Bangor University

DOCTOR OF PHILOSOPHY

Identification and functional characterisation of germ line genes in human cancer cells

Aldeailej, Ibrahim

Award date:
2013

Awarding institution:
Bangor University

[Link to publication](#)

Bangor University

School of Biological Sciences

Identification and functional characterisation of germ line genes in human cancer cells

Ph.D. Thesis 2013

IBRAHIM ALDEAILEJ

Declaration and Consent

Details of the Work

I hereby agree to deposit the following item in the digital repository maintained by Bangor University and/or in any other repository authorized for use by Bangor University.

Author Name: IBRAHIM MOHAMMED ALDEAILEJ

Title: Identification and functional characterisation of germ line genes in human cancer cells

Supervisor/Department: Dr. Ramsay James McFarlane/ School of Biological Sciences

Funding body (if any): kingdom of Saudi Arabia Government

Qualification/Degree obtained: Ph.D.

This item is a product of my own research endeavours and is covered by the agreement below in which the item is referred to as "the Work". It is identical in content to that deposited in the Library, subject to point 4 below.

Non-exclusive Rights

Rights granted to the digital repository through this agreement are entirely non-exclusive. I am free to publish the Work in its present version or future versions elsewhere.

I agree that Bangor University may electronically store, copy or translate the Work to any approved medium or format for the purpose of future preservation and accessibility. Bangor University is not under any obligation to reproduce or display the Work in the same formats or resolutions in which it was originally deposited.

Bangor University Digital Repository

I understand that work deposited in the digital repository will be accessible to a wide variety of people and institutions, including automated agents and search engines via the World Wide Web.

I understand that once the Work is deposited, the item and its metadata may be incorporated into public access catalogues or services, national databases of electronic theses and dissertations such as the British Library's EThOS or any service provided by the National Library of Wales.

I understand that the Work may be made available via the National Library of Wales Online Electronic Theses Service under the declared terms and conditions of use (http://www.llgc.org.uk/index.php?id=4676). I agree that as part of this service the National Library of Wales may electronically store, copy or convert the Work to any approved medium or format for the purpose of future preservation and accessibility. The National Library of Wales is not under any obligation to reproduce or display the Work in the same formats or resolutions in which it was originally deposited.

<u>Statement 1</u>:

This work has not previously been accepted in substance for any degree and is not being concurrently submitted in candidature for any degree unless as agreed by the University for approved dual awards.

Signed ………………………………………… (candidate)

Date ………………………………………………

<u>Statement 2</u>:

This thesis is the result of my own investigations, except where otherwise stated. Where correction services have been used, the extent and nature of the correction is clearly marked in a footnote(s).

All other sources are acknowledged by footnotes and/or a bibliography.

Signed ………………………………………… (candidate)

Date ………………………………………………

<u>Statement 3</u>:

I hereby give consent for my thesis, if accepted, to be available for photocopying, for inter-library loan and for electronic storage (subject to any constraints as defined in statement 4), and for the title and summary to be made available to outside organisations.

Signed ………………………………………… (candidate)

Date ………………………………………………

NB: Candidates on whose behalf a bar on access has been approved by the Academic Registry should use the following version of **Statement 3:**

<u>Statement 3 (bar)</u>:

I hereby give consent for my thesis, if accepted, to be available for photocopying, for inter-library loans and for electronic storage (subject to any constraints as defined in statement 4), after expiry of a bar on access.

Signed ………………………………………… (candidate)

Date ………………………………………………

Statement 4:

Choose **one** of the following options

a) I agree to deposit an electronic copy of my thesis (the Work) in the Bangor University (BU) Institutional Digital Repository, the British Library ETHOS system, and/or in any other repository authorized for use by Bangor University and where necessary have gained the required permissions for the use of third party material.	
b) I agree to deposit an electronic copy of my thesis (the Work) in the Bangor University (BU) Institutional Digital Repository, the British Library ETHOS system, and/or in any other repository authorized for use by Bangor University when the approved **bar on access** has been lifted.	
c) I agree to submit my thesis (the Work) electronically via Bangor University's e-submission system, however I **opt-out** of the electronic deposit to the Bangor University (BU) Institutional Digital Repository, the British Library ETHOS system, and/or in any other repository authorized for use by Bangor University, due to lack of permissions for use of third party material.	

Options B should only be used if a bar on access has been approved by the University.
In addition to the above I also agree to the following:

1. That I am the author or have the authority of the author(s) to make this agreement and do hereby give Bangor University the right to make available the Work in the way described above.

2. That the electronic copy of the Work deposited in the digital repository and covered by this agreement, is identical in content to the paper copy of the Work deposited in the Bangor University Library, subject to point 4 below.

3. That I have exercised reasonable care to ensure that the Work is original and, to the best of my knowledge, does not breach any laws – including those relating to defamation, libel and copyright.

4. That I have, in instances where the intellectual property of other authors or copyright holders is included in the Work, and where appropriate, gained explicit permission for the inclusion of that material in the Work, and in the electronic form of the Work as accessed through the open access digital repository, *or* that I have identified and removed that material for which adequate and appropriate permission has not been obtained and which will be inaccessible via the digital repository.

5. That Bangor University does not hold any obligation to take legal action on behalf of the Depositor, or other rights holders, in the event of a breach of intellectual property rights, or any other right, in the material deposited.

6. That I will indemnify and keep indemnified Bangor University and the National Library of Wales from and against any loss, liability, claim or damage, including without limitation any related legal fees and court costs (on a full indemnity bases), related to any breach by myself of any term of this agreement.

Signature: …………………………………… Date:…………………………………………….

iii

Abstract

Cancer is a leading cause of death worldwide and this is at least in part due to limitations in current therapies and late diagnosis. Thus, improving the tools to diagnose cancer at early stages and the development of new therapeutic targets is essential. One group of proteins that might be helpful for both diagnosis and immunotherapy targeting is known as the cancer/testis antigens (CTAs). CTA genes are expressed in the normal testis and should not be expressed in other healthy somatic cells, however these genes are expressed in various cancer cells. Therefore, identifying new bona fide CTA genes has great clinical importance. In this study, different strategies were used to identify and characterise new CTA genes. The results presented here identified eleven candidate CTA genes.

Two CTA genes, *SPO11* and *PRDM9* were validated at the protein level. SPO11 and PRDM9 proteins were detected only in the normal testis and not in any other normal tissues. PRDM9 was detected in different types of cancer and SPO11 was detected in all the cancer cell lines and most of the cancer tissues which were used in this study. These results suggest that SPO11 might be essential for the cancer cells. SPO11 was also found to be associated with the DNA, which might indicate that SPO11 was bound to the DNA, giving rise to the possibility of DSB formation in cancer cells. The presence of SPO11 during mitotic cell division might lead to incorrect replication or/and formation of DSBs during mitosis, which might lead to different chromosome rearrangements and ultimately to cancer, suggesting that SPO11 could be an oncogenic driver. Therefore, defects in SPO11 might cause cancer cells to undergo apoptosis, which might explain the level of cell death observed after the cancer cells were treated with siRNA and TALENs. In addition, knockdown of PRDM9 was shown to reduce SPO11-DNA binding in the cancer cells which suggested that PRDM9 may have a meiotic-like function in cancer cells, which opens the chromatin and allow SPO11 access and DSB formation.

CTA genes are important during meiosis. Identification of new CTA genes expressed in different cancer tissues and cell lines indicate that they may be potentially good tools for early diagnosis or/and cancer therapy targets.

Acknowledgments

Abbreviation

ACTRT1	actin-related protein T1
ADAM2	metallopeptidase domain 2
AEBSF	4-(2-aminoethyl) benzenesulfonyl fluoride
AEs	axial elements
ALL	Acute lymphoblastic leukaemia
BAGE	melanoma antigen family
BRDT	bromodomain, testis-specific
C1orf65	chromosome 1 open reading frame 65
C4orf51	chromosome 4 open reading frame 51
C7orf31	chromosome 7 open reading frame 31
C10orf82	chromosome 10 open reading frame 82
C11orf91	chromosome 11 open reading frame 91
C12orf42	chromosome 12 open reading frame 42
C19orf67	chromosome 19 open reading frame 67
C20orf79	chromosome 20 open reading frame 79
C22orf33	chromosome 22 open reading frame 33
CALM2	calmodulin 2 (phosphorylase kinase, delta)
CATSPER3	cation channel sperm-associated protein 3
CCDC146	coiled-coil domain containing 146
CCDC18	coiled-coil domain containing 18
CCDC38	coiled-coil domain containing 38
CCDC79	coiled-coil domain containing 79
CE	central element
CR	complete response
CTA	cancer testis antigen
CTAG2	cancer/testis antigen 2
C-terminal	carboxy-terminal domain
CTLs	cytotoxic T cells
CTLs	Cytolytic T lymphocyte
CTNNA2	catenin (cadherin-associated protein), alpha 2
CTp11	cancer/testis-associated protein of 11 kD
CYLC2	cylicin, basic protein of sperm head cytoskeleton 2

DAC	5-aza-2'-deoxycytidine
DC	Dendritic cells
dHJ	double-Holliday junction
DKK1	dickkopf-1
DMEM	Dulbecco's Modified Eagle Medium
DSB	double-strand break
ECACC	European Collection of Cell Cultures
ELDA	Extreme limiting dilution analysis
EOC	epithelial ovarian cancer
ERK	mitogen-activated protein kinase 1
ESCC	esophageal squamous cell carcinoma
EST	expressed sequence tag
FAM133A	family with sequence similarity 133, member A
FBS	foetal bovine serum
GLT6D1	glycosyltransferase 6 domain containing 1
GPAT2	glycerol-3-phosphate acyltransferase 2
HCA587	MAGEC2 melanoma antigen family C, 2
HCC	hepatocellular carcinoma
HDAC	Histone deacetylases
HORMAD1	ORMA domain-containing protein 1
HORMAD2	ORMA domain-containing protein 2
IGF	insulin-like growth factor
IHC	Immunohistochemistry
IMP-3	mRNA binding protein 3
IQCF5	IQ motif containing F5
JARID1B	jumonji/ARID domain-containing protein 1B
LEs	lateral elements
LIPI	lipase member I
LUZP4	leucine zipper protein 4
LY6K	lymphocyte antigen 6 complex locus K
MAGE-C1	melanoma antigen family C, 1
MBD3L1	methyl-CpG binding domain protein 3-like 1
MEM	Minimum Essential Medium
MHC	major histocompatibility complex

MI	metaphase I
MII	metaphase II
MM	multiple myeloma
MPSS	massively parallel signature sequencing
MRN	MRE11–RAD50–NBS1
NCBI	National Center for Biotechnology Information
NK	natural killer
NMC	NUT midline carcinoma
N-terminal	amino-terminal domain
NUT	nuclear protein in testis
PAGE5	P antigen family, member 5
PAX5	paired box 5
PBK	PDZ binding kinase
PBLs	peripheral blood lymphocytes
PBLs	peripheral blood lymphocytes
PBMC	peripheral blood mononuclear cell
Piwil2	piwi-like RNA-mediated gene silencing 2
PRDM9	PR domain zinc finger protein 9
PTPN20B	protein tyrosine phosphatase, non-receptor type 20B
PVRIG	poliovirus receptor related immunoglobulin domain containing
RLNL	regional lymph node lymphocytes
RLNL	regional lymph node lymphocytes
RPMI	Roswell Park Memorial Institute
RVD	repeat-variable di-residue
SAGE1	sarcoma antigen 1
SC	synaptonemal complex
SCM	stem cell medium
SD	stable disease
SDSA	synthesis-dependent strand annealing
SEREX	serological analysis of cDNA expression libraries
siRNA	Small interfering RNA
SMC1	structural maintenance of chromosomes 1
SMC1α	structural maintenance of chromosomes 1A
SMC3	structural maintenance of chromosomes 3

SPAG9	sperm associated antigen 9
SSX1	synovial sarcoma, X breakpoint 1
STAG3	stromal antigen 3
STK31	serine/threonine kinase 31
SYCE1	synaptonemal complex central element protein 1
SYCE2	synaptonemal complex central element protein 2
SYCE3	synaptonemal complex central element protein 3
SYCP1	synaptonemal complex protein 1
SYCP2	synaptonemal complex protein 2
SYCP3	synaptonemal complex protein 3
TAAs	tumour-associated antigens
TAG-1	transient axonal glycoprotein 1
TALEs	transcription activator like effectors
TDRD1	tudor domain containing 1
TDRD1	tudor domain containing 1
TEX12	testis-expressed protein 12
TEX15	testis expressed 15
TF	transverse filament
TIL	tumour-infiltrating lymphocytes
TIL	tumour-infiltrating lymphocytes
TRK	neurotrophic tyrosine kinase, receptor, type 1
TSGs	Tumour suppressor genes
TTK	TTK protein kinase
TUBA1B	tubulin alpha-1B chain
WNT	wingless-type MMTV integration site

Contents

List of figures

List of tables

Chapter 7

1   Introduction

1.1   Cancer overview

Cancer is one of the main diseases that causes death worldwide; for instance, in the US, one of four deaths is caused by cancer (Siegel et al., 2012). In addition, in the US, some cancers, such as leukaemia and brain cancer, are the second most frequent causes of death among children (Siegel et al., 2012).

Cancer comprises a large group of diseases characterised by the abnormal growth of cells in the body which is caused by genetic or epigenetic changes that lead to uncontrolled cell proliferation (Sharma et al., 2010). These uncontrolled cells can spread (metastasise) to different parts of the body and lead to secondary tumours in other organs (Brábek et al., 2010). The risk of being affected by cancer can be increased by different factors, such as environment, age, lifestyle, viruses, or bacterial infection.

On other hand, there are a number of cancers that are caused by inherited germ line mutations. For instance, two studies of the North American population demonstrated that for 13%−15% of women diagnosed with ovarian carcinoma it is caused by germline mutations in the *BRCA1* or *BRCA2* genes (Pennington and Swisher, 2012). The germline mutation passes from the parent to their children and will affect a single copy of the gene in every cell of the body. Heterozygosity is lost when the second copy of the gene becomes mutated, possibly only in a single cell, which will establish the tumour. In addition, heterozygous germline mutations in the fumarate hydratase (*FH*) gene caused hereditary leiomyomatosis and renal cell cancer (HLRCC) which is a tumour predisposition syndrome (Lehtonen et al., 2006).

Advances in DNA sequence technology has increased knowledge of cancer at different levels, including biomarker identification for early diagnosis, and drug targeting (Meyerson et al., 2010).

1.2 Hallmarks of Cancer

Normal cells develop the neoplastic state through one or more of the cancer hallmarks that determine neoplastic organisation. The hallmarks of cancer include: sustaining proliferative signalling, evading growth suppressors, resisting cell death, enabling replicative immortality, inducing angiogenesis, activating invasion and metastasis, genome instability and mutation, tumour-promoting inflammation, reprogramming energy metabolism and evading immune destruction (Hanahan and Weinberg, 2011). Thus, understanding the hallmarks of cancer can help in designing therapeutic drugs to target cancer (Figure1.1).
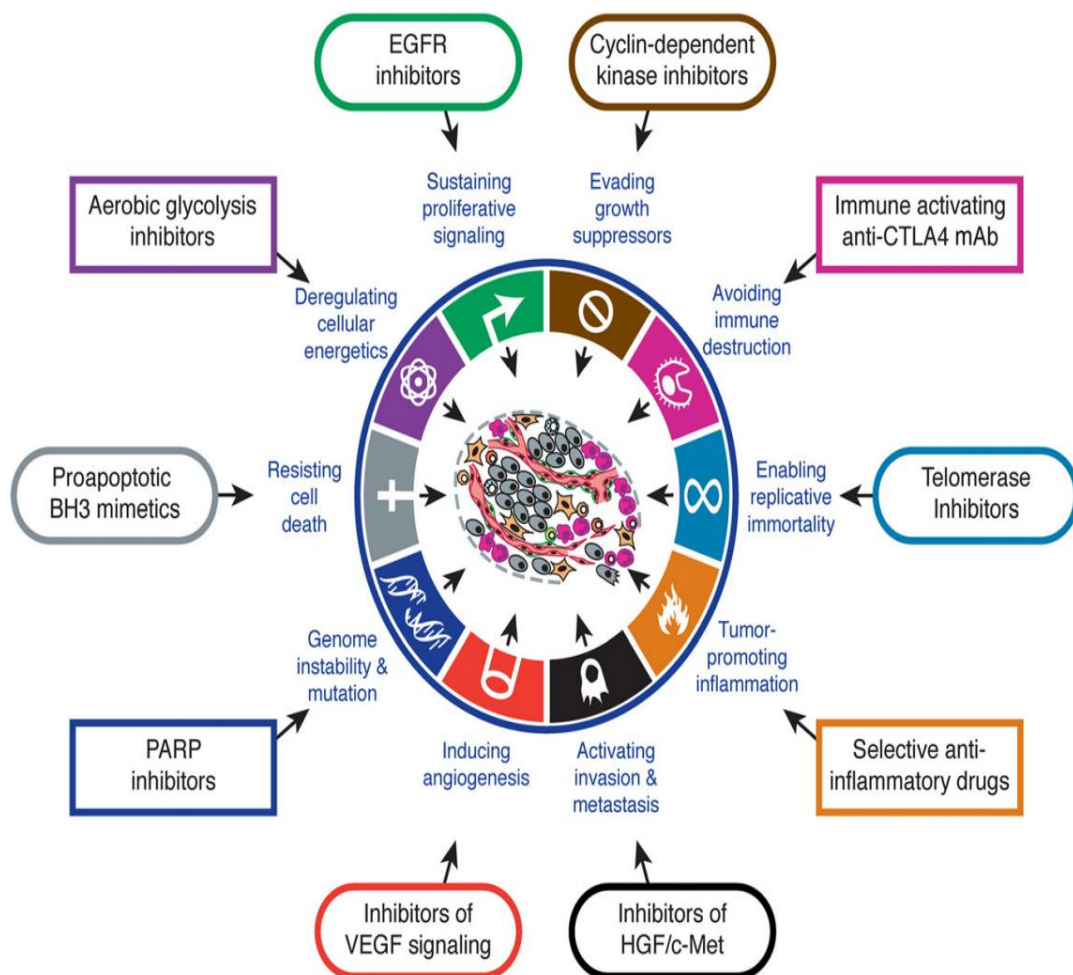
Figure 1.1. Therapeutic Targeting of the Hallmarks of Cancer. Examples of therapies targeting cancer hallmarks (Hanahan and Weinberg, 2011).

Throughout the cell cycle and during cell growth, normal cells carefully control the release and production of growth promoting signals including the maintenance signals that control energy metabolism and cell survival. Two types of these signals are recognised, one type that involves cell surface binding factors and another that acts intracellularly (for example, on kinase domains). However, in cancer cells, these signals become deregulated, which causes the cells to become 'masters of their own destiny' (Hanahan and Weinberg, 2000; 2011). The cancer cells may then begin to produce their own growth factors or/and may stimulate normal cells to associate with the tumour by cell to cell signalling (Hembruff et al., 2010).

Another hallmark of cancer is evasion of growth suppressors. Under normal conditions, tumour suppressor genes such as *p53* and *Rb* suppress abnormal cell growth and proliferation (Cairns et al., 2011). Thus, a lack of these tumour suppressor genes will lead to abnormal proliferation; for example, a null *Rb* leads to the progression of neoplasia while a null of *p53* can lead to leukaemia (Hanahan and Weinberg, 2011). The apoptotic programme targets cancer cells during tumorigenesis or as result of cancer therapy; therefore, a defect in the apoptotic programme is a hallmark of cancer (Hanahan and Weinberg, 2011). For instance, the apoptotic system responds to a cell damage signal, but the apoptotic process might be defective in the interactions between three factions of the Bcl-2 protein family (Adams and Cory, 2007).

Enabling replicative immortality is another hallmark of cancer. Cancer cells have unlimited capacity to replicate to reach the macroscopic tumour stage. This enabling of replicative immortality occurs rarely, due to natural cell senescence or elimination, but might occur due to delays in cell death or cell elimination (Hanahan and Weinberg, 2011). In addition, the telomeres that protect the ends of the chromosomes are involved in the unlimited proliferation of cancer cells as pathways for telomere maintenance must be activated (Blasco, 2005).

Both normal and cancer tissues require angiogenesis to provide nutrients and oxygen and to evacuate carbon dioxide and metabolic wastes. Therefore, during the tumour progression, new vessels assist in the expansion of the neoplastic growths, making angiogenesis another of the hallmarks of cancer (Raica et al., 2009). Further hallmarks of cancer include activating invasion and metastasis. When cells that duplicate are in the same organ as primary tumour, this is called invasion. When cancer spreads from one organ to another that is not directly connected with the primary site, it is called metastasis

and is achieved by an association between the cancer cells and other cells through the extracellular matrix (ECM) (Hanahan and Weinberg, 2011).

Recently, genome instability and mutation have been reviewed as hallmarks of cancer; most of these hallmarks depend on a change in the genome of the neoplastic cells (Hanahan and Weinberg, 2011). For instance, DNA methylation and histone modification can inactivate tumour suppressor genes (Cedar and Bergman, 2009). Inflammation, which is usually regarded as a reaction that protects the body against infection, can also lead to cancer, making chronic inflammation yet another hallmark of cancer (Aggarwal et al., 2006).

Deregulation of energy metabolism has also been reported as a hallmark of cancer (Hanahan and Weinberg, 2011). For instance, abnormal glycolytic fuelling can lead to mutation in tumour suppressor genes such as *p53*, as well as association with different oncogenes such as *Ras* (Jones and Thompson, 2009). The immune system can play an important role in resisting or eradicating the formation of cancer. However, cancer cells/ tumours have the ability to avoid the immune system through as yet poorly defined mechanisms. Therefore, evading immune destruction is a key hallmark of cancer (Hanahan and Weinberg, 2011). For this reason, using combinations of chemotherapy and immunotherapy is an attractive prospect to increase the efficiency of immunotherapy as a cancer treatment (See section 1.6.8.2).

1.3 Conventional treatments for cancer

Cancers are traditionally treated with surgery, radiotherapy, and chemotherapy. These conventional treatments have distinct advantages for cancer patients, and each has potential negative side effects. Many cancer patients experience a recurrence following cancer surgery (Eichler and Plotkin, 2008). The side effects of radiotherapy include fatigue, nausea, anorexia, skin irritation, hair loss, and changes in taste bud perception. In addition, there are other side effects to long-term radiotherapy, such as memory loss, gait dysfunction, incontinence, and endocrine dysfunction (Eichler and Plotkin, 2008).

Cancer chemotherapy can be more cost-effective (Eichler and Plotkin, 2008); side effects include hair loss, fatigue, diarrhoea, dizziness upon standing up, loss of libido, abdominal pain, weight gain, anxiety, loss of appetite, and irritability (Carelle et al., 2002). As an alternative, many studies have been carried out to investigate the potential of cancer immunotherapy treatments, although these have yet to be widely applied.

1.4 Cancer immunotherapy

Cancer immunotherapy might be an alternative treatment for conventional cancer treatments in the future. Therefore, many researcher clinicians focus developing cancer immunotherapy. The overarching aim is to use immunotherapy to target cancer cells without harming the healthy cells. There are various mechanisms to use immune system against growing cancer cells such as, natural killer (NK) cells, cytotoxic T cells (CTL), natural killer T cells, and, in some cases, antibodies. Dendritic cells (DC) play a central role in the antitumor immunity in solid tumors by coordinating the activities of the NK cells, CTL and natural killer T cells (Iclozan and Gabrilovich, 2012).

There is another promising approach of cancer immunotherapy treatments which involves the targeting of genes expressed normally in the testis but not in other healthy somatic cells. However, these genes are expressed in different type of cancers (see section 1.6). These genes are known as cancer/testis antigen genes (CTA genes) such as *MAGE-C1/CT7*, which is highly expressed in Multiple myeloma (MM) (de Carvalho et al., 2012). Given that the testis is the site for male meiosis and there is a potential for CTA genes to be oncogenic (for example, see section 1.6.6), it is important to have a full understanding of meiosis and mitosis.

1.5 Mitosis and Meiosis

Mitotic division is the process of a single cell division that normally produces two identical daughter cells from a single parental cell. During meiosis, a single diploid cell in the ovaries and testes of mammals divides to form four haploid gamete cells, ova and sperm cells respectively (Table 1.1).

1.5.1 Mitosis

During mitotic S-phase, DNA replicates once to produce two sister chromatids per chromosome. Prior to anaphase, when sister chromatids separate, the sister chromatids are tightly linked to each other by a protein complex called cohesins (see Section 1.5.2.5) (Nasmyth, 2011; Uhlmann, 2004). This association, called sister chromatid cohesion, allows spindle microtubules to attach to the kinetochores correctly (Gregan et al., 2011; Hauf and Watanabe, 2004) and generates opposing forces on sister chromatids. At the

metaphase to anaphase transition cohesion is disrupted, allowing the sister chromatids to separate and the spindle to pull the sister chromatids to opposite poles of the cell (Daum et al., 2011; Scholey et al., 2003).

Mitotic cell division is divided into different stages (Figure 1.2):

1. **Interphase:** During interphase, the chromosomes become extended and thin which make them less distinct (Maeshima et al., 2010).

- **Prophase:** During this stage the sister chromates are condensed into shorter, thicker fibres. The centrioles duplicate and migrate to opposite poles of the cell, and the spindle begins assembly (Scholey et al., 2003).

- **Prometaphase:** During this stage, the nuclear envelope breaks (in open mitoses) into fragments that allow the spindle to attach to a small nodule-like structure, called the kinetochore, which is present at the outer surface of the centromere of each chromatid (Scholey et al., 2003).

- **Metaphase:** During this stage, the chromosomes are aligned at the centre of the cell on the metaphase plate and attached to the spindle microtubule, prior to the signal for chromatid separation (Scholey et al., 2003; Walczak et al., 2010).

- **Anaphase:** During this stage, the cohesion between the sister chromatids is disrupted, and they are pulled to opposite poles of the cell (Haering and Nasmyth, 2003; Walczak et al., 2010).

- **Telophase:** During this stage, the chromatid becomes an independent chromosome, and the spindle is disassembled. Finally, two groups of chromosomes are enveloped by a new nucleic membrane (Walczak et al., 2010).

- **Cytokinesis:** During this stage, the cell cytoplasm separates, yielding two identical daughter cells (Walczak et al., 2010).
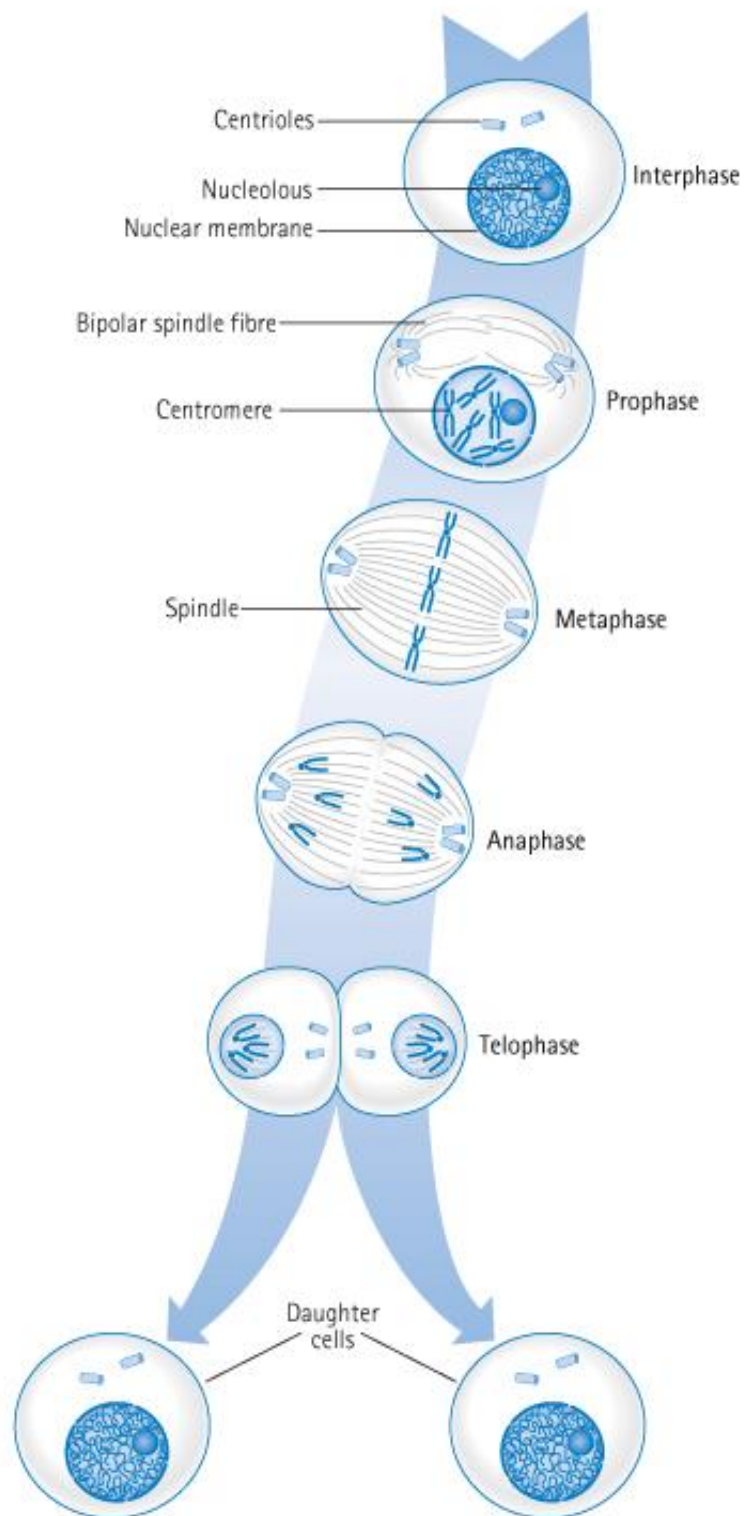
Figure 1.2 The stages of mitosis. The stages of mitosis, starting with interphase and then prophase, where the sister chromatids are condensed, the centrioles migrate to opposite poles of the cell, and the spindle begins assembly. During metaphase, the sister chromatids are aligned at the centre of the cell; then, the chromatids are pulled to opposite poles of the cell during anaphase. During telophase, the spindle is disassembled, and the two groups of chromosomes are enveloped by a new nucleic membrane. Finally, the daughter cells separate during cytokinesis (Egel and Lankenau, 2007).

1.5.2 Meiosis

Meiosis is initiated with one round of chromosome duplication (meiotic S-phase) that is followed by two rounds of chromosome segregation, known as meiosis I (reductional) and meiosis II (equational) (Egel and Lankenau, 2007). Each division has four stages: prophase, metaphase, anaphase, and telophase (Figure 1.3).

1.5.2.1 Meiosis I

Prophase I: During this stage, the cohesins pair sister chromatids together and recombination occurs between the homologues. Then, in most organisms the homologues become closely associated in a process called synapsis (Qiao et al., 2012). In this part of meiosis I, many species of eukaryotes have primary meiotic arrests during oocyte development that is maintained for a few days (*Drosophila*) or for decades (humans). Then as result of hormonal or developmental stimulation, oocytes release the first arrest, and enter a second arrest at metaphase I (MI), metaphase II (MII), then the second arrest release for fertilisation and the completion of meiosis in vertebrates (*Xenopus* and mammals) (Von Stetina and Orr-Weaver, 2011), a similar arrest is not noted in male gametogenesis.

Prophase I is divided into four sub-stages: leptotene, zygotene, pachytene, diplotene and diakinesis.

- o **Leptotene:** Recombination is initiated by cleavage of the DNA double helix at many locations (see Section 1.5.2.3).

- o **Zygotene:** During synapsis, the homologues draw closer to each other through a protein complex called the synaptonemal complex (SC), which begins to be assembled between homologues (discussed in Section 1.5.2.4) (Qiao et al., 2012). Each pair of synapsed homologous chromosomes is known as a bivalent (Blanco-Rodríguez, 2012).

- o **Pachytene:** At this stage, the chromosomes become shorter and thicker (Page et al., 2003), and the SC assembly is completed. At the end of this stage crossovers are completed (Kleckner, 1996). There are important checkpoints at this stage, called pachytene checkpoints, which have the

responsibility of arresting meiosis if there is a failure in chromosome synapsis and/or recombination, in order to allow the cell to repair the error or to activate the apoptotic programme (Pellestor et al., 2011).

- o **Diplotene:** This stage is marked by the bivalent beginning to separate (Handel and Schimenti, 2010). However, the homologous chromosomes are held together as a result of crossing over by cohesion connections between sister chromatids distal to chiasmata, and this is responsible for holding homologous chromosomes together (Buonomo et al., 2000). In normal meiosis, each bivalent has at least one chiasma, and the long chromosomes have three or more (Espagne et al., 2011).

- o **Diakinesis:** More condensation occurs in this stage (Lesch and Page, 2012). In addition, by the end of this sub-stage, the spindle formation is initiated and the nuclease membrane breaks down (Öllinger et al., 2010).

- **Metaphase I:** During this stage, the bivalents attach to the meiotic spindle and are aligned at the metaphase plate, which is the centre of the cell (Petronczki et al., 2003).

- **Anaphase I:** During this stage, the cohesin cleaves from the bivalent (homologous arm), which allows the homologous chromosomes to separate (chromosomes segregation) and move to the opposite poles (Brar and Amon, 2008). The cohesin at the centromere is protected by human Bub1 and human Shugoshin (Sgo1), which keep the sister chromatids together until anaphase II but permit homologue segregation (Tang et al., 2004).

- **Telophase I:** During this stage, the nuclear membrane reassembles around each group of homologues at each pole (Egel and Lankenau, 2007).

1.5.2.2 Meiosis II

The stages in this division are similar to those in mitotic division and result in four haploid cells, known as spermatids (male) or ova (female). However, most mammals have a meiotic arrest during oocyte development (Von Stetina and Orr-Weaver, 2011) (Figure 1.3).

9
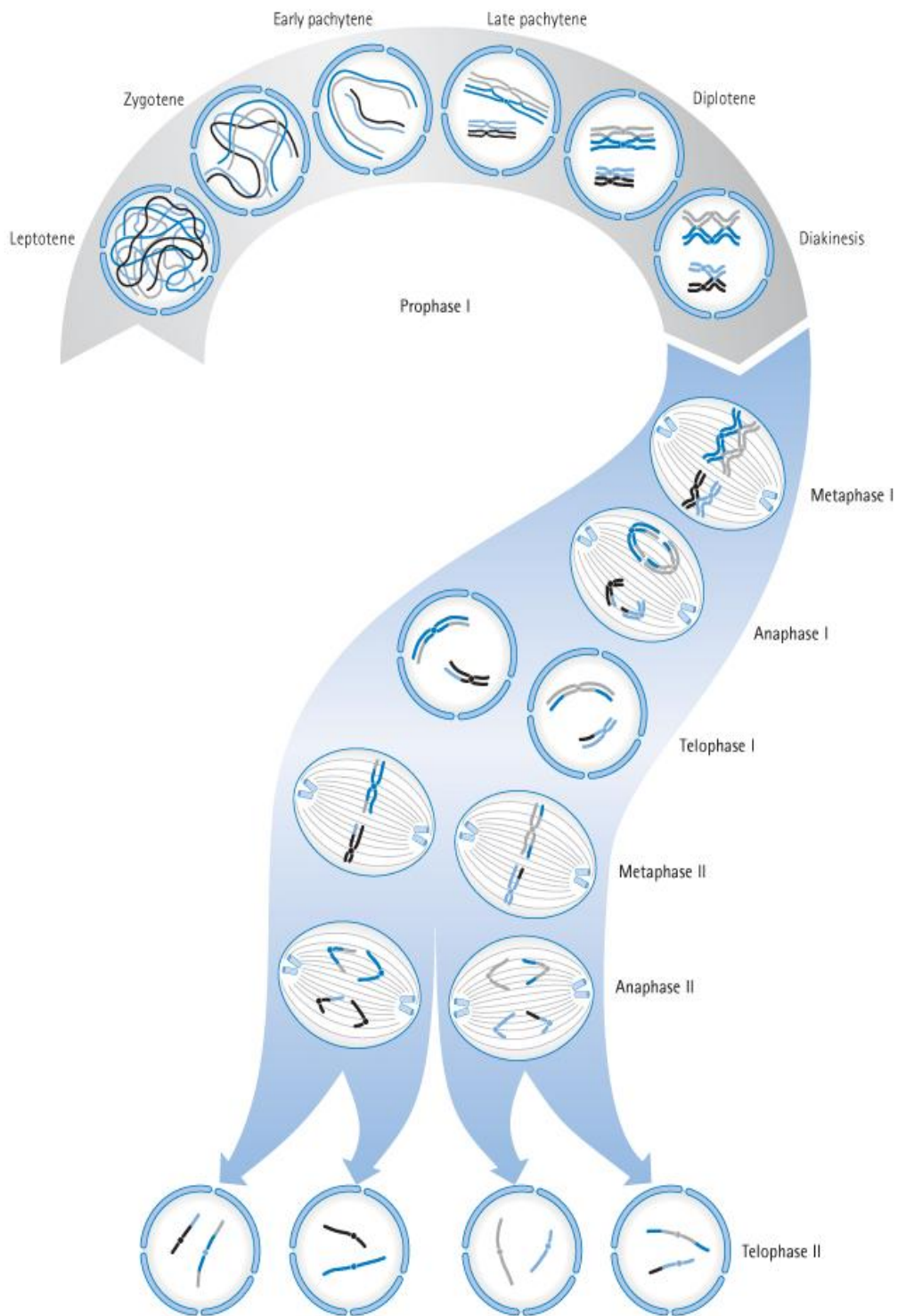
Figure 1.3 The meiosis process: Meiosis I stages, consisting of the following sub-stages: prophase I, metaphase I, anaphase I, and telophase I. The meiosis II stages result in four haploid cells (Egel and Lankenau, 2007) (see the text for more details).

1.5.2.3 Meiotic recombination

The process of recombination links homologues together in a bivalent during prophase I of meiosis I; this is important for chromosome alignment/segregation in meiosis I. Recombination allows the generation of a new combination of alleles in the offspring and serves as an evolutionary driver. Defects in the frequency or position of recombination may lead to chromosome non-disjunction, which causes aneuploidy disorders, such as Down syndrome (Abruzzo and Hassold, 2006). In addition, double-strand break (DSB) repair abnormality during meiotic recombination can cause chromosome translocations (Richardson et al., 1998).

Recombination in meiosis I occurs at preferred locations on the homologues, which causes a high frequency of recombination, called recombination hotspots (Cheung et al., 2010). In mammals the PRDM9 protein controls some meiotic recombination hotspot distribution in the genome by binding to specific DNA sequences that establish open chromatin for Spo11 to initiate the meiotic recombination by generating a DSB (Baudat et al., 2010). In the budding yeast, after the DNA replication, the axial element components Red1, Hop1, cohesin and the pre-DSB recombinosome subunits Mer2, Rec114, and Mei4 bind to the sites of axis. The Mer2 is phosphorylated by S-Cdk, which will recruit Rec114 and Mei4. Spo11 will then bind to the chromatid after condensation and sister chromatids are conjoined in the developing axis for cleavage of the DNA within one of the hotspots (Figure 1.4) (Panizza et al., 2011).

Spo11 remains covalently bound to the 5' end of the breaks, and short oligonucleotides and Spo11 protein are removed from the 5' ends by the Mre11-Rad50-Nbs1 (MRN) protein complex, leading to the generation of single-strand 3' ends (Longhese et al., 2010). Then, DSB resection occurs in both directions mediated by Exo1 in the 5′-3′ direction away from the DSB and Mre11 in the 3′-5′ direction towards the DSB end (Garcia et al., 2011). The generated 3' ends are coated by recombinases, Rad51 and Dmc1, which mediate inter duplex strand invasion, thus, forming the D-loop. Rad51 is required for both meiosis and mitosis, whilst Dmc1 is restricted to meiosis and is thought to facilitate inter homologue strand invasion (Serrentino and Borde, 2012) (Figure 1.5).

The D-loop can be dissociated following limited replication primed by the invading 3' end when the single-strand 3' ends are displaced leading to the synthesis-dependent strand

annealing (SDSA) pathway (Paigen and Petkov, 2010). A structure termed a double-Holliday junction (dHJ) is formed when the second end is joined to the homologous chromosome (Youds and Boulton, 2011). The dHJ can then be resolved by cleavage as a result of interaction with different enzymes, such as Mus81-Mms4(EME1) complex, Slx1/4 (BTBD12) and GEN1; dHJ resolution leads to crossover or non-crossover (Figure 1.5), but the major crossover resolution pathway in budding yeast is Exo1-Mlh1-3 and Sgs1 mediated (Zakharyevich et al., 2012).
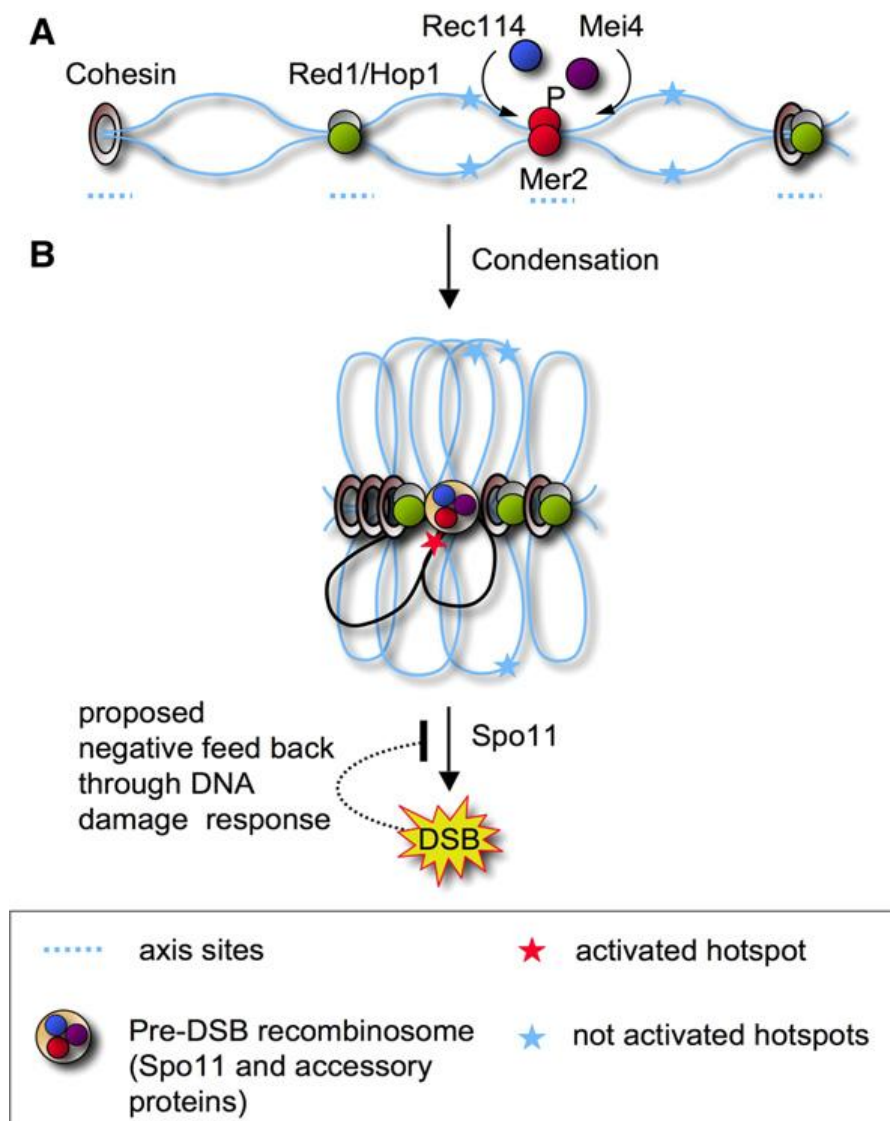
Figure 1.4 Pre-DSB recombinosome binding to the DNA to establish the DSB: A) The axial element components Red1, Hop1, cohesin and the pre-DSB recombinosome subunits Mer2, Rec114, and Mei4 bind to the sites of axis after DNA replication. **B)** Spo11 will bind to the chromatid after condensation and sister chromatids are conjoined in the developing axis for cleavage of the DNA with one of the hotspots (Panizza et al., 2011).
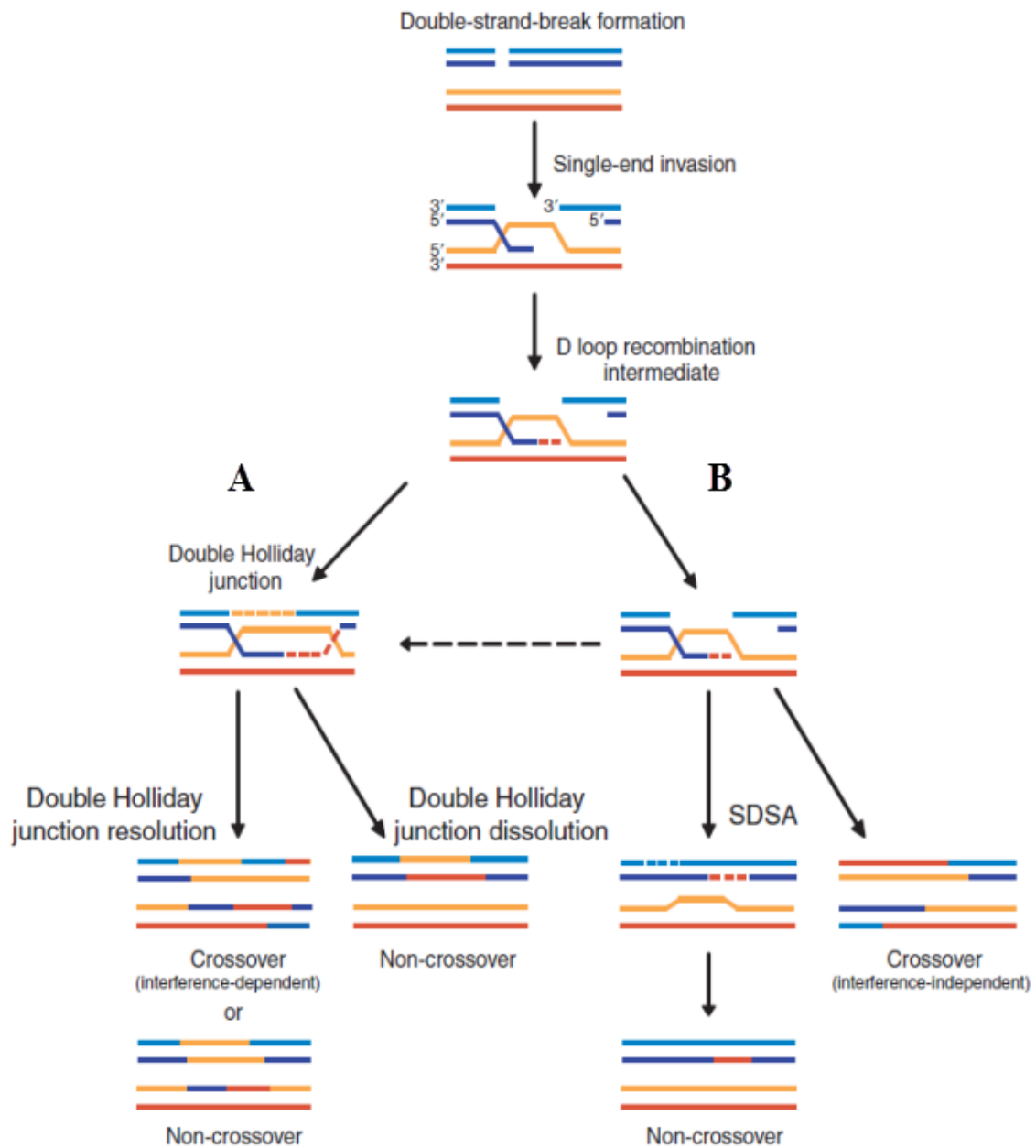
Figure 1.5 A model for the mechanism of homologous recombination in meiotic prophase I. SPO11 generates DSBs. The 5' end is removed by MRN complex to generate 3' end, which then initiates a single-end invasion D- loop intermediate. (**A**) If the second end is joined to the homologus a double-Holliday junction (dHj) is formed. The dHj can be resolved to form either a crossover or a non-crossover. Otherwise, the junction can be dissolved to form a non-crossover. (**B**) Instead of forming a dHj, the D loop can be dissociated and the invading strand can associate with the opposite end of the original break following limited de novo DNA synthesis; this is synthesis-dependent strand annealing (SDSA) and non-crossovers are formed. Alternatively, the intermediate can be acted upon by enzymes, such as Mus81, that can form interference-independent crossovers (Youds and Boulton, 2011).

1.5.2.4 Synaptonemal complex

The synaptonemal complex (SC) is a protein complex formed between two homologous chromosomes during meiotic prophase I, which causes stable association of the homologous chromosomes (Page et al., 2008). Defects in synapsis can result in different consequences in the meiosis process, such as infertility or aneuploidy in mammals (Fraune et al., 2012). In humans, oocyte aneuploidy which may be caused by defects in synapsis can lead to miscarriages (Garcia-Cruz et al., 2008). The SC contains three different structural elements: lateral elements, transverse filaments, and central element (Figure 1.6) (Costa and Cooke, 2007).

HORMA-domain proteins (HORMAD1 and HORMAD2) promote SC formation by playing an important role in homology searching (Wojtasz et al., 2009). The SC initiates assembly when the axial elements (AEs) are formed in each chromosome during the leptotene to zygotene stages. These AEs are then termed lateral elements (LEs) which contain SYCP2 and SYCP3 proteins and cohesin (Fraune et al., 2012). Subsequently, the transverse filament is formed by SYCP1 (Hamer et al., 2006), which has two terminal domains: a carboxy-terminal domain (C-terminal), associated with the lateral elements, and an amino-terminal domain (N-terminal), which interacts with the central elements (Liu et al., 1996) (Figure 1.6).

The central element of the SC contains SYCE1 and SYCE2, which interact with the SYCP1 of the transverse filaments (Costa et al., 2005). Hamer et al. (2006) identified testis-expressed protein 12 (TEX12), which is located in the central element. TEX12 is essential for the association of SYCE2 and forming the central element (Hamer et al., 2008). In addition, SYCE3, another protein involved in the central element, has been identified; SYCP1 interacts with SYCE3 to form the bridge between the transverse filament and central element (Figure 1.6) (Schramm et al., 2011). This complex holds the homologous chromosomes together until disassembly at the diplotene stage (Bisig et al., 2012).
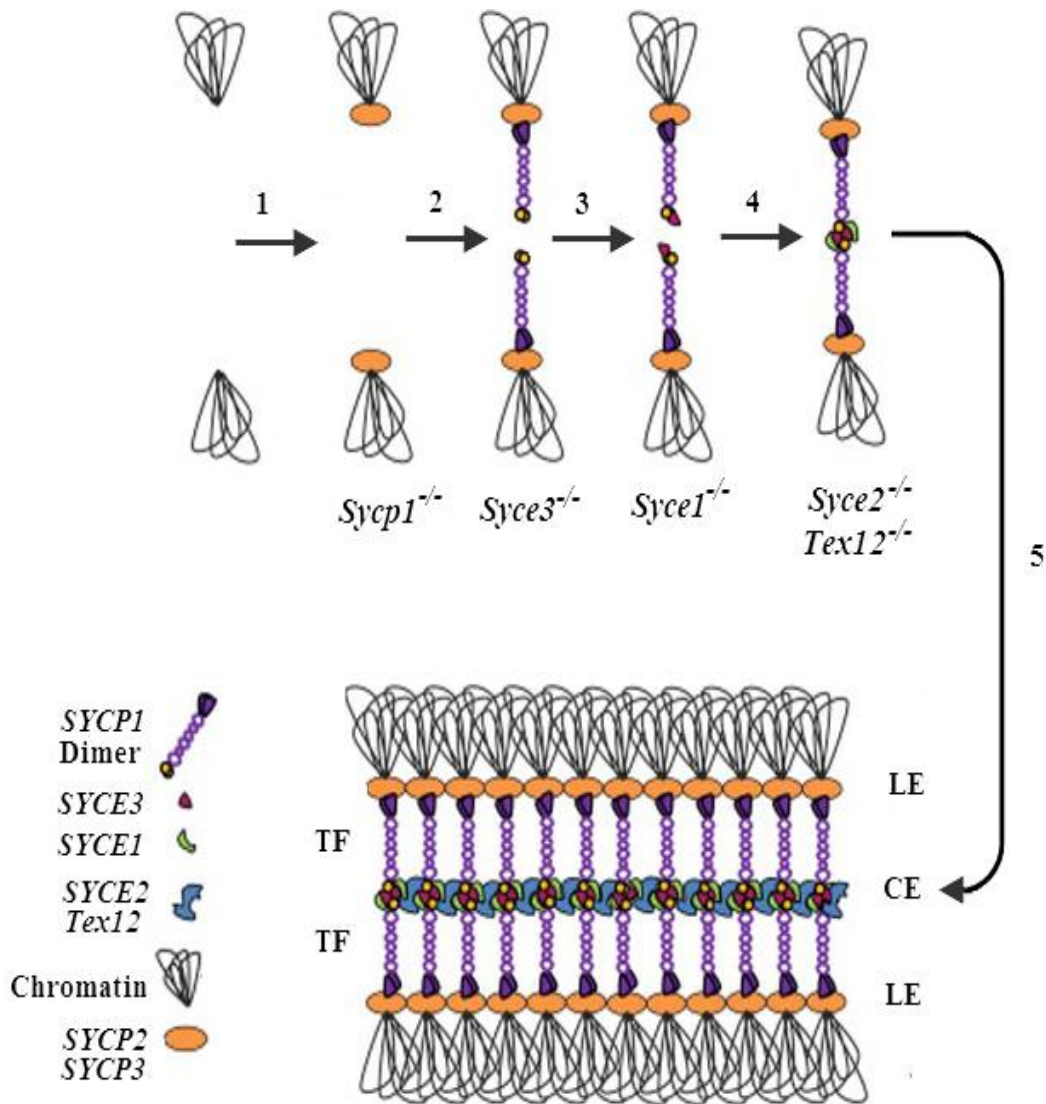
Figure 1.6 Synaptonemal complex structures. 1) The SC cannot form when SYCP1 is deleted; 2) The SC cannot form when SYCP3 is deleted; 3) The SC cannot form when SYCE1 is deleted; 4) The SC cannot form when SYCE2 and Tex12 are deleted; 5) The SC formed between two homologous containing lateral elements (LEs), transverse filament (TF) and central element (CE). Modified from (Fraune et al., 2012).

1.5.2.5 Cohesin complex

The cohesin complex plays an important role in the linking of the sister chromatids during both mitosis and meiosis (Figure 1.7). This link is initiated at S-phase and is maintained until anaphase (Gandhi et al., 2006). Chromatid cohesion defects may lead to aneuploidy and/or cancer (Barber et al., 2008; Mann et al., 2005). Moreover, mutation in cohesion genes *SMC3* and *SMC1* can lead to Cornelia de Lange syndrome and Phocomelia syndrome (Deardorff et al., 2007; 2012).

During mitosis, the cohesin complex contains four subunits: SMC1α and SMC3, which are related to a family of proteins termed structural maintenance chromosomes (SMC), and another two subunits not related to this family, called SCC1 (Rad21) and SCC3 (Mehta et al., 2012). In vertebrate, SCC3 has two related homologs known as stromalin antigens 1 and 2 (SA1 and SA2) (Mehta et al., 2012). In meiosis SMC1α can be replaced with SMC1β (Revenkova et al., 2004), while SA1 and SA2 can be replaced with STAG3 (Pezzi et al., 2000). In meiosis, SCC1 can also be replaced by REC8 (Revenkova and Jessberger, 2006) and recently an additional mammalian meiosis-specific SSC1/REC8 paralogue has been identified, Rad21-like protein (Rad21L) (Gutiérrez-Caballero et al., 2011).

Another recent study, reported three distinct meiotic cohesin complexes, one containing REC8 and another containing Rad21L and the last one containing Rad21^{Scc1} (Uhlmann, 2011). The one contain Rad21L is propose to act as a basis for lateral-element formation for the SC, but only Rad21L recruits SYCP1. Once recombination is complete, Rad21L is phosphorylated and then dissociates from chromosomes, helping consequent synaptonemal-complex disassembly. Then the meiotic cohesin complexes containing Rad21^{Scc1} is recruited to chromosomes (Figure 1.8) (Uhlmann, 2011).

In mitosis all cohesin complex is removed from sister chromatids starting in prophase by arm cohesin removal, and completed in metaphase (Nasmyth, 2011). The mechanistic triggers for cohesion arm removal during prophase are complex and not fully characterised. However, there are three possibilities. The first is as a result of chromosome condensation. The second is because sister chromatid resolution can favour the directionality of the topoisomerase-driven events. The third is that the cohesin is removed without cleaving any of the cohesin subunit, causing the subsequent destruction of the cohesin by separase. In addition, removing the cohesin arms during prophase might

depend on two mitotic kinases: polo-like kinase 1, which consists of phosphorylate Scc1/Rad21 and SA1/SA2 are subunits of cohesion, and Aurora B kinase associates with this. The centromeric/pericentromeric cohesin are protected of the prophase pathway by Sgo1. Then, during the metaphase to anaphase, this cohesion is disrupted by cleavage of Scc1/Rad21 by separase (Mehta et al., 2012).

In meiosis, the removal of cohesin complex is achieved in two steps, the first step by cleavage of REC8 subunit by separase from the arm cohesion during metaphase I to anaphase I, while the centromeric and pericentromeric cohesion is protected until removal during metaphase II to anaphase II by separase, as a second step which allows the sister chromatids to separate to the opposite pole (Mehta et al., 2012).
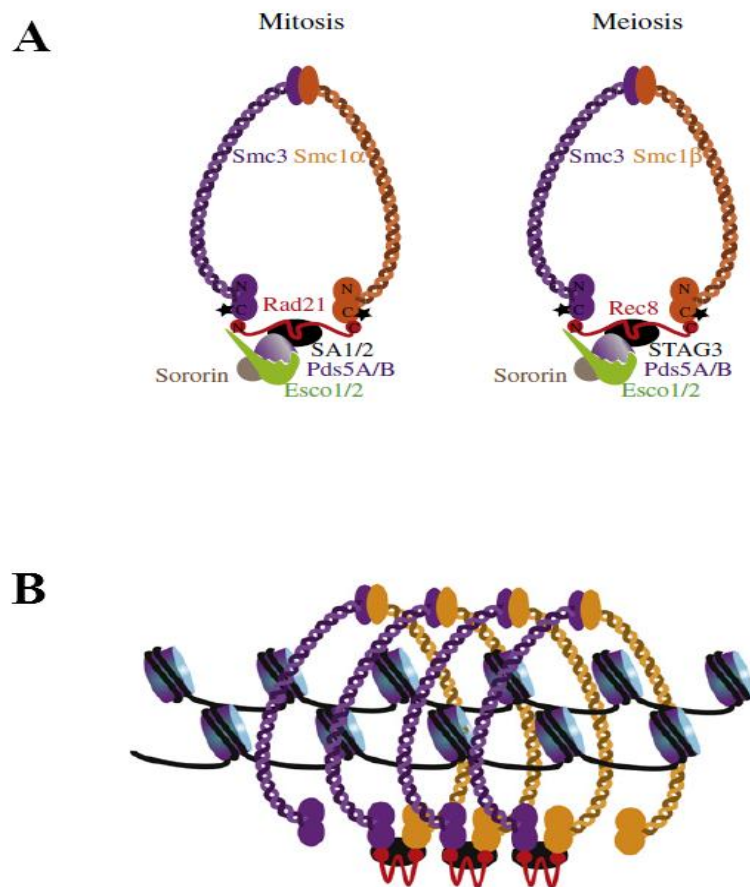
Figure 1.7. Cohesin complex structure. (**A**) The cohesin complex structure in meiosis and mitosis; (**B**) The cohesin complex holds sister chromatids together. Modified from (Mehta et al., 2012).
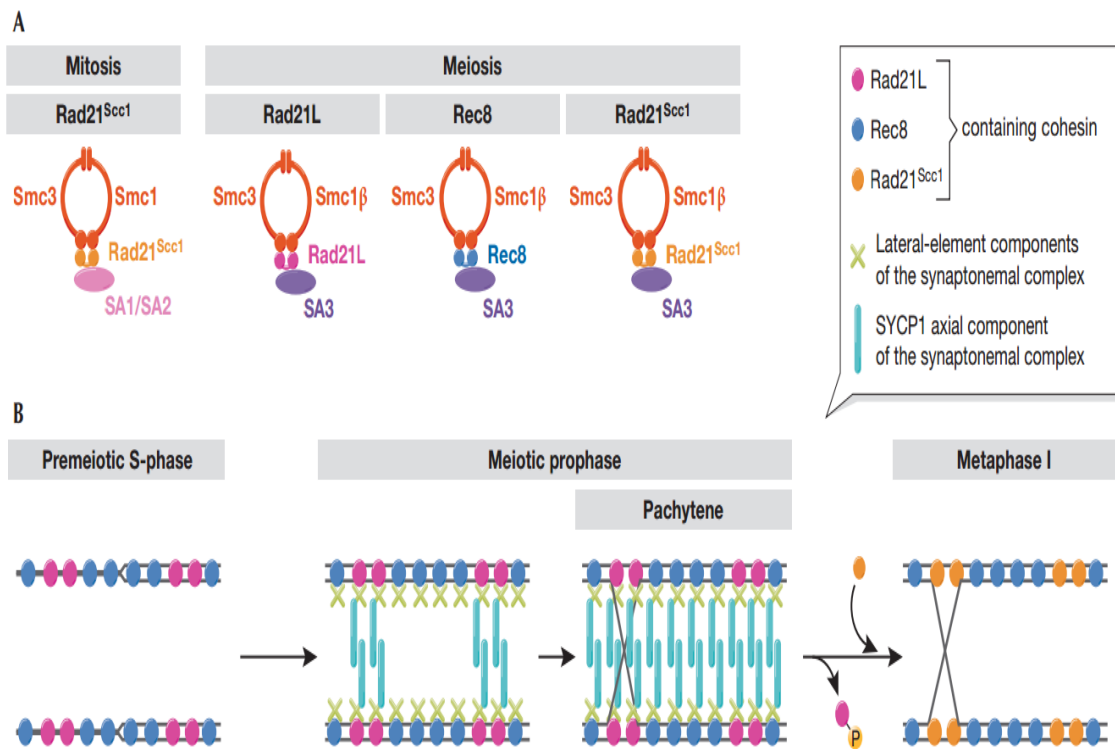
Figure 1.8. Rad21L, a new cohesin subunit with unprecedented features. (**A**) Cohesin structure of mitosis and three main cohesin meiotic complexes. (**B**) Model for the localization of cohesin complexes during meiosis. Rec8 and Rad21L cohesin complexes establish sister chromatid cohesion during premeiotic S-phase and act as a basis for lateral-element formation for SC, but only Rad21L recruits SYCP1. Once recombination is complete, Rad21L is phosphorylated and then dissociates from chromosomes, facilitating subsequent synaptonemal-complex disassembly. Rad21[Scc1] containing cohesin is then recruited to chromosomes (Uhlmann, 2011).

Table 1.1 Comparison between different phases of mitosis and meiosis cell division

	Mitosis	Meiosis
Number of segregation events	One	Two
Location	All dividing somatic cells and germ line cells prior to the formation of primary oocytes or spermatocytes	The two divisions in gametogenesis
DSB	Mostly not programmed, arising as result of exogenous factors, such as UV and chemicals.	Programmed, arising by endogenous factors (SPO11)
Synaptonemal complex	Not assembled	Assembled
Cohesin complex	Consists of SMC1α, SMC3, SCC1, and SCC3	Consists of a condination of cohesion proteins including, SMC1β , SMC3, STAG3, REC8 and RAD21L
Inter homologus crossover	Very uncommon	Common at different locations on the homologous chromosomes
Outcome	Two identical daughter cells; each has diploid chromosomes	Four haploid gamete cells

1.6 Cancer testis antigens (CTAs)

In 1991, Van der Bruggen and his colleagues successfully identified the first CTA genes; they were cloned from cells of a patient who had melanoma, and were called the melanoma antigen family (*MAGE*) (Van der Bruggen et al., 1991). The CTAs represent an important family of tumour-associated antigens (TAAs) (van Duin et al., 2011). According to the CTA database, 136 CTA families have been identified, including 253 supposed CTAs, about half of which are encoded by genes located on the X chromosome (van Duin et al., 2011).

CTAs are proteins normally found in male germ cells; they are not found normally in adult somatic cells outside the testes. In some cases, these antigens also can be found in the ovaries and trophoblasts. In addition, CTAs are found in different types of cancer. The expression of CTA genes in cancer cells can lead to abnormal chromosome segregation, which causes chromosome rearrangement (Simpson et al., 2005). Thus, CTAs have the potential to be used as cancer biomarkers for early diagnosis that can lead to a better prognosis (van Duin et al., 2011). Moreover, these antigens are promising for cancer immunotherapy and vaccination and may also serve as drug targets (discussed in 1.6.6).

1.6.1 Classification of CTAs

CTAs are divided into two broad classes, depending on the chromosomal location of their genes. The first class is CT-X antigens. Their genes are located on the X chromosome, and about 10% of all X chromosome genes are CTA genes (Ross et al., 2005). According to the CTA database (Almeida et al., 2009), about 50% of CTA genes are located on the X chromosome. The CT-X antigens genes, such as *NY-ESO-1*, are normally expressed in spermatogonia (Jungbluth et al., 2001). In addition, some CT-X antigens, such as *MAGE-1* and *MAGE-4*, have been identified in spermatogonia and primary spermatocytes (Takahashi et al., 1995). The second class is the non-X CT antigens, that are autosomally encoded. The non-X CT antigen genes, such as *SCP1*, are expressed in spermatocytes (Türeci et al., 1998). However, there are some non-X CT antigen genes, such as *TDRD1* and *TEX15*, that are expressed in germ line spermatogonia (Loriot et al., 2003).

CTAs are also divided into three classes based on gene expression across normal tissue (de Carvalho et al., 2012). The first class is testis-restricted, in which expression is restricted

to the adult testis and placenta. Testis/brain-restricted, another class of CTA genes, has expression restricted to the adult testis and all, or some of the central nervous system tissues. The third class is testis-selective, which are expressed in the adult testis/placenta and a small number of any other selective normal tissues (de Carvalho et al., 2012).

1.6.2   Identification of CTAs

There are different strategies for identifying CTAs. Cytolytic T lymphocyte (CTLs) was the first strategy used to identify CTAs. Van der Bruggen et al. (1991) identified MAGE-1 by using $CD8^+$ (T-cells) from patient-derived malignant melanoma samples.

Later, the serological analysis of cDNA expression libraries (SEREX) was established as another strategy for identifying CTAs. This method uses diluted serum from cancer patients to isolate/analyse expressed cDNA libraries prepared from tumours (Sahin et al., 1997). Many CTAs have been identified using this technique, such as New York oesophageal squamous cell carcinoma 1 (*NY-ESO-1*) (Chen et al., 1997) and synaptonemal complex protein 1 (*SCP1*) (Türeci et al., 1998).

Database mining is another strategy for identifying CTAs. *ADAM* was identified as metallopeptidase domain 2 (*ADAM2*), P antigen family, member 5 (prostate associated) (*PAGE5*), and lipase member I (*LIPI*), were all identified by using the database mining strategy (Scanlan et al., 2002). Chen et al. (2005a) identified cancer/testis antigen family 45 (*CT45*) with another strategy, massively parallel signature sequencing (MPSS). MPSS is a technique that can detect all mRNA species expressed in the cell line of a tissue sample (Chen et al., 2005a)

1.6.3   Function of CTAs

Functions of most CTAs are poorly understood, in either the germ line or cancers. Some CTA genes have specific function during meiosis such as, SPO11 which has an important role in meiotic recombination by initiating the recombination process by cleavage of the double-strand DNA (see Section 1.5.2.3) (Paigen and Petkov, 2012). In addition, SPO11 has specific function in mediating chromosome alignment during meiotic homologous synapsis (Boateng et al., 2013). Additionally, *HORMAD1* and *HORMAD2*, which have

been reported to be CTAs, have multiple roles in the DSB process and SC formation during meiotic recombination (Wojtasz et al., 2009).

Some CTAs, such as the MAGE family, play important roles in the process of tumorigenesis (Fátima et al., 2012). Another CTA gene, *TSGA10*, encodes one of the sperm tail components, and may be associated with an organelle, such as the centrosome, which has an important role in cell division. The *TSGA10* gene also has been confirmed to significantly overexpress in brain tumours (Behnam et al., 2009). Helicase-like features catalyse the unwinding of duplex nucleic acids in an ATP-dependent manner, which is involved in nucleic acid transactions; the helicase-like features are found in two CTAs, CAGE and HAGE (Umate and Tuteja, 2011). Another CTA gene is *BRDT*, which has an ATP-independent action, suggesting a structural role for the protein in the remodelling of acetylated chromatin (Pivot-Pajot et al., 2003).

1.6.4 Epigenetics association with CTA genes expression

Epigenetic factors are those which influence the genome to alter the phenotype without changing the genotype, such as chromatin acetylation and methylation involved in tissue-specific patterns of gene expression (Godfrey et al., 2007). There are different epigenetic processes, such as DNA methylation and histone posttranslational modifications (Sun et al., 2012). DNA methylation is the most common process for epigenetic regulation of gene expression (Bird, 2007).

Histones are naturally positively charged and histone acetylation neutralises this change to reduce the association with DNA and facilitate transcription (Kouzarides, 2007). Histone acetylation is frequently observed in active promoters, with low levels spread throughout the genome (Wang et al., 2008). Histone deacetylases (HDAC) remove acetyl groups from histone tails, whilst histone acetyl transferases (HATs) add them, the combined activity of these factors regulates histone dynamics (Sun et al., 2012).

Histone hyperacetylation and histone deacetylation can negatively regulate gene expression by either downregulating or upregulating genes in cancer cells. Hyperacetylation of histone H3 and H4 has been observed to promote CTA gene expression. For example, *LAGE1, MAGEA3,* and *TRAG3*, which confirms the association between histone hyperacetylation and CTA gene expression (Yawata et al., 2010). In

addition, histone deacetylation increases the expression of *NY-ESO1* in lung cancer cells (Weiser et al., 2001).

Epigenetic processes are associated with CTA genes expression in cancer cells. One of these associations is DNA hypermethylation or hypomethylation (Smet and Loriot, 2013). For example, promoter DNA hypomethylation increases the expression of some CTA genes, such as B melanoma antigen family (*BAGE*), cancer testis antigen (*CAGE*), and melanoma antigen family A (*MAGE-A*) (De Smet and Loriot, 2010). In addition, DNA hypomethylation in CML cell lines and patients is associated with overexpression of *HAGE* (Roman-Gomez et al., 2007). However, DNA hypermethylation at the promoter region is associated with CTA gene silencing (Yawata et al., 2010).

A recent study, found specific DNA hypomethylation of CTA gene promoters in the normal testis and cancer cells but not in the healthy somatic cells (Kim et al., 2013). For instance, promoter hypomethylation is the molecular mechanism directly responsible for the high expression levels of the *HAGE* gene in CML (Roman-Gomez et al., 2007). High methylation is association with the repression of *MAGE-A1*, while demethylation results in induction of *MAGE-A1* (De Smet et al., 1999). Furthermore, demethylation is associated with derepression of *NY-ESO-1* expression in lung cancer (Hong et al., 2005).

1.6.5   Oncogenic activity association with CTA genes

Proto-oncogenes encode proteins involved in all aspects of controlling cell dynamics, including growth factors, growth-factor receptors, protein kinases, and nuclear factors regulating gene expression proteins that generate second messengers such as ERK*,* TRK*,* RAS*,* WNT*,* and MYC (Cammack et al., 2006). However, mutations in proto-oncogenes or alterations in their expression profile can change them to oncogenes (Adjei, 2001).

Many CTA genes have been demonstrated to be proto-oncogenes and/or oncogenes (Cheng et al., 2011). For instance, *Piwil2* is an oncogene and a CTA gene (Mirandola et al., 2011), because it has expression restricted to the normal testis and several human cancer including, breast, prostate, gastrointestinal, ovarian cancer (Lee et al., 2006). Piwil2 promotes cell proliferation and inhibits the apoptotic pathway (Lee et al., 2006). A recent study, reported that *Piwil2* over expression in cancer cells modulated chromatin dynamic during DNA repair (Wang et al., 2011).

1.6.6   Tumour suppressor activity of CTA genes

Tumour suppressor genes (TSGs) control and/or protect the cell from incorrect cell growth and inhibit cellular migration and metastasis (Hayslip and Montero, 2006). Inactivation or mutation in tumour suppressor genes can lead to genomic instability, which can cause tumours (Lengauer et al., 1998). The *p53* gene is a TSG that controls the cell cycle and leads to apoptosis by induction of the cyclin-dependent kinase inhibitor p21 (Kawamura et al., 2009) or cell cycle arrest when programming of the cell cycle is incorrect (Farnebo et al., 2010). Thus, inactivation of *p53* commonly leads to cancer (Junttila et al., 2010).

TSGs are negatively regulated by different types of genes. For example, *p53* is regulated by the CTA, *CAGE*, which also increases resistance to drugs, leading to limited apoptotic effects (Kim et al., 2010). In addition, expression of the CTA gene *MAGE-A* blocks the interaction between p53 and chromatin, which inhibit the function of p53 (Marcar et al., 2010). A melanoma-associated CTA gene, *PAGE5*, positively regulates antiapoptotic genes, such as metallothionein 2A and interleukin 8 genes, and also inhibits apoptotic genes, such as the dickkopf-1 (*DKK1*) gene, where *DKK1* expression was p53-independent (Nylund et al., 2012).

1.6.7   CTAs in diagnosis

A recent study evaluated the presence of CTA gene expression of all three CTA gene classes—testis-restricted, testis/brain-restricted, and testis-selective—in newly diagnosed and recurrent multiple myeloma (MM) patients (van Duin et al., 2011). Interestingly, they found *MAGEC1*, *MAGEB2*, and *SSX1* from the testis-restricted class with a high frequency of expression (71%, 47% and 30%, respectively) in newly diagnosed patients, and expression (61%, 28% and 30%, respectively) in recurrent patients. In addition, they found a high frequency of *FAM133A*, *CTNNA2*, *CAGE1*, and *MAGEC2* gene expression in the testis/brain-restricted CTA class in newly diagnosed (86.3%, 60.6%, 56.3%, and 29.1%, respectively) and recurrent (79.2%, 26.5%, 91.7, and 9.5, respectively) MM patients. From the testis-selective class, they found *SPAG9*, *CTAGE5*, *PBK*, *ZNF165*, and *JARID1B* expressed in newly diagnosed (100%, 95.6%, 94.1%, 83.1%, and 82.5%, respectively) and recurrent (99.6%, 48.5%, 86.4%, 13.6% and 33.7%, respectively) patients (van Duin et al., 2011).

Additinally, different CTAs were detected in different tissues and blood samples obtained from cancer patients. For example, expression of *MAGE*-1, *SSX*-1, *CT11*, and *HCA587* CTA genes was evaluated in 105 tissues from hepatocellular carcinoma (HCC) patients at cancer stages I and II (43 patients) and cancer stages III and IV (62 patients); the results of expression for these genes were 75.2% for *MAGE1*, 72.4% for *SSX*-1, 62.9% for *CTp11*, and 56.2% for *HCA587* (Zhao et al., 2004). In addition, the expression for at least one of these antigen genes in these tissue samples was about 93.3%, 72.4% for two genes, 46.6% for three genes, and 37.1% for four genes, indicating some degree of co-expression (Zhao et al., 2004).

Mou and colleagues (2002) evaluated the presence of MAGE-1 and MAGE-3 antigens (both of which are CTAs) in blood and tissue samples from 30 HCC patients. The results of this study indicated 63.3% were positive for at least one antigen in peripheral blood mononuclear cell (PBMC) samples and 83.3% for HCC tissue samples (Mou et al., 2002). In another study, sperm-associated antigen 9 (SPAG9), another CTA, was detected in 90% of epithelial ovarian cancer (EOC) tissues (Garg et al., 2007).

In a study of frequency of CTA gene expression in breast cancer, *MAGE-A* showed the most frequent CT expression (77/454, 17.0%), and the second rate of frequency was *CT7* (13.7%), followed by *NY-ESO-1* (11.2%) and *CT45* (10.1%). Other genes showed frequencies of less than 10%: *MAGEC2* (8.4%), *GAGE* (3.5%), *SAGE1* (2.2%), and *NXF2* (1.8%) (Chen et al., 2011).

In another recent study, MAGE-A10 was screened by using immunohistochemistry on different cancer tissues, with the following results: 38% detection in malignant melanoma, 34.9% detection in lung squamous cell carcinoma, 31.3% detection in endometrium serous adenocarcinoma, 32.2% detection in skin basalioma, 31.3% detection in urinary bladder infiltrating urothelial carcinoma, and 22.5% detection in stomach adenocarcinoma, intestinal type (Schultz-Thater et al., 2011).

1.6.8 CTAs as an adoptive immunotherapy and cancer vaccination

1.6.8.1 CTA in adoptive immunotherapy and cancer vaccination

Immunotherapy has re-emerged as a potential form of cancer therapy (Mellman et al., 2011). Identification of cancer antigens provides the ability to identify cancer-specific genes in patients for early diagnoses, as well as to develop an immunogenic vaccine targeted toward these antigens (Rosa et al., 2012).

Adoptive immunotherapy is a treatment approach in which cells with anti-tumour reactivity are administered to a tumour-bearing host to mediate the regression of established tumour (Perez et al., 2007). For instance, autologous CD4$^+$ T-cells were isolated from a 52 year-old patient with recurrent metastatic melanoma associated with the CTA NY-ESO-1. After autologous cell expansion *in vitro*, these cells responded to peptides derived from NY-ESO-1. The cells were infused into the patient, and after two months, there was no longer evidence of the disease; two years later, the patient was still disease free (Hunder et al., 2008).

Another study used three CTA antigenic peptides from each of the following CTAs: TTK protein kinase (TTK), lymphocyte antigen 6 complex locus K (LY6K), and insulin-like growth factor (IGF)-II mRNA binding protein 3 (IMP-3) that were present in more than 90% of oesophageal cancers (Yamabuki et al., 2006). Immunohistochemistry demonstrated LY6K and IMP-3 were cytoplasmic, and TTK was located in the cytoplasm and nucleus of oesophageal cancer cells (Mizukami et al., 2008). The antigenic peptides stimulated CTLs that recognised and killed oesophageal squamous cell carcinoma (ESCC) cells, endogenously expressing these antigens *in vitro* (Suda et al., 2007). Furthermore, responses to antigen-specific T-cells were seen in 80% of patients for LY6K, 70% for TTK, and 40% for IMP-3 in tumour-infiltrating lymphocytes (TIL), regional lymph node lymphocytes (RLNL), and peripheral blood lymphocytes (PBLs) obtained from HLA-A*2402 positive patients with ESCC. These antigenic peptides were approved for safety, feasibility, immunological response, and clinical effectiveness of the vaccination by measuring complete response (CR), stable disease (SD), or objective response after vaccination (Mizukami et al., 2008).

Immunogenic cancer vaccines are being developed to encourage the immune system to respond in cancer patients (Gure et al., 2002). Cancer vaccination also would be very useful to initiate protective immunity before cancer is established (Slingluff and Speiser, 2005). The majority of cancer vaccinations are antigens targeting T-cell response, such as CD4$^+$ and CD8$^+$ (Greten and Jaffee, 1999).

1.6.8.2 Combining CTA cancer adoptive immunotherapy and chemotherapy

Different cancer therapy including conventional therapy (chemotherapy and radiation therapy), molecular-targeted therapy, and immunotherapy have been combined as try to treat the cancer patients (Krishnadas et al., 2013a). For instance, Demethylating agents and histone deacetylase (HDAC) inhibitors activate essential genes for apoptotic pathways as molecular-targeted therapy; that also leads to increase in the sensitivity of the cancer cells to the antitumour agents (Natsume et al., 2008).

Using 5-aza-2'-deoxycytidine (DAC) to treat ovarian cell lines for 3- to 7 days increased the expression of some CTA genes (11/12): *MAGE-A1*, *MAGE-A3*, *MAGE-A4*, *MAGE-A6*, *MAGE-A10*, *MAGE-A12*, *NY-ESO-1*, *TAG-1*, *TAG-2a*, *TAG-2b*, and *TAG-2c*. In addition to those expression increases, increases were seen for major histocompatibility complex (MHC) class I encoded molecules which are required for antigen presentation and recognition by antigen-specific cytotoxic T cells (Adair and Hogan, 2009).

In the clinic, a patient with stage IV neuroblastoma who was treated with conventional cancer therapy including chemotherapy, radiotherapy and monoclonal antibodies. Then the patient was treated with combining DAC and a DC vaccine targeting *NY-ESO-1*, *MAGE-A1* and *MAGE-A3*; the patient had three sets of combined treatment. After a year of the first combined treatment, there was no evidence of tumour in the patient (Krishnadas et al., 2013b). This study, supports the idea of using the chemotherapy based on demethylation combined with vaccination of CTAs, increase the efficiency of antigen presentation and recognition a DC vaccine targeting CTAs.

1.7   Transcription activatorlike effectors

Transcription activator like effectors (TALEs) are obtained from the plant pathogens in the genus *Xanthomonas*; the TALEs are a family of proteins that bind to a specific DNA sequence and transcriptionally activate gene expression (Christian et al., 2010). The function of this protein-DNA binding is to modulate gene expression in the target cells making them more amenable to pathogen attack (Cermak et al., 2011). The TALEs can be combined with the nuclease domains which creates TALENs that can be used to target and knockout specific genes and gene replacements (Li et al., 2011). In addition, there is a promising future in the use of this protocol in human gene therapy; for example, to engineer genes that cause inherited disorders (Mussolino and Cathomen, 2012).

TALENs consist of many repeat regions; each repeat corresponds to a nucleotide in the target binding site; each repeat contains 33 or 34 amino acids (Mussolino and Cathomen, 2012) and the differences between the TALs is having an important polymorphism among position 12 and 13 of the 33/34, called a repeat-variable di-residue (RVD) (Zhang et al., 2011). RVDs are changeable based on the nucleotide to which the RVD is going to bind, such as NI to A, HD to C, NG to T and NN to G or A (Figure 1.9) (Cermak et al., 2011).
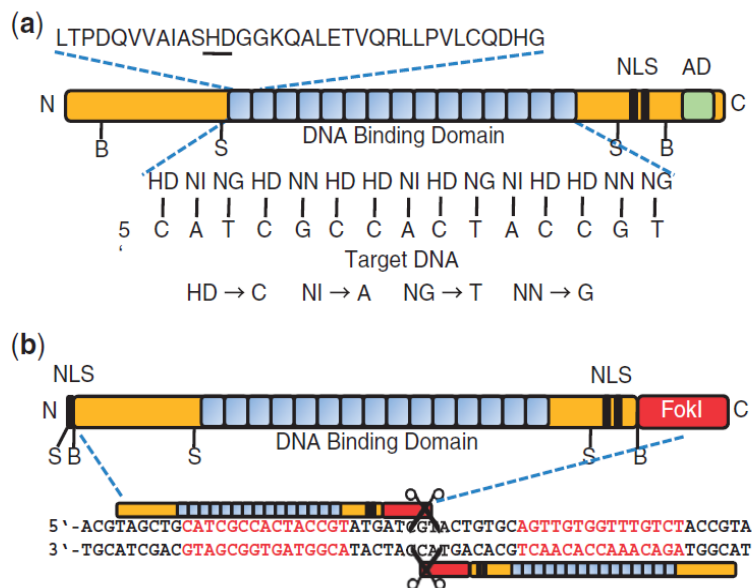
Figure 1.9. TAL effector and TALEN structure. (a) TAL effector structure, showing a consensus repeat sequence with the repeat-variable di-residue (RVD) underlined; the sequence of RVDs determines the target nucleotide sequence. (b) Structure of a TALEN with two monomeric TALENs required to bind the target nucleotide sequence to enable FokI to cleave DNA (NLS: nuclear localization signal(s); AD: transcriptional activation domain; B: BamHI; S: SphI).

28

Golden Gate cloning is used to organise the TALEN RVDs in order based on the DNA target sequence. The Golden Gate technique is a rapid cloning technique, result from a designed mixture of digestion and ligation. Cermak et al., (2011) designed Golden Gate cloning in two steps by using complete set of plasmids to organise the TALEN RVDs in order. The first step involves assembling the RVDs in order from 1 to 10 in the pFUS_A vector and the complete sequence of the RVDs from 11 to the penultimate in the pFUS_B vector. The second step is to assemble the pFUS_A, pFUS_B and pLR vector, which contain the last RVD in the pTAL1, 2, 3, or 4 vectors (Figure 1.10).
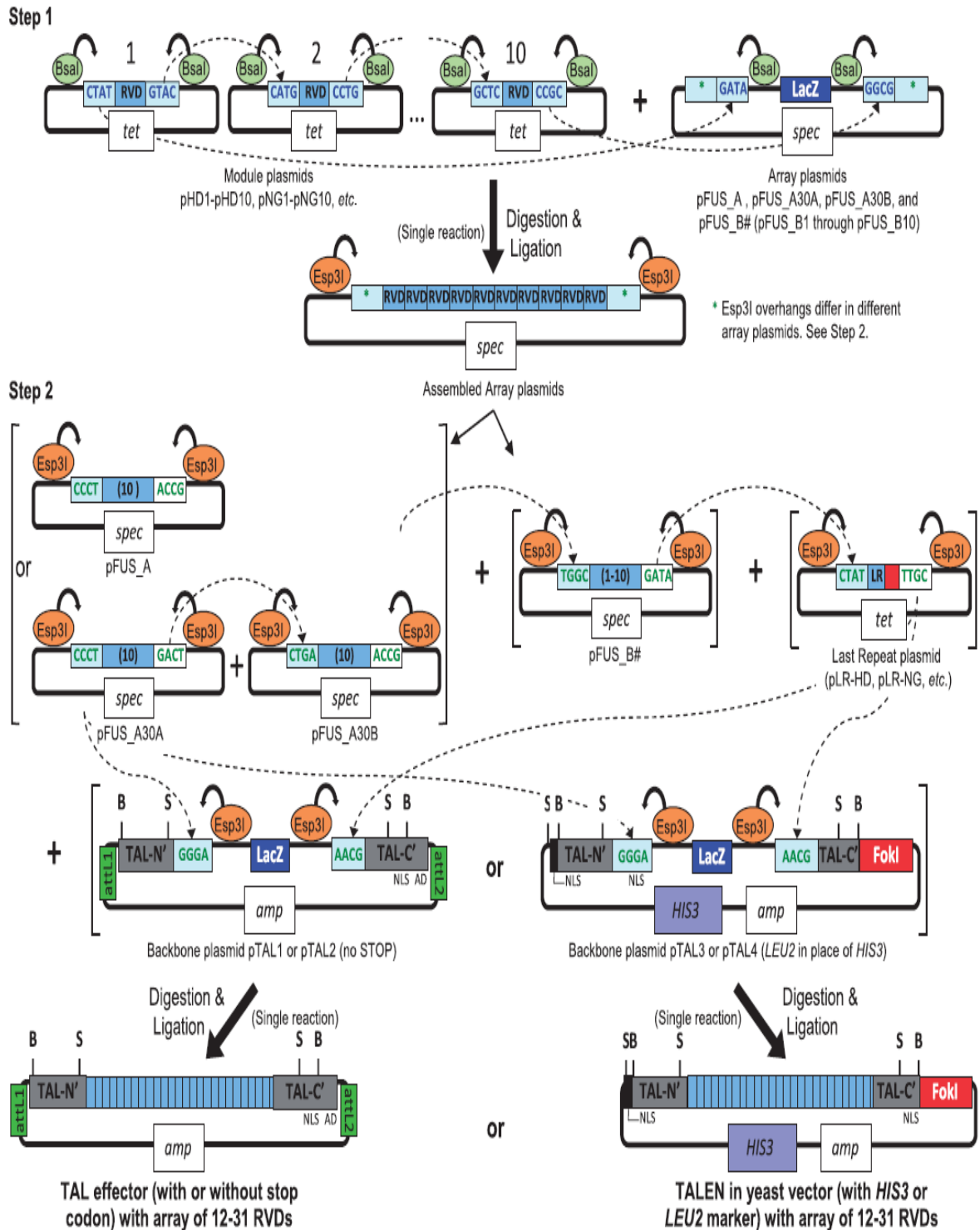
Figure 1.10. Golden Gate assembly of custom TAL effector and TALEN constructs. Step 1: assemble the repeat array in order by using mixture of ligation and digestion (using the type IIS restriction endonucleases BsaI); Step 2: place this into a backbone plasmid to create full length constructs (using the type IIS restriction endonucleases Esp3I). (NLS: nuclear localization signal[s]; AD: transcriptional activation domain; tet: tetracycline resistance; spec: spectinomycin resistance; amp: ampicillin resistance; attL1 and attL2: recombination sites for Gateway cloning; B: BamHI; S: SphI) (Cermak et al., 2011).

30

1.8 Aims and objectives

The main aims of this study was to identify novel CTA genes by manually searching the literature for human meiotic recombination regulator genes and validate the genes identified by bioinformatics as human meiotic genes, which was achieved by carrying out RT-PCR using RNA from 21 normal human tissues with normal testis tissue as positive control. The genes exhibiting a testis-restricted expression profile in normal tissues were analysed for evidence of expression in 33 cancer cells/tissues to obtain gene expression profiles for these candidate genes. Then the expression of the validated CTA candidate genes were analysed in patient-derived cancer microarray data for 13 cancer types using the CancerMA database tool. In addition, assess the levels of SPO11 and PRDM9 protein in different normal and cancerous tissues by western blot and immunohistochemistry.

SPO11 gene knockout from the cancer cells by using the transcription activator-like effector nuclease (TALENs) technique was another aim to assess whether SPO11 has a functional role in cancer cells. In addition, the effect of SPO11-siRNA and TALENs treatment on the cancer cell growth needs to be assessed.

Study the role of SPO11 by characterising the possible function for SPO11 in cancer cells by determining whether SPO11 is covalently bound to DNA. In addition, there are different genes associated with SPO11 in the meiotic cell division; thus, another aim was to assess the effects of individual knockdown of ATM, Rad50 and PRDM9 on SPO11 binding to DNA.

Study the role of PRDM9 in cancer cells was another aim by testing the localisation of PRDM9 (nuclear or cytoplasmic). In addition, the effects of *PRDM9* knockdown on the levels of K3H4-me and the association of PRDM9 with chromatin were examined. Lastly, the relationship between *PRDM9* and *Rik* human orthologue genes was to be explored.

2 Materials and methods

2.1 Source of the cell lines

The embryonal carcinoma cell line (NTERA-2 clone D1cells) was a gift from Prof. P.W. Andrews (University of Sheffield). One of the ovarian cell lines (A2780) was kindly provided by Prof. P. Workman (Cancer Research UK Centre for Cancer Therapeutics, Surrey, UK). The liver cancer cell line (HepG2) was a gift from Dr. J. Muller (University of Warwick). The other ovarian cell lines (PEO14 and TO14), breast cell lines (MCF7 and MDA-MB-453), colon cell lines (HT29, HCT116, T84, LoVo and SW480), lung cell line (H460), astrocytoma cell line (1321N1) and melanoma cell lines (G361, MM127, COLO800 and COLO857) were obtained from European Collection of Cell Cultures (ECACC).

2.2 Routine cell culture

The NTERA2, 1321N1, SW480, HepG2, A2780 and MDA-MB-453 cells were cultured in Dulbecco's Modified Eagle Medium (DMEM) with GlutaMAX (Invitrogen 61965-026) supplemented with 10% foetal bovine serum (FBS) (Invitrogen 10270098). The HT29, HCT116 and G361 cells were cultured in McCoy's 5a with GlutaMAX (Invitrogen 36600-021) supplemented with 10% FBS. The H460, COLO800 and COLO857 cells were cultured in Roswell Park Memorial Institute (RPMI) 1640 medium with GlutaMAX (Invitrogen 61870-010) supplemented with 10% FBS. The MM127 cells were cultured in RPMI 1640 medium with GlutaMAX and HEPES (Invitrogen 72400021) supplemented with 10% FBS. The TO14 and PEO14 cells were cultured in RPMI 1640 medium with GlutaMAX supplemented with 10% FBS and 2 mM sodium pyruvate. The MCF-7 cells were cultured in Minimum Essential Medium (MEM) with GlutaMAX (Invitrogen 41090-028) supplemented with 10% FBS and 1% nonessential Amino Acids (NEAA). The LoVo cells were cultured in Ham's F-12 Nutrient Mixture (F-12) with GlutaMAX (Invitrogen 31765-027) supplemented with 10% FBS. The T84 cells were cultured in DMEM/F12 (1:1) with GlutaMAX (Invitrogen 31331-028) supplemented with 10% FBS. All cell lines were cultured at 37C° in 5% CO_2 except for NTERA2, which was cultured at 37 °C in 10% CO_2.

2.3   Total RNA isolation and cDNA synthesis

For this procedure, 3 x 10^6 cells were collected at the confluent stage in 1 ml of TRIzol reagent (Invitrogen 15596-026) and then incubated for 5 mins at room temperature. A 0.2 ml volume of chloroform was added to the TRIzol, shaken vigorously for 15 secs. and incubated for 5 mins at room temperature. After centrifugation at 12,000 xg at 4°C for 15 mins, the aqueous phase was transferred to a new tube and 500 µl isopropanol was added to precipitate the RNA. After incubation for 10 mins at room temperature, the mixture was centrifuged at 4°C for 20 mins at 12,000 xg. The supernatant was removed and the pellet was collected and washed by re-suspension in 75% ethanol and centrifuged for 5 mins at 7500 xg. The pellet was then dried and re-suspended in RNase-free water containing DNase; the DNase was activated by incubation at 37°C for 10 mins and inactivated by incubation at 75°C for 10 mins. Finally, the RNA concentration was measured with a NanoDrop (ND_1000) spectrophotometer. The SuperScript III First Strand synthesis kit (Invitrogen, 18080-051) was used to synthesise cDNA from 1 µg of the total RNA (following the manufacturer's instructions).

2.4   Reverse-Transcriptase Polymerase Chain Reaction (RT-PCR)

Gene codon sequences were obtained from the National Center for Biotechnology Information (NCBI). Primers were designed for each gene codon sequence. RT-PCR was adjusted by adding ~150 ng/µl cDNA, 10 pmol/µl of each primer. Primers were designed to span at least one intron between the forward and reverse to distinguish cDNA from gDNA; the inter exonic PCR product size is significantly smaller than the equivalent gDNA. 25 µl BioMix Red (Bioline BIO-25005) was added to a final volume of 50 µl. The target sequence was amplified with initial heating at 96°C for 5 mins, followed by 40 cycles of denaturing at 96°C for 30 secs., annealing temperature (as will be described in the primer tables 2.1, 2.2 and 2.3) for 30 secs. and extension at 72°C for 40 secs., followed by a final extension step at 72°C for 5 mins. The products were run on 1% agarose gels containing ethidium bromide. The 100 bp DNA marker (NEB, N0467) was used.

Table 2.1. Primers for EST analysis

Gene	Primer direction *	Primer sequence (5' to 3')	Tm (°C)	Target size (bp)
ACTRT1	F	GGGATGACATGGAGAAACTC	58.4	591
	R	CCATTTTTGAGAGTCCTGGG		
CYLC2	F	GCCCTGTTATTTCCCAAACC	58.4	680
	R	GCATCCTTCGATTCATCACC		
C20orf79	F	CAGTTCGAGGTTCTGGGTTC	60.5	369
	R	GCTAAGCAGAACCTTGCCAC		
CCDC38	F	GCTGTCCTTTCAGAAGATGC	58.4	652
	R	GCCGCCATTCTTTCTGTTTC		
MBD3L1	F	CTGGCTTGAGCACCTCAATC	58.4	343
	R	GCAGGAATTATCTCCACCGC		
CCDC79	F	CTGCCACATTGTGCTTCAC	58.4	686
	R	CATTTCGGAACAACTGGGAG		
C22orf33	F	GATCCTCCTCGAGAGAGAAC	60.5	426
	R	GCCAGTGTTCTAAGTCCCTC		
SUN3	F	GAAGACCAAGTCGAGATGGC	60.5	481
	R	GGTGTCCCCAGTTGCTAAAG		
C1orf65	F	CGGATCAGAAGGTCCAGATG	60.5	637
	R	CGCATCTTCCTCTGTTCCTC		
LUZP4	F	GGAATCGCCTTCAAGACAGC	60.5	547
	R	CACAAGATCTCCCTGGCTAC		
C4orf51	F	CAGGATGAAACACGATGGTC	58.4	430
	R	CCTTGCTTTCAGAATCGCAC		

Gene		Sequence	Tm (°C)	Size (bp)
GLT6D1	F	GCTCTCAGACTGGTTTCATC	58.4	580
	R	GAAATCTCCCTGTCCAAACG		
IQCF5	F	CATGACAGAAGGTCTGCAG	58.4	281
	R	GCCAATAGACCTGGATGATG		
CCDC18	F	GATTGAGCTTACTGGCACTG	58.4	539
	R	CTCTGTGCTCACGAATAGTC		
CALM2	F	GACTGAAGAGCAGATTGCAG	60.5	316
	R	CATCACATGGCGAAGTTCTG		
TDRD1	F	CTTTCAGGGAATACGGTGCC	58.4	673
	R	CAGGTGGCTAGAGGTGATTG		
PTPN20B	F	CAGACAGCCATCAAGGATTG	58.4	685
	R	CATCCACACATAGGAACACC		
C12orf42	F	CATAGTCCCCAGGTGTTCTG	60.5	508
	R	GCCTTTTCCGACGGGATTTC		
CATSPER3	F	CTCATGGGCAAACAGTTCAC	58.4	570
	R	CAGCTCACTGAAACTTGTGC		
C19orf67	F	GAGACCAAGTACAGAAGGAG	58.4	562
	R	GAATAAAGGTCATCCTCGGC		
C11orf91	F	CTATTTCCCGTCCCTGTACG	60.5	461
	R	CGTCTTTTAGCGCCTTCAGG		
PAX5	F	GATCCAAACCAAAGGTCGCC	60.5	588
	R	GATTGGCCTTCATGTCGTCC		

* F: forward; R: reverse

Table 2.2 Primers for analysis of microarray genes

Gene	Primer direction *	Primer sequence (5' to 3')	Tm (°C)	Target size (bp)
NUT	F	CACCACCAGTTGCTCAACTG	60.5	632
	R	CTCCTTCACAGCTTCTGGTG		
C10orf82	F	GAGAAACCTGCCAATCACAC	58.4	365
	R	CCATGACAGTGTATCTCGTG		
CCDC146	F	GCAGCTTCGCAAAGATACG	58.4	624
	R	GCTTGTTTCATGGACAGCTC		
TUBA1B	F	GCCAAGTGACAAGACCATTG	58.4	630
	R	CCATCAAATCTCAGGGAAGC		
GPAT2	F	GATACTGTTGCGTGGCTTTG	58.4	490
	R	CTTTCTGCTCAATCGCTGTC		
C10orf82	F	GAGAAACCTGCCAATCACAC	58.4	365
	R	CCATGACAGTGTATCTCGTG		
STK31	F	CTGCAAAGAGCTGGAGATAG	58.4	618
	R	GCTTCTGTGTCAACATCCAC		
STAG3	F	CAGTGGAGGCTGTCAGATTAC	60.5	591
	R	GAGTGACCTTCTCTGCATCAG		
PVRIG	F	GTGCTGCTGACCTTGTGTGTC	57	491
	R	CGCAGCAGATGAAGGAGGTAG		
C7orf31	F	CAATTGAACACCCCTACCAC	58.4	646
	R	GTACAATCTGGACAGGAACG		

* F: forward; R: reverse

Table 2.3 Primers for analysis of recombination genes

Gene	Primer direction *	Primer sequence (5' to 3')	Tm (°C)	Target size (bp)
PRDM9	F	CAGGCTCAGAAACCAGTGTC	60	655
	R	GTTCCTGGCCGTATTCATCC		
SYCP1	F	CAGCAGGAGAATAAGGCCTTG	61	675
	R	GGCAGATGTCCACAGATAGTC		
SYCP3	F	GGGTGAAGTGCAGAATATGCTG	57	467
	R	CTTGCTGCTGAGTTTCCATC		
HORMAD1	F	GCCCAGGATCTACACAGTTAG	60.5	486
	R	CCATTCGTTCTCTCTCAGTGG		
HORMAD2	F	GAGAGCTCTTATGGAGAACGC	60.5	707
	R	CTGGAGCACTCAGAACTTTGC		
SYCE1	F	CTGCTCAAGGAAGAGAAGCTG	60.5	318
	R	CTCTTCCTCTTGTGTGCTCTG		
SYCE2	F	CTTCTCCTCTCTGGACTCAAG	60.5	339
	R	CATCTGAGTCTTAGGCTCTGC		
REC8	F	GTTGGTGAAGCGCGAATACC	60.5	444
	R	GGAACTTCAGGAGGGATCTC		
TEX12	F	CCACAGCTGTCCTCTCTTGG	63	258
	R	CCTCTGTCGCAGGAACTCTC		
SYCP2	F	CTTGGGAGACCTGGCAAAATG	60.5	354
	R	GATGAAGCCTCTGTTGTTCGC		
STAG3	In Table 2.2			

* F: forward; R: reverse

2.5 Total protein extraction from cell lines

Whole cells were lysed in lysis buffer [50 mM Tris-HCl pH 7.4, 200 mM sodium chloride, 0.5% Triton X-100, 1 mM AEBSF (4-(2-aminoethyl) benzenesulfonyl fluoride (Sigma A8456) with one complete mini, EDTA-free protease inhibitor cocktail tablet/10 ml (Roche 11836170001)]. Total protein concentration was measured using the Pierce ® BCA Protein Assay Kit (Thermo Scientific, 23227) following the manufacturer's instructions. An equal volume of sample buffer, Laemmli 2× Concentrate (Sigma S3401), was added to the cell lysate. The lysate was then boiled at 100°C for 5 mins.

2.6 Extraction of cytoplasmic and nuclear protein fractions from cell lines

The cells were lysed in hypotonic buffer (50 mM Tris-HCl pH 7.4, 0.1 M sucrose, 1 mM AEBSF with one complete mini, EDTA-free protease inhibitor cocktail tablet/10 ml) and an equal volume of lysis buffer C (1% triton, 10 mM magnesium chloride, 1 mM AEBSF with one complete mini, EDTA-free protease inhibitor cocktail tablet/10 ml) were added. The lysed cells were incubated on ice for 30 mins and then centrifuged at 6000 xg for 2 mins. The supernatant, which contained the cytoplasm, was transferred to a new tube. The pellet, which contained the nucleus, was resuspended in lysis buffer N (50 mM Tris-HCl pH 7.4, 100 mM potassium acetate (KAc), 1 mM AEBSF with one complete mini, EDTA-free protease inhibitor cocktail tablet/10 ml). The protein concentration was measured for both cytoplasmic and nuclear fractions using the Pierce ® BCA Protein Assay Kit. An equal volume of sample buffer, Laemmli 2× Concentrate, was added to the cytoplasmic and nuclear extracts. The lysates were then boiled at 100°C for 5 mins.

2.7 Western blotting

A 25 µg sample of the protein for each extract was loaded into a Novex® 4-12% Tris-Glycine Mini Gel 1.0 mm (Invitrogen, EC60352BOX). In addition, the protein marker (Bio-Rad, 161-0374) was used. The gel was run in 1X MOPS SDS Running Buffer (Invitrogen, NP0001) for 2 hrs at 100 volts. The proteins were transferred to an Immobilon-P PVDF membrane (Millipore, IPVH00010) which was activated by wetting the PVDF membrane in methanol. The transfer was completed in 1x transfer buffer (380 mM glycine, 50 mM Tris) at 400 mA for 4 hrs. The membrane was washed several time in

dH$_2$O and then it was blocked in 5% skimmed milk powder in PBS/Tween 20 (0.3% w/v) (milk solution) for one hour at room temperature. The primary antibody was diluted in milk solution (Table 2.4) and incubated with the membrane overnight at 4°C. The membrane was then washed for 10 mins twice with milk solution. The membrane was then incubated in secondary antibody diluted in milk solution (Table 2.5) for one hour at room temperature. The membrane was washed twice for 10 min in milk solution and twice for 10 mins in PBS/Tween 20 (0.3% w/v). Super Signal West Pico Chemiluminescent ECL substrate (Pierce, 34080) was then used to detect the protein after exposure to CL-XPosure Film (Thermo Scientific, 34088).

Table 2.4 Primary antibodies

Ab. against	Cat.No.	Source	Host	Clonality	W.B. dilution	IHC dilution
α-Tubulin	T 6072	Sigma	Mouse	Monoclonal	1/6000	-
Lamin B	Sc-6217	Santa Cruz	Goat	Polyclonal	1/1000	-
GAPDH	Sc-365062	Santa Cruz	Mouse	Monoclonal	1/1000	-
SPO11	H00023626-A01	Abnova	Mouse	Polyclonal	1/500	1/50
PRDM9	Ab85654	Abcam	Rabbit	Polyclonal	1/1000	1/50
ATM	Ab2629	Abcam	Goat	Polyclonal	1/3000	-
MAGEC1	Ab61404	Abcam	Mouse	Monoclonal	1/500	-
H3K4-3me	Ab8580	Abcam	Rabbit	Polyclonal	1/1000	-
Rad50	Ab89	Abcam	Mouse	Monoclonal	1/1000	-

Table 2.5 Secondary antibodies

Antibody	Cat.No.	Source	Conjugate	W.B. dilution
Donkey anti-rabbit	711-035-152	Jackson Immunoresearch	HRP	1/40000
Donkey anti-mouse	711-035-150	Jackson Immunoresearch	HRP	1/40000
Rabbit anti-goat	A5420	Sigma	HRP	1/40000

2.8 Immunohistochemistry

Adapted from (Kim et al., 2011a)

Paraffin sections were cut to 4 µm and placed onto slides. The sections then de-paraffinised by incubation at 70°C for 20 mins. Staining was performed using a Leica Bond Max automated immunostainer. Antigen retrieval was performed by heat induced epitope retrieval (HIER) for 20 mins [Bond Epitope Retrieval solution 1 (Leica AR9961), which is low pH, was used for anti-SPO11 antibody (Abnova H00023626-A01) and Bond Epitope Retrieval solution 2 (Leica AR9640), which is high pH, was used for anti-PRDM9 antibody (Abcam ab85654)].

The slides were washed and then incubated for 1 hour at room temperature with primary antibodies diluted in antibody diluent with Background Reducing Components (Dako S3022). After washing the slides, post primary AP (Polymer Refine Red Detection Kit, Leica DS9390) was applied for 30 mins. The slides were washed and then incubated for 30 mins with polymer AP (Polymer Refine Red Detection Kit, Leica DS9390). Substrate Chromogen was applied by incubating the slides with Mixed Red Refine for 15 mins (Polymer Refine Red Detection Kit, Leica DS9390). The slides were washed and incubated with hematoxylin for 5 mins. Finally, the slides were washed, dehydrated, cleared with xylene and mounted with a coverslip.

2.9 Gene knockdown using siRNA

The required cells were seeded (1.5x105) into each well of 6 well plates (each well contain 2 ml of fresh appropriate medium) and then incubated at 37°C. A transfection mix for the first hit of siRNA was prepared for each well by adding 600 pmol siRNA (Table 2.6) to 100 µl of medium serum free medium containing 6 µl of Hiperfect Transfection Reagent (Qiagen 301705); this siRNA mixture was incubated at room temperature for 30 mins. In addition, a non-interference mixture was prepared for use as a negative control by using Negative Control siRNA (Qiagen 1022076) and preparing this in the same way as the siRNA mixture preparation. The siRNA mixture and the negative control were added to the cells in the 6 well plates. Untreated cells were prepared as controls at the same time of transfection. After 48 hrs, the media were refreshed and the second hit of the transfection was applied in the same way as the first hit. After 24 hrs from the second hit, the cells were harvested and prepared for western blotting (see western blotting methods, Section 2.7). All samples from untreated cells, non–interference controls, and the cells treated with siRNA were loaded in equal concentrations onto the western blot gel.

For SPO11 knockdown, also the required cells were seeded (8 x10^4) into each well of 6 well plates (each well contain 2 ml of fresh appropriate medium) and then incubated at 37°C. The second day a transfection mix for the first hit of was prepared for each well by adding 500 pmol on target plus smart pool SPO11 (Thermo Scientific CatNo. L-020043-0-0005) to 190 µl of medium serum free medium containing 4 µl of DarmaFECT4 Transfection Reagent (Thermo Scientific Cat No. T-2004-01); this siRNA mixture was incubated at room temperature for 30 mins. In addition, a non-interference mixture was prepared for use as a negative control by using on target plus non-targeting (Thermo Scientific Cat No. D-001830-10-05) and preparing this in the same way as the on target plus smart pool SPO11 mixture preparation. The on target plus smart pool SPO11 mixture and the negative control were added to the cells in the 6 well plates. Untreated cells were prepared as controls at the same time of transfection. After 48 hrs, the media were refreshed and the second hit of the transfection was applied in the same way as the first hit. After 24 hrs from the second hit, the cells were harvested and prepared for western blotting.

Table 2.6 siRNAs

Gene target	Product name	Catalogue No.	Target sequance (5' to 3')	Stock conc.
Negative control	Negative Control siRNA	1022076	AATTCTCCGAACGTGTCACGT	5 nMol
SPO11	Hs_SPO11_1 FlexiTube siRNA	SI00100366	CAGAGTGTACTTACCTAACAA	1 nMol
SPO11	Hs_SPO11_2 FlexiTube siRNA	SI00100373	ACAACTAATGTTAACGCATAA	1 nMol
SPO11	Hs_SPO11_4 FlexiTube siRNA	SI00100387	TACCTTCTACGATACAACTAA	1 nMol
PRDM9	Hs_PRDM9_7 FlexiTube siRNA	SI04299890	CCACACAGCCGTAATGACAAA	1 nMol
RAD50	Hs_RAD50_4 FlexiTube siRNA	SI00080717	CTGGCTACATAGTAAATCAAA	1 nMol
RAD50	Hs_RAD50_3 FlexiTube siRNA	SI00080710	CTGCGACTTGCTCCAGATAAA	1 nMol
ATM	Hs_ATM_5 FlexiTube siRNA	SI00299299	AAGGCTATTCAGTGTGCGAGA	1 nMol

2.10 Applying the TALEN technique to disrupt the *SPO11* gene

Adapted from (Cermak et al., 2011).

The *SPO11* gene has two different isoforms; the difference between the two isoforms is that Exon 2 found in isoform a is missing in isoform b. A TALEN was designed to Exon 3.

This is a two-step process. The first step was the TALEN itself and the second step was the recombinant insert that contained two arms; we called one the 5' end arm which was located before the TALEN sequence and the other was called the 3' arm, which was located after the TALEN sequence. These two arms were cloned into the bML3 (neoR) vector.

The TALEN step was started by selecting the TALEN repeat variable di-residue RVD sequences based on the target sequence in Exon 3, using the TAL Effector Nucleotide Targeter 2.0 on the Cornell University website:

(https://boglab.plp.iastate.edu/node/add/talen last accessed in 2/2012) (Table 2.7).

2.7 TALEN target and the RVDs sequence

TALEN target	Forward								Space				Reverse					
	5' CTTCAGATGGTATCCCAT TGCACCACCAGAAAG ATCAAAAGTGATTCACC 3'																	
	The forward sequence																	
F*	C	T	T	C	A	G	A	T	G	G	T	A	T	C	C	C	A	T
TAL1	pHD1	pNG2	pNG3	pHD4	pNI5	pNN6	pNI7	pNG8	pNN9	pNN10	pNG1	pNI2	pNG3	pHD4	pHD5	pHD6	pNI7	pLR-NG
	The reverse sequence																	
F*	A	T	C	A	A	A	A	G	T	G	A	T	T	C	A	C		C
R*	G	G	T	G	A	A	T	C	A	C	T	T	T	T	G	A		T
TAL2	pNN1	pNN2	pNG3	pNN4	pNI5	pNI6	pNG7	pHD8	pNI9	pHD10	pNG1	pNG2	pNG3	pNG4	pNN5	pNI6		pLR-NG

* F: Forward; R: Reverse

Using the Golden Gate TALEN and TAL Effector Kit (Addgene, Cat# 1000000016), 150 ng of each RVD from 1−10 was cloned into vector pFUS_A (150 ng) while 150 ng of each RVD from 11−17 in the TAL1 (forward) (RVDs 1−7 were used for this) was cloned into vector pFUS_B (150 ng). The same procedure was used for TAL2 (reverse) and then 10 units of *BsaI* (NEB, Cat#R0535), 400 cohesive end units of T4 DNA Ligase, 2 µl of 10x T4 DNA Ligase Reaction Buffer in a final volume of 20 µl, made up with sterile dH$_2$O. The thermocycler was used to incubate the RVD reactions at 37°C for 5 mins, 16°C for 10 mins 10 cycles, 50°C for 5 mins and 80°C for 5 mins. A 1 µl volume of 10 mM ATP (NEB, Cat#9804) and 10 units of Plasmid-Safe™ ATP-Dependent DNase (Epicentre® Biotechnologies Cat# E3101K) were added to each tube and then incubated at 37°C for 1 hour.

A 5 µl sample of the product was transformed into 50 µl of 5-alpha Competent *E. coli* (High Efficiency) (NEB, Cat# C2987), which were then incubated on ice for 30 mins followed by heat shock at 42°C for 30 secs and then incubated on ice for 5 mins; 950 µl of SOC Outgrowth Medium (NEB, Cat# B9020) was added to the transformed Competent *E. coli* cells and incubated for 1 hour at 37°C. The cells were plated onto Luria-Bertani agar medium (LB-agar) containing 50 µg/ml spectinomycin, with isopropylthio-β-galactoside (IPTG) and 5-bromo-4-chloro-indolyl-β-D-galactopyranoside (X-gal) for screening the clones as blue and white clones. The plates were incubated for 24 hrs at 37°C.

Three white clones were screened by diluting the clones in 20 µl of sterile dH$_2$O and then 2 µl of this solution was mixed with 10 pmol/µl of each primer TAL_F1 (5' TTGATGCCTGGCAGTTCCCT 3') and TAL_R2 (5' CGAACCGAACAGGCTTATGT 3') and 25 µl BioMix Red in a final volume of 50 µl. The target sequence was amplified by initial heating at 96°C for 5 mins, followed by 35 cycles of denaturing at 96°C for 30 secs, annealing temperature at 55°C for 30 secs and extension at 72°C for 85 secs, followed by a final extension step at 72°C for 5 mins. The correct clones showed a clear band at about 1000 bp, smearing and a faint band starting at 200 bp. The correct clones were grown overnight in LB medium containing 50 µg/ml spectinomycin. Minipreps were prepared for the plasmids pFUS_A, pFUS_B for TAL1 and pFUS_A, pFUS_B for TAL2.

The pFUS_A, pFUS_B for TAL1 was cloned into pTAL4 vector by adding 150 ng of each pFUS_A, pFUS_B for TAL1, 150 ng of pLR-NG vector (the last RVD in Table 2.7), 75 ng of pTAL4, 10 µl of Esp3l (FISHER Cat# FERER0452), 400 cohesive end units of T4 DNA Ligase, 2 µl of 10x T4 DNA Ligase Reaction Buffer and finally the volume was

completed with dH$_2$O to 20 µl. The pFUS_A, pFUS_B for TAL2 was cloned into pTAL4 vector in the same manner as described for TAL1. The reaction mix was incubated at 37°C for 10 mins, followed by incubation at 16°C for 15 mins then it was incubated at 37°C for 15 mins, followed by final incubation 80°C for 5 mins. A 950 µl volume of SOC Medium was added to the transformed competent *E. coli* cells and incubated for 1 hour at 37°C. The cells were plated onto LB- agar media containing 50 µg/ml ampicillin with IPTG and X-gal; the plates were incubated for 24 hour at 37°C.

White clones were picked and screened by diluting the clone in 20 µl of sterile dH$_2$O; 2 µl of this dilution was mixed with 10 pmol/µl of each forward (5' TTGGCGTCGGCAAACAGTGG 3') and reverse (5' GGCGACGAGGTGGTCGTTGG 3') primer and 25 µl BioMix Red in a final volume 50 µl. The target sequence was amplified with initial heating at 96°C for 5 mins, followed by 35 cycles of denaturing at 96°C for 30 secs, annealing temperature at 55°C for 30 secs and extension at 72°C for 85 secs, followed by a final extension step at 72°C for 5 mins. The correct clones had a clear band at about 2000 bp and smears above and below that band. The correct clones were grown overnight in LB media containing 50 µg/ml ampicillin. Minipreps were made of the plasmids TAL1 in pTAL4 and TAL2 in pTAL4 and these were checked by sequencing using seq TALEN 5.1 (5' CATCGCGCAATGCACTGAC 3') forward primer and TAL-R2.

The pTAL4 containing TAL1 and TAL2 individually were cloned into pcDNA3.1 (-). This clone was achieved by digesting pcDNA3.1(-) and TAL1 in pTAL4 vectors, which contained TAL1 and TAL2, with 20 units *XhoI* (NEB Cat# R0146) and 20 units of *Afl*II (NEB Cat# R0520), then ligating and transforming. A 1 µg amount of the pcDNA3.1(-) vector was digested with 20 units of *XhoI* and 20 units of *Afl*II, 6 µl of NEbuffer 4 (10X) in a reaction volume made up to 60 µl with sterile dH$_2$O and incubated at 37°C for 2 hrs; the pcDNA 3.1 (-) digested products were purified from the gel. 1 µg of each TAL1 and TAL2 in pTAL4 vector was digested with 20 units of *XhoI* and 50 units of *ApaI* (NEB, Cat# R0114), 6 µl of NEB buffer 4 (10X) and a complete the reaction volume made up to 60 µl with sterile dH$_2$O and incubated at 37°C for 2 hrs; the products at about 4200 bp were purified from the gel, digested again with 20 units of *Afl*II and the products at about 4 kbp were purified. The inserts were ligated into the pcDNA 3.1 (-) vectors at a ratio of 8:3 according to strength of the band of each one in the gel. The reaction mixture was 1 µl of quick ligation (NEB, Cat# M2200), 10 µl of ligation buffer (10X), in a volume made up

to 20 µl with sterile dH$_2$O; ligation was carried out by incubating at room temperature for 5 mins and then the ligation was chilled on ice. A 5 µl volume of the ligation reaction was transformed to 25 µl of competent *E. coli* cells. The cells and the ligation was then incubated on ice for 30 mins, then heat shock at 42 °C for 30 secs and placed on ice for 5 mins. A 300 µl volume of SOC medium was added to the transformed competent *E. coli* cells and incubated for 1 hour at 37°C. The cells were plated onto LB- agar media containing 50 µg/ml ampicillin; the plates were incubated for 24 hrs at 37°C. A total of 50 clones for each TAL were picked and screened by diluting the clone in 20 µl of sterilised dH$_2$O and 2 µl of this solution was mixed with 10 pmol/µl of each primer: [forward (5' TTGGCGTCGGCAAACAGTGG 3') and reverse (5' GGCGACGAGGTGGTCGTTGG 3')] and 25 µl BioMix Red in final volume of 50 µl. The target sequence was amplified with initial heating at 96°C for 5 mins, followed by 35 cycles of denaturing at 96°C for 30 secs, annealing temperature at 55°C for 30 secs and extension at 72°C for 85 secs, followed by a final extension step at 72°C for 5 mins. The correct clones were grown overnight in LB media containing 50 µg/ml ampicillin. Minipreps were prepared of the plasmids TAL1 in pTAL4 and TAL2 in pTAL4 and these were checked by sequencing using seq TALEN 5.1 (5' CATCGCGCAATGCACTGAC 3') forward primer and TAL-R2.

The second step was to prepare the recombinant insert, which was achieved by cloning the 5' arm and then the 3' arm into bML3 (neoR). Total genomic DNA was purified from the NTERA2 cell line using the Wizard® Genomic DNA Purification Kit (Promega, Cat#A1120) following the manufacturer's instructions. The arm's primers were designed and then the cleavage and the restriction enzyme sequences were added to the beginning of each primer (Table 2.8).

The arms were amplified by adding ~300 ng DNA, 10 pmol/µl of each primer and 25 µl BioMix Red in final volume of 50 µl, then the PCR mix was heated at 96°C for 5 mins, followed by 35 cycles of denaturing at 96°C for 30 secs, annealing temperature at 62.5°C for 30 secs and extension at 72°C for 30 secs, followed by a final extension step at 72°C for 5 mins. The arm's PCR products were purified from the gel using the QIAquick PCR Purification Kit (Qiagen, Cat#28104) following the manufacturer's instructions.

First, the 5' arm was cloned into the bML3(neoR) vector by digesting the bML3(neoR) vector and the 5' arm PCR products each individually with SacI and SpeI for 2 hrs at 37°C. The ligation was achieved by using 50 ng of the digested vector and a ratio of 1:5 of

the PCR purified products for the 5' arm, mixed with 1µl of quick ligation, 10 µl of ligation buffer (10X) in a total volume of 20 µl. The ligation mix was incubated at room temperature for 5 mins and then chilled on ice; 5 µl of the ligation mix was transformed into 25 µl of 5-alpha Competent *E. coli* (High Efficiency) by incubating the cells and the ligation on ice for 30 min, then heat shock at 42°C for 30 secs and placing on ice for 5 mins. A 300 µl volume of SOC medium was added to the transformed competent *E. coli* cells and incubated for 1 hour at 37 °C.

The cells were plated onto LB- agar media containing 50 µg/ml ampicillin; the plates were incubated for 24 hrs at 37°C. A total of 50 clones were picked and screened by diluting the clone in 20 µl of sterile dH₂O and 2 µl of this dilution mixed with 10 pmol/µl of each primer F 5' arm, R 5' arm and 25µl BioMix Red in a final volume of 50 µl. The target sequence was amplified with initial heating at 96°C for 5 mins, followed by 35 cycles of denaturing at 96°C for 30 secs, annealing temperature at 62.5°C for 30 secs and extension at 72°C for 30 secs, followed by a final extension step at 72°C for 5 mins. The correct clones were grown overnight in LB media containing 50 µg/ml ampicillin. Minipreps were prepared for the 5' arm in the bML3(neoR) vector. The same processes were repeated to clone the 3' end arm into the bML3(neoR) vector containing the 5' arm. However, the restriction enzymes were replaced by *Eco*RV and *Kpn*I.

Table 2.8 Arm primers

Primer	Cuter	Primer sequence 5' to 3'	Tm (°C)	Size (bp)
F 5' arm	*Sac*I	TCCGAGCTCGGGTGCAATTCTCACATATGCC	62.5	807
R 5' arm	*Spe*I	GGACTAGTCCCACATTTCTTCTCAATTTAAGCAC		
F 3' arm	*Eco*RV	GCGGATATCCCTGTTTTTAATAGATCACTTTCATACAT	62.5	821
R 3' arm	*Kpn*I	CGGGGTACCCCTAGGCGACAGAGCAAGAC		

At this stage, three vectors were ready to use with the cells: the first vector was bML3 (neoR) containing both homology arms cloned into it. The second vector was pcDNA 3.1 (-) with the TAL1 cloned into it. The third vector was pcDNA 3.1 (-) with the TAL2 cloned into it. These three vectors were inserted into the cell line at the same time by either chemical transfection or electroporation.

2.10.1 Chemical transfection

On the first day, 5×10^5 HCT116 cells were seeded into a T25 flask. The next day, a vector mixture was prepared by mixing 250 µl of McCoy's 5a serum free medium with 10 µg of bML3 (neoR) containing both homology arms, 1 µg of pcDNA 3.1 (-) containing TAL1 and 1 µg of pcDNA 3.1 (-) containing TAL2. In addition, the transfection mixture was prepared by mixing 250 µl of McCoy's 5a serum free medium with Lipofectamine 2000 (Invitrogen, cat. No. 11668-027). Both mixtures were incubated for 5 mins at room temperature. The vectors and transfection mixtures were combined and incubated at room temperature for 20 mins.

The mixture was then added to the HCT116 cells after refreshing the media and incubated at 37ºC in 10% CO_2. After 24 hrs, approximately 5×10^4 cells were transferred into each 10 cm^2 plates and 300 µg/ml of G418 was added at the same time. The cells were grown for 12 days; the media and G418 were refreshed after 6 days. Each single colony was picked using a Cloning Cylinder, 10 mm x 10 mm diameter (Sigma, cat. No. C2059-1EA), and transferred to 24 well plates and 300 µg/ml of G418 was added at the same time. The cells were grown in a T75 flask until they reached the confluent stage and then half of the flask contents was frozen and the rest of the contents was used for total protein lysates and DNA extraction using the Wizard® Genomic DNA Purification Kit (Promega Cat#A1120) following the manufacturer's instruction.

2.10.2 Electroporation transfection

The NTERA2 cells were grown in a T75 flask to the confluent stage. The cells were then washed with 1x PBS and trypsinised. A sample of 5×10^6 cells was centrifuged at 1500 xg for 5 mins. The cells were resuspended in 500 µl ice-cold 1X PBS and transferred into cold 0.4 cm MicroPulser Cuvettes (Biorad, Cat. No. 165-2088). The vectors were added as 40 µg of bML3 (neoR) containing both homology arms, 5 µg of pcDNA 3.1 (-) containing TAL1 and 5 µg of pcDNA 3.1 (-) containing TAL2. All mixtures were incubated in ice for 10 min and then the electroporation transfection was achieved using a Gene Pulser Xcell™ Eukaryotic System at 320V and 200µF or 250V and 500 µF. The cells were then incubated on ice for 20 mins.

The cells were split into two T75 flasks. After 48 hrs, the cells were trypsinised and transferred to 24 well plates (1×10^3/ well) and a 10 cm plate (5×10^4/ plate) and then 300

µg/ml of G418 was added at the same time. The media and G418 were refreshed every 6 days. After 15–20 days, a single colony from the 10 cm plates was transferred into a 24 well plate using a Cloning Cylinder, 10 mm x 10 mm diameter; and the cells in the original 24 well plates were grown; the media and G418 were refreshed every 6 days. The growth of the surviving cells was continued in a T75 flask until the cells reached the confluent stage and then half of the flask contents was frozen and the rest of the flask contents was used for total protein lysates and DNA extraction using the Wizard® Genomic DNA Purification Kit.

The reductions in the protein level were observed by western blotting for the two colonies. Then re-electroporation transfection was applied for these two colonies using the same protocol as described above, and then10 µl of each of the 500 µl preparations was plated onto the 10 cm plate. After 48 hrs, the medium was refreshed and 300 µg/ml of G418 was added. After 15-20 days, a few cells had survived; the single colonies on the 10 cm plates were transferred into 24 well plates using a Cloning Cylinder, 10 mm x 10 mm diameter. The surviving cells were grown to the confluent stage in a T75 flask. Half of the flask contents was frozen, and the rest of the flask contents was used for total protein lysates and DNA extraction using the Wizard® Genomic DNA Purification Kit.

2.11 Chromatin association

Adapted from (Bermudez et al., 2012).

Whole cells were lysed using lysis buffer [50 mM Tris-HCl pH 7.4, 200 mM sodium chloride, 0.5% Triton X-100, 1 mM AEBSF (4-(2-aminoethyl) benzenesulfonyl fluoride; Sigma A8456) with one complete mini, EDTA-free protease inhibitor cocktail tablet/10 ml (Roche, 11836170001)]. An equal volume of sample buffer, Laemmli $2\times$ Concentrate (Sigma, S3401), was added to the cell lysates.

Cells were collected at each stage, washed using 1x PBS and counted. The cells were lysed in lysis buffer Ch (50 mM Hepes-NaOH (pH 7.5), 100 mM NaCl, 5 mM $MgCl_2$, 1 mM EDTA, 0.5% Triton X-100, 1 mM ATP, phosphatase, and protease inhibitors) and incubated on ice for 10 mins. The samples were then centrifuged at 15,000 xg for 10 mins. The supernatant was transferred to a clean Eppendorf tube containing an equal volume of Laemmli buffer.

The pellet was resuspended in lysis buffer Ch containing 0.4 M NaCl and incubated on ice for 1 hour, then centrifuged at 8000 xg for 10 mins. The supernatant was transferred to a clean Eppendorf tube containing an equal volume of Laemmli buffer.

The pellet was resuspended in lysis buffer Ch containing 1 M NaCl, and then sonicated at 3 microns for 10 secs (1 secs on and 1 secs off) using a SoniPrep 150. The samples were incubated on ice for one hour, and centrifuged at 8000 xg for 10 mins. The supernatant was transferred to a clean Eppendorf containing an equal volume of Laemmli buffer.

All the lysates were boiled at 100ºC for 5 mins and western blot analysis was carried out.

2.12 Detection of covalent DNA-bound SPO11

Adapted from (Hartsuiker, 2011).

The cells were trypsinised, washed twice, and then 2.5–6 x 10^5 cells were lysed in fresh 1.1 ml lysis buffer (8 M guanidine HCl, 30 mM Tris pH 7.5, 10 mM EDTA, 1 % Sarcosyl, adjusted to pH 7.5 with 10 M NaOH). The lysed cells were incubated at 65ºC for 15 min and then the lysate was centrifuged at 16,000 xg for 5 mins.

CsCl gradients (1.45 g/ml density: 60.90 g CsCl dissolved in 100 ml dH$_2$0. The refractive index (RI) was 1.3764; 1.50 g/ml density: 68.48 g CsCl in 100 ml H$_2$O, RI 1.3815; 1.72 g/ml density: 98.04 g CsCl in 100 ml dH$_2$O, RI 1.4012; 1.82 g/ml density: 111.94 g CsCl in 100 ml H$_2$O, RI 1.4104) were loaded into polyallomer centrifuge tubes (Beckman Coulter Cat. No. 326819) beginning with CsCl 1.82 g/ml then very carefully layering 1 ml of CsCl 1.72 g/ml on top of the first layer; repeating this for the 1.50 g/ml and 1.45 g/ml CsCl solutions. A 1 ml sample of the lysed cells was then loaded as the top layer. The gradients were centrifuged for 24 hrs at 30,000 r.p.m. at 25ºC in a Beckman SW55Ti rotor.

The remainder of the lysed cells was used for DNA quantification. The remaining cell lysate was incubated at 65ºC for 5 mins and centrifuged for 2 mins at 16,000 xg, then 10 µl of the supernatant was added to 90 µl of TE containing 0.5 µg/ml Rnase A (Sigma, Cat No. R6513) and incubated for 3 hrs at 37ºC. The mix was centrifuged for 2 mins at 16,000 xg to remove any insoluble material, and then 50 µl of the supernatant was added to 50 µl of a 1:200 dilution of Quant-iT PicoGreen dsDNA reagent (Invitrogen, Cat. No. P7581)

mixed in TE, and incubated for 5 mins at room temperature. A blank control (50 μl TE) and DNA standard (50 μl 100 ng/ml Lambda DNA [NEB, N3011] in TE) was prepared in parallel. An Invitrogen Qubit was calibrated using the blank control and DNA standard and then the DNA concentration in the samples was measured.

After 24 hrs, the tubes were removed from the ultracentrifuge. A centrifuge tube containing the gradient was clamped in a retort stand. Silicone tubing was fitted into a peristaltic pump and the end silicone tubing was attached to a needle. The needle was inserted into the bottom of centrifuge tube at a 45° angle. Using the peristaltic pump, the gradient was slowly pumped out of the tube and each 0.5 ml fraction was collected in a labelled Eppendorf tube.

A nitrocellulose membrane (Whatman, Cat. No. 10402096) was wetted in 1X PBS and applied to a slot blotter (Hoefer PR648 slot blot filtration manifold unit). The fractions were loaded onto the slot blot at equal loadings for each sample: based on DNA concentration measurements, the loadings for the slot blot were calculated as 150 ng for each sample. Once the samples were sucked through the membrane, the membrane was dried face up on a piece of blotting paper. The DNA was cross-linked to the membrane using a stratalinker (auto-crosslink, 120,000 microjoules).

The membrane was blocked in milk solution (3% non-fat dry milk, 0.1% Tween 20 in PBS) for 30 mins on a shaker and then incubated overnight at 4°C in anti-SPO11 antibody (Abnova, Cat. No. H00023626-A01), which was diluted 1/500 in milk solution. The membrane was then washed in milk solution twice for 10 min each time and then incubated for 1 hour at room temperature in Donkey anti-mouse as the secondary antibody (Jackson Immunoresearch, Cat. No. 711-035-150, also diluted in milk solution). The membrane was washed twice for 5 min in milk solution and three times for 5 mins in PBS/Tween 20 (0.3% w/v). Pierce ECL Plus Western Blotting Substrate (Pierce 32132) was used to detect SPO11 after exposure for 15 mins to CL-XPosure Film (Thermo scientific, 34088).

2.13 The growth of colon cancer cells (Colonospheres and parental) treated with siRNA and TALENs

Colonospheres generated individually from parental HCT116 and SW480 were cultured in fresh serum-free stem cell medium (SCM) (DMEM/F12 (1:1) supplemented with 1X B27 (Life Technologies 17504-044), 20 ng/ml Epidermal Growth Factor (EGF) (Life Technologies PHG0311), 10 ng/ml fibroblast growth factor (FGF) (Life Technologies PHG0014) and 1X Penicillin-Streptomycin antibiotic) in an ultralow attachment 10 cm dish (Corning, Costar 3262). The cells were cultured for 4 days at 37ºC in 5% CO_2 and the media were refreshed after 2 days. The cells were then washed with 1X PBS, resuspended in 1 ml of Accutase (Invitrogen, A11105-01) and incubated for 10 mins at room temperature to create single cells. The volume was then made to 10 ml with SCM media.

The cells were seeded into 96 well plates as 100 cells, 10 cells and a single cell in 100 µl of SCM media. then the transfection with the first hit of siRNA mixture was prepared for each well by adding 300 pmol SPO11 siRNA (Table 2.6) in 5 µl of serum free DMEM/F12 (1:1) containing 0.3 µl of Hiperfect Transfection Reagent (Qiagen, 301705); the siRNA mixture was incubated at room temperature for 30 mins. In addition, a non-interference mixture was prepared as a negative control by using Negative Control siRNA (Qiagen, 1022076) and prepared in the same way as the siRNA mixture preparation. The siRNA mixture, negative control and Hiperfect Transfection Reagent without addition were added to the cells individually (6 wells for each condition) in parallel with untreated cells.

The cells were treated with TALEN (See 2.10) prepared for each well by adding 200 ng of each SPO11 TAL1 and TAL2 in 5 µl of serum free DMEM/F12 (1:1) containing 0.25 µl of Lipofectamine® 2000 Transfection Reagent (Life Technologies, 11668-027). The TALEN mixture was incubated at room temperature for 30 mins. In addition, TALEN with a homology arm mixture was prepared similarly to the TALEN mixture preparation but with the addition of 600 ng of the homology arms. The TALEN mixture, TALEN with homology arms mixture and Lipofectamine® 2000 Transfection Reagent without addition (as a negative control) were added to the cells individually (6 wells for each condition) in parallel with untreated cells.

The same experiment was repeated with parental HCT116 and SW480 cells. However, the second hit was done on the second day of the cell seeding in the same manner as the first hit but in a 50 µl total volume of SCM media, which was added to the first 100 µl of SCM. The cell images were taken after 10 days respectively.

2.14 Extreme limiting dilution analysis

Adapted from (Hu and Smyth, 2009)

HCT116 colonospheres were prepared as described in Section 2.13 and then the cells were seeded as 100 and 10 cells into 96 Well Clear Flat Bottom Ultra Low Attachment Microplates (Corning, Costar 3474). The cells were then treated with siRNA as different siRNAs, negative control and Hiperfect Transfection Reagent, as described in 2.13. In addition, the cells then treated with TALEN (TAL1 and TAL2), TALEN (TAL1 and TAL2) with homology arms, empty vectors and Lipofectamine® 2000 Transfection Reagent without addition (as a negative control) individually (6 wells for each condition) in parallel with untreated cells. After 8 days from the cell seeding, the number of wells showing formation of colonospheres was counted. The frequency of sphere forming cells in a particular cell type was determined using the ELDA webtool at:
 http://bioinf.wehi.edu.au/software/elda.

3 Identification of novel cancer/testis genes: meiotic chromosome regulator genes

3.1 Introduction

During meiosis specific genes mediate distinct and important roles in chromosome dynamics (Table 3.1); some of these genes are involved in meiotic recombination (see section 1.5.2.3). Recombination ensures accurate homologous chromosome segregation to generate haploid gametes (Petronczki et al., 2003). Recombination intermediates are process to form crossover or non-crossover products. During meiosis, at least one obligate crossover occurs per chromosome and, in mice, approximately 10% of recombination events result in crossovers (Cole et al., 2010).

Many genes involved in mediating meiotic recombination mechanisms are specifically expressed in meiosis. However, some of these genes are abnormally expressed and have an important role in different types of cancer; the associated protein products are known as cancer/testis antigens (CTAs) (Cheng et al., 2011). The expression of CTA genes in cancer cells can lead to abnormal chromosome segregation, which can be associated with chromosome rearrangement (Simpson et al., 2005).

SPO11 (CT35) is a meiosis specific protein that binds to DNA to initiate recombination by forming DNA DSBs. The *SPO11* gene has been reported to be expressed in melanoma and cervical cancer cells (Koslowski et al., 2002). In addition, SYCP1 (CT8) has been identified as a CTA (Meuwissen et al., 1997; Türeci et al., 1998). SYCP1 is one of the protein components of the SC (transverse filament) and is required to form a bridge between the central and lateral elements of the SC in order to assemble the SC structure (Costa et al., 2005). SYCE1 (CT76) is another protein component of the SC which has been identified as a CTA (van Geel et al., 2002). HORMAD1 (CT46) and HORMAD2 (CT46.2) have also both been identified as CTAs (Chen et al., 2005b; Liu et al., 2012; Pangas et al., 2004), and both normally have a specific function during meiosis (Table 3.1).

The CTAs are restricted to the testis in normal adult cells, but not expressed in other normal somatic cells except for some genes in a limited number of normal tissues, and are highly expressed in cancer tissues (Simpson et al., 2005). Thus, these genes can be used as biomarkers for cancer screening in the early stages (see section 1.6.5) (Grizzi et al., 2007). In addition, identification of CTAs provides potential cancer specific immunotherapy and vaccination targets (see section 1.6.6) (Hemminger et al., 2012). For instance, Hunder et al. (2008) successfully used a CTA, NY-ESO-1, to treat a metastatic melanoma patient with recurrent disease.

This project aimed to determine whether a cohort of genes which are involved in meiotic genome dynamics are candidate CTA genes. RNA from twenty-one human normal tissues, including testis as positive control, was analysed for gene expression profiles. The genes exhibiting a testis-restricted expression profile in normal tissues were analysed for evidence of expression in 33 cancer cells/tissues to obtain gene expression profiles for these candidate genes (Figure 3.1).

Table 3.1. The function of meiosis recombination genes

Gene	Function of gene product	Reference
HORMAD1	SC formation and promotes homologue alignment.	(Daniel et al., 2011)
HORMAD2	Quality control mechanism that recognizes unsynapsis and recruits ATR activity during mammalian meiosis.	(Kogo et al., 2012)
PRDM9	Regulates meiotic recombination hot spots in mice and humans; required for synapsis and forms the sex body (X and Y).	(Berg et al., 2010; Hayashi et al., 2005; Sasaki and Matsui, 2008)
REC8	Component of the meiotic cohesin complex (see section 1.5.2.5).	
SPO11	Initiates meiotic recombination by forming DSBs.	(Henderson and Keeney, 2004;

		Keeney and Neale, 2006)
STAG3	Component of the meiotic cohesin complex (see section 1.5.2.5).	
SYCE1	Component of the SC (see section 1.5.2.4).	
SYCE2	Component of the SC (see section 1.5.2.4).	
SYCP1	Component of the SC (see section 1.5.2.4).	
SYCP2	Component of the SC (see section 1.5.2.4).	
SYCP3	Component of the SC (see section 1.5.2.4).	
TEX12	Component of the SC (see section 1.5.2.4).	

Identification of novel CTA gene candidates

Manual searching in the literature for human meiotic recombination regulator genes

Ⓐ

RT-PCR using 21 human normal tissues to validate gene expression profiles

ⓘ

Expressed in different normal tissues

ⓘⓘ

Expressed only in:

1) Testis-restricted (Only in normal testis)

2) Testis/brain-restricted (Only in normal testis/CNS)

3) Testis-selective (Only in normal testis/selective normal tissue)

Ⓑ

Validate these genes with RT-PCR using 33 cancer tissues and cell lines

Excluded from genes lists

Might encode novel CTAs

Figure 3.1. Strategy to identify novel CTA genes. (**A**) Using RT-PCR with 21 human normal tissues and based on the RT-PCR results of the gene expression profiles in different normal tissues the genes were divided into: i) expressed in different normal tissues; these genes were excluded from the recombination genes list; ii) the genes expressed only in the 1) testis, 2) testis/CNS, or 3) testis/selective normal tissues; (**B**) The genes from group ii were validated with 33 cancer tissues or cancer cell lines.

3.2 Results

3.2.1 RT-PCR with normal tissues and cancer tissues/cell lines

In this chapter meiotic recombination regulator genes were tested to identify novel CTA genes. cDNAs were made from RNA from 21 normal tissues, including testis tissue. The genes exhibiting a testis-restricted expression profile in normal tissues were analysed for expression in 33 cancer cells/tissues to obtain gene expression profiles for these candidates. *β-actin* gene expression was used as control for the cDNA quality; *MAGEC1*, *SSX2* (testis restricted), and *SYCP1* (testis/brain restricted) were used as controls for known CTA genes. All genes involved in the meiotic recombination process, such as SC genes [*SYCP1* (as control), *SYCP2*, *SYCP3*, *TEX12*, *SYCE1*, *SYCE2*], meiosis cohesin complex (*REC8* and *STAG3*), *HORMAD1*, *HORMAD2*, and *PRDM9*, were tested for there expression profile in normal tissues.

The analysis showed a number of these genes were expressed in different normal tissues, therefore, these genes were excluded of the study (Figures 3.2 and 3.5). However, expression of *PRDM9* is restricted to the testis, while *SYCP3* had expression restricted to the testis and thymus (Figures 3.3 and 3.5) indicating they could be good candidates for CTA genes. All the results were confirmed by sequencing selective RT-PCR products (Table 3.2).

PRDM9 and *SYCP3* were analysed for expression in 33 cancer tissues and cancer cell lines (Figures 3.4 and 3.6). The *PRDM9* gene was expressed only in the normal testis and not in other normal tissues; thus, this gene belongs to the testis-restricted category (Figures 3.3 and 3.5). In addition, it was expressed in different cancer tissues and cell lines, such as embryonal carcinoma (NTERA2), astrocytoma (1321N1), colon cancer cells (LoVo), prostate cancer cells (PC-3), breast cancer tissue and cell line (MCF-7), ovarian cancer cells (A2780, PE014, and TO14), melanoma cells (G361 and COLO857), and leukaemia cells (K-562) (Figures 3.4 and 3.6).

SYCP3 was expressed in the normal testis and thymus; thus, this gene belongs to the testis-selective category (Figures 3.3 and 3.5). In addition, it is expressed in different cancer tissues and cell lines, such as colon cancer cells (HT29 and HCT116), prostate cancer cells (PC-3), cervical cancer cells (Hela-S3), ovarian cancer cells (A2780, PE014, and TO14), and melanoma cells (G361 and MM127) (Figures 3.4 and 3.6).
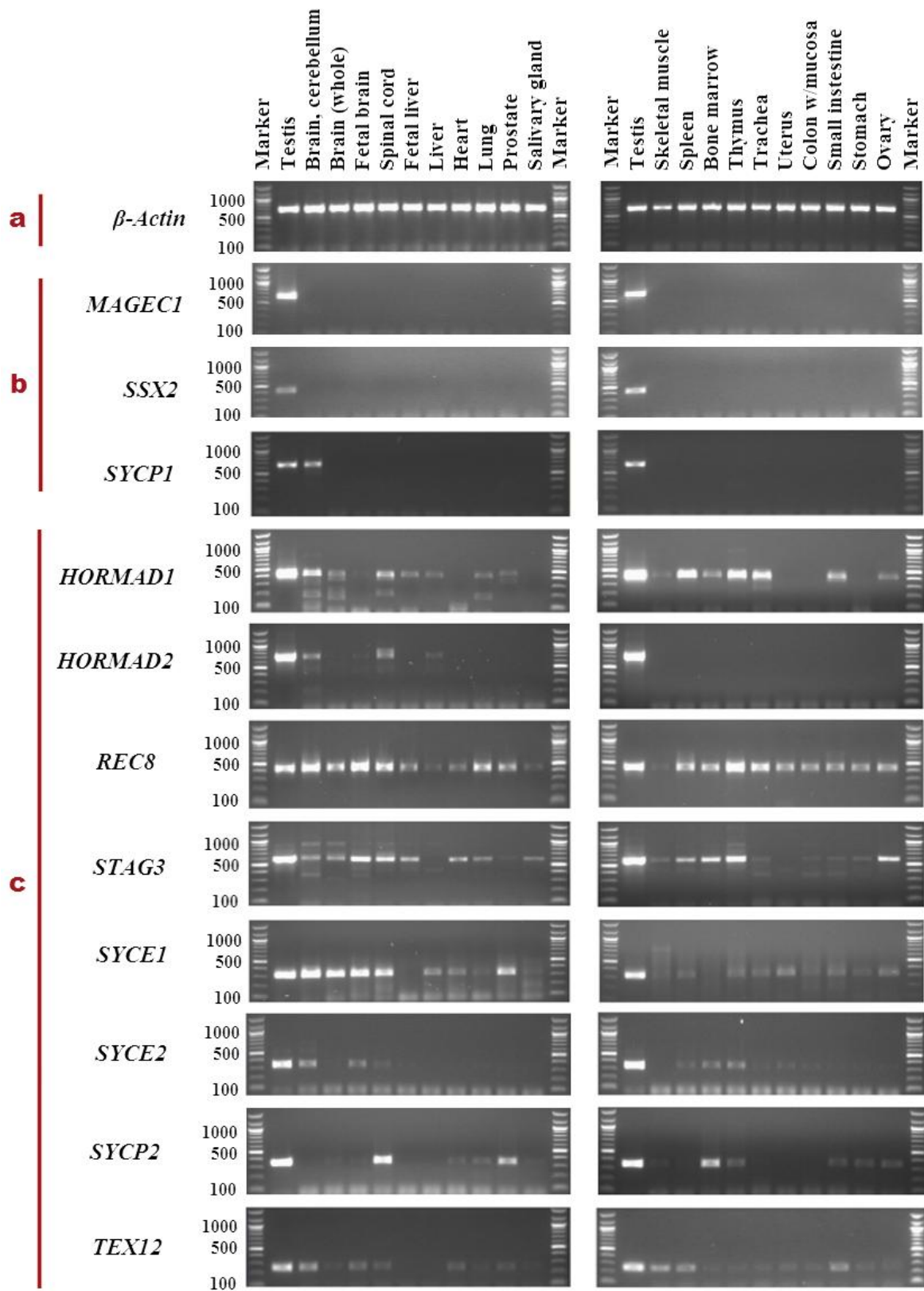
Figure 3.2. RT-PCR results for normal tissues for excluded meiosis recombination genes. (**a**) *β-actin* as control for cDNA quality; (**b**) *MAGEC1*, *SSX2*, and *SYCP1* as controls for CTA genes; (**c**) *HORMAD1*, *HORMAD2*, *SYCE1*, *SYCE2*, *TEX12*, *SYCP2*, *REC8*, and *STAG3* are expressed in different normal tissues (repeated twice).

58
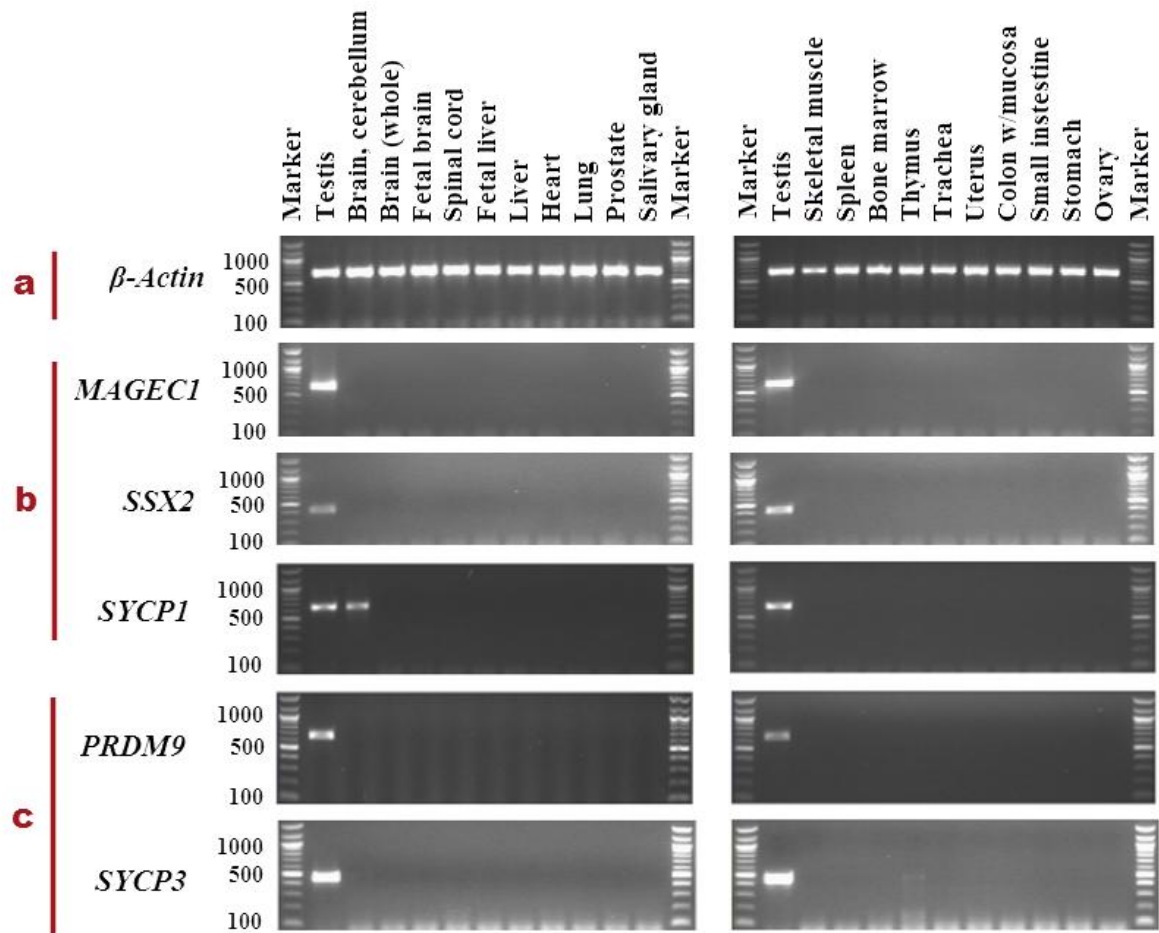
Figure 3.3. RT-PCR results for some of meiosis recombination genes in normal tissues. (**a**) *β-actin* as control for cDNA quality; (**b**) *MAGEC1*, *SSX2*, and *SYCP1* as control for CTA genes; (**c**) The expression analysis for new CTA gene candidates *SYCP3* is expressed in the normal testis and thymus; *PRDM9* is expressed only in the normal testis (repeated twice).
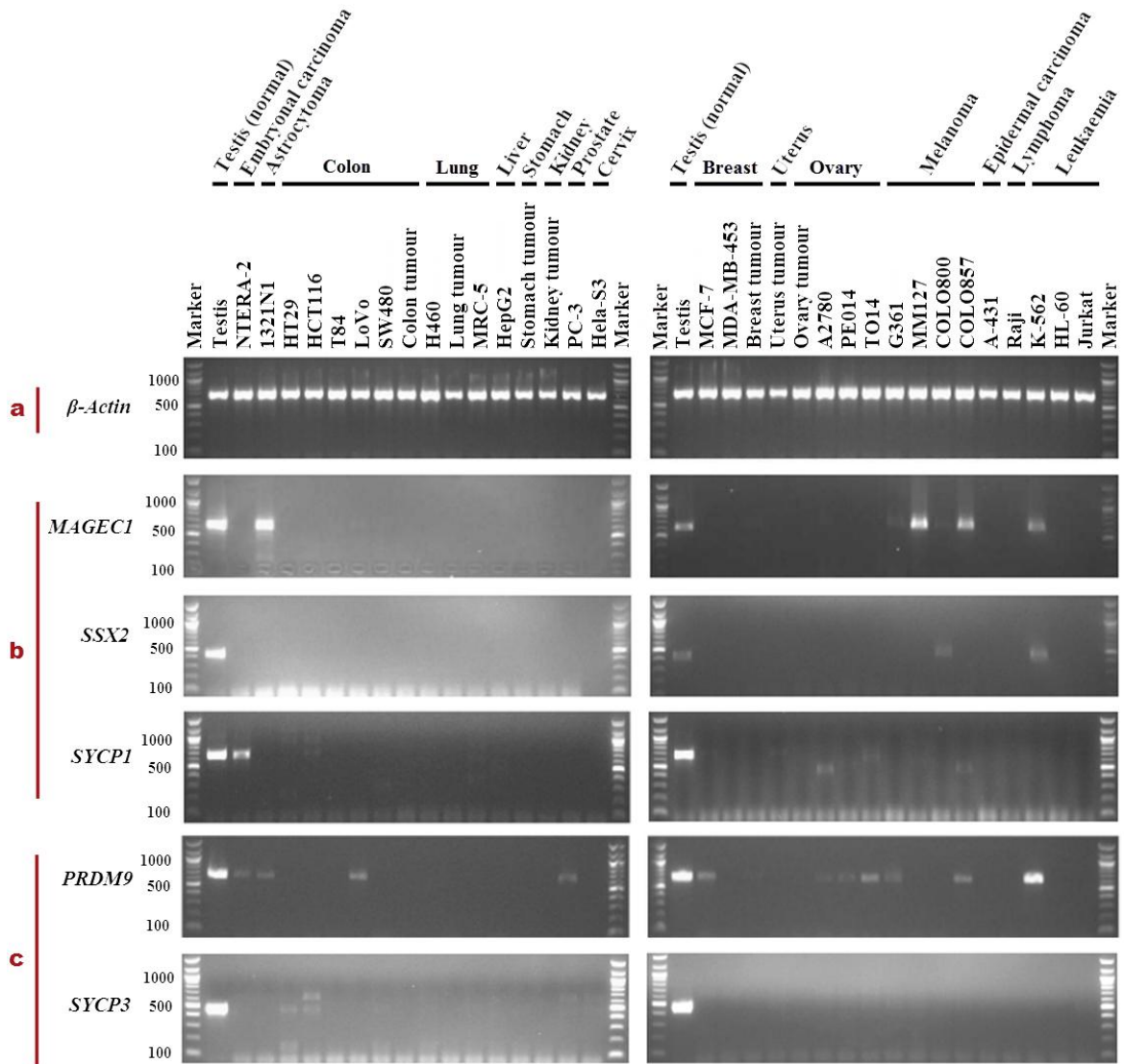
Figure 3.4. RT-PCR results for the good CTAs candidate of recombination genes in cancer tissues and cell lines. (**a**) *β-actin* as control for cDNA quality; (**b**) *MAGEC1*, *SSX2*, and *SYCP1* as control for CTA genes; (**c**) *SYCP3* and *PRDM9* are expressed in different cancer tissues and cell lines (there are faint bands of SYCP3 with PC-3, Hela-S3, A2780, PE014, TO14, G361 and MM127, which are visible on the computer screen) (repeated twice).
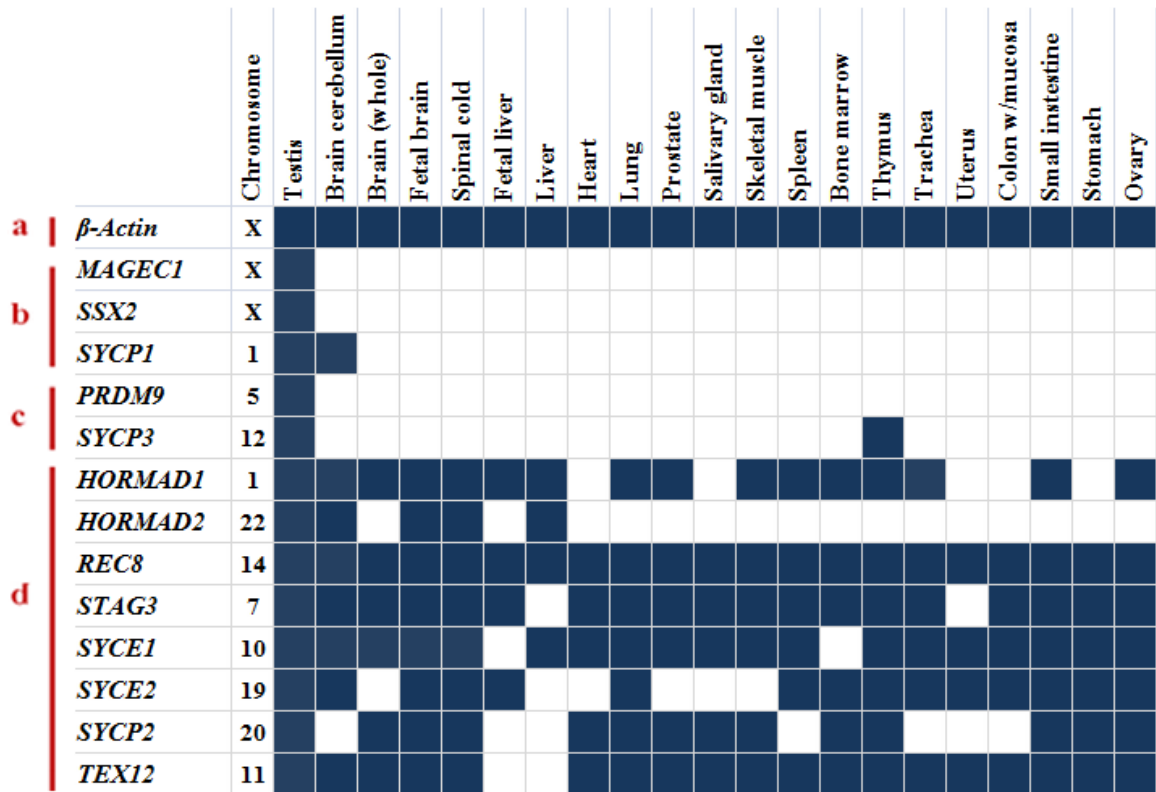
Figure 3.5. Summary of RT-PCR results in normal tissues. (**a**) Expression of *β-actin* as control for cDNA quality; (**b**) *MAGEC1*, *SSX2* and *SYCP1* as controls for CTA genes; (**c**) Expression of *SYCP3* and *PRDM9* in normal tissues shows these two genes might be good CTA genes; (**d**) The expression of *HORMAD1*, *HORMAD2*, *SYCE1*, *SYCE2*, *TEX12*, *SYCP2*, *REC8* and *STAG3* in different normal tissues (dark blue: gene expressed, white: does not expressed).
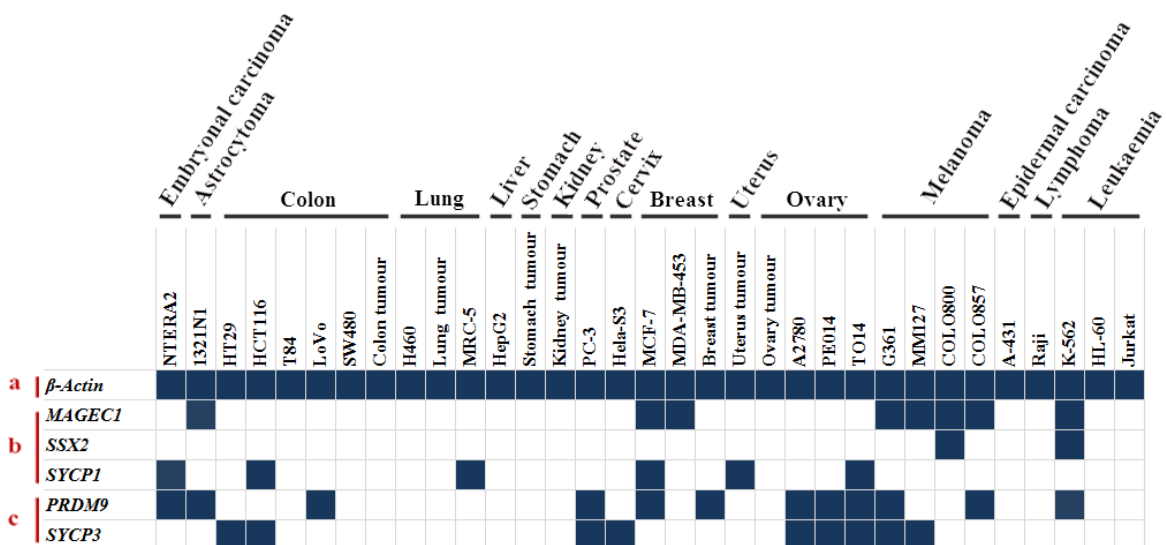
Figure 3.6. Summary of RT-PCR results for *SYCP3* and *PRDM9* in cancer tissues and cell lines. (**a**) Expression of *β-actin* as control for cDNA quality; (**b**) Expression of *MAGEC1*, *SSX2*, and *SYCP1* as a control for CTA genes in cancer tissues and cell lines; (**c**) Expression of two new potential CTA genes, *SYCP3* and *PRDM9*, in cancer tissues and cancer cell lines (dark blue: gene expressed, white: does not expressed).

Table 3.2. Summary of the sequencing results for recombination genes

Gene	Primer	Expected size (bp)	Approximate product size (bp)	Normal tissue or cancer cell line	Sequence size (bp)	The identity from NCBI between the RT-PCR products and the genes
HORMAD1	F	486	486	Spleen	383	99%
HORMAD2	F	707	707	Brain, cerebellum	632	99%
HORMAD2	F	707	707	Liver	527	99%
PRDM9	F	655	655	MCF-7	116	98% *PRDM9* 95% *PRDM7*
PRDM9	F	655	655	K-562	413	99% *PRDM9* 96% *PRDM7*
REC8	F	444	444	Bone marrow	397	99%
STAG3	F	591	591	Testis	555	99%
STAG3	F	591	591	Bone marrow	535	99%
STAG3	F	591	490	Bone marrow	81	94% GGA2
SYCE1	F	318	318	Prostate	274	100%
SYCE2	F	339	339	Bone marrow	182	99%
SYCP1	F	675	675	NTERA2	391	99%
SYCP1	F	675	675	G-361	178	100%
SYCP2	F	354	354	Spinal cord	141	99%
SYCP2	F	354	354	Bone marrow	152	100%
SYCP3	F	467	467	HT29	323	99%
SYCP3	F	467	467	Jurkat	320	99%
TEX12	F	258	258	Spleen	182	100%

3.2.2 Meta-analysis results

Expression meta-analysis assesses the expression of genes in clinical cancer samples by analysing patient-derived cancer microarray data for 13 cancer types was carried out through the CancerMA database tool (http://www.cancerma.org.uk/index.html) (Feichtinger et al., 2012b). This analysis was applied to the candidate genes *PRDM9* and *SYCP3*. *SPO11*, which was identified as a CTA gene, along with the CTA control genes *MAGEC1*, *SSX2*, and *SYCP1* were also included. The results of the meta-analysis indicated up-regulation of *MAGEC1*, *SSX2*, *SYCP1*, *SYCP3*, and *PRDM9* in some of the 13 cancer types (Figure 3.5). Notably, all genes were up-regulated in ovarian cancers. Moreover, whilst *PRDM9* exhibited expression in a range of cancer types as measured by RT-PCR, it only gave a meta up-regulation for ovarian tumours.
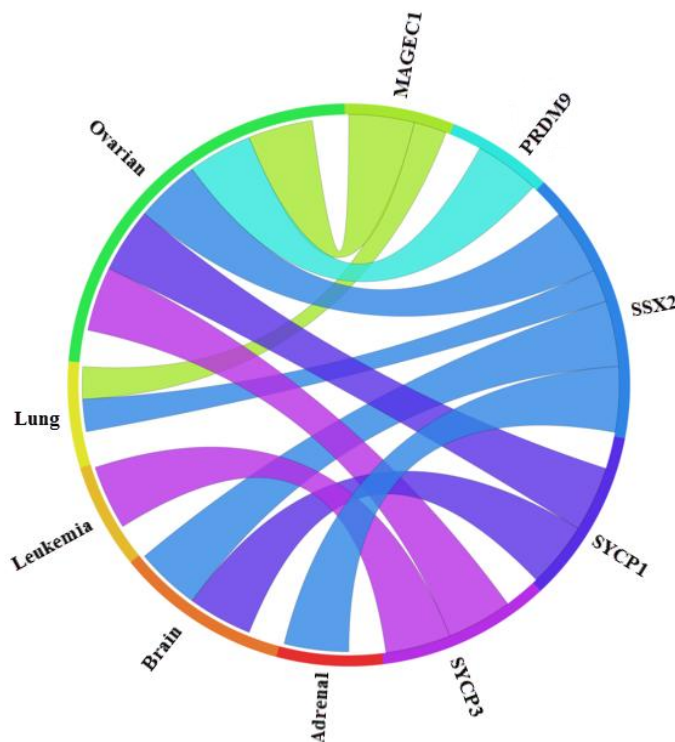
Figure 3.7. The Circos plot for the good candidate of recombination genes and control genes: The Circos plot shows the meta-change in gene expression in relation to corresponding cancer types for the six genes that present as a good candidate of recombination and control genes following RT-PCR analysis; these are represented on microarrays. Five of the six genes show significant up-regulation for combined cancer data sets. Each connection between a gene and a cancer type indicates a statistically significant mean up-regulation for that cancer type derived from a number of combined array studies for cancer tissue *vs*. normal tissue. The weight of the connection corresponds to the magnitude of the meta-change in gene expression.

3.3 Discussion

3.3.1 Gene expression of the meiosis specific genes

In the present study, some of the genes previously identified as CTA genes, such as *HORMAD1* (CT46) (Chen et al., 2005b; Pangas et al., 2004) and *HORMAD2* (CT46.2) (Liu et al., 2012), were found to be expressed in different normal tissues (Figure 3.7). Hence, these genes were excluded from the study. In a previous study, weak expression of *HORMAD1* was detected in brain, colon, breast, spleen, and placenta (Chen et al., 2005b). *HORMAD2* expression was detected in testis and liver (Liu et al., 2012). These findings suggest the *HORMAD* genes are not testis-restricted CTA genes.

Other meiosis-specific genes, *SYCE1, SYCE2, TEX12, SYCP2* (members of SC), *REC8* and *STAG3* (members of cohesin complex) showed high expression in different normal tissues (Feichtinger et al., 2012a). In addition, the expression of *SYCE1* was detected in different normal tissues (Hofmann et al., 2008). In the fission yeast, specific post-transcriptional mRNA degradation inhibits the production of the Rec8 protein in the mitotic cells (Harigaya et al., 2006). If this inhibition is also applicable in mammalian cells, it may account for the expression of the meiosis-specific genes in the somatic cells and could indicate that whilst there is mRNA, there may not be protein.

3.3.2 *PDRM9* identified as novel potential CTA gene

PRDM9 is a zinc finger protein (Kota and Feil, 2010). It binds to its recognition sites which results in activation of histone H3K4 methyltransferase activity (Neale, 2010). The chromatin modification is thought to conferring hotspot activity, which allows SPO11 to initiate recombination by generating DSBs at these sites (Buard et al., 2009). In 20 mouse strains, the PRDM9 zinc finger was sequenced and five different zinc finger repeats were identified; each zinc finger mediates binding to a specific site of the DNA (Parvanov et al., 2010).

In this study, the *PRDM9* gene was expressed only in the normal testis and not in other normal tissues; thus, this gene belongs to the testis-restricted category (Figure 3.3). In addition, it was widely expressed in different cancer tissues and cell lines, including

embryonal carcinoma, astrocytoma, colon cancer, prostate cancer, breast cancer, ovarian cancer, melanoma, and leukaemia. Thus, if PRDM9 has the same activity in cancer cells as it does in meiosis, this would mean it could modify the chromatin and allows SPO11 to form a DSB.

Meisetz which is mouse orthology gene of *PRDM9* has a function in meiotic transcriptional regulation, this activates expression of other testis-specific genes such as *RIK* gene (Hayashi et al., 2005). Therefore, PRDM9 might transcriptional activity or modify the chromatin structure in the somatic cells and drive oncogenic transcriptional activation. whilst this is speculation, this could be tested by depleting PRDM9 in cancer cell lines and assessing transcriptional changes (Feichtinger et al., 2012a).

A recent study (Hussin et al., 2013) has reported that rare *PRDM9* alleles are linked to genomic rearrangements and an excess of these rare *PRDM9* alleles can also lead to aneuploidies, and that both are associated with childhood leukemogenesis. These findings may support the expression of the *PRDM9* in leukaemia observed in the present study. In addition, the meta-analysis observation of significant up-regulation of *PRDM9* in ovarian cancers supports the *PRDM9* expression in ovarian cancer cell lines observed in the present study.

This gene is testis-restricted and is expressed in different types of cancer, making it an important and promising biomarker and potential therapeutic target for different types of cancer. Thus, this gene will be studied in more detail (See Chapter 7) in order to investigate the PRDM9 protein in normal and cancer tissues and cell lines.

3.3.3   SYCP3 identified as a potential CTA gene

SYCP3 is a component of the lateral elements in the SC (See 1.5.2.4). A previous study identified *SYCP3* as a CTA gene which has testis-restricted expression in normal tissues and is expressed in tumours of soft tissue, ovary and brain (Mobasheri et al., 2007). However, in the present study, *SYCP3* was detected in the normal tissues of the testis and the thymus, which might shifts it from the testis-restricted group to a testis-selective group. Another possibility of the expression differences in the normal tissues between the pervious study and present study could be that the thymus tissue which has been used in this study was aberrant. In addition, *SYCP3* in the present study showed expression in

cancers of the colon, prostate, cervix, and ovary, and in melanoma, so it seems likely *SYCP3* is a good CTA gene candidate.

A meta-analysis based on 13 different microarrays of cancer tissues was carried out for *SYCP3* expression. This analysis showed up-regulation of *SYCP3* in ovarian cancer and leukaemia. Therefore, the meta-analysis supported the expression of the *SYCP3* in ovarian cancer. *SYCP3* expression was detected in 47% of ALL patients (Niemeyer et al., 2003), which support the up-regulation results for *SYCP3* in leukaemia cells.

Another recent study has shown a different view of the relationship between expression of *SYCP3* during mitosis and cancer. Accumulation of DSBs was observed in somatic cells that expressed *SYCP3*. In addition, the expression of *SYCP3* during cell division increased the risk of aneuploidy (Hosoya et al., 2011). SYCP3 is capable of forming a complex with BRCA2 inhibiting the interaction between RAD51 and BRCA2, thereby affecting homologue recombination repair in response to DNA damage (Hosoya et al., 2011). Thus, *SYCP3* expression could be oncogenic by interfering with normal chromosome segregation and DNA damage repair.

3.4 Conclusions

This chapter focused on meiotic chromosome regulator genes in order to identify novel CTAs. Ten genes were analysed in 21 normal tissues, using the testis as a control. Some of these genes (*SPO11*, *HORMAD1* and *HORMAD2*) had been previously identified in other studies as CTA genes. However, in this study *HORMAD1*and *HORMAD2* were shown to be expressed in more than two normal tissues, in addition to the testis. Other meiosis specific genes, *SYCE1, SYCE2, TEX12, SYCP2, REC8* and STAG3 were also highly expressed in different normal tissues. Therefore, these genes were excluded from further study.

Of these 10 genes, only *PRDM9* and *SYCP3* were identified as good candidates to encode CTAs. *PRDM9* belongs to the testis-restricted category while *SYCP3* might belong to a testis-selective category, although taking all data together it seem likely that *SYCP3* is testis restricted. Both *PRDM9* and *SYCP3* were expressed in different types of cancers, as confirmed by meta-analysis. Thus, these two genes are important and promising as biomarkers and immunotherapy targets for different types of cancer.

4 Identification of novel CTA gene candidates from a bioinformatics search

4.1 Introduction

As previous indicated highly restricted cancer/testis antigens (CTAs) are found in male germ cells; they are expressed in normal adult testes and are termed testis-restricted. Another group of CTA genes are expressed in the normal testis and the central nervous system, and are termed testis/brain-restricted. Some of these genes are expressed in some normal tissues and are placed in a special group termed testis-selective (de Carvalho et al., 2012). These genes are widely expressed in different cancer types.

Different strategies are available for identifying CTAs. One of these strategies was to use a bioinformatics approach to characterise CTA genes (Hofmann et al., 2008). A data mining strategy identified ADAM as a metallopeptidase domain 2 (*ADAM2*), P antigen family, member 5 (prostate associated) (*PAGE5*), and lipase member I (*LIPI*) (Scanlan et al., 2002). Furthermore, large scale post genomics technologies have been used to drive successful CTA genes screens (for example, see Chen et al., 2005a).

In this chapter, RT-PCR was carried out to validate genes identified by bioinformatics tools (Figure 4.1). This search was initiated by searching for mouse meiotic genes from GermOnline (www.germonline.org/), and then these genes were mapped to human orthologous genes. The human orthologues were then filtered using Mitocheck to avoid genes that were expressed during mitosis (http://www.mitocheck.org/). The genes were passed through Mitocheck and then checked through two different programmes to check the expression in cancer tissues: the first method was the expressed sequence tag (EST) from UniGene (Table 4.1; http://www.cancerest.org.uk/; Feichtinger et al., 2013) and the second method was cancer microarray data from ArrayExpress (Table 4.2; http://www.cancerest.org.uk/; Feichtinger et al., 2012b).
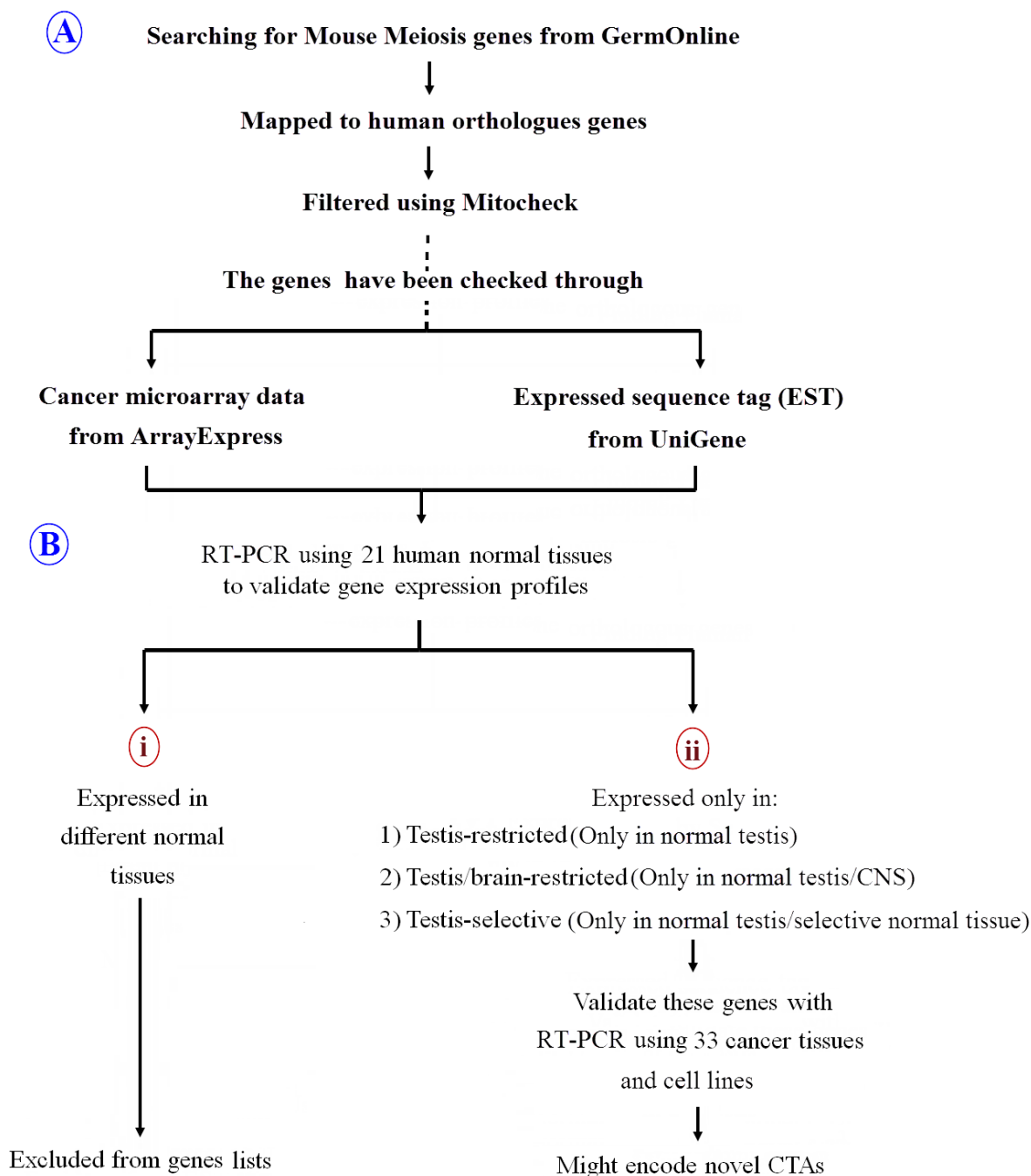
Figure 4.1. Strategy to identify novel CTA genes through bioinformatic tools. (A) Shows the bioinformatics process used to identify the genes. (B) Using RT-PCR with 21 human normal tissues and based on the RT-PCR results of the gene expression profiles in different normal tissues, the genes were divided into the following categories: **i)** expressed in different normal tissues; these genes were excluded from the further study; **ii)** the genes expressed only in the 1) testis, 2) testis/CNS, or 3) testis/selective normal tissues; The genes from group ii were validated with 33 cancer tissues or cancer cell lines.

The results from these searches were 10 genes belonging to the microarray search and 21 genes belonging to the EST search [other genes were identified, but these were allocated to this specific study; (Feichtinger et al., 2012a)]. These genes were all tested by me by RT-PCR on 21 normal human tissues including testis. The genes were predicted to be expressed either only in the testis, or in the testis and CNS, or in the testis and two or fewer normal tissues. Genes matching one of these three profiles were examined by RT-PCR using RNA extracted from 33 cancer tissues and cancer cell lines. The CTA candidate genes were then subjected to microarray meta-analysis to determine the relationship between these genes and 13 types of cancers.

Table 4.1 The list of genes analysed in this study that were identified by analysed of EST data sets

Gene	Function of gene product	Reference
ACTRT1	A major component of the calyx in the perinuclear theca of mammalian sperm heads.	(Heid et al., 2002)
C1orf65	Unknown	
C4orf51	Unknown	
C11orf91	Unknown	
C12orf42	Unknown	(Sampietro et al., 2011)
C20orf79	Unknown	
C22orf33	Spermatogenesis associated.	(Puri et al., 2011)
CALM2	Involved in the pathway that regulates the centrosome cycle and progression through cytokinesis and mediates the control of several protein kinases and phosphatises.	(Jukic et al., 2010)
CATSPER3	Play an important role in sperm hyperactivated motility.	(Jin et al., 2007)
CCDC18	Involved in spindle pole and centrosome function.	(Sharp et al., 2011)
CCDC38	May regulate pulmonary function.	(Artigas et al., 2011)

CCDC79	Unknown	
CYLC2	A specific component of the cytoskeleton of sperm heads.	(Hess et al., 1995)
GLT6D1	Unknown	
IQCF5	Unknown	
LUZP4	Also known as HOM-TES-85 and involved in transcriptional processes.	(Türeci et al., 2002)
MBD3L1	Most likely functions when in association with other factors and plays a role during the development of postmeiotic male germ cells.	(Jiang et al., 2002)
PAX5	Essential for commitment of lymphoid progenitors to the B lymphocyte lineage and regulates the process of spermatogenesis.	(Branford et al., 1997; Cobaleda et al., 2007)
PTPN20B	Involved in the microtubule network.	(Fodero-Tavoletti et al., 2005)
SUN3	The SUN-domain interacts with the KASH-domain to form SUN-KASH protein complexes and then plays a role in alignment of homologous chromosomes, their pairing and recombination in meiosis. In addition, SUN-domain proteins regulate apoptosis and survival of the germline.	(Fridkin et al., 2009)
TDRD1	A Tudor domain protein that functions during spermatogenesis.	(Kojima et al., 2009)

Table 4.2. The list of genes analysis in this study that were identified by analysed of microarray data sets.

Gene	Function of gene product	Reference
C7orf31	Unknown	
C10orf82	Unknown	
CCDC146	Unknown	(Kim et al., 2011b)
GPAT2	May have a role in testis development and function.	(Wang et al., 2007)
NUT	Unknown, but there are rare cancers caused by fusion of *BRD4* and *NUT* as result of a chromosomal translocation, t(15;19)(q13;p13).	(French et al., 2007; Reynoird et al., 2010)
PVRIG	Unknown	
STAG3	Member of the cohesin complex (see section 1.5.2.5).	
STK31	Unknown	
SYCP2	Member of SC (see 1.5.2.4).	
TUBA1B	The major component of microtubules.	(Zhu et al., 2012)

4.2 Results

4.2.1 EST derived genes

The 21 genes that were identified using EST bioinformatic tool (http://www.cancerest.org.uk/) were validated by 40 cycle RT-PCR (to take the PCR to the limits of sensitivity) using cDNA synthesised from RNA from 21 normal human tissues, including the testis, which was predicted to be positive. In addition, the *β-Actin* gene was used as control for the cDNAs quality. Two CTA genes (*MAGEC1* and *SSX2*) were used as CTA gene positive controls. The genes that were expressed only in the normal testis or normal testis and selective tissues (two or fewer) were carried further for analysis of cDNA synthesised from RNA from 33 cancer tissues and cancer cell lines.

The test on the different normal tissues revealed 8 genes *CCDC18, CLAM2, TDRD1, PTPN20B, C12orf42, CATSPER3, C11orf91* and *PAX5* that were expressed in different normal tissues (more than two) including the testis (Figures 4.2 and 4.8). These genes were excluded from further study. The second group contained 11 genes, *ACTRT1, CCDC38, C22orf33, SUN3, C1orf65, LUZP4, C4orf51, GLT6D1, CYLC2*, *CCDC79* and *C20orf79* which had expression restricted to the testis in the normal tissues panel (Figures 4.3 and 4.8). The third group obtained from normal tissue consisted of two testis-selective genes, *MBD3L1* and *IQCF5*, which were expressed in the normal testis and two or fewer of the other normal tissues (Figures 4.4 and 4.8).

The testis-restricted and the testis-selective genes were further investigated in 33 cancer tissues and cell lines. The testis-restricted genes were divided into two groups based on the RT-PCR results on cancer RNAs. The first group was *ACTRT1, CCDC38, C22orf33, C1orf65*, *LUZP4* and *C20orf79,* which were expressed in different cancer types (Figures 4.5 and 4.9). The second group was *SUN3, C4orf51, GLT6D1, CYLC2* and *CCDC79*, which not expressed in any of the cancer cells used in present study (Figures 4.6 and 4.9). The testis-selective genes *IQCF5* and *MBD3L1* were expressed in different types of cancers (Figures 4.7 and 4.9). Sample RT-PCR products were confirmed by sequencing to validate the correct target cDNA was being amplified (Table 4.3).
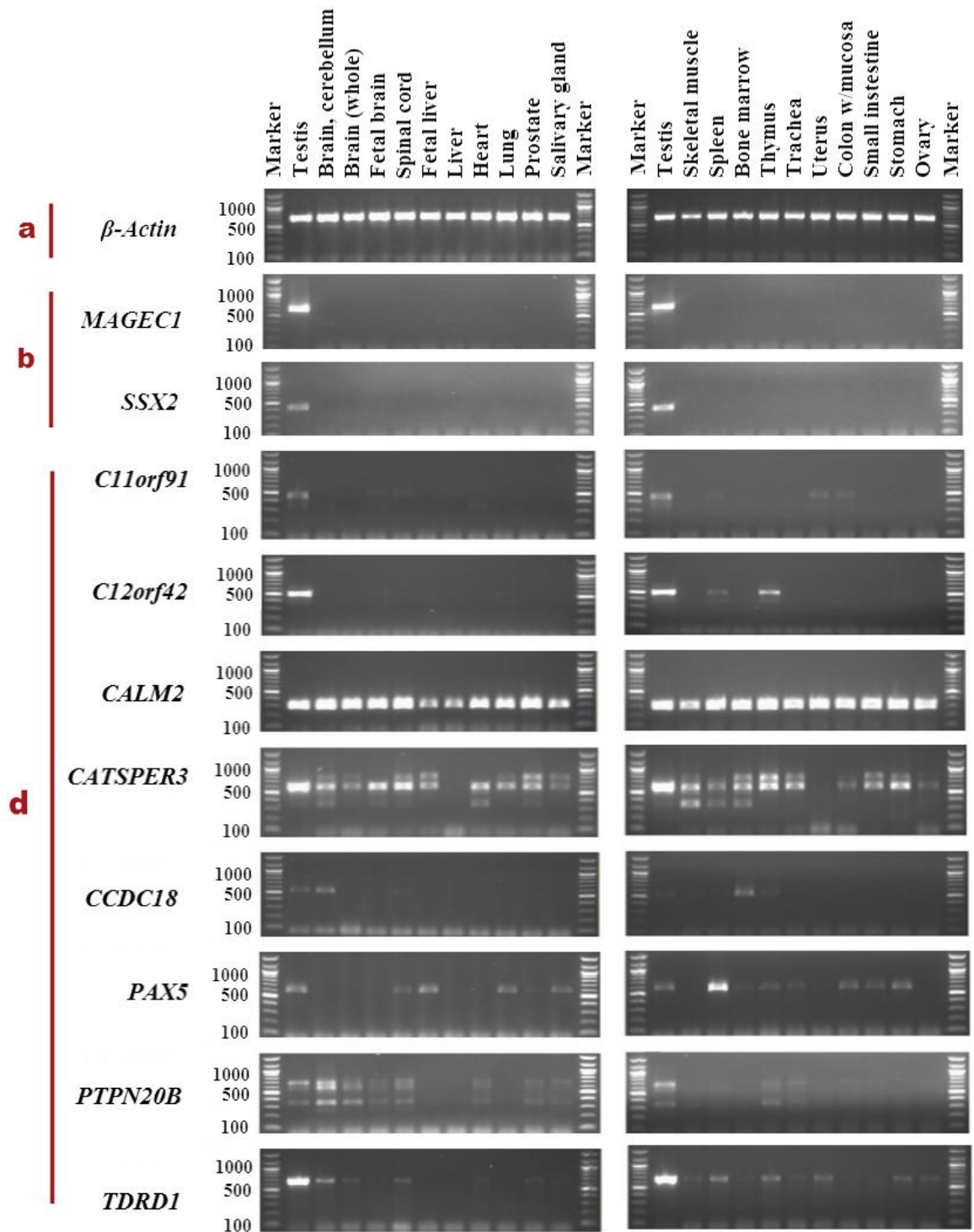
Figure 4.2. RT-PCR results for the EST derived gene list that were excluded from further study following analysis of normal tissues cDNA. (**a**) *β-actin* served as a control for tissue cDNA; (**b**) *MAGEC1* and *SSX2* served as controls for CTA genes; (**c**) Some of the EST derived genes were expressed in different normal tissues (done once).
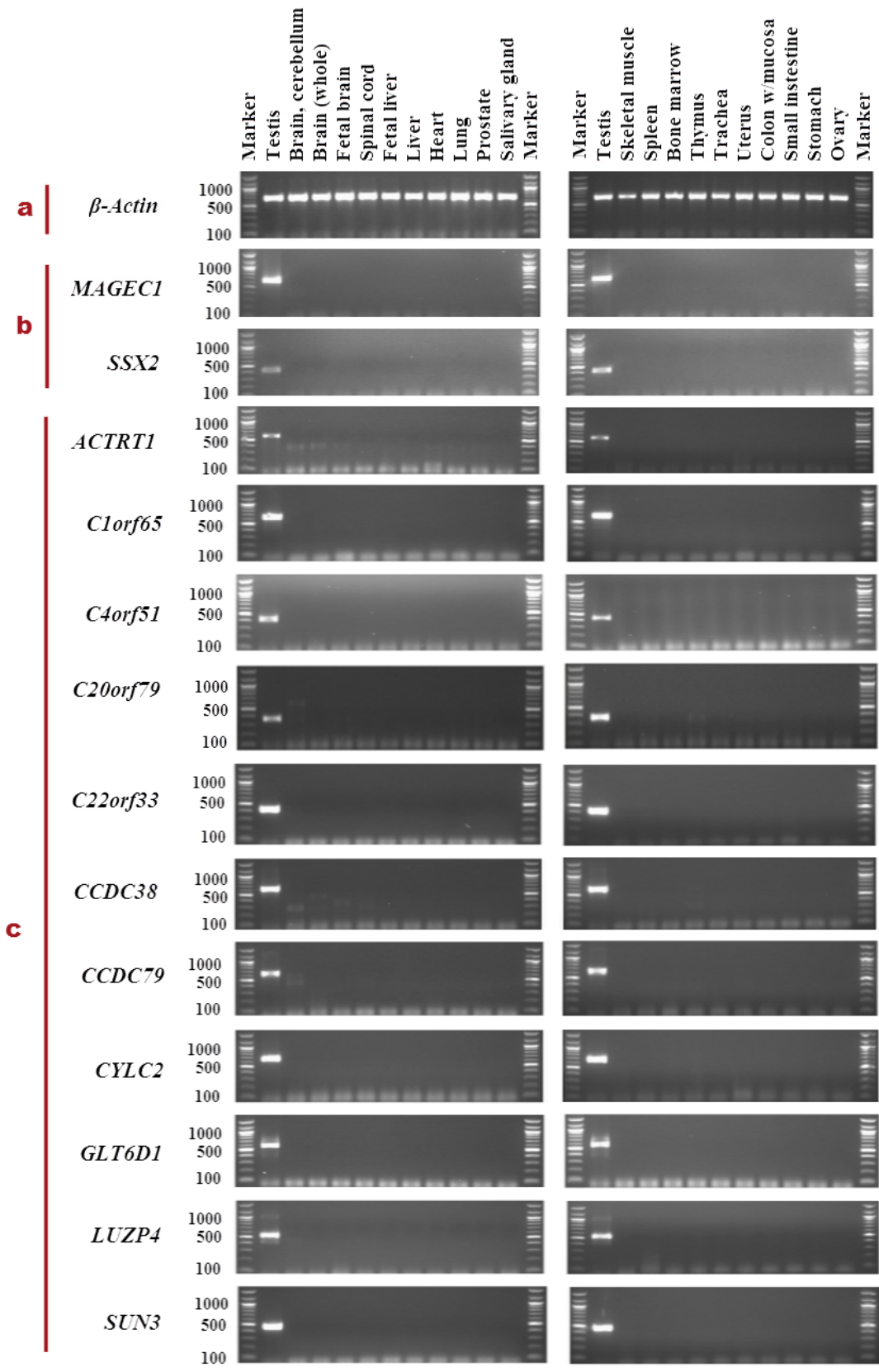
Figure 4.3. RT-PCR results for cDNA from normal tissues for EST derived genes: testis restricted genes. (**a**) β-actin served as a control for tissue cDNA; (**b**) *MAGEC1* and *SSX2* served as controls for CTA genes; (**c**) Some of the EST derived genes were restricted in expression to the normal testis (done once).
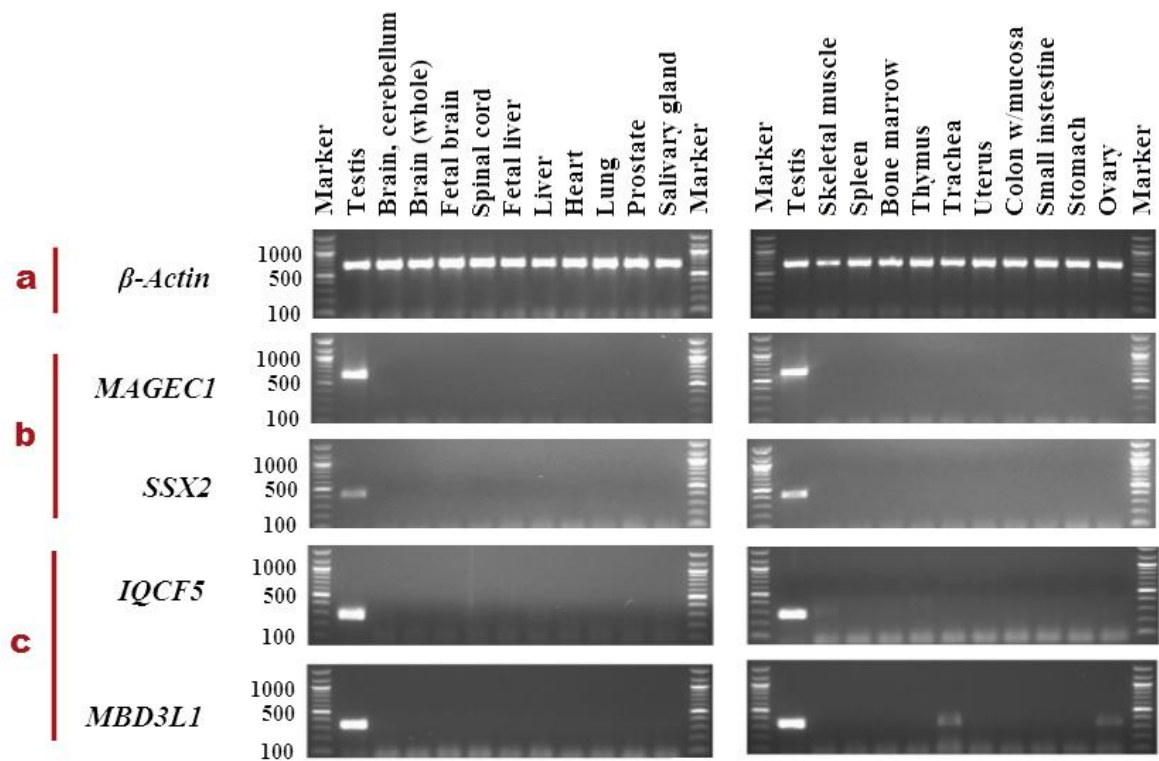
Figure 4.4. RT-PCR results for cDNA from normal tissues for EST derived genes: testis-selective genes. (**a**) β-actin as control for tissue cDNA; (**b**) *MAGEC1* and *SSX2* served as controls for CTA genes; (**c**) Some of the EST derived genes were expressed in normal testis and two or fewer of other normal tissues (done once).
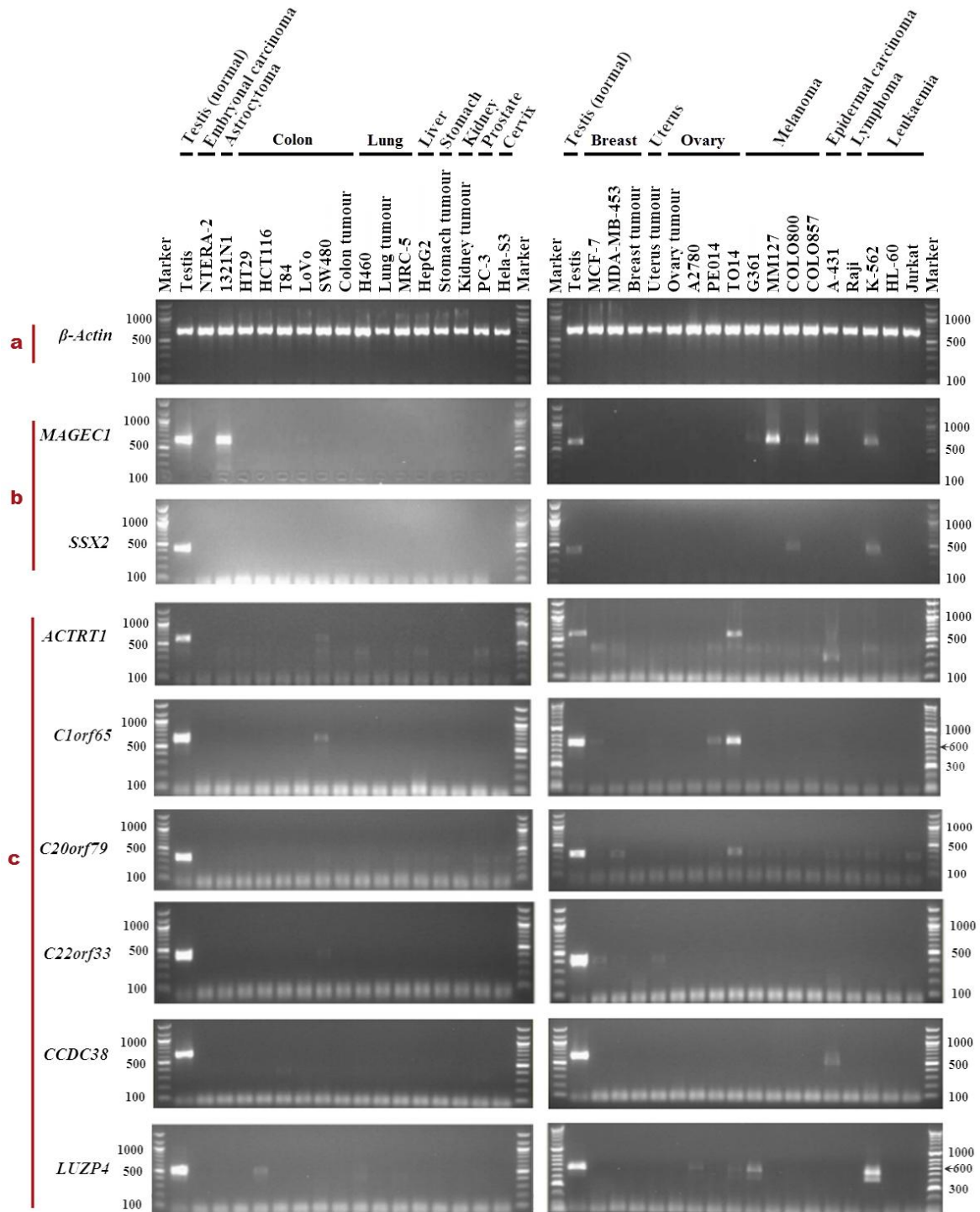
Figure 4.5. RT-PCR results for the good candidate CTA genes of EST derived genes in cancer tissues and cell lines. (**a**) β-actin served as a control for tissue and cell line cDNA; (**b**) *MAGEC1* and *SSX2* served as controls for CTA genes; (**c**) Some of the EST derived genes expressed in different cancer tissues and cell lines (done once).

76
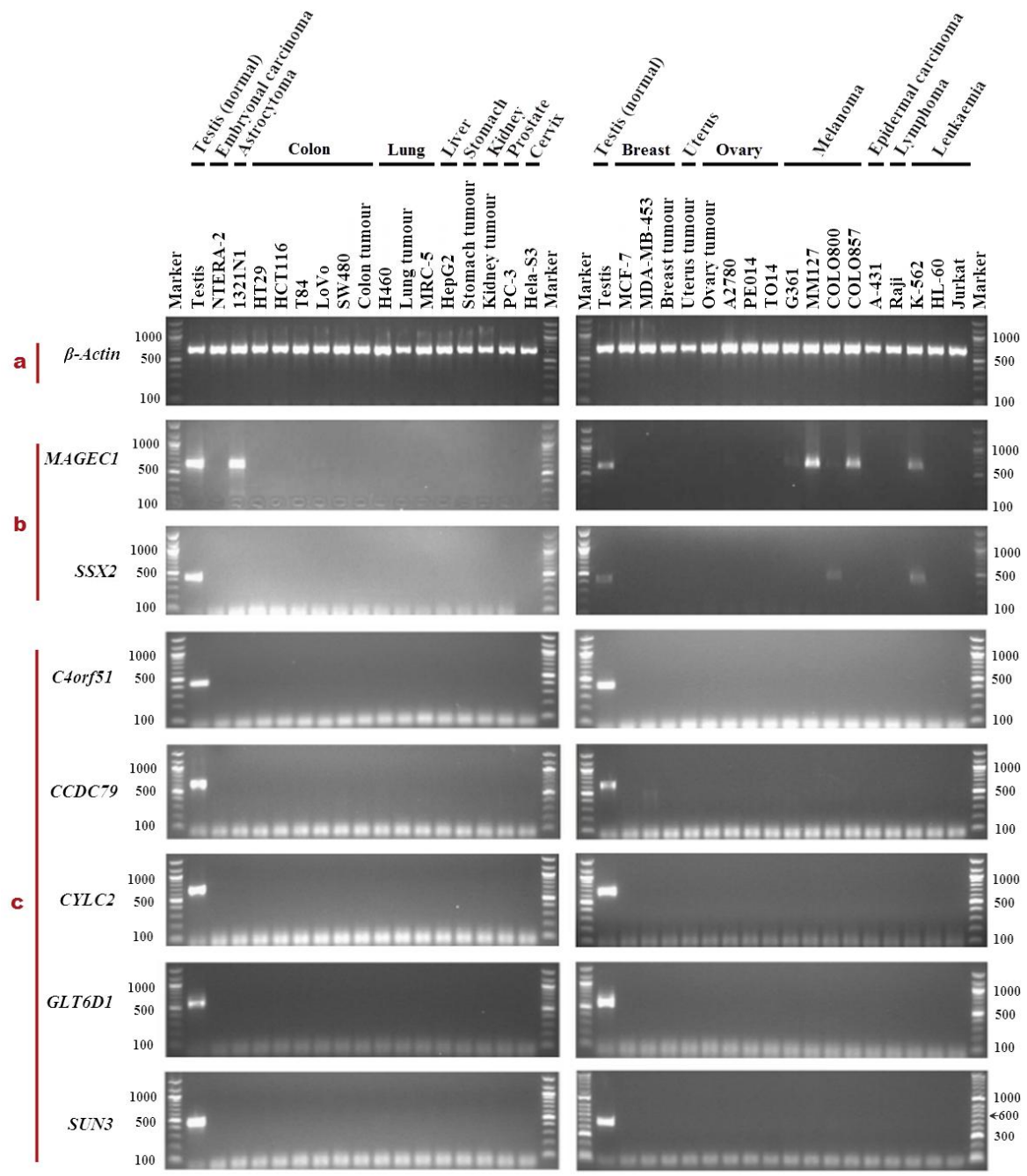
Figure 4.6. RT-PCR results for the good candidate CTA genes of EST derived genes in cancer tissues and cell lines. (**a**) β-actin served as a control for tissue and cell line cDNA; (**b**) *MAGEC1* and *SSX2* served as controls for CTA genes; (**c**) Some of the EST derived genes were expressed only in the normal testis (done once).

77
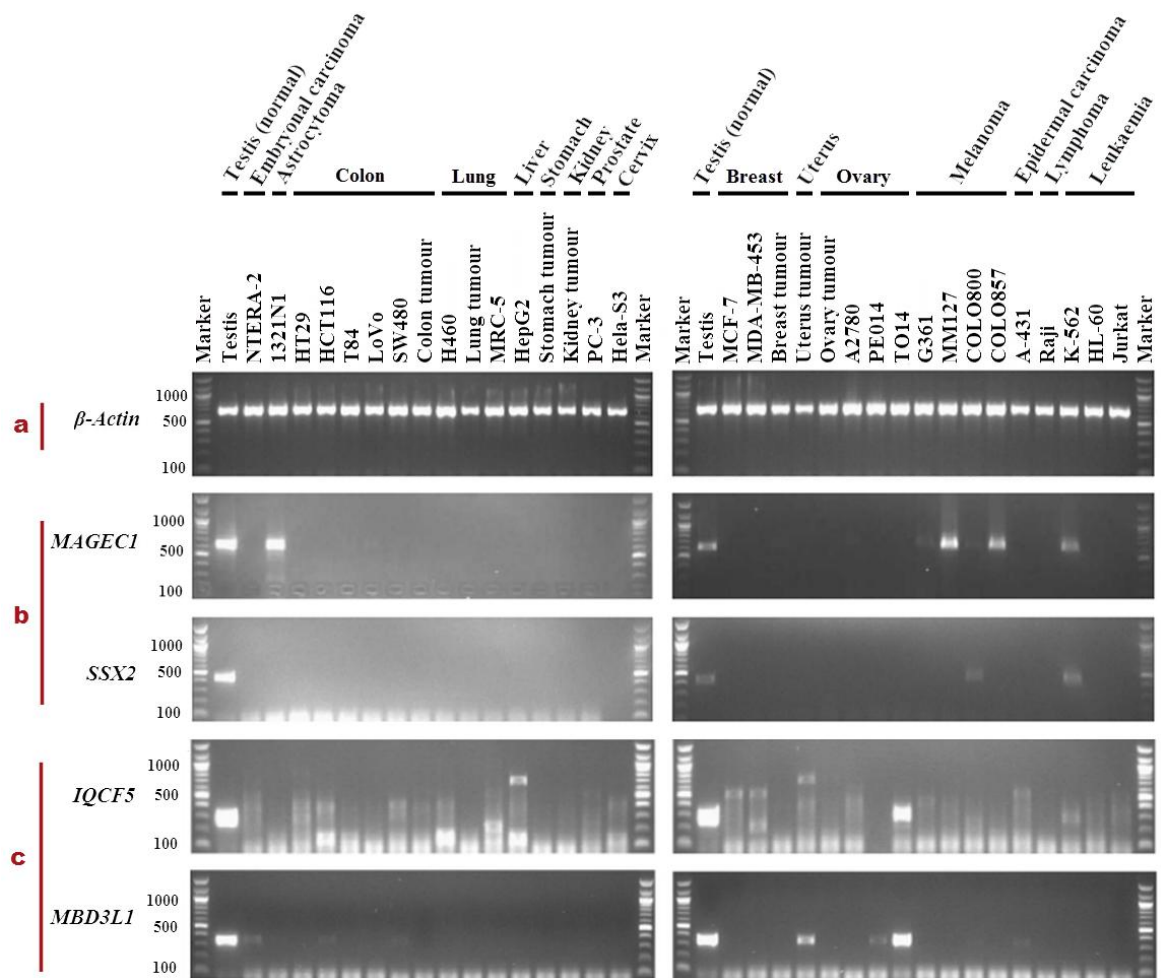
Figure 4.7 RT-PCR results for the good candidate CTA genes of EST derived genes (testis selective category) in cancer tissues and cell lines. (**a**) β-actin served as a control for tissue and cell line cDNA; (**b**) *MAGEC1* and *SSX2* served as controls for CTA genes; (**c**) Some of the EST derived genes (testis selective category) expressed in different cancer tissues and cell lines (done once).

Table 4.3. Summary of the sequencing results for EST derived genes.

Gene	Primer	Expected size (bp)	approximate product size (bp)	Normal tissue or cancer cell line	Sequence size (bp)	The identity from NCBI between the RT-PCR products and the genes
ACTRT1	F	591	400	Brain, cerebellum	195	97% LMTK2
ACTRT1	F	591	400	Brain (whole)	150	99% LMTK2
ACTRT1	F	591	400	TO14	72	Failed
ACTRT1	F	591	591	TO14	553	100%
C1orf65	F	637	637	SW480	148	100%
C1orf65	F	637	550	SW480	69	100%
C1orf65	F	637	637	TO14	375	99%
C1orf65	F	637	550	TO14	95	99%
C11orf91	F	461	461	Spleen	68	98%
C11orf91	F	461	461	Colon w/ mucosa	77	96%
C12orf42	F	508	508	Spleen	53	96%
C12orf42	F	508	508	Thymus	202	99%
C20orf79	F	369	369	Testis	331	99%
C20orf79	F	369	369	Thymus	293	100% (E(sp1)
C20orf79	F	369	369	PO14	96	100%
C22orf33	F	426	426	SW480	70	99%
C22orf33	F	426	426	MCF-7	283	99%
CCDC18	F	539	539	Bone marrow	310	99%
CCDC38	F	652	300	Brain, cerebellum	253	99% Homo sapiens chromosome 3 clone RP11-334L22 map 3p (AC037193.4)
CCDC38	F	652	390	Brain (whole)	221	98% Homo sapiens chromosome 3 clone RP11-334L22 map 3p (AC037193.4)

CCDC38	F	652	490	Brain (whole)	205	99%
CCDC38	F	652	652	A-431	66	100%
CCDC38	F	652	700	A-431	74	100%
CCDC79	F	686	686	testis	110	99%
CCDC79	F	686	550	Brain, cerebellum	89	98% RUNX1T1
CCDC79	F	686	550	MDA-MB-453	41	100% THITE_2119020
IQCF5	F	281	281	Testis	240	99%
IQCF5	F	281	400	HT29	131	99% AHCYL1
IQCF5	F	281	281	HT29	238	100%
IQCF5	F	281	700	HeP G2	600	99% C3
IQCF5	F	281	600	MDA-MB-453	236	100% AL359736.19
IQCF5	F	281	281	MDA-MB-453	68	99% PI4KA
IQCF5	F	281	250	MDA-MB-453	178	99% THBS1
IQCF5	F	281	281	PO14	238	100%
IQCF5	F	281	250	PO14	172	99% THBS1
LUZP4	F	547	400	K-562	28	99%
LUZP4	F	547	547	K-562	39	100%
LUZP4	F	547	900	K-562	44	95%
MBD3L1	F	343	343	Trachea	295	100%

Figure 4.8. Summary of RT-PCR results in normal tissues for all EST derived genes. (**a**) Expression of β-actin served as a control for the tissue cDNA; (**b**) *MAGEC1* and *SSX2* served as controls for the CTA genes; (**c**) Some of EST genes were good candidate genes and were testis restricted genes and testis selective genes; (**d**) some of the EST derived genes were expressed in different normal tissues (dark blue: gene expressed, white: does not expressed).

	Gene	Chromosome	Testis	Brain cerebellum	Brain (whole)	Fetal brain	Spinal cold	Fetal liver	Liver	Heart	Lung	Prostate	Salivary gland	Skeletal muscle	Spleen	Bone marrow	Thymus	Trachea	Uterus	Colon w/mucosa	Small instestine	Stomach	Ovary
a	β-Actin	X	■	■	■	■	■	■	■	■	■	■	■	■	■	■	■	■	■	■	■	■	■
b	MAGEC1	X	■																				
	SSX2	X	■																				
c	ACTRT1	X	■																				
	CCDC38	12	■																				
	C22orf33	22	■																				
	C1orf65	1	■																				
	LUZP4	X	■																				
	SUN3	7	■																				
	C4orf51	4	■																				
	GLT6D1	9	■																				
	CYLC2	9	■																				
	CCDC79	16	■																				
	C20orf79	20	■														■						
	IQCF5	3	■											■									
	MBD3L1	19	■														■						■
d	CCDC18	1	■	■	■		■							■		■							
	CALM2	2	■	■	■	■	■	■	■	■	■	■	■	■	■	■	■	■	■	■	■	■	■
	TDRD1	10	■	■	■				■		■	■	■	■	■	■	■	■	■	■	■	■	■
	PTPN20B	10	■	■	■	■	■	■		■	■	■	■		■	■	■	■	■	■	■	■	■
	C12orf42	12	■		■	■	■				■				■		■				■		
	CATSPER3	5	■	■	■	■	■	■		■	■	■	■	■	■		■	■		■	■	■	■
	C19orf76	19	■				■					■		■		■							
	C11orf91	11	■	■		■	■							■						■	■		
	PAX5	9	■			■	■	■		■		■			■		■		■	■		■	

81

Figure 4.9. Summary of RT-PCR results for the good CTA candidate genes from EST derived genes in cancer tissues and cell lines. (**a**) Expression of β-actin served as a control for the tissues and cell lines; (**b**) Expression of *MAGEC1* and *SSX2* served as controls for CTA genes in cancer tissues and cell lines; (**c**) Expression of the good CTA candidate genes from the testis-restricted category in different cancer tissues and cell lines; (d) Some of the good CTA candidate genes from the testis-restricted category were not expressed in any cancer tissues and cell lines; (e) Expression of the good CTA candidate genes from the testis-selective category in different cancer tissues and cell lines (dark blue: gene expressed, white: does not expressed).

4.2.2 Microarray derived genes

The 10 genes that were identified by a microarray bioinformatics comparison forerunner to cancer MA (http://www.cancerma.org.uk/) were validated by 40 cycles of RT-PCR using cDNA synthesised from RNA from 21 normal tissues, including the testis as a positive control. In addition, the *β-Actin* gene was used as control for the cDNA quality. Two CTA genes (*MAGEC1* and *SSX2*) were used as CTA controls. The genes that were expressed only in normal testis or in normal testis and normal CNS were studied further with cDNA synthesised from RNA from 33 cancer tissues and cancer cell lines.

The test on the different normal tissues resulted in 8 genes, *CCDC146, TUBA1B, GPAT2, STK31, STAG3, PVRIG, SYCP2* and *C7orf31,* being demonstrated to be expressed in different normal tissues (more than two) including the testis (Figures 4.10 and 4.13). Therefore, these genes were excluded from further study. The second group obtained was the *C10orf82* gene, which was demonstrated to have expression restricted to the normal testis; while *NUT* was expressed in the normal testis and very weak expression in fetal brain and small intestine (Figures 4.11 and 4.13).

Expression of these two genes (*C10orf82* and *NUT*) was further analysed using RNA from 33 cancer tissues and cell lines. *C10orf82* was a testis restricted gene without any expression in the cancers; *NUT* was restricted to colon cancer cell lines and ovarian cancer tissues and cell lines (Figures 4.12 and 4.14). *NUT* RT-PCR products in ovarian cancer tissues and cell lines were confirmed by sequencing (Table 4.4).
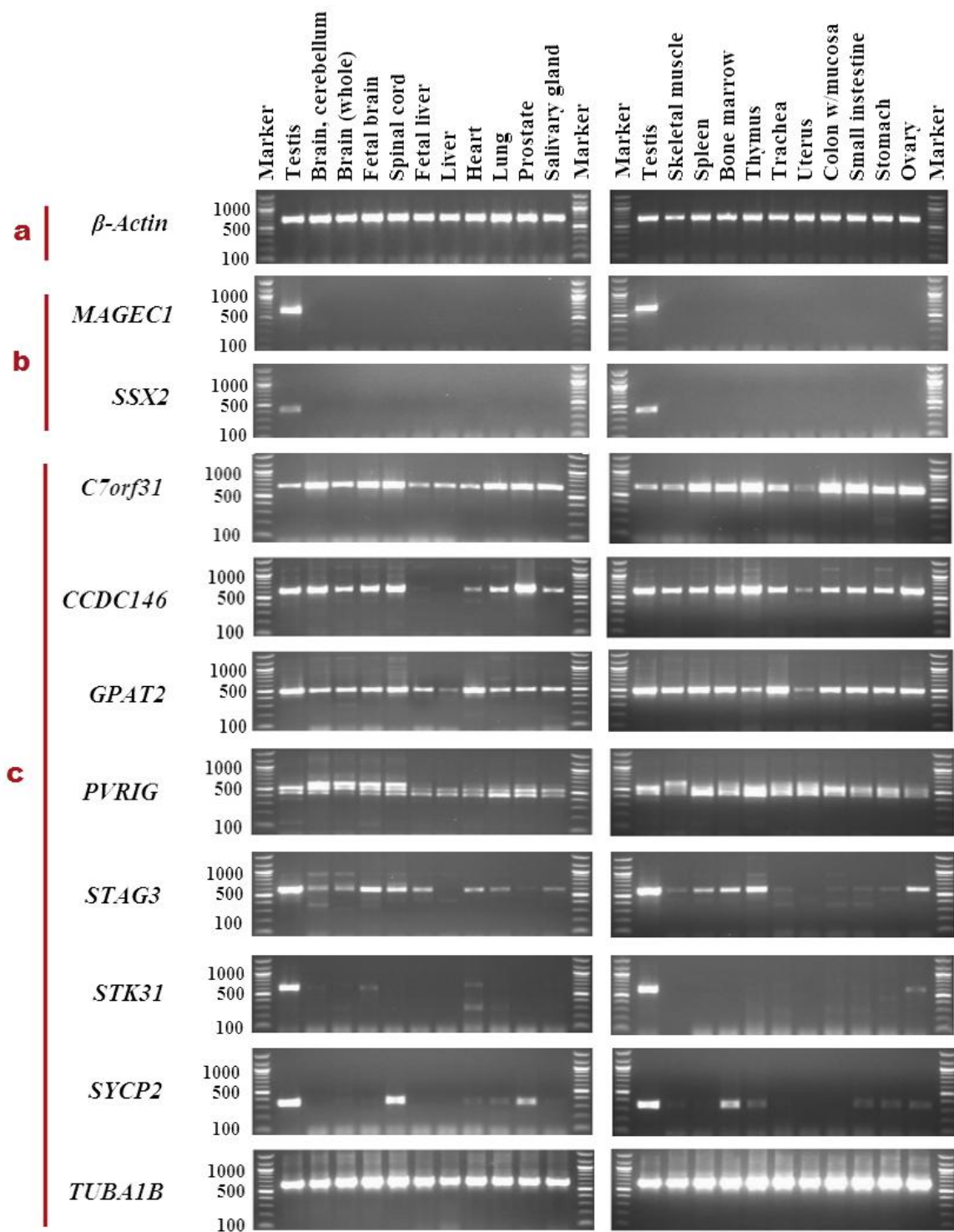
Figure 4.10. RT-PCR results for microarray derived genes in normal tissues for the excluded genes. (**a**) β-actin served as a control for tissue cDNA; (**b**) *MAGEC1* and *SSX2* served as controls for CTA genes; (**c**) Some of the microarray derived genes were expressed in different normal tissues (repeated twice).

84
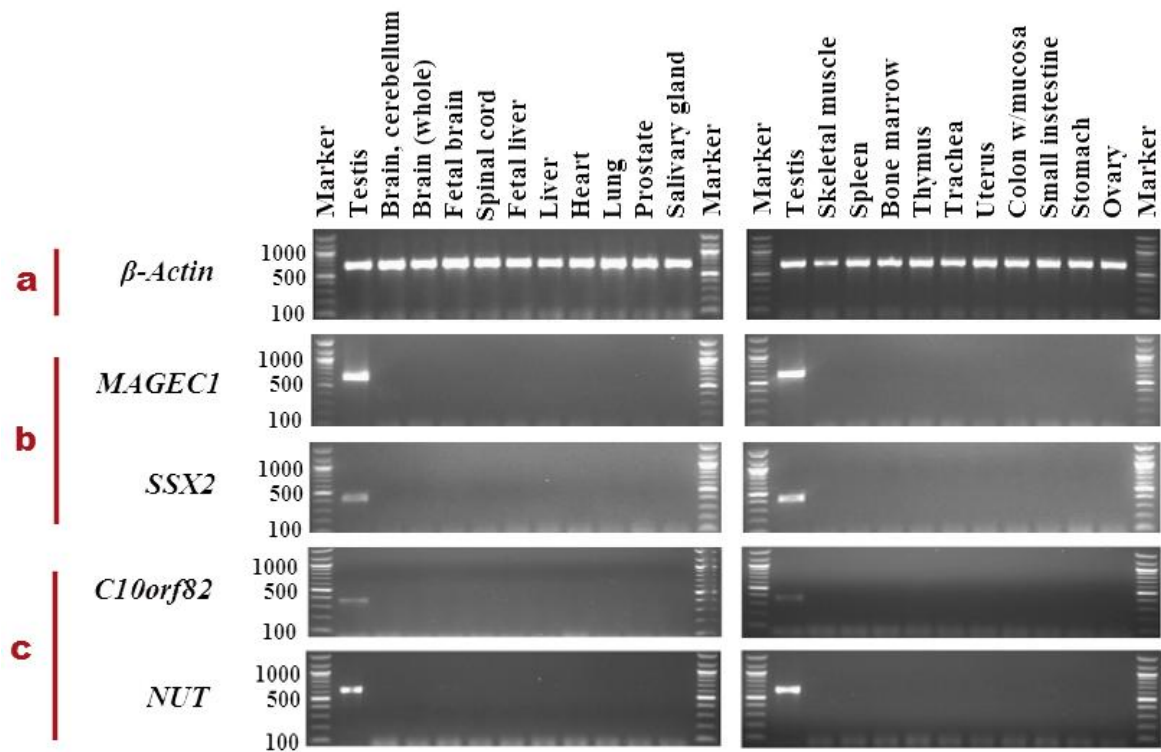
Figure 4.11. RT-PCR results for microarray derived genes in normal tissues for the good CTA candidate genes. (**a**) β-actin served as a control for tissue cDNA; (**b**) *MAGEC1* and *SSX2* served as controls for CTA genes; (**c**) Some of the microarray derived genes were restricted expression to the normal testis (repeated twice).
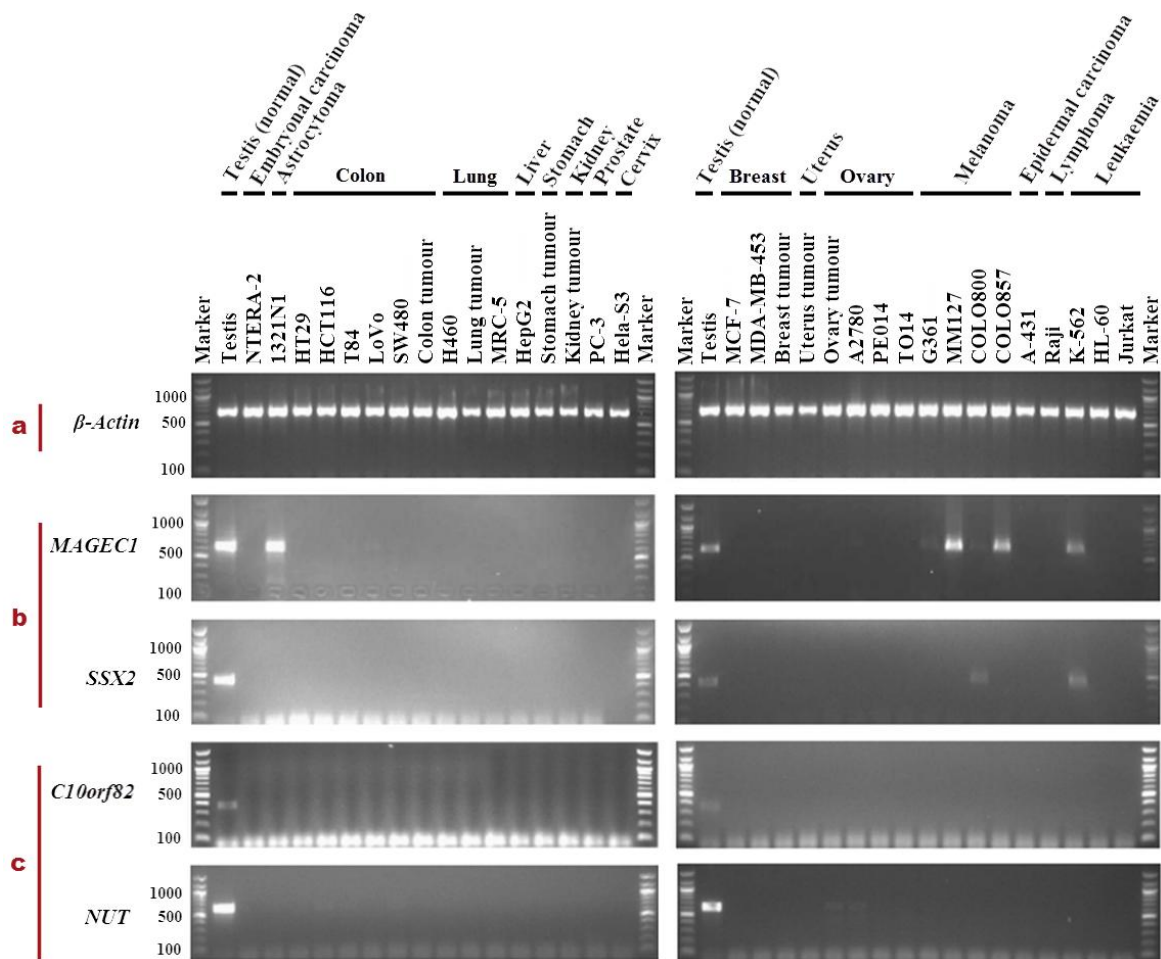
Figure 4.12. RT-PCR results for the good CTA candidates from microarray derived genes. (**a**) β-actin served as a control for tissue and cell lines cDNA; (**b**) *MAGEC1* and *SSX2* served as controls for CTA genes; (**c**) *C10orf82* was expressed in different cancer tissues and cell lines, while *NUT* expression was restricted to the normal testis (repeated twice).

Table 4.4. Summary of the sequencing results for microarray derived genes

Gene	Primer	Expected size (bp)	approximate product size (bp)	Normal tissue or cancer cell line	Sequence size (bp)	The identity from NCBI between the RT-PCR products and the genes
NUT	F2	623	623	Ovary Tumour	64	98%
NUT	F2	623	623	A2780	102	99%

86

	Gene	Chromosome	Testis	Brain cerebellum	Brain (whole)	Fetal brain	Spinal cold	Fetal liver	Liver	Heart	Lung	Prostate	Salivary gland	Skeletal muscle	Spleen	Bone marrow	Thymus	Trachea	Uterus	Colon w/mucosa	Small instestine	Stomach	Ovary
a	β-Actin	X	■	■	■	■	■	■	■	■	■	■	■	■	■	■	■	■	■	■	■	■	■
b	MAGEC1	X	■	□	□	□	□	□	□	□	□	□	□	□	□	□	□	□	□	□	□	□	□
	SSX2	X	■	□	□	□	□	□	□	□	□	□	□	□	□	□	□	□	□	□	□	□	□
c	C10orf82	10	■	□	□	□	□	□	□	□	□	□	□	□	□	□	□	□	□	□	□	□	□
	NUT	15	■	□	□	■	□	□	□	□	□	□	□	□	□	□	□	□	□	□	■	□	□
d	C7orf31	7	■	■	■	■	■	■	■	■	■	■	■	■	■	■	■	■	■	■	■	■	■
	CCDC146	7	■	■	■	■	■	■	□	■	■	■	■	■	■	■	■	■	■	■	■	■	■
	GPAT2	2	■	■	■	■	■	■	■	■	■	■	■	■	■	■	■	■	■	■	■	■	■
	PVRIG	7	■	■	■	■	■	■	■	■	■	■	■	■	■	■	■	■	■	■	■	■	■
	STAG3	7	■	■	■	■	■	□	■	■	■	■	■	■	■	■	■	■	■	■	■	■	■
	STK31	7	■	■	■	■	■	■	■	■	■	□	■	□	■	■	■	■	□	■	■	■	■
	SYCP2	20	■	□	■	■	□	■	■	■	■	■	■	■	■	■	■	■	□	■	■	■	■
	TUBA1B	12	■	■	■	■	■	■	■	■	■	■	■	■	■	■	■	■	■	■	■	■	■
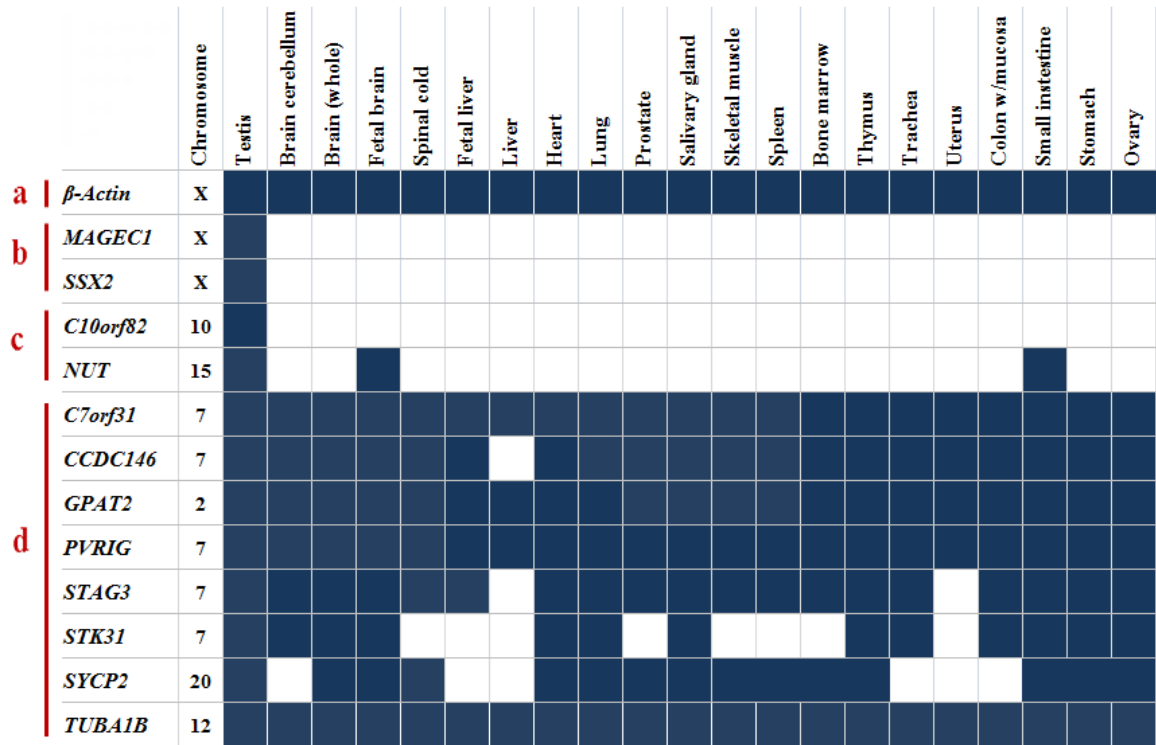
Figure 4.13. Summary of RT-PCR results in normal tissues for all microarray derived genes. (**a**) Expression of β-actin served as a control for the tissue cDNA; (**b**) *MAGEC1* and *SSX2* served as controls for CTA genes; (**c**) Some of microarray genes that were good CTA candidate genes were testis restricted genes and testis selective genes; (**d**) some of the microarray derived gens were expressed in different normal tissues (dark blue: gene expressed, white: does not expressed).
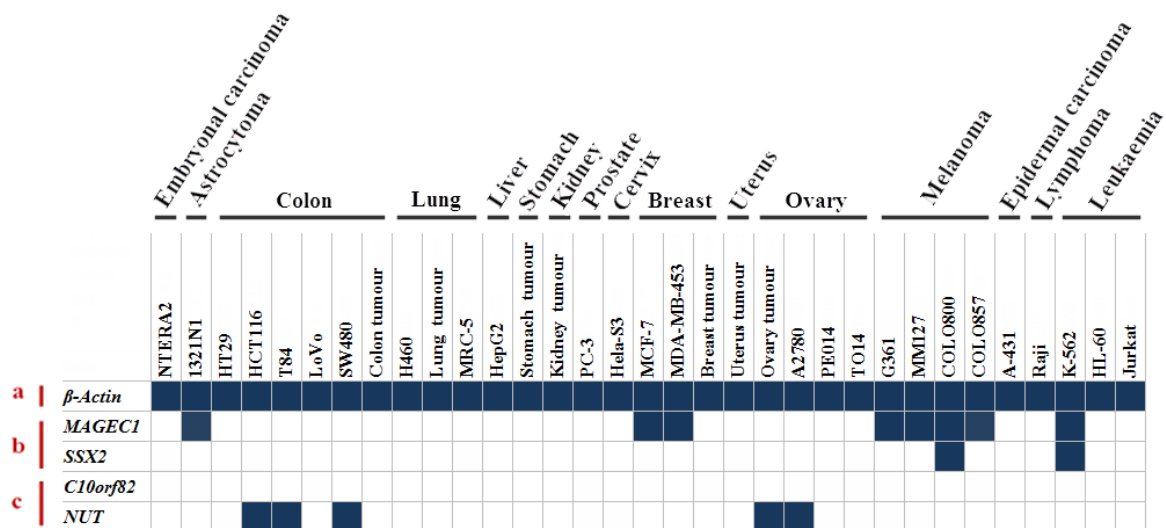
Figure 4.14. Summary of RT-PCR results for the good CTA candidate genes from microarray derived genes in cancer tissues and cell lines. (**a**) Expression of β-actin served as a control for the tissues and cell lines; (**b**) Expression of *MAGEC1* and *SSX2* served as controls for CTA genes in cancer tissues and cell lines; (**c**) Expression of the good CTA candidate genes; *C10orf82* was not expressed in any cancer tissue and cancer cell line; while the *NUT* was expressed in colon and ovarian cancers (dark blue: gene expressed, white: does not expressed).

4.2.3 Microarray meta-analysis for candidate CTA genes identified

A meta-analysis of microarray data derived from 13 cancer types (80 data sets) of cancer *vs.* normal tissues from patients was carried out through the CancerMA database (http://www.cancerma.org.uk/ ; Feichtinger et al., 2012b). The meta-analysis was achieved by running the good candidate CTA genes that were expressed in cancer and the genes expressed only in the normal testis with no expression in the cancer: *ACTRT1, CCDC38, C22orf33, C1orf65, LUZP4, SUN3, C4orf51, GLT6D1, CYLC2, CCDC79, C20orf79, IQCF5* and *MBD3L1* from the EST gene libraries and *C10orf82 and NUT (C15orf55)* from the microarray gene libraries, through the CancerMA database tool. The results of this analysis indicated up-regulation of *CCDC79, SYLC2, LUZP4, MBD3L1* and *NUT* in ovarian cancer; while *CCDC38* was up-regulated in brain cancer (Figure 3.11).
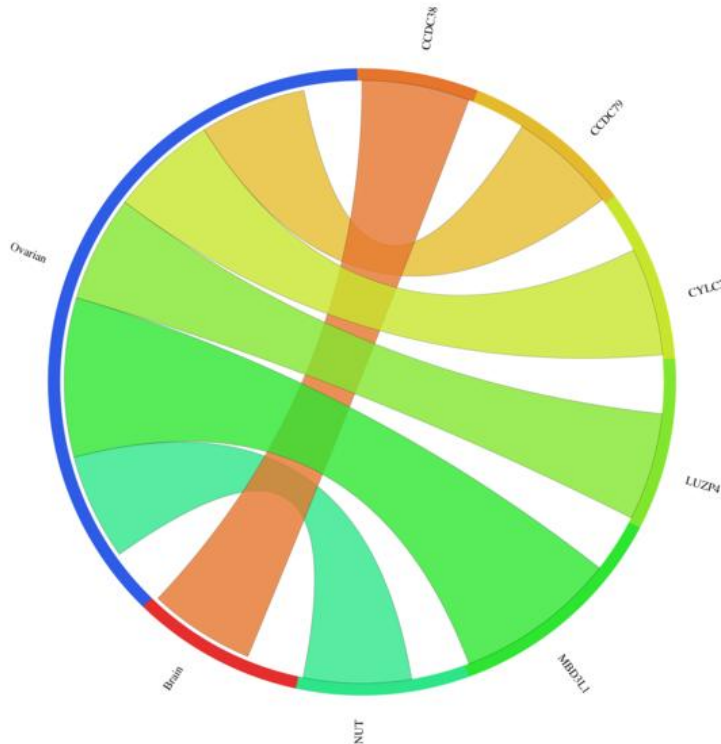
Figure 4.15. The Circos plot for the good candidate genes and the testis restricted genes: The Circos plot shows the meta-change in gene expression in relation to corresponding cancer types for the 15 genes, which gave a testis-only expression profile following RT-PCR analysis; these are represented on microarrays. Six of the 15 genes show significant up-regulation for combined cancer data sets (*CCDC79, SYLC2, LUZP4, MBD3L1* and *NUT* in ovarian cancer, while *CCDC38* was up-regulated with brain cancer). Each connection between a gene and a cancer type indicates a statistically significant mean up-regulation for that cancer type derived from a number of combined array studies for cancer tissue *vs.* normal tissue. The weight of the connection corresponds to the magnitude of the meta change in gene expression.

4.3 Discussion
4.3.1 Genes from the EST and microarray libraries showed expression restricted to the normal testis

Six genes, *SUN3, C4orf51, GLT6D1, CYLC2, CCDC79* (from the EST library) and *C10orf82* (from the microarray library), out of 31 genes showed expression restricted to the normal testis but not expressed in any of the other normal or cancer tissues/cells used in the present study. Thus, given that these genes are orthologues of meiotic spermatocyte genes, their function appears to be testis specific with no cancer activation. Some of the functions of these genes are known and others are unknown (see Tables 4.1 and 4.2).

On the other hand, the present study only used 33 cancer tissues/cells, which means that these genes might be expressed in other cancers not included in the present study. For instance, a meta-analysis was carried out on these six genes through the CancerMA online tool, which is based on microarray data from 80 cancer array sets for 13 type of cancer (Feichtinger et al., 2012b); the results of this analysis shows significant up-regulation for *CYLC2* and *CCDC79* in ovarian cancer (Feichtinger et al., 2012a). However, the RT-PCR results for both *CYLC2* and *CCDC79* in the present study did not indicate any expression in the ovarian cancer tissue or the three different ovarian cell lines (A2780, PE014 and TO14) that were used.

4.3.2 Genes from EST and microarray libraries identified as CTA genes

Nine of 31 genes from both the EST and microarray libraries were identified as possible CTA genes. Three genes, *IQCF5, MBD3L1* (EST library) and *NUT* (Microarray library), belonged to the testis-selective category, because they were expressed in two or fewer of the normal tissues and the testis; and expressed in several type of cancers. The other six genes, *ACTRT1, CCDC38, C22orf33, C1orf65, LUZP4* and *C20orf79,* belonged to the testis-restricted category, because their expression was restricted to the testis; and they were expressed in several type of cancers. Some of functions of these genes are known and others are unknown (See Tables 4.1 and 4.2).

Meta-analysis was carried out for the genes that showed significant up-regulation for *MBD3L1* and *NUT* with ovarian cancer, which confirmed the RT-PCR results. In addition, the meta-analysis results showed significant up-regulation for *CCDC38* with brain cancer, while the present study showed no expression of *CCDC38* in the single human brain astrocytoma cell line that was used.

LUZP4 (CT-8/HOM-TES-85), which is one of the EST derived genes examined in the present study, was identified as a CTA gene (Türeci et al., 2002). The present study showed that *LUZP4* is testis-restricted gene. In addition, Türeci et al. (2002) detected *LUZP4* in colon, lung, ovary, and melanoma, which confirm the present study results. Meta-analysis was carried out on *LUZP4* through the CancerMA online tool, which is based on microarray data from 13 type of cancers (Feichtinger et al., 2012b); the analysis shows significant up-regulation of *LUZP4* in ovarian cancer.

The nuclear protein of the testis (*NUT*) gene is a testis specific gene of unknown function (Teo et al., 2011). However, NUT has been detected in a rare and aggressive cancer known as NUT midline carcinoma (NMC) (Stelow and French, 2009). Most patients with this cancer die within one year of developing symptoms (French, 2010). NMC occurs as result of fusions between *NUT* and *BRD4*, resulting in an oncogene which is caused by t(15;19) (q13;p13.1) (Ziai et al., 2010). This type of cancer has been detected in tumours of the larynx, oral cavity, lung, breast, prostate, ovary, colon, uterus, kidney, pancreas, and bladder using a monoclonal antibody against NUT (Haack et al., 2009). The use of the FISH technique for both *NUT* and *BRD4* is another useful molecular approach for detecting NMC (Hsieh et al., 2011). We cannot dismiss the possibility that the *NUT* gene expression we are measuring is due to a *NUT-BRD* fusion.

A previous study showed that the fusions between *NUT* and *BRD4* cause *NUT* to interact with *p300* (*BRD4-NUT/p300*). This interaction leads to transcriptionally inactive hyperacetylated chromatin domains that inactivate *p53* (Reynoird et al., 2010). Therefore, knockdown of *BRD4-NUT* releases *p300*, to allow activation of *p53* and promotion of cell differentiation and apoptosis (Reynoird et al., 2010). Thus, *NUT* is a good CTA genes candidate, which shows significant change in the chromosome structure, and inactivates *p53*. In the present study, *NUT* was detected in the ovarian tumour and one of the ovarian cell lines, suggesting that this gene could be a good tool for both diagnosis and immunotherapy in patients with this aggressive cancer.

These genes were expressed clearly in different type of cancers and were restricted to normal testis only, or with fewer than two other additional normal tissues. Therefore, these genes are important and promising as biomarkers and immunotherapy targets for different types of cancer. However, further studies are required for these genes, such as study of the protein presence in normal and cancer tissues using western blot and/or immunohistochemistry.

4.3.3   Gene expression of the meiosis specific genes

In a previous study, *TDRD1* was identified as a CTA gene (Loriot et al., 2003). However, weakly positive signals were detected in different normal tissues testis, brain, breast, colon, spleen, ovary and thymus using 30 cycles of RT-PCR (Loriot et al., 2003). In the present study, 40 cycles of RT-PCR were applied for different normal tissues, which resulted in detection of *TDRD1* expression in different normal tissues: testis, brain cerebellum, whole brain, fetal brain, spinal cord, heart, prostate, salivary gland, skeletal muscle, spleen, bone marrow, thymus, trachea, uterus, colon, small intestine, stomach and ovary. Therefore, *TDRD1*was excluded from further study.

Other genes, *CCDC18, CLAM2, TDRD1, PTPN20B, C12orf42, CATSPER3, C11orf91, PAX5* (EST gene library), *CCDC146, TUBA1B, GPAT2, STK31, STAG3, PVRIG, SYCP2* and *C7orf31* (microarray gene library), exhibited extensive expression in different normal tissues. In the fission yeast, specific post-transcriptional mRNA degradation inhibits the production of the Rec8 protein from *Rec8* mRNA in mitotic cells (Harigaya et al., 2006). If such a post transcription pathway also occurs in mammalian cells, it may account for the expression of the meiosis-specific genes in the somatic cells. In addition, some of the normal tissues from which the RNA was extracted were obtained *post mortem* and many of the donors were elderly, which may lead to neoplastic changes in the tissues and that change might have showed expression of the candidate genes (Feichtinger et al., 2012a).

4.5   Conclusions

In this chapter, bioinformatic tools have been used to identify human meiosis-specific genes. The search started by searching for mouse meiosis genes from GermOnline, and then these genes were mapped to human orthologue genes. The human orthologue genes were then filtered using Mitocheck to avoid genes that were expressed during the mitosis process. The genes that passed through the Mitocheck were checked through two different programmes to check their expression in the cancer tissues; the first method was an expressed sequence tag (EST) from UniGene and the second method was cancer microarray data from ArrayExpress.

The results from these searches were 10 genes belonging to the microarray search and 21 genes belonging to the EST search. These genes were all tested using RT-PCR in 21

normal human tissues, including testis, which was expected to be positive. The genes that were expressed in more than two normal tissues and the testis were excluded from further study. The good candidate genes, *IQCF5, MBD3L1*, *NUT, ACTRT1, CCDC38, C22orf33, C1orf65, LUZP4* and *C20orf79*, and *NUT* were studied further in 33 cancer tissues and cancer cell lines and showed expression in different types of cancers. The expression of these genes in the cancer cell might lead to genomic change or inhibit important genes such as, *NTU* in the cancer cells. CTA genes are promising for cancer diagnosis and cancer immunotherapy. However, these genes require further investigation at the protein level in normal and cancer tissues.

Other genes, *SUN3, C4orf51, GLT6D1, CYLC2, CCDC79* and *C10orf82,* showed expression restricted to the testis but were not expressed in the other normal or cancer tissues/cells that were used. However, meta-analysis showed that *CYLC2* and *CCDC79* were up-regulated in ovarian cancer. Thus, these genes require more studies: more types of cancer should be used, and additional ovarian cancer samples should be used especially for *CYLC2* and *CCDC79*.

5 A role of SPO11 in cancer cells?

5.1 Introduction

During meiosis, inter-homologue recombination allows for the generation of a new combination of alleles in the offspring due to chromosome crossovers (Paigen and Petkov, 2010). The recombination process is initiated by the SPO11 protein, which creates a DSB in one chromatid (Paigen and Petkov, 2012). In *Saccharomyces cerevisiae*, meiotic recombination results from a pathway for the formation and subsequent processing of DNA double-strand breaks (DSBs). Six of these genes are required to form DSBs, *Spo11, Me14, Mer2, Rec102, Rec104* and *Rec114*. Thus, null mutation in one of these genes blocks DSB formation that will lead to blocking recombination (Keeney et al., 1997). In addition, there another three genes, *Red1, Hop1* and *Mek1/Mre4*, that function to encode components or modulators of chromosomes or chromatin structure required for full level of DSBs (Mao-Draayer et al., 1996).The repair of the DSB is then initiated by removing Spo11 from the DNA to generate a 3' single-stranded end; this step is performed by the Mre11-Rad50-Nbs1 (MRN) protein complex (Longhese et al., 2010), and then Exo1 and Mre11 bidirectional resection of DNA DSB (Garcia et al., 2011). In some cases this processed end invades an homologous duplex to initiate the formation of the inter-homologous connections needed for correct meiotic chromosome segregation.

Spo11 is a topoisomerase II-like protein (Bergerat et al., 1997) and it has endonuclease activity that mediates DSB formation (Bergerat et al., 1997). In *Saccharomyces cerevisiae*, Spo11 plays additional roles during meiosis and is required for the formation of the axial element (AE), the synaptonemal complex (SC) and the spindle; additionally, it aids in the maintenance of meiotic chromosome condensation (Boateng et al., 2013; Celerin et al., 2000; Loidl, 2013). In budding yeast, Spo11 also has an important role in replication control but this has been poorly explored (Cha et al., 2000). Spo11 initiates a DSB via the Y135 residue (Bergerat et al., 1997). The Spo11-Y135F mutant protein has been shown to localise to hotspot DNA but does not form DSBs (Prieler et al., 2005). Therefore, DSB formation is affected by a *spo11–Y135F* mutation as this residue is directly involved in DSB catalysis; however, this mutant is competent for DNA replication, whereas the

Spo11Δ mutant has altered DNA replication kinetics indicating a DSB-independent function in meiotic DNA replication (Cha et al., 2000).

Homozygous null mutation of *SPO11* in mice can lead to arrest and spermatocyte apoptosis during the early prophase to mid-pachynema meiosis (Romanienko and Camerini-Otero, 2000). In both male and females knockout of the *SPO11* results in infertility (Romanienko and Camerini-Otero, 2000). The absence of *SPO11* can prevent initiation of meiotic recombination, which adversely affects chromosomes segregation (Bellani et al., 2005).

Different proteins, such as ATM kinase, are associated with SPO11, thereby controlling the number of SPO11-generated DSBs (Lange et al., 2011). In addition, Rad51 and Dmc1 show a functional association with Spo11 at different meiotic stages: leptonema, early zygonema, late zygonema and early pachynema. For instance, a recent study in mice has presented this association with three different genotypes, where wild-type mice (Spo11^{wt}) were compared with mice heterozygous for a Spo11 null allele (Spo11^{het}) or overexpressing Spo11 from a transgene (Spo11^{wt+tg}) during the early meiosis leptonema stage. Rad51 was decreased by 15% and Dmc1 was decreased by 30% with Spo11^{het}; whereas both Rad51 and Dmc1 were increased by 25% in the Spo11^{wt+tg} genotype (Cole et al., 2012), indicating an alteration in DSB levels as measured by Rad51/Dmc1 association directly correlated to Spo11 level.

SPO11 is a meiosis-specific gene, which means in males it is expressed in the normal adult testis but not in the other normal tissues. However, it has been found to be expressed in several different types of cancer such as melanoma, cervical cancer and lung cancer cell lines (Koslowski et al., 2002).

As *SPO11* was identified as a cancer/testis gene (Koslowski et al., 2002), the aim of the research described in this chapter was to investigate level of SPO11 protein in different normal and cancer tissues by western blot and immunohistochemistry. Additionally, a chromatin association assay was used to assess any potential SPO11 function in different cell lines. The transcription activator-like effector nuclease (TALENs) technique was applied to knockout the *SPO11* gene from the cancer cell lines to assess whether SPO11 has function in cancer cells.

5.2 Results

5.2.1 SPO11 protein levels in normal tissue and cancer cells

SPO11 was identified as a potential CTA gene based on RT-PCR result in both normal and cancer tissues (Koslowski et al., 2002). In addition, *SPO11* expression was detected in the normal testis based on northern blot data (Romanienko and Camerini-Otero, 1999). Here, SPO11 protein levels were assessed in four human cancer cell lines: HCT116, SW480, HepG2 and NTERA2 (Figure 5.1). Moreover, siRNA was used to attempt to determine the specificity of the commercial antibodies (Figure 5.1). The band obtained on western blots using the Abnova anti-SPO11 antibody (Table 2.4) gave a band of approximately the correct predicted size of 44 kDa (Figure 5.1). However, the knockdown with different siRNA failed.
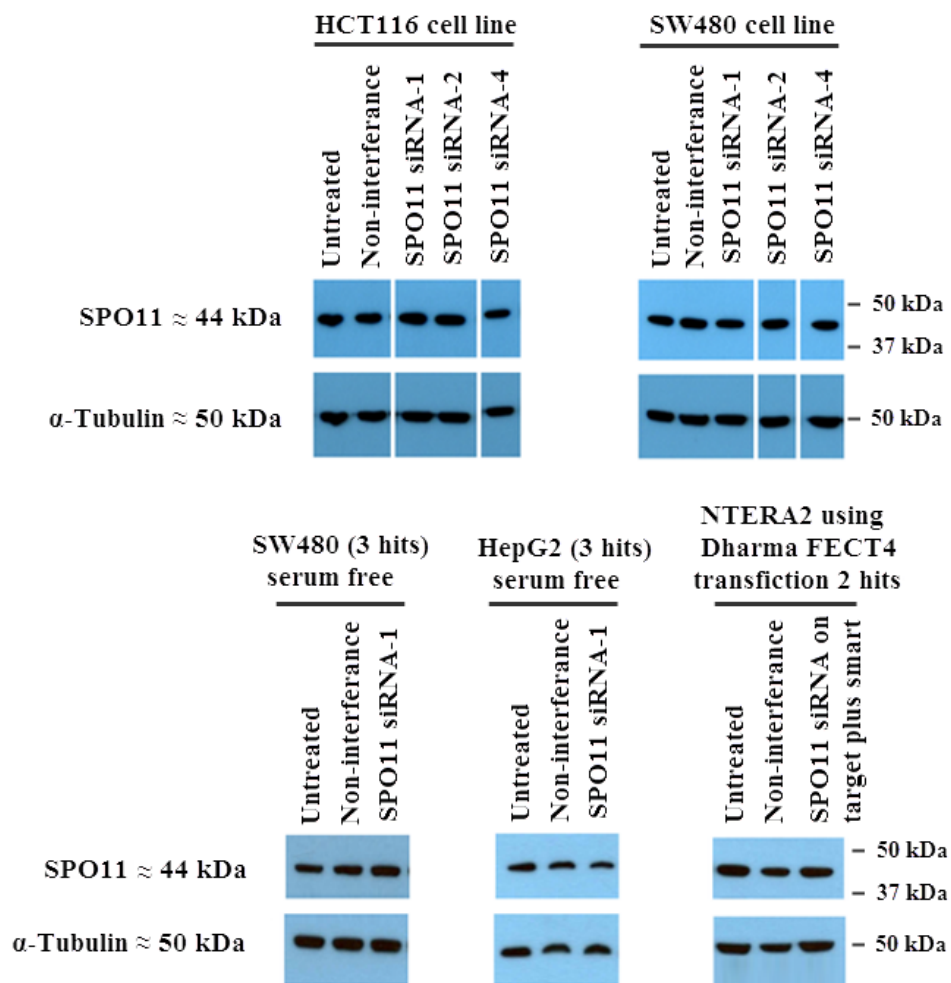

Figure 5.1 SPO11 levels in cancer cells. Western blots of whole cells extracts using commercial anti-SPO11 antibody shows a single band of the correct predicted size in all four cell lines (HCT116, SW480, HepG2 AND NTERA2). siRNA failed to reduce the levels of this protein (repeated three times).

To further ascertain whether the 44 kDa band is SPO11, the protein levels were then analysed in whole cells extracts (WCE) from 14 different normal tissues including testis tissue and 17 different cancer cell lines. GAPDH was used as control to test the quality of the WCE, and anti-MAGE-C1 antibodies were used as a CTA control. A band corresponding to the size of SPO11 (that will be referred to as SPO11) was observed in the normal testis, but not in the other normal tissues except the spinal cord, which showed a smear below the expected size. Surprisingly, western blots of different cancer cell lines including embryonal carcinoma, astrocytoma, colon, lung, liver, breast, ovary and melanoma showed a band corresponding to the correct size for SPO11 at high levels in all the cell lines used in the present study (Figure 5.2).

To explore this further, cells were fractionated into nuclear and cytoplasm extracts to identify the location of what is thought to be SPO11 protein. In the cell lines NTERA2, G361, LoVo, MCF-7, A2780, PE014 and TO14, SPO11 was detected strongly in the nucleus and weakly in the cytoplasm. However, in the HCT116 cells, it was detected in the nucleus only (Figure 5.3).

The protein levels were then examined in normal and cancer tissues by immunohistochemistry (IHC) (Table 5.1) using the normal testis as a positive control (Figure 5.4) and in normal and cancerous colon and ovary tissues (Figure 5.5) and liver and lung tissues (cancerous lung only) (Figure 5.6). SPO11 was detected in the normal testis but not in other normal tissues (colon, ovary and liver). These results confirmed the anti-SPO11 antibody is detecting a testis-specific protein. SPO11 was detected in all liver and lung cancer tissues used. However, it was only detected in about half of the ovarian cancer tissues and about 88% of the colon cancer tissues used in the present study.
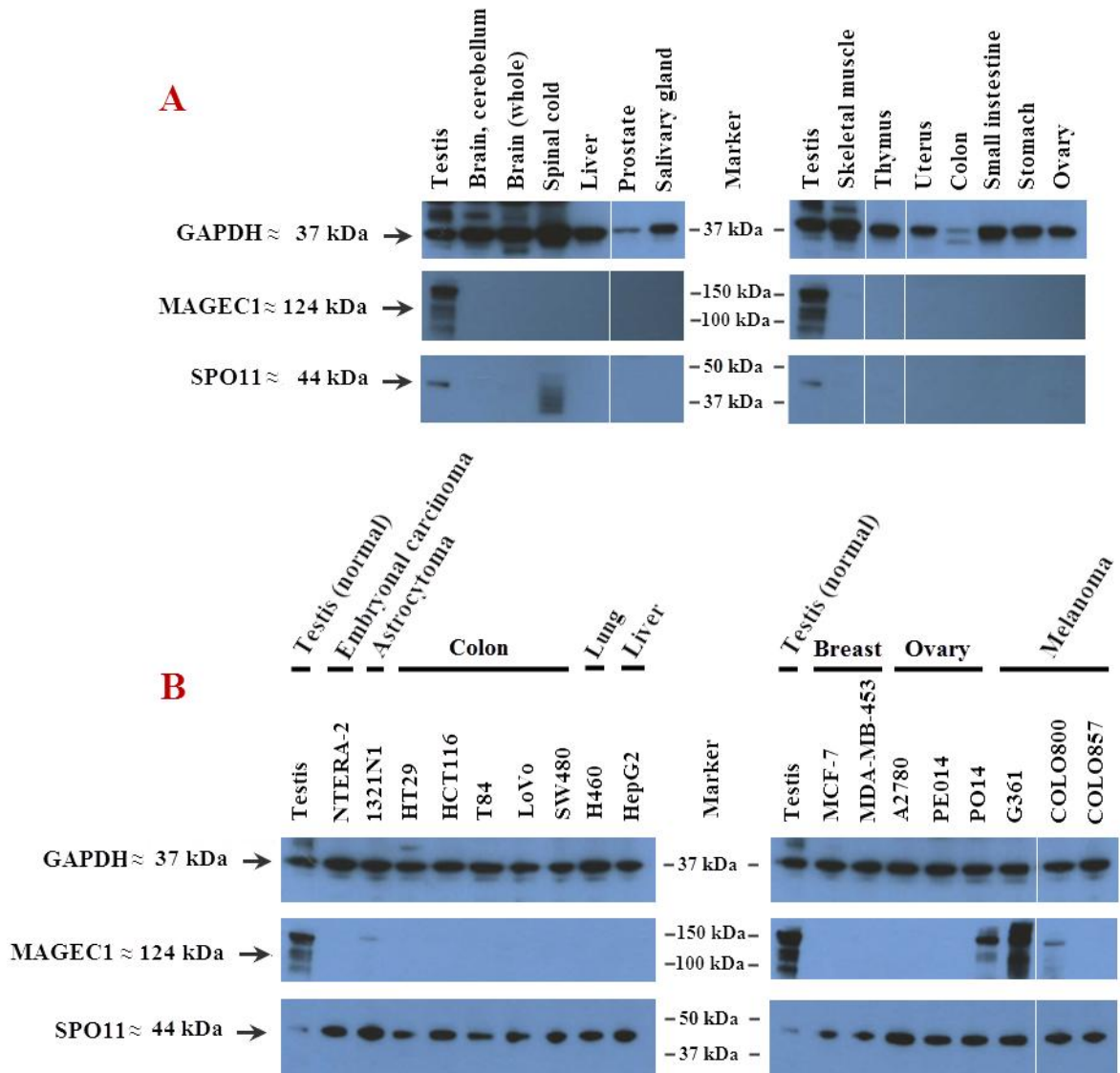
Figure 5.2 Western blot for SPO11 in normal tissues and a cancer cell lines. (A) Shows GAPDH as a control for the normal tissues, MAGE-C1 as a CTA control, and SPO11 that was present in the normal testis only. **(B)** Shows GAPDH as a control for the cancer cell lines, MAGEC1 as a CTA control is present in melanoma and one of the ovarian cancers; SPO11 was present in all cell lines (the normal tissues were repeated twice, and the cancer cell line repeated three times).
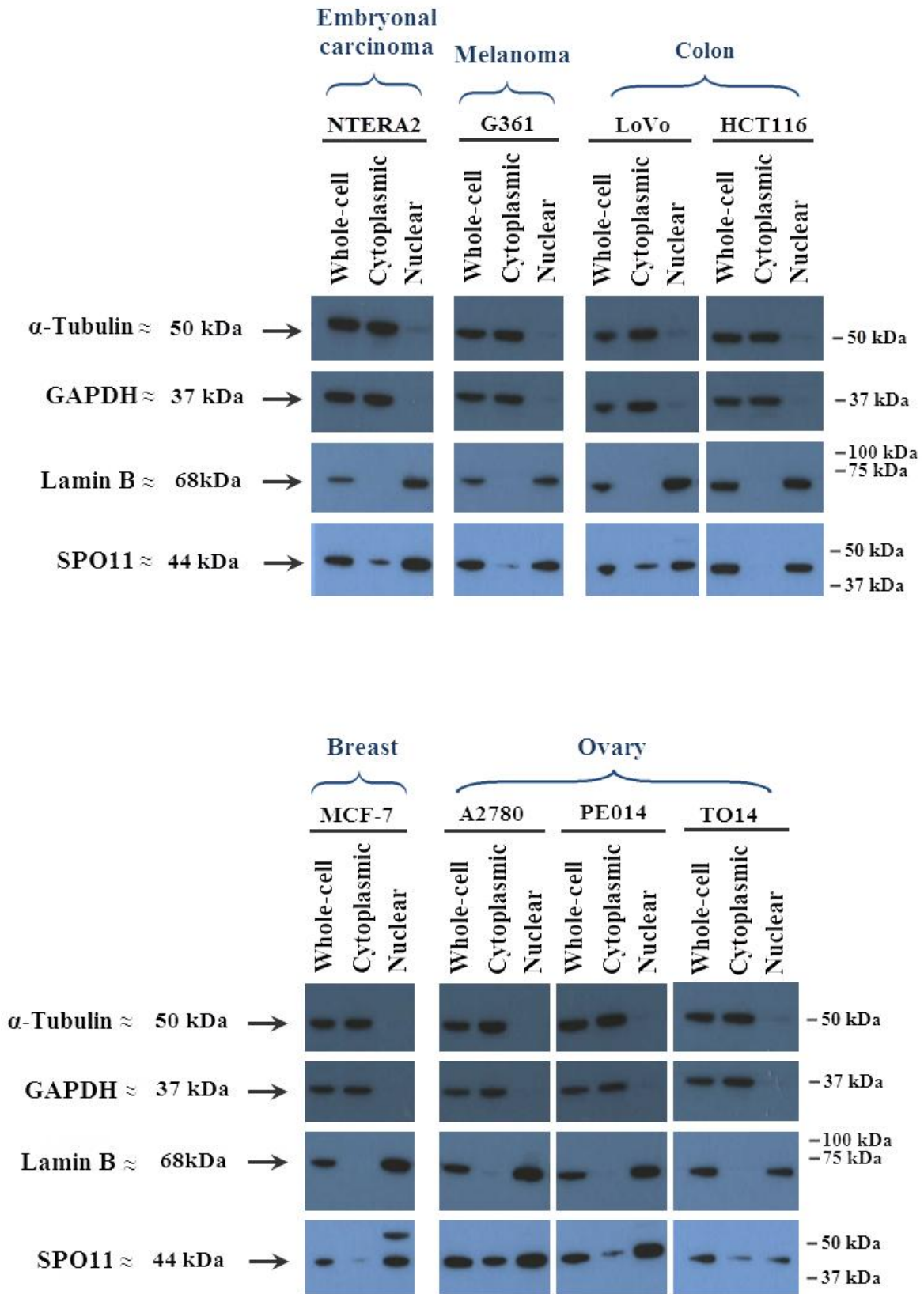
Figure 5.3 Western blot for SPO11 in different cell lines fractionations. Shows SPO11 present in both cytoplasm (low levels) and nucleus (high levels) in embryonal carcinoma, melanoma, two colon cancers, breast cancer, and three ovarian cancer cell lines. In HCT116 cells it was seen only in the nucleus (repeated twice).

Table 5.1. SPO11 IHC results for different organ tissues.

Organ	Normal tissues		Cancer tissues	
	Positive	Negative	Positive	Negative
Testis	3/3	0/3	-	-
Colon	0/8	8/8	7/8	1/8
Ovary	0/1	1/1	3/7	4/7
Liver	0/2	2/2	4/4	0/4
Lung	-	-	6/6	0/6

Normal testis tissues
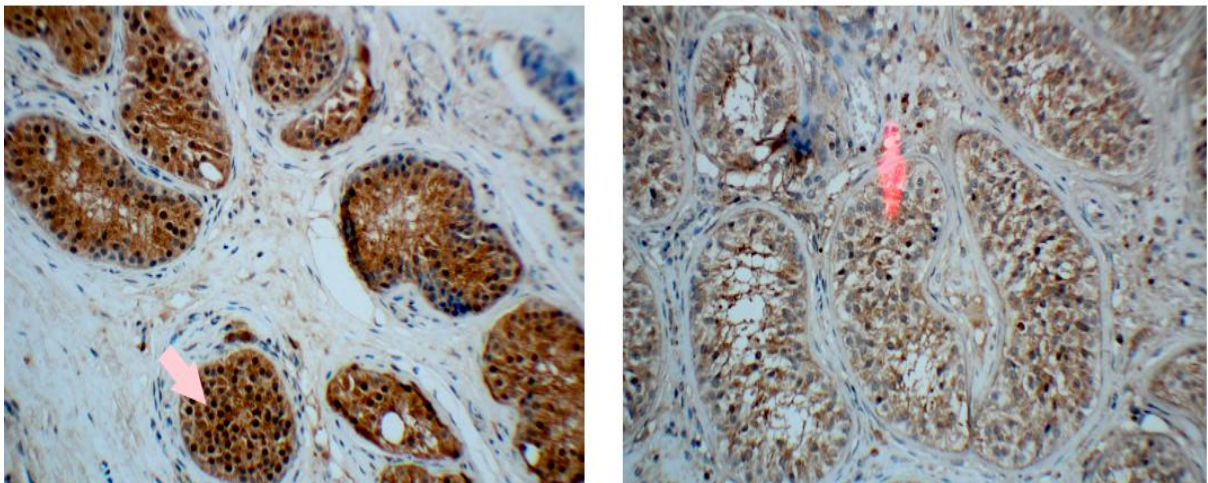
Figure 5.4 SPO11 IHC results for normal human testis tissue. Normal testis tissues were used as a positive control for CTAs. The arrows in both images show the seminiferous tubules stained brown by anti-SPO11 antibody, which presents as positive. (These results were generated with cooperation with a pathologist consultant and were repeated several times with different samples from the same organ; see Table 5.1).

	Normal tissue	Cancer tissue
Colon		
Ovary		
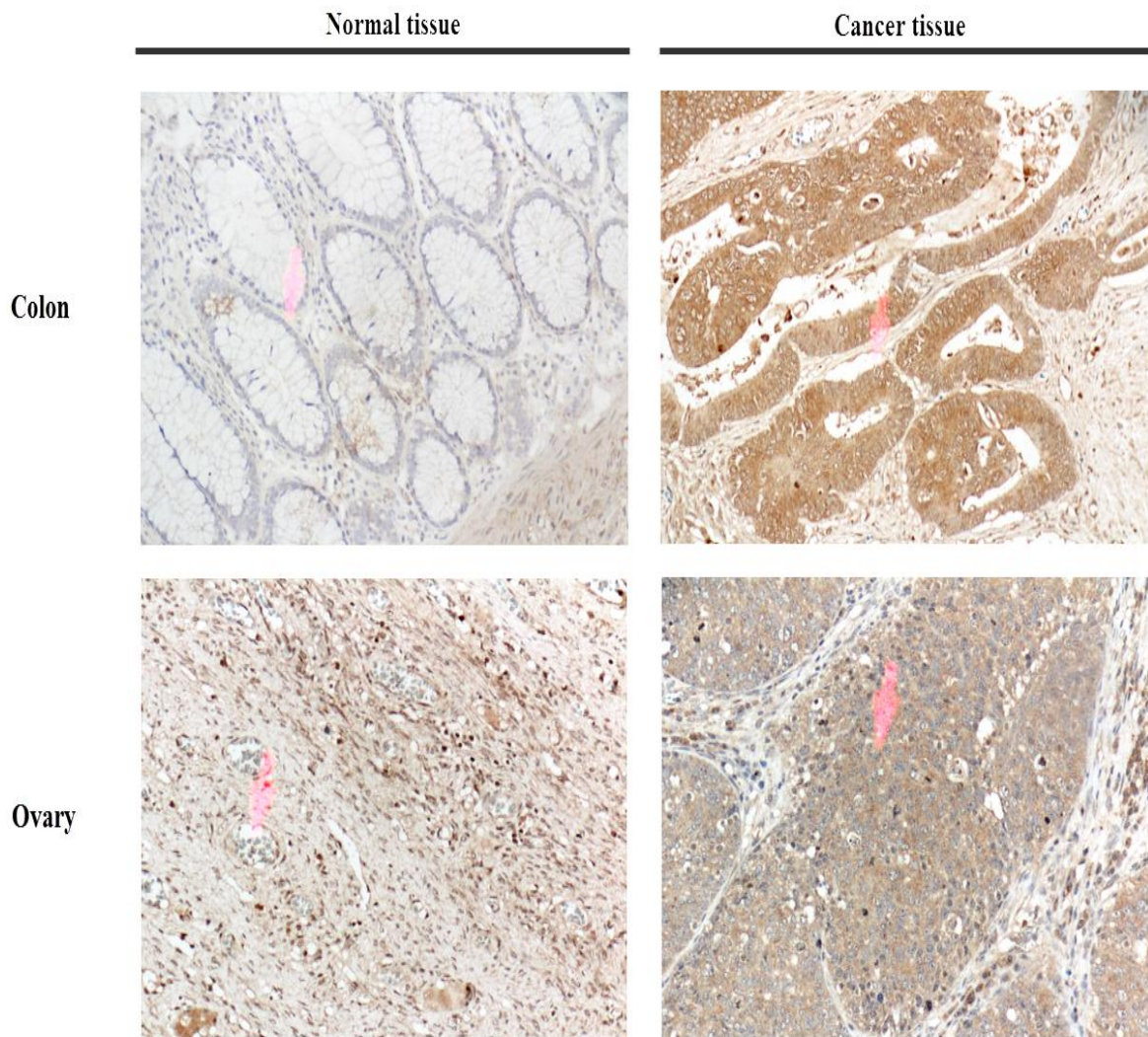
Figure 5.5 SPO11 IHC results in normal and cancerous tissues from the colon and ovary. Normal colon tissues are shown at the top left. The arrow points to the crypts in this section stained with haematoxylin, which present as negative. Moderately differentiated adenocarcinoma tissues are shown at the top right. The arrow points to the differentiated adenocarcinoma weakly stained brown by anti-SPO11 antibody, which presents as positive (the tissues were obtained from the same patient). Normal ovarian tissues are shown at the bottom left. The arrow points to the oocyte in this section stained with haematoxylin, which presents as negative. Papillary serous adenocarcinoma grade III tissues are shown on the bottom right. These are weakly stained brown by anti-SPO11 antibody and present as positive. (These results were generated with cooperation with a pathologist consultant and were repeated several times with different samples from the same organ; see Table 5.1).
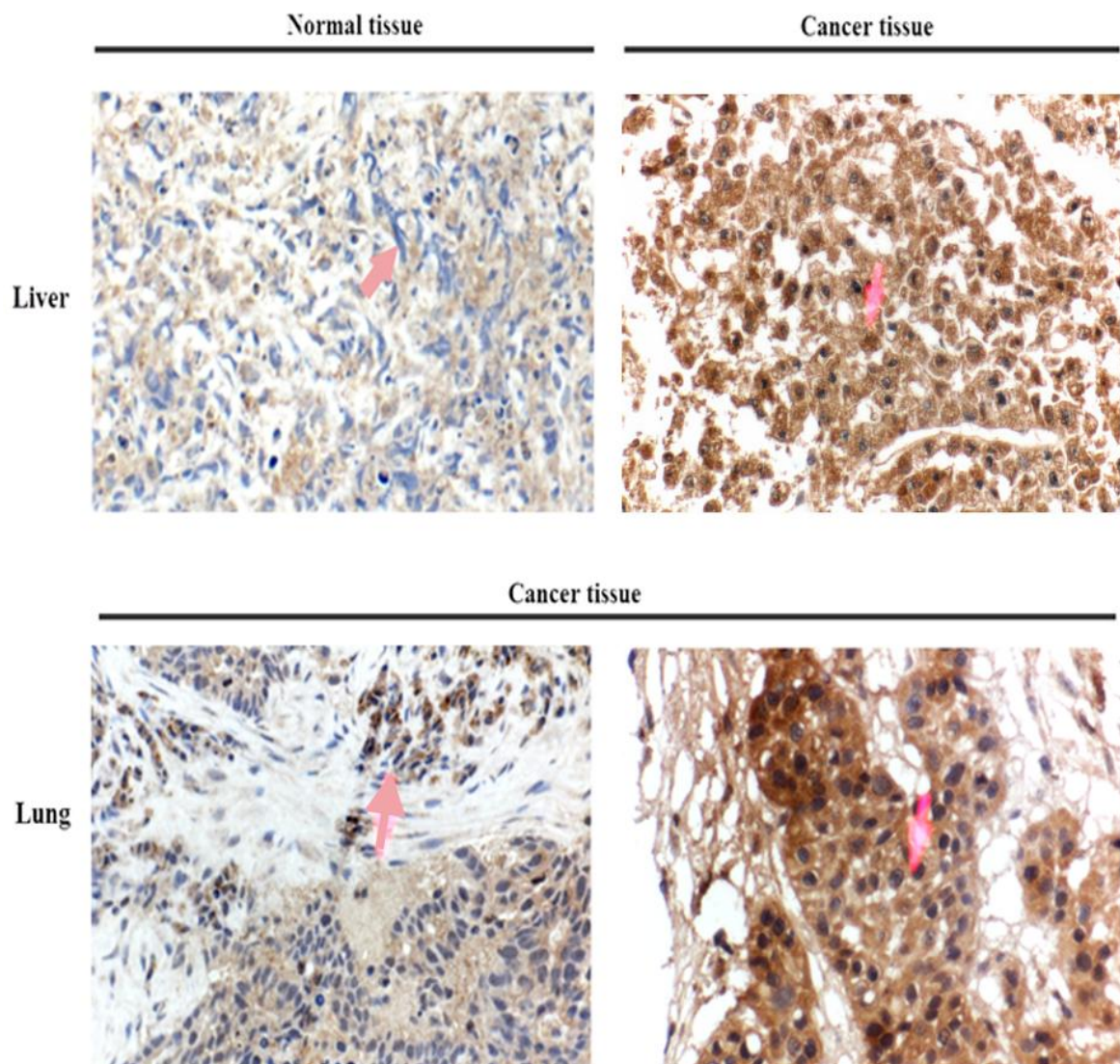
Figure 5.6 SPO11 IHC results normal and cancerous tissues from the liver and lung. (A) Normal liver tissues are shown on the left. One arrow points at the cords of hepatocytes stained with haematoxylin, which present as negative. The other arrow points at the differentiated adenocarcinoma tissues (on the right) stained brown by anti-SPO11 antibodies, which present as positive. **(B)** Lung cancer tissues; the left image shows a focal positive reaction. The arrow shows adenocarcinoma stained brown by anti-SPO11 antibodies. The right image shows squamous cell carcinoma, moderately differentiated and with strong positive brown staining by anti-SPO11 antibodies. (These results were generated with cooperation with a pathologist consultant and were repeated several times with different samples from the same organ; see Table 5.1).

5.2.2 Chromatin association assay for SPO11

The association between the SPO11 and chromatin was tested by increased salt concentration treatment of chromatin extracts. In this assay the lysates were treated with increasing concentrations of salt (NaCl). The 0.1 M Ch lysate corresponds to the proteins with no chromatin association; the 0.4 M Ch lysate corresponds to proteins that display weak chromatin association; and the 1 M Ch lysate corresponds to strongly associated chromatin proteins. The increasing salt concentration disrupts the protein interactions (protein–chromatin associations). Therefore, the protein can be seen if the protein of interest is chromatin associated strongly/weakly or not chromatin associated. It will not identify any covalent binding to DNA by a given protein.

In addition, to determine if any association occurred before or after metaphase, the cells were treated with colcemid, which breaks the spindle accumulating cells in metaphase. Different cell lines were used in this experiment, including two colon cancer cell lines (HCT116 and SW480), an embryonal carcinoma line (NTERA2) and an ovarian cancer line (A2780). Anti H3K4-3me, anti-lamin-B and anti α-tubulin were used as positive controls. The majority of SPO11 was not associated with chromatin or was washed off with 0.1 M NaCl, which means free SPO11 does not tightly associate with chromatin (Figure 5.7). In addition, some SPO11 might be covalently bound to the DNA.
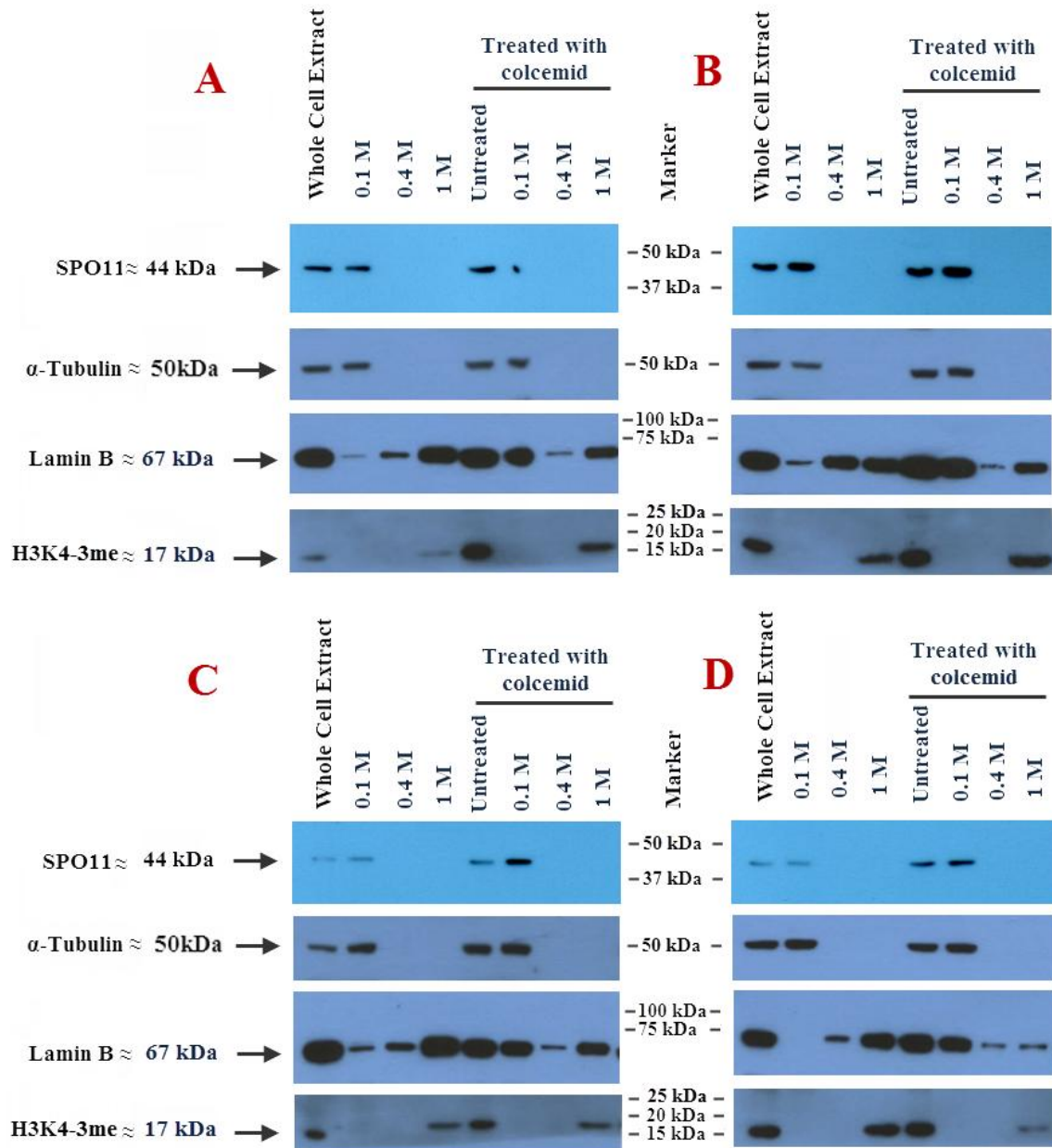
Figure 5.7 Chromatin association test for SPO11. All cell lines used show no association between SPO11 and chromatin; the H3K4 (used as a control) shows strong association with chromatin. **(A)** HCT116 cell line; **(B)** SW480 cell line; **(C)** 2780 cell line. **(D)** NTERA2 cell line (done once).

5.2.3 Knocking out *SPO11* using the TALEN technique

TALEN is a new tool for knocking out genes (see Section 1.9). For this study, TALENs were designed to knockout *SPO11*; the deletion strategy was designed to remove exon 3 of the *SPO11* gene (Figure 5.8). The TALENs were designed for this aim through Golden Gate cloning, which is a rapid cloning technique (Cermak et al., 2011). In addition, the homology arms were designed to generate deletion within exon 3.

The RVD array HD NG NG HD NI NN NI NG NN NN NG NI NI NG HD HD HD NI NG will target the forward sequence 5'- CTTCAGATGGTATCCCAT -3', and the RVD array NN NN NG NN NI NI NG HD NI HD NG NG NG NG NN NI NG will target the reverse sequence 5'- GGTGAATCACTTTTGAT -3'. The RVD from 1–10 was cloned into pFUS-A plasmid for each forward and reverse sequence individually. RVD from 11–17 of the forward and 11–16 in the reverse was cloned into pFUS-B plasmid individually. The mixture was then transformed into *E. coli* cells and which were plated onto LB agar. Three white colonies from each transformation were then screened and overnight cultures were inoculated. Plasmid DNA was isolated and the intermediary arrays were fused, along with a last repeat, and put into the desired context using one of the four backbone plasmids (pTAL4) thus fusing the *Fok*I element. Three white colonies from each transformation were then screened and overnight cultures were started. Complete constructes were then cloned into pcDNA3.1 for transfection.

The homology arms were cloned into bML3 (neoR). The reason for using the homology arms is to replace the TALEN target region. A neomycin resistance gene was used for selection after transfecting the cells with the TALEN and homology arms.

Two cell lines were then transfected using different transfection methods. The first cell line, HCT116, was transfected chemically using Lipofectamine 2000. WCE from individual neomycin resistant clones were subjected to western blotting. Reductions in SPO11 levels were seen for colonies No.13 and 14 (Figure 5.9). The second cell line, NTERA2, underwent transfection by electroporation, followed by western blotting of the cell lysates from neomycin resistant colones. Colony analysis showed a partial reduction in SPO11 levels in colonies 2, 4, 7, 16, 17, 25, 27 and 28 (Figure 5.10). However, this is

only a primary observation (as time was limited for this study). A Southern blot should be performed to confirm this observation and to check if there is a heterozygote.

The western blot analysis revealed that there did not appear to be any homozygous *SPO11* negative lines. The reduction of the SPO11 levels in the colonies 13 and 14 for HCT116 and in some NTERA2 colonies could indicate possible heterozygous deletions. Southern blot analysis of these clones is on-going to determine their *SPO11* status.
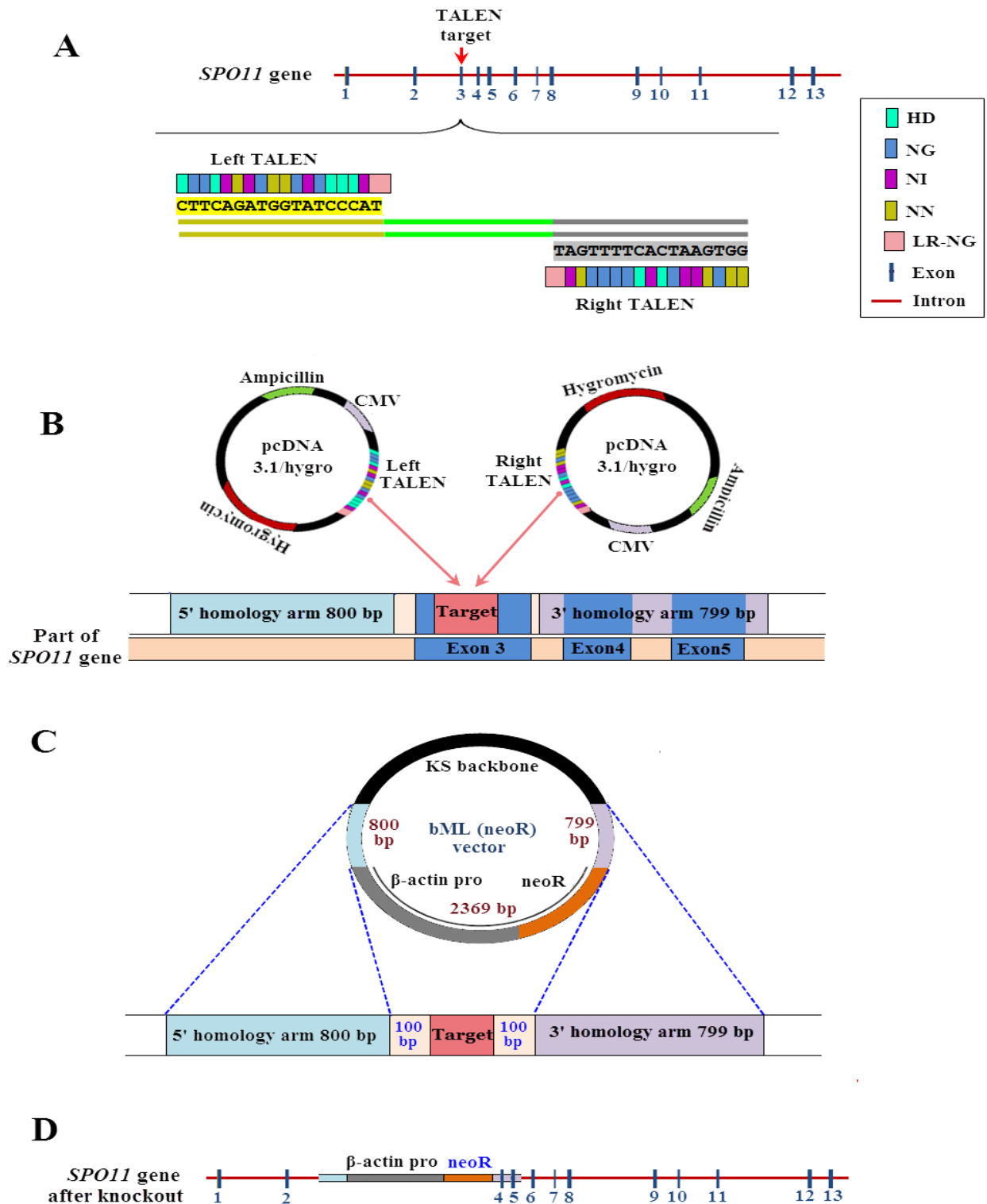
Figure 5.8 TALEN technique targeting *SPO11* gene. The TALEN technique applied to target *SPO11* gene in multi-steps. **(A)** Shows the third exon of *SPO11* as a TALEN target; and shows the TALEN designed based on the nucleases binding target. **(B)** Shows the right and the left TALEN cloned individually into pcDNA 3.1/hygro vectors that generates a frame shift by remove 89 bp of Exon 3 **(C)** Shows the 5' and 3' homology arms both cloned into bML (neoR) vector and then the target in the *SPO11* gene. **(D)** The *SPO11* gene sequence after disruption of part of the third exon and repair with the homology arms in the bML (neoR) vector.
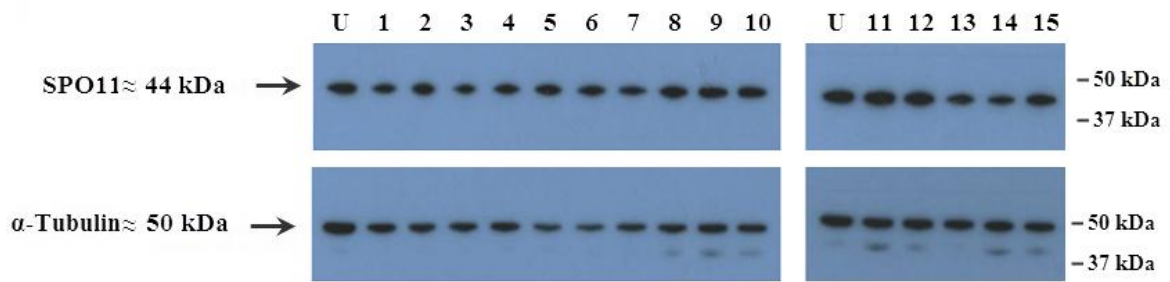
Figure 5.9. Western blots of HCT116 colonies following chemical transfection with TALENs and homology arms. The SPO11 protein levels compared with α-tubulin; only the colonies 13 and 14 show a reduction in SPO11 protein (done once).
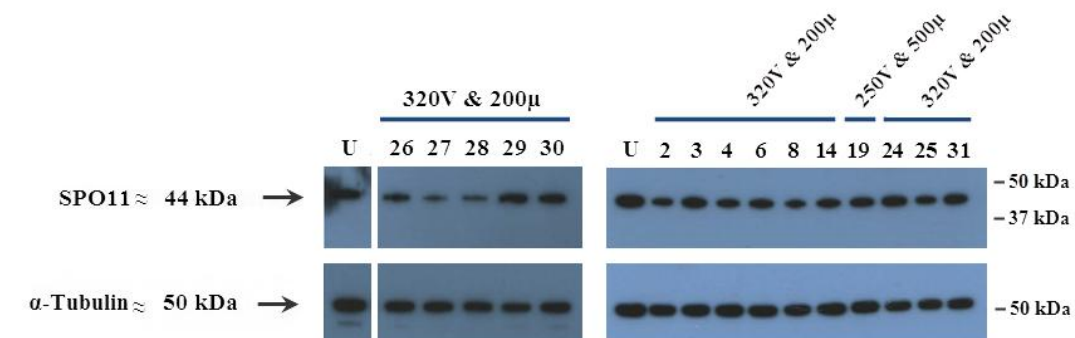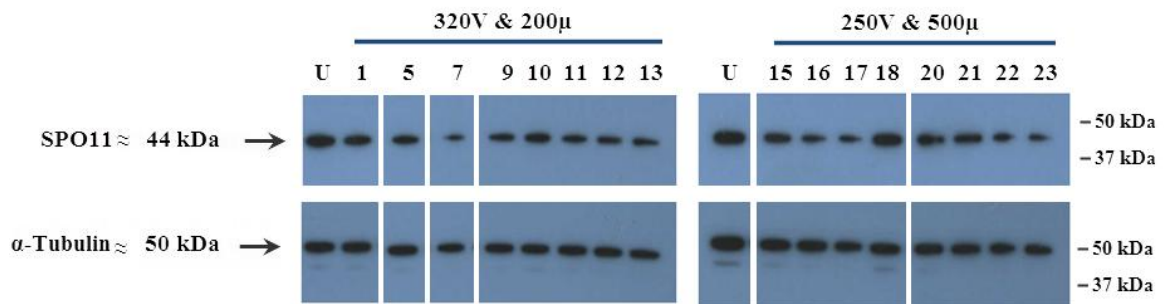
Figure 5.10. Western blots of NTERA2 colonies following electroporation transfection by with TALENs and homology arms. The SPO11 protein levels compared with α-tubulin; the strongest reductions in SPO11 protein were in colonies 2, 4, 7, 16, 17, 25, 27 and 28 (done once and samples: 2, 3, 4, 6, 8, 14, 19, 24 and 25 were repeated twice).

5.2.4 The growth of colon cancer cells transfected with siRNA and TALENs

The previous western blot and siRNA results demonstrated that we could not obtain a reduction in SPO11 levels with siRNA. One possibility is that the antibodies are not specific. However, the band size is correct and normal human tissues the band only detected in the testis [with an ill-defined smear being picked up in the spinal cord extract; (Figure 5.2 A)]. An alternative explanation could be that *SPO11* is essential to the cancer cells and so cells are refractory to siRNA mediated reduction. The lack of any TALEN derived homozygous deletion lines could support this hypothesis. Moreover, *SPO11* is remarkable in that it appear to be present in all cell lines tested and many cancerous tissues (see above) implying it is required for growth. We set out to test this hypothesis by using an extreme limiting dilution assay (ELDA), a standard cell survival assay.

5.2.4.1 *The growth of colon cancer cells transfected with siRNA*

Two colon cell lines were cultured as colonosphere colonies. The spheres were disrupted and cells were seeded in serial dilution of 100, 10 and 1 cell per well. The colonosphere colonies for both cell lines were restored to the parental, non-spheroid form using normal 96 well plates, which allow the cells to attach to the surface. These cells were transfected twice with non-interference HiPerFect transfection (as negative controls) and different siRNAs. The first transfection was performed at the same time of the cell seeding; the second was four days after the cell seeding.

The first results were obtained 5 days after the transfection. The numbers of surviving cells transfected with siRNA-4 against *SPO11* at both 10 and 100 cell seedings were much lower than the numbers of cells that survived following the untreated, non-interference, transfection only, siRNA-1, and siRNA-2 transfection (for a results summary, see Tables 5.2 and 5.3) (see also the results in the appendix). The second set of results was obtained 10 days after transfection. The numbers of surviving cells transfected with siRNA-4 at both 10 and 100 cell seedings were much lower (as described in Tables 5.2 and 5.3) than the numbers of cells that survived in the untreated and control conditions, or following transfection with siRNA-1 and siRNA-2 (Figure 5.11a and b; 5.12 a and b) (for a results summary, see Tables 5.2 and 5.3).

The final set of results was obtained 20 days after transfection. The numbers of cells surviving after transfection with siRNA-4, at both 10 and 100 cell seedings, remains much lower (as described in Tables 5.2 and 5.3) than the numbers of cells that survived in the untreated and the control conditions, or following siRNA-1and siRNA-2 transfection (for a results summary, see Tables 5.2 and 5.3) (see also the results in the appendix).

Table 5.2. Summary of the SW480 cell growth after transfection with siRNA, following result is a summary of the growth in one of the six wells, the growth in which was all similar (± 10%)

Cell line	Days after Transfection	Treatment	100 cells	10 cells	1 cell
SW480	Day 5	Untreated	≈30% confluent	10 colonies	Single colony
		Non-interference	≈30% confluent	8 colonies	Single colony
		Transfection only	≈30% confluent	8 colonies	Three colonies
		SPO11 siRNA-1	≈20% confluent	7 colonies	Single colony
		SPO11 siRNA-2	≈30% confluent	6 colonies	Single colony
		SPO11 siRNA-4	Two colonies	3 colonies	0
SW480	Day 10	Untreated	≈60% confluent	10 colonies	Single colony
		Non-interference	≈60% confluent	8 colonies	Single colony
		Transfection only	≈60% confluent	7 colonies	0
		SPO11 siRNA-1	≈30% confluent	6 colonies	0
		SPO11 siRNA-2	≈50% confluent	9 colonies	Single colony
		SPO11 siRNA-4	Single colony	0	0
SW480	Day 20	Untreated	≈80% confluent	10 colonies	Single colony
		Non-interference	≈80% confluent	10 colonies	Two colonies
		Transfection only	≈80% confluent	8 colonies	0
		SPO11 siRNA-1	≈50% confluent	6 colonies	0
		SPO11 siRNA-2	≈50% confluent	11 colonies	Two colonies
		SPO11 siRNA-4	Two colonies	0	0

Table 5.3. Summary of the HCT116 cell growth after transfection with siRNA, following result is a summary of the growth in one of the six wells, the growth in which was all similar (± 10%)

Cell line	Days after Transfection	Treatment	100 cells	10 cells	1 cell
HCT116	Day 5	Untreated	≈80% confluent	9 colonies	Single colony
		Non-interference	≈70% confluent	11 colonies	Single colony
		Transfection only	≈80% confluent	9 colonies	0
		SPO11 siRNA-1	≈50% confluent	8 colonies	Two colonies
		SPO11 siRNA-2	≈50% confluent	8 colonies	Two colonies
		SPO11 siRNA-4	≈12 colonies	3 colonies	0
HCT116	Day 10	Untreated	≈Confluent	≈50% confluent	Single colony
		Non-interference	≈Confluent	≈60% confluent	Two colonies
		Transfection only	≈Confluent	≈50% confluent	Three colonies
		SPO11 siRNA-1	≈90% confluent	≈30% confluent	Three colonies
		SPO11 siRNA-2	≈Confluent	≈40% confluent	Two colonies
		SPO11 siRNA-4	≈60% confluent	6 colonies	0
HCT116	Day 20	Untreated	Over grown	≈90% confluent	Single colony
		Non-interference	Over grown	≈90% confluent	Three colonies
		Transfection only	Over grown	≈90% confluent	Two colonies
		SPO11 siRNA-1	Over grown	≈80% confluent	Three colonies
		SPO11 siRNA-2	Over grown	≈Confluent	Two colonies
		SPO11 siRNA-4	≈90% confluent	≈80% confluent	0

Figure 5.11a. Growth of the SW480 cell line 10 days after transfection with different siRNA, with 10 cells seeded. Non-interference and HiPerFect transfection (as negative controls) and untreated cells were used to compare the growth of cells transfected with different siRNA (the arrows point to the cell colonies as an example to show the cell growth in this figure). The growth of cells transfected with SPO11-siRNA4 is negatively affected compared to the growth of the untreated and transfection control cells (done once).
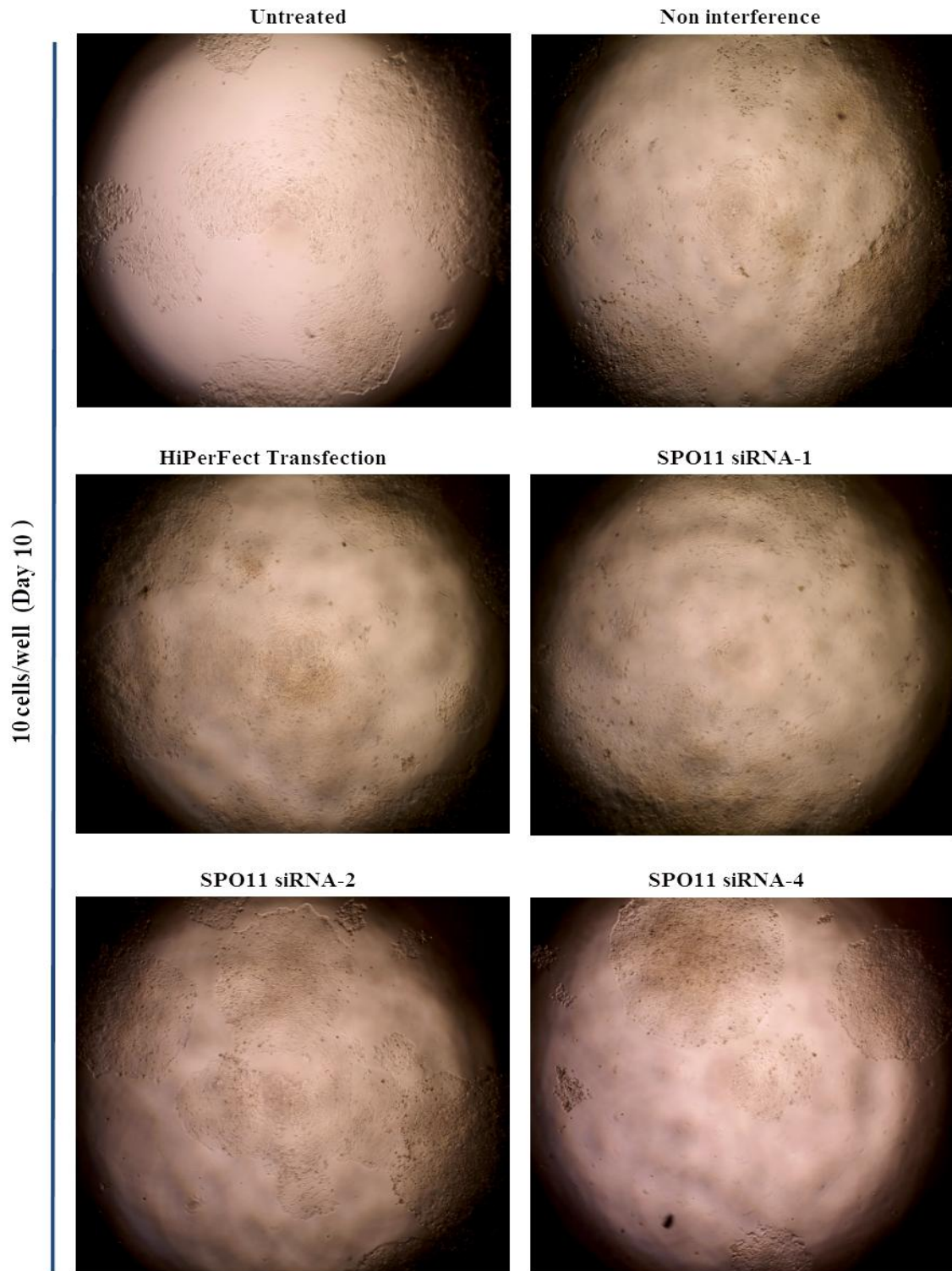
Figure 5.11b. Growth of the HCT116 cell line 10 days after transfection with different siRNAs, with 10 cells seeded. Non-interference and HiPerFect transfection (as negative controls) and untreated cells were used to compare the growth of cells transfected with different siRNAs. The growth of cells transfected with SPO11-siRNA4 is negatively affected compared to the growth of untreated and transfection control cells (done once).

Untreated | Non interference

HiPerFect Transfection | SPO11 siRNA-1

SPO11 siRNA-2 | SPO11 siRNA-4

100 cells/well (Day 10)
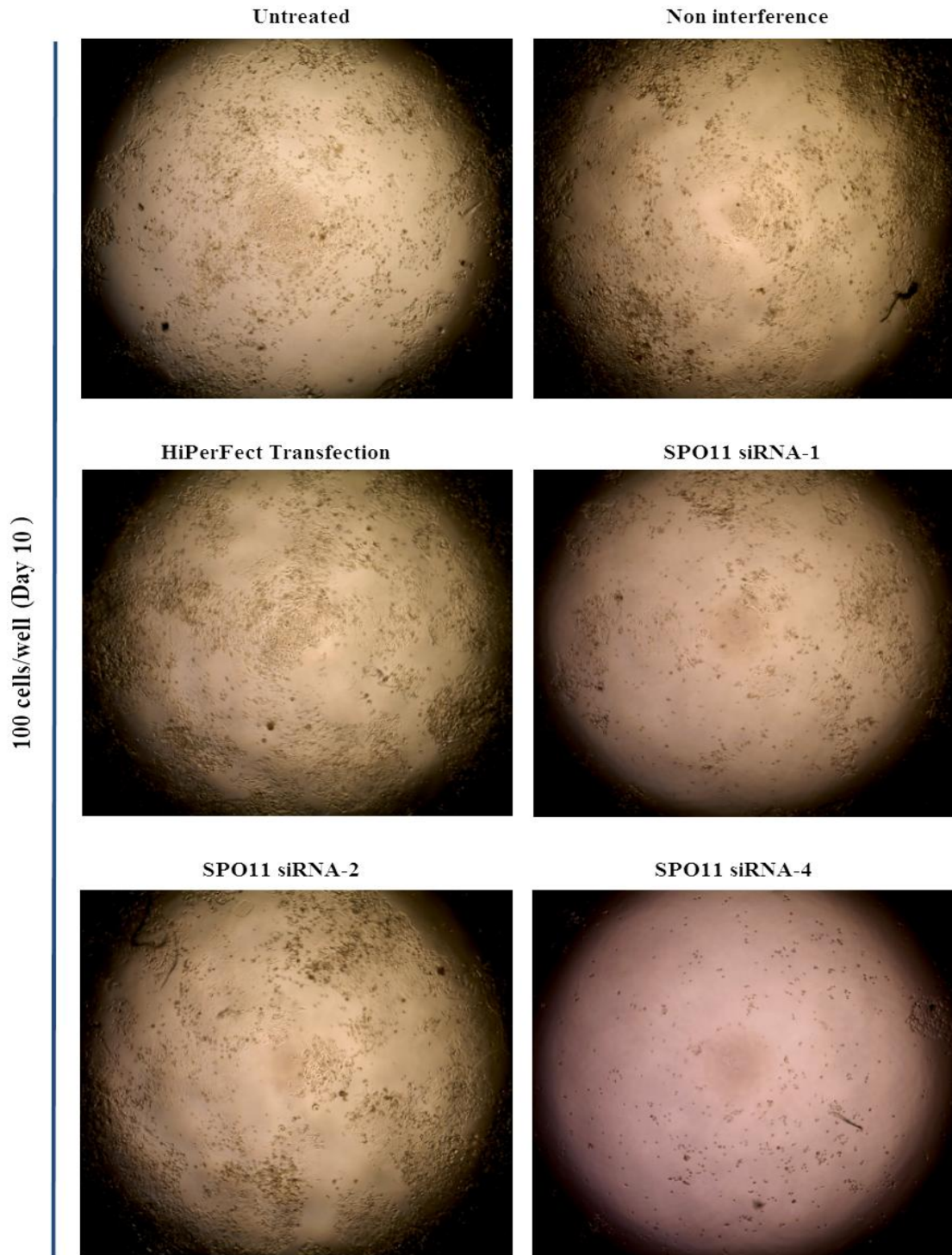
Figure 5.12a. Growth of the SW480 cell line 10 days after transfection with different siRNAs, with 100 cells seeded. Non-interference and HiPerFect transfection (as negative controls) and untreated cells were used to compare the growth of cells transfected with different siRNAs. The growth of cells transfected with SPO11-siRNA4 is negatively affected compared to the growth of untreated and transfection control cells (done once).

Untreated · Non interference

HiPerFect Transfection · SPO11 siRNA-1
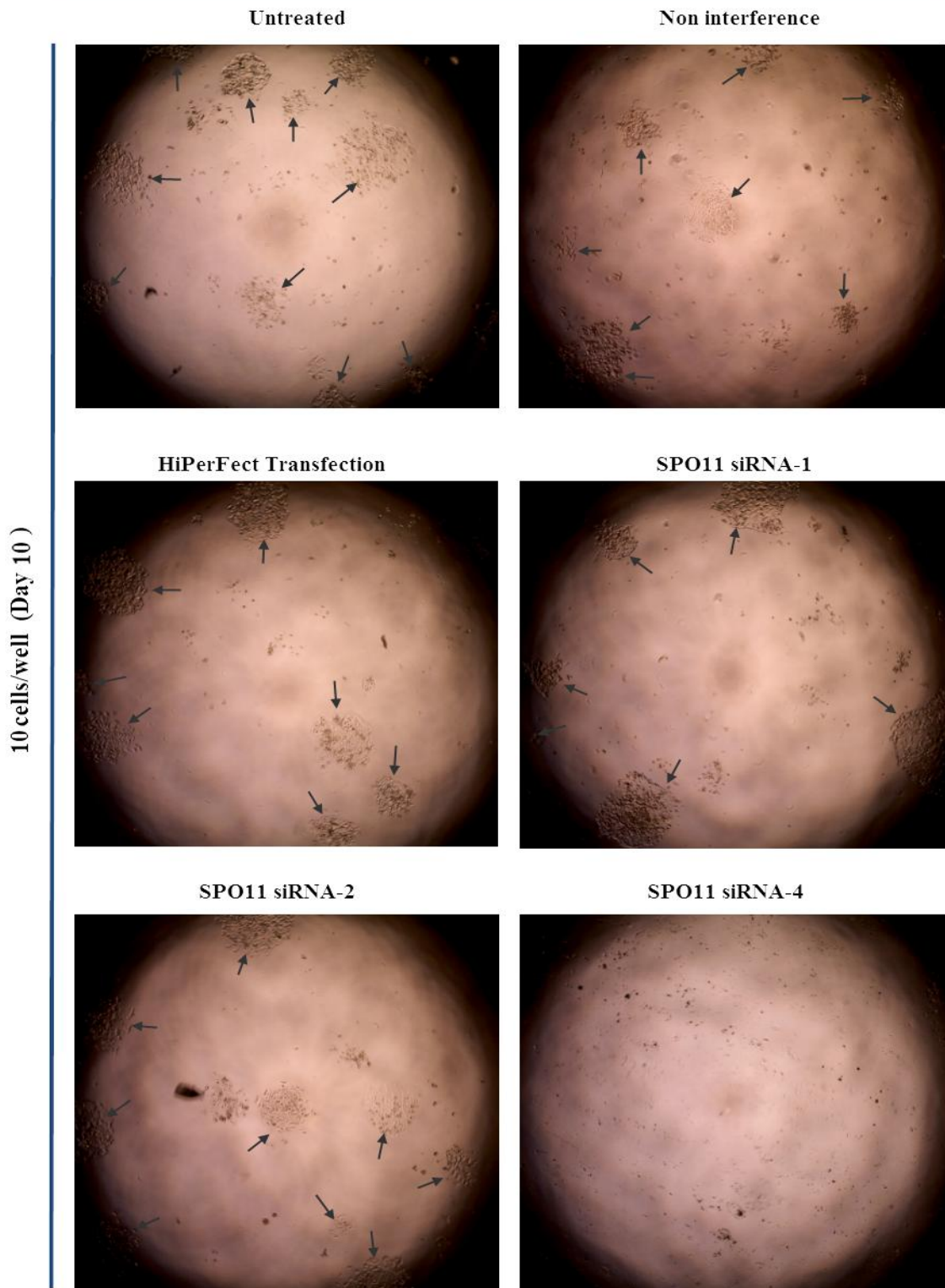
SPO11 siRNA-2 · SPO11 siRNA-4

100 cells/well (Day 10)

Figure 5.12b. HCT116 cell line 10 days after transfection with different siRNA with 100 cells seeded. Non-interference and HiPerFect transfection (as negative controls) and untreated cells were used to compare the growth of cells transfected with different siRNAs. The growth of cells transfected with SPO11-siRNA4 is negatively affected compared to the growth of untreated and transfection control cells (done once).

114

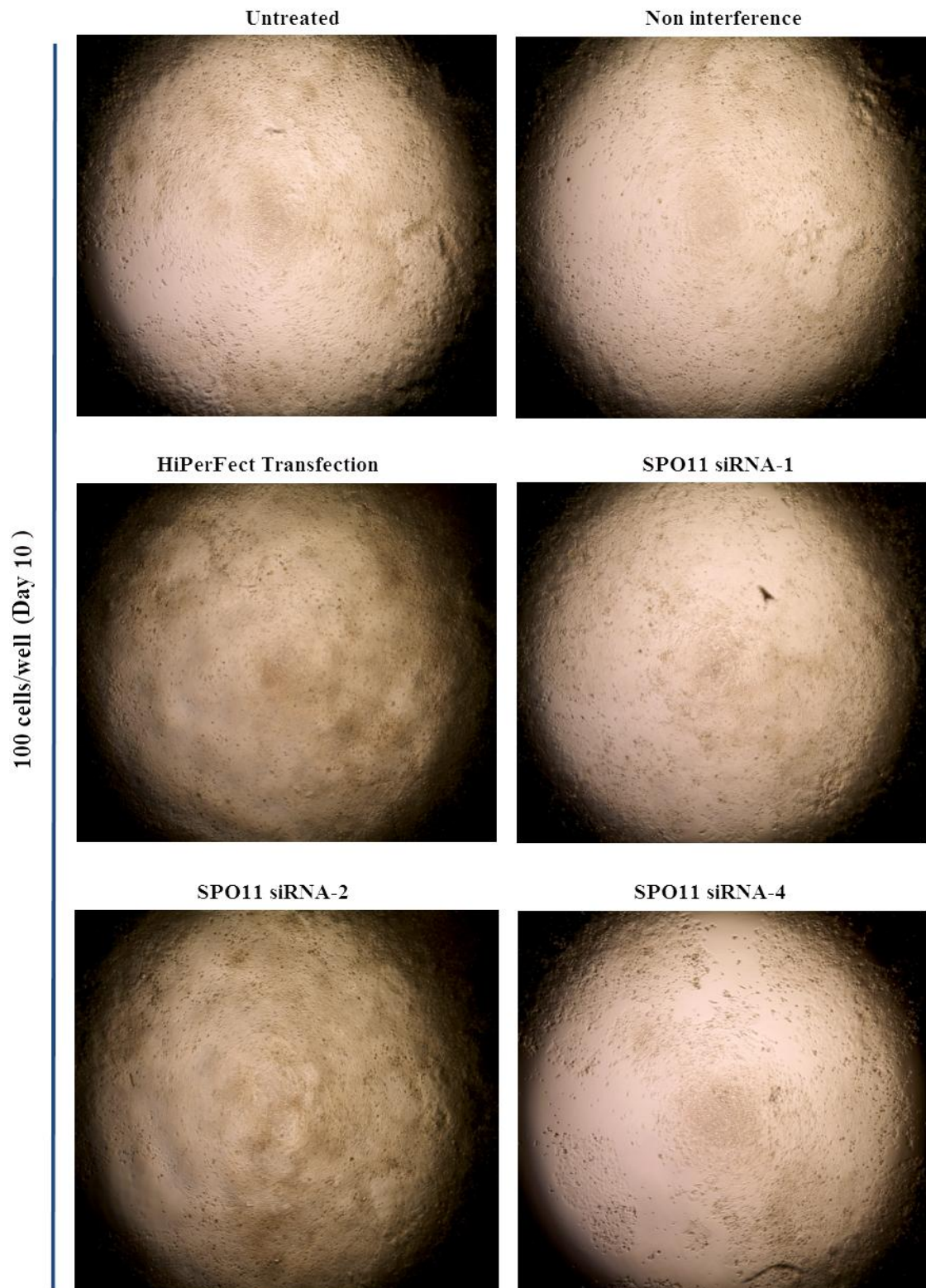### 5.2.4.2 The growth of colon cancer cells transfected with TALENs

The colonosphere of HCT116 and SW480 were disrupted and seeded in serial dilution as 100, 10 and 1 cell per well. The colonosphere colonies for both cell lines were restored to the parental form using normal 96 well plates, which allow the cells to attach to the surface. These cells were transfected twice with TALEN and TALEN with homology arms and Lipofectamine 2000 (as negative control). The first transfection was performed at the same time of the cell seeding; the second was four days after the cell seeding.

The first results were obtained 5 days after transfection. The SW480 cells at 10 and 100 cell seedings, transfected with TALENs and TALENs with homology arms, and the negative control were adversely affected by Lipofectamine 2000. HCT116 cells transfected with TALENs and TALENs with homology arms and the negative control were also adversely affected by Lipofectamine 2000 but some growth was seen in the negative control; no growth was seen in cells transfected with TALENs and TALENs with homology arms when the seeding started at 10 cells. However, when 100 cells were uses, the HCT116 cells showed the same growth as the negative control and the cells transfected with TALENs only, while no growth was seen with the cells transfected with TALENs with homology arms (for a results summary, see Table 5.4) (see also the results in the appendix).

The second results were obtained 10 days after transfection. The SW480 cells, at 10 cell seeding, that were transfected with TALENs and TALENs with homology arms and the negative control were adversely affected by Lipofectamine 2000 (for a results summary, see Table 5.4) (See also the results in the appendix). However, the SW480 cells at a 100 cell seeding showed no growth at all after transfection with TALENs and TALENs with homology arms, while some growth was seen in the negative control comparing to untreated cells (Figure 5.14) (for a results summary, see Table 5.4).

Ten days after transfection, the HCT116 cells transfected with TALENs and TALENs with homology arms and the negative control were adversely affected by Lipofectamine 2000 but some growth was apparent in the negative control; in contrast, no growth was visible in the cells transfected with TALENs and TALENs with homology arms when the seeding started at 10 cells (Figure 5.13). However, when seeding started with 100 HCT116 cells, good growth was seen in the negative control and untreated cells and some

growth was noted in the cells transfected with TALENs only. No growth was seen with the cells transfected with TALENs with homology arms (Figure 5.15) (for a results summary, see Table 5.4)

The final set of results was obtained 20 days after transfection. The SW480 cells with 10 cell seeding, transfected with TALENs and TALENs with homology arms and negative control were adversely affected by Lipofectamine 2000 (for a results summary, see Table 5.4) (see also the results in the appendix). However, the SW480 cells at 100 cell seeding transfected with TALENs and TALENs with homology arms showed no growth at all, while some growth was observed for the negative control compared to the untreated cells (Figure 5.17) (for a results summary, see Table 5.4).

After 20 days, HCT116 cells transfected with TALENs and TALENs with homology arms, and negative controls at 10 cell seedings showed good growth in the untreated cells and negative controls, while only a single colony appeared with the cells transfected with TALENs only, but there was no growth by the cells transfected with TALENs with homology arms (Figure 5.16) (for a results summary, see Table 5.4). However, when 100 cell seeding was used, HCT116 cells showed good growth in the negative control and untreated cells and some growth with the cells with TALENs only, but no growth with the cells transfected with TALENs with homology arms (Figure 5.18) (for a results summary, see Table 5.4).

Table 5.4. Summary of the cell growth after transfection with TALENs, following result is a summary of the growth in one of the six wells, the growth in which was all similar (± 10%)

Cell line	Days after Transfection	Treatment	100 cells	10 cells	1 cell
SW480	Day 5	Untreated	≈20% confluent	9 colonies	0
		Lipofectamine 2000	6 colonies	2 colonies	0
		TALENs	0	0	0
		TALENS and arms	0	0	0
SW480	Day 10	Untreated	≈60% confluent	9 colonies	0
		Lipofectamine 2000	16 colonies	0	0
		TALENs	0	0	0
		TALENS and arms	0	0	0
SW480	Day 20	Untreated	≈Confluent	9	0
		Lipofectamine 2000	11 colonies	single colony	0
		TALENs	0	0	0
		TALENS and arms	0	0	0
HCT116	Day 5	Untreated	≈80% confluent	9 colonies	single colony
		Lipofectamine 2000	15 colonies	2 colonies	0
		TALENs	13 colonies	single colony	0
		TALENS and arms	0	0	0
HCT116	Day 10	Untreated	≈Confluent	≈50% confluent	single colony
		Lipofectamine 2000	≈40% confluent	5 colonies	0
		TALENs	11 colonies	single colony	0
		TALENS and arms	0	0	0
HCT116	Day 20	Untreated	Over grown	≈90% confluent	≈40% confluent
		Lipofectamine 2000	Over grown	≈60% confluent	0
		TALENs	≈60% confluent	single colony	0
		TALENS and arms	0	0	0

Figure 5.13 HCT116 cells 10 days after transfection with TALENs and TALENs with homology arms, with 10 cells seeded. Untreated cells and Lipofectamine 2000 treated cells (as negative control) were used to compare the cell growth after transfection with TALENs and TALENs with homology arms. The negative control cells showed lower growth than the untreated cells, while no growth was observed with the cells transfected with TALENs and TALENs with homology arms, compared to the negative control and untreated cells (done once).

118

SW480 cell line

Untreated

Lipofectamine 2000

100 cells/well (Day 10)

Lipofectamine2000 and TALENs

Lipofectamine 2000, TALENs and homolgy arms

Figure 5.14 SW480 cells 10 days after transfection with TALENs and TALENs with homology arms, with 100 cells seeded. Untreated and Lipofectamine 2000 treated cells (as negative controls) were used to compare the cell growth following transfection with TALENs and TALENs with homology arms. The negative control cells showed lower growth than the untreated cells, while no growth was observed with the cells with TALENs and with TALENs with homology arms compared to the negative controls, and untreated cells (done once).

Untreated | Lipofectamine 2000

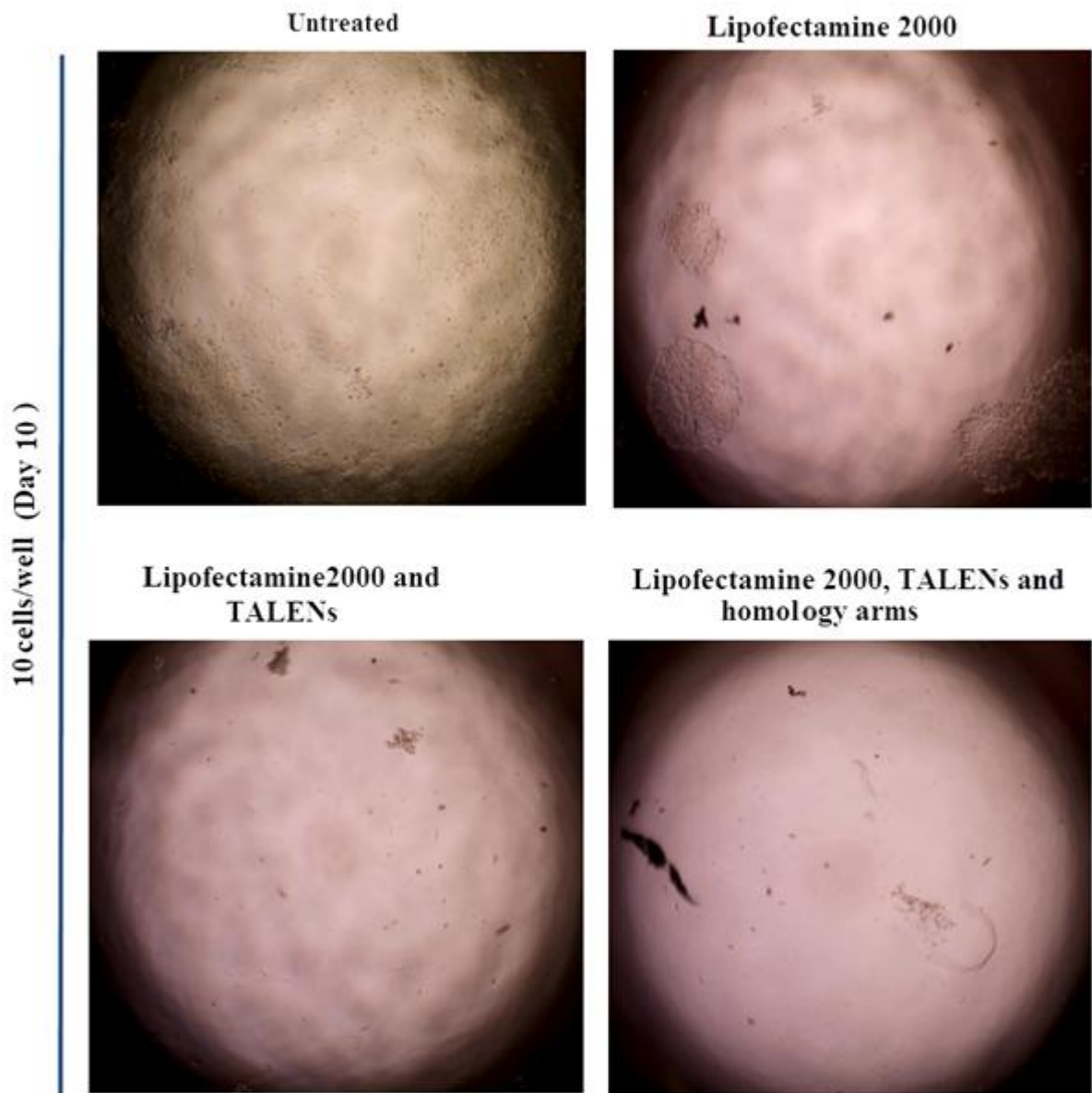Lipofectamine2000 and TALENs | Lipofectamine 2000, TALENs and homolgy arms

Figure 5.15. HCT116 cells 10 days after transfection with TALENs and TALENs with homology arms, with 100 cells seeded. Untreated and Lipofectamine 2000 treated cells (as negative controls) were used to compare the cell growth following transfection with TALENs and TALENs with homology arms. The negative control cells showed lower growth than the untreated cells, while only few colonies were observed with TALENs; no growth was observed with the cells with TALENs with homology arms (done once).

Untreated

Lipofectamine 2000

10 cells/well (Day 20)

Lipofectamine2000 and TALENs

Lipofectamine 2000, TALENs and homolgy arms

Figure 5.16. HCT116 cells 20 days after transfection with TALENs and TALENs with homology arms, with 10 cells seeded. Untreated and Lipofectamine 2000 treated cells (as negative controls) were used to compare the cell growth following transfection with TALENs and TALENs with homology arms. The negative control cells showed lower growth than the untreated cells, while only single colony was observed with TALENs no growth was observed with the cells with TALENs with homology arms (done once).

Untreated

Lipofectamine 2000

Lipofectamine2000 and TALENs

Lipofectamine 2000, TALENs and homolgy arms
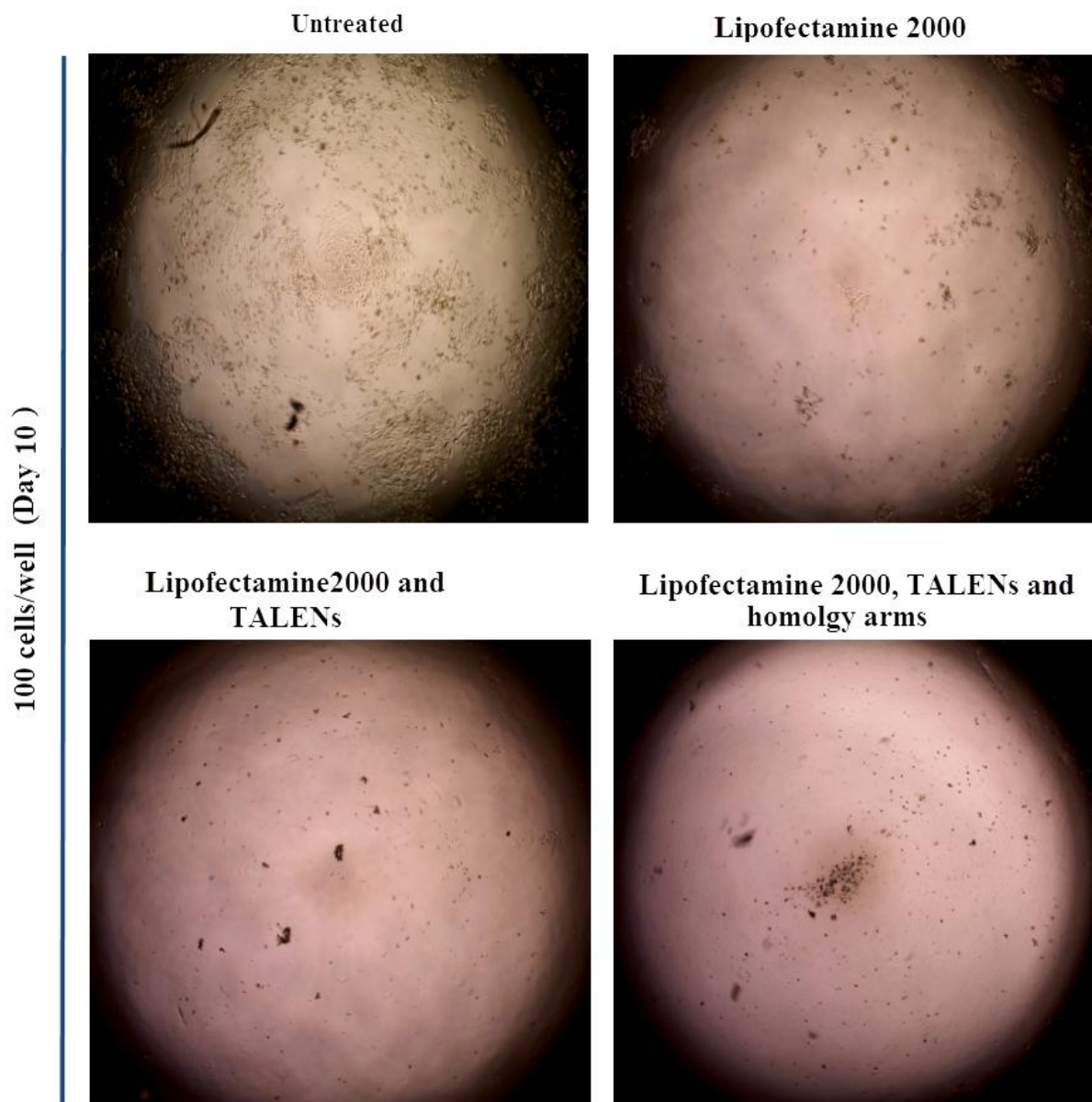
100 cells/well (Day 20)
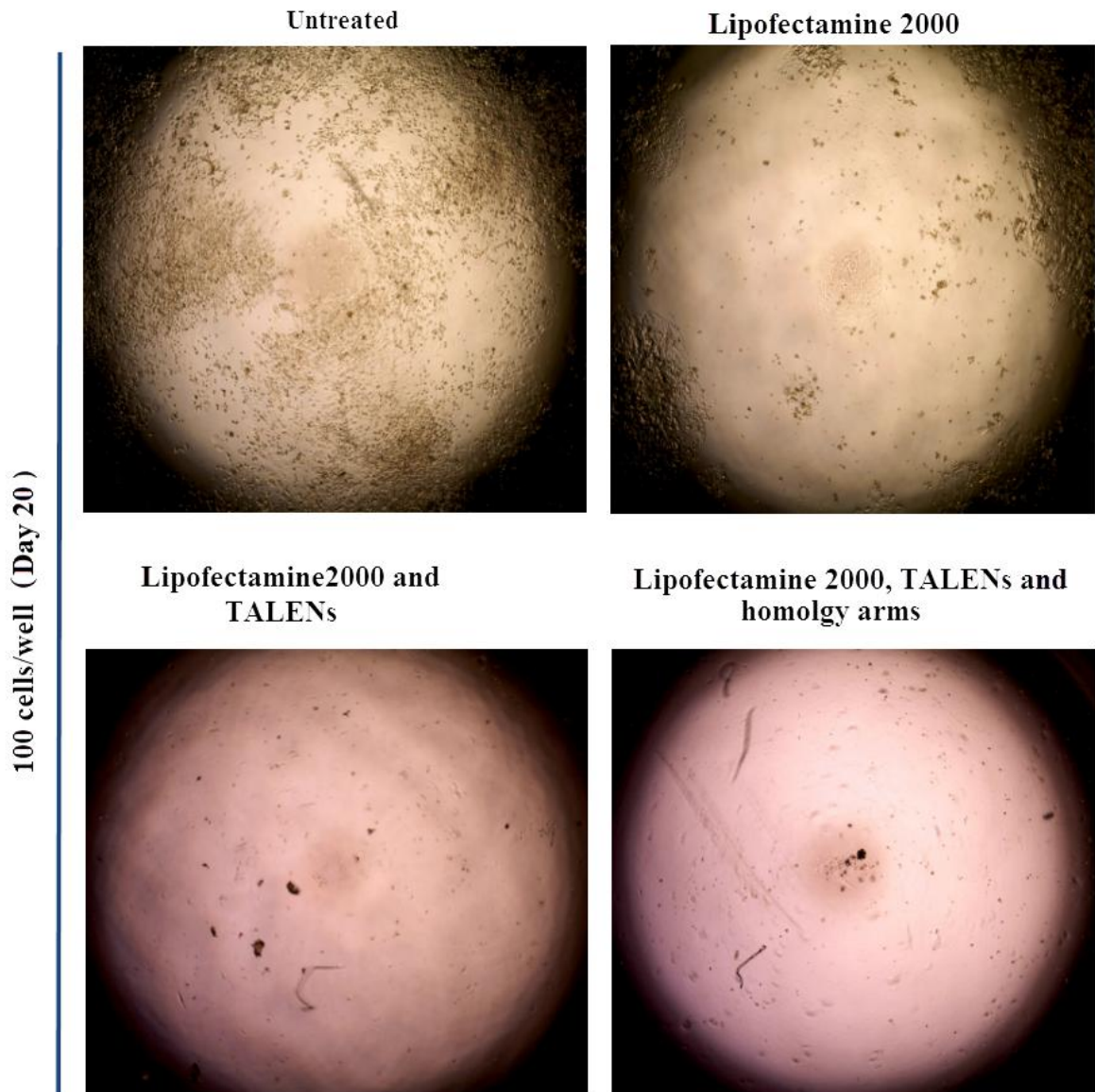
Figure 5.17. SW480 cells 20 days after transfection with TALEN and TALEN with homology arms, with 100 cells seeded. Untreated and Lipofectamine 2000 treated cells (as negative controls) were used to compare the cell growth following transfection with TALENs and TALENs with homology arms. The negative control cells showed lower growth than the untreated cells, while no growth was observed with the cells with TALENs and with TALENs with homology arms (done once).

122

Untreated

Lipofectamine 2000

Lipofectamine2000 and TALENs

Lipofectamine 2000, TALENs and homolgy arms
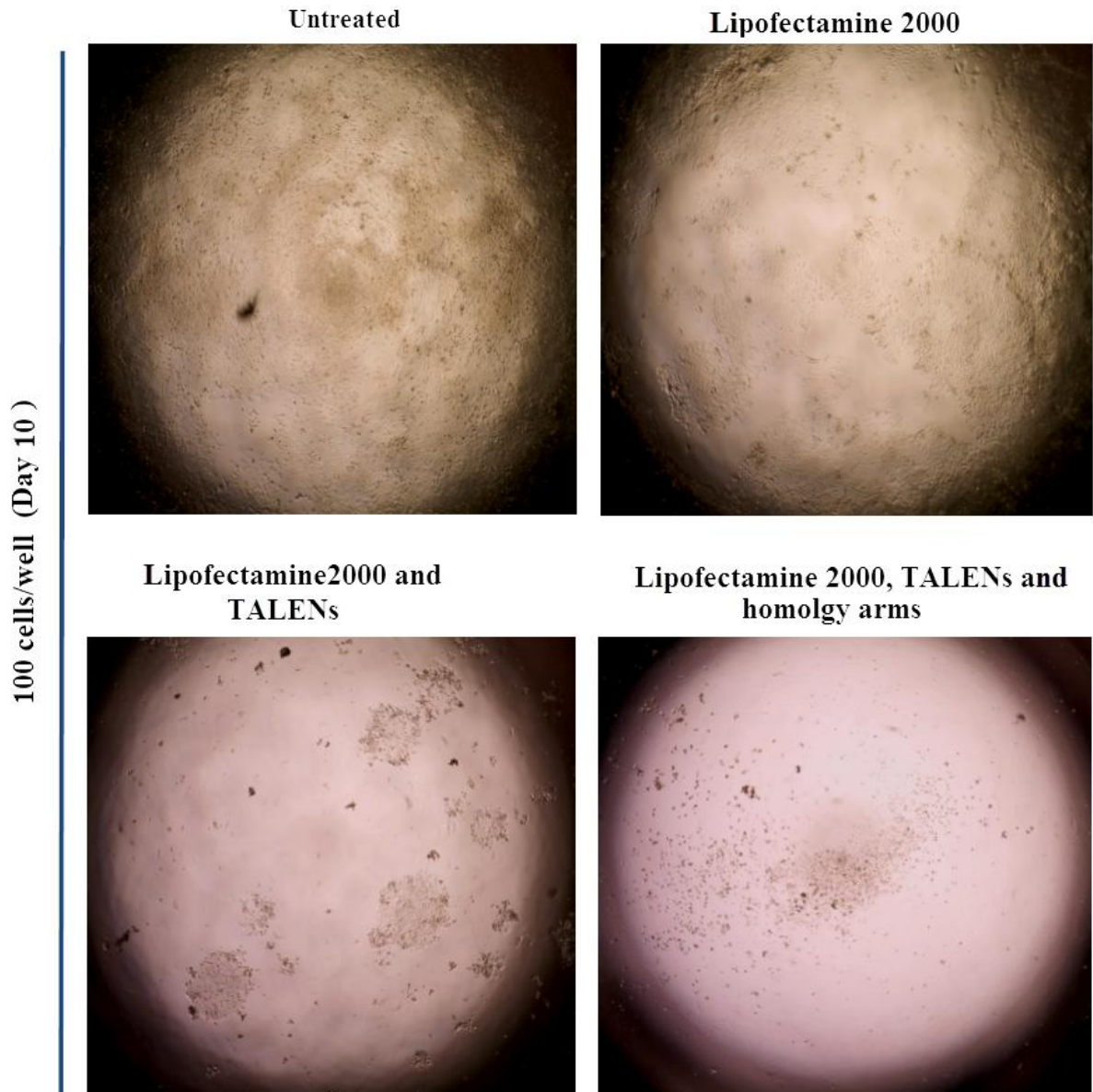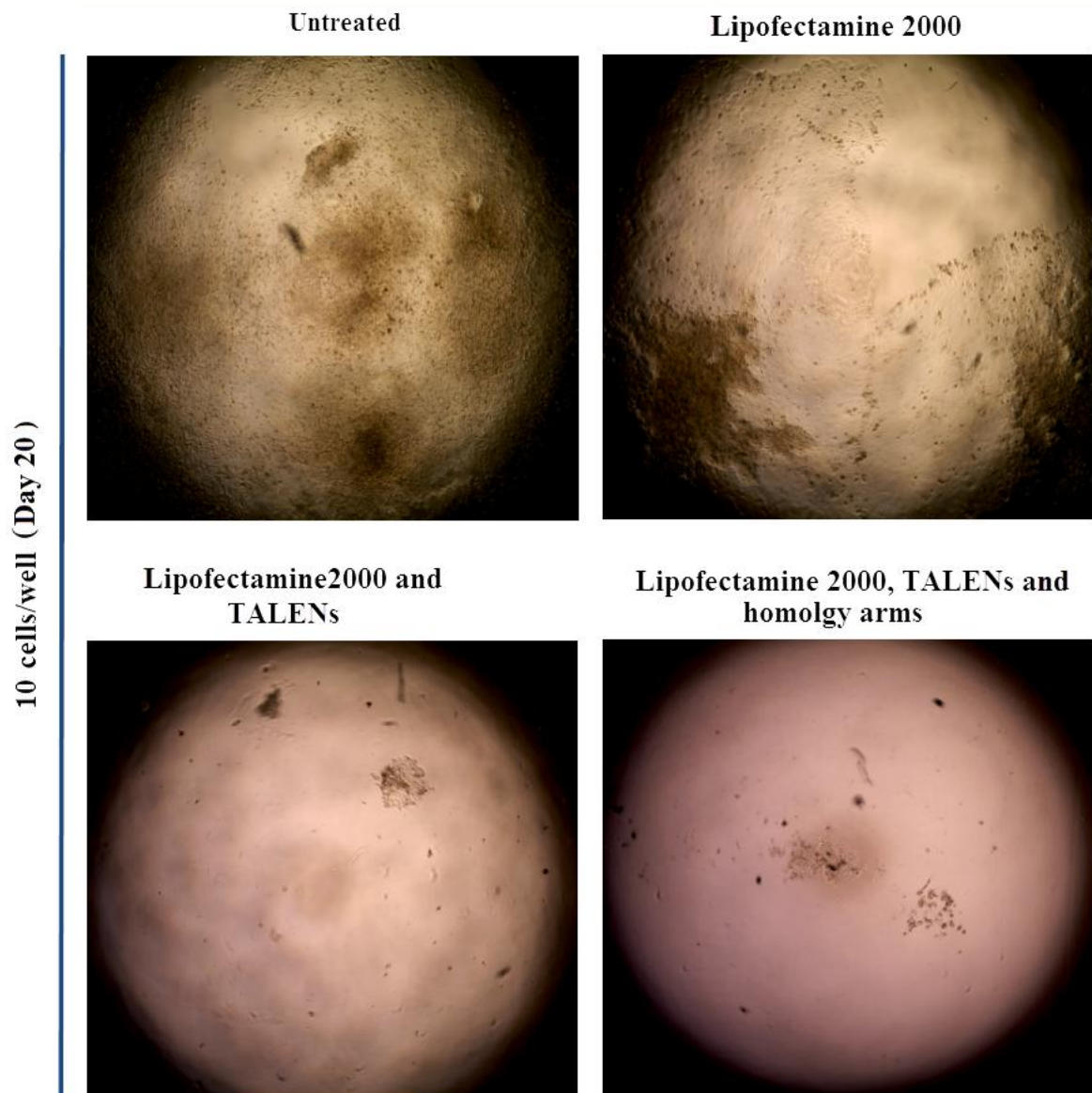
100 cells/well (Day 20)
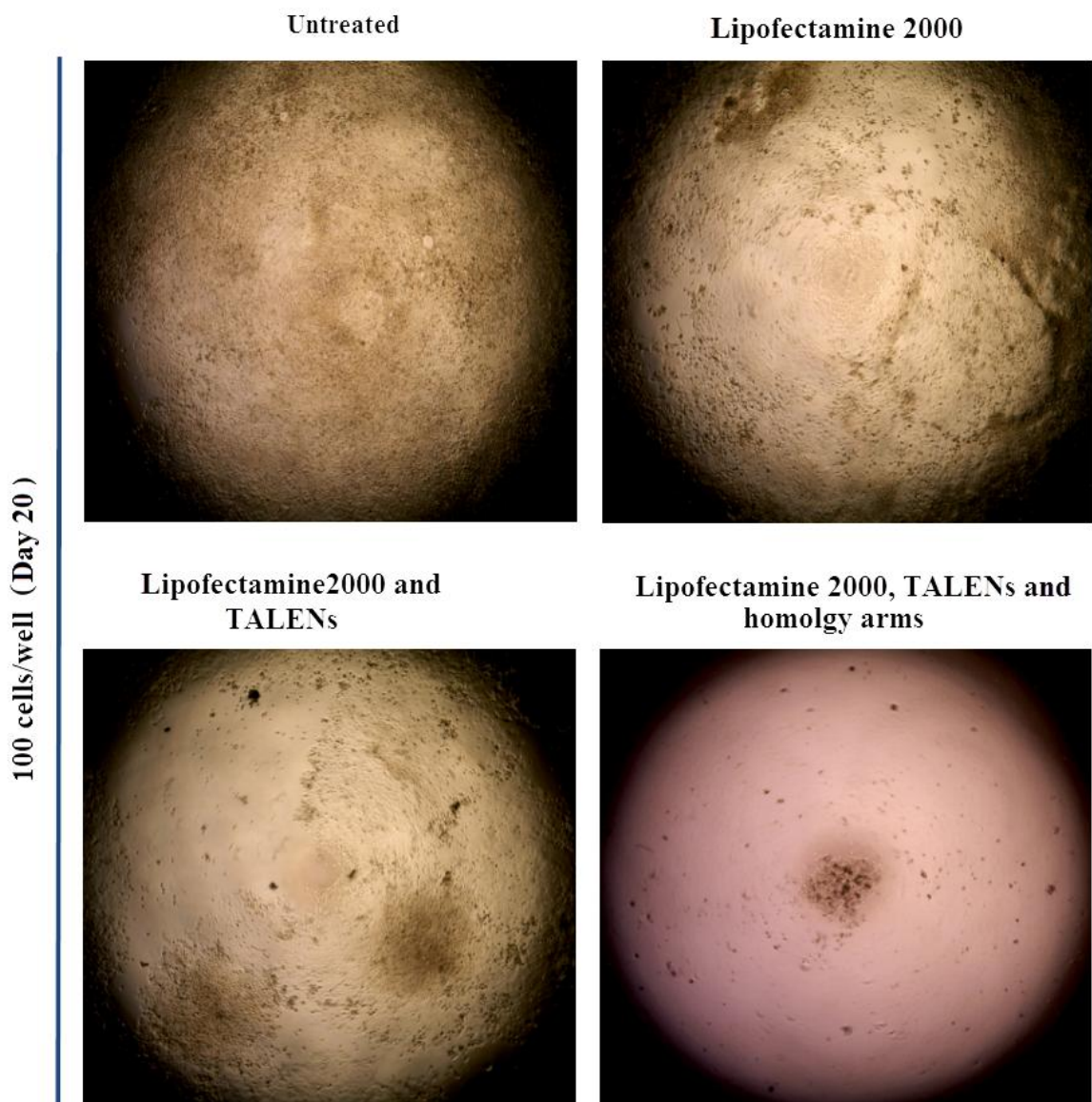
Figure 5.18. HCT116 cells 20 days after transfection with TALENs and TALENs with homology arms, with 100 cells seeded. Untreated and Lipofectamine 2000 (as negative control) were used to compare the cells growth with TALENs and TALENs with homology arms. The negative controls and cells transfected with TALENs showed lower growth than the untreated cells, while no growth was observed for the cells with TALENs with homology arms (done once).

5.2.4.3 The growth of parental colon cancer cells transfected with TALENs

SW480 and HCT116 parental (non-spheroid) cells were transfected with empty vectors (as negative control), TALENs and TALENs with homology arms. The SW480 cells grew more slowly than the HCT116 cells; therefore, for the SW480 line, only 100 cells were seeded while 10 and 100 cells were seeded for the HCT116 line. The cells were transfected twice, once at the same time as the cell seeding and another 24 hours later.

The results were obtained 10 days after the first transfection. The SW480 results show different levels of confluence among the untreated, Lipofectamine 2000-treated and empty vector transfected cells, while only four colonies were observed in the cells transfected with only TALENs and no growth was observed in the cells transfected with TALENs and arms (Table 5.5) (Figure 5.19).

The HCT116 10 cells seeding results showed a different level of confluence with untreated, Lipofectamine 2000-treated and empty vector transfected cells, while only a single colony was observed in the cells transfected with only TALENs and two colonies were observed in the cells transfected with TALENs and arms (Table 5.5) (Figure 5.20). In addition, the HCT116 100 cells seeding results showed a different level of confluence with all treatment conditions, but the cells transfected with TALENs and arms had a much lower confluence level when compared to the other treatments (Table 5.5) (Figure 5.21).

Table 5.5. Summary of the parental cell growth after transfection with TALENs, following result is a summary of the growth in one of the six wells, the growth in which was all similar (± 10%)

| Cell line	SW480	HCT116	
Cells seeding No.	100 cells	10 cells	100 cells
Untreated	≈ Confluent	≈80% confluent	Over grown
Lipofectamine 2000	≈30% confluent	≈80% confluent	Over grown
Empty vectors	≈20% confluent	≈30% confluent	≈80% confluent
TALENs	Four colonies	Single colony	≈70% confluent
TALENS and arms	0	Two colonies	≈20% confluent

Figure 5.19 SW480 cells 10 days after transfection with TALENs and TALENs with homology arms, with 100 cells seeded. Lipofectamine 2000, empty vectors (as a negative control) and untreated cells were used to compare the cell growth with TALENs and TALENs with homology arms. The negative controls and empty vector-treated cells showed lower growth than the untreated cells. The cells transfected with TALENs showed growth of only three colonies, while no growth was seen with the cells with TALENs with homology arms, when compared to the negative control, the cells transfected with TALENs and the untreated cells (done once).

125

Untreated

Lipofectamine 2000

10 cells/well

Lipofectamine 2000 and
empty vectors

Lipofectamine2000 and
TALENs

Lipofectamine 2000, TALENs and
homolgy arms
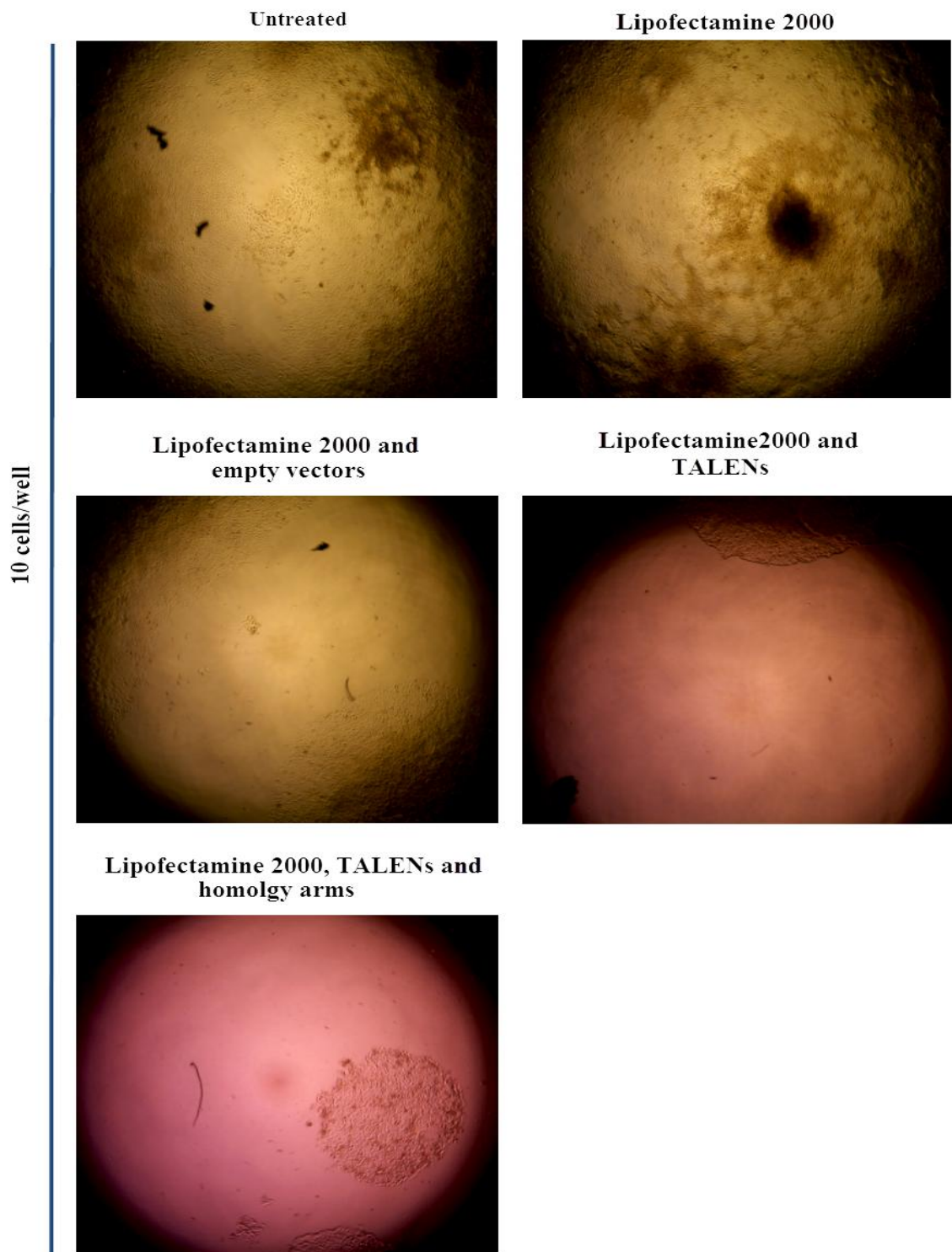
Figure 5.20. HCT116 cells 10 days after transfection with TALENs and TALENs with homology arms, with 10 cells seeded. Lipofectamine 2000, empty vectors (as a negative control) and untreated cells were used to compare the cell growth with TALENS and TALENs with homology arms. The negative controls and empty vector-transfected cells showed lower growth than the untreated cells. The cells transfected with TALENs and with TALENs with homology arms showed growth of one and two colonies respectively (done once).
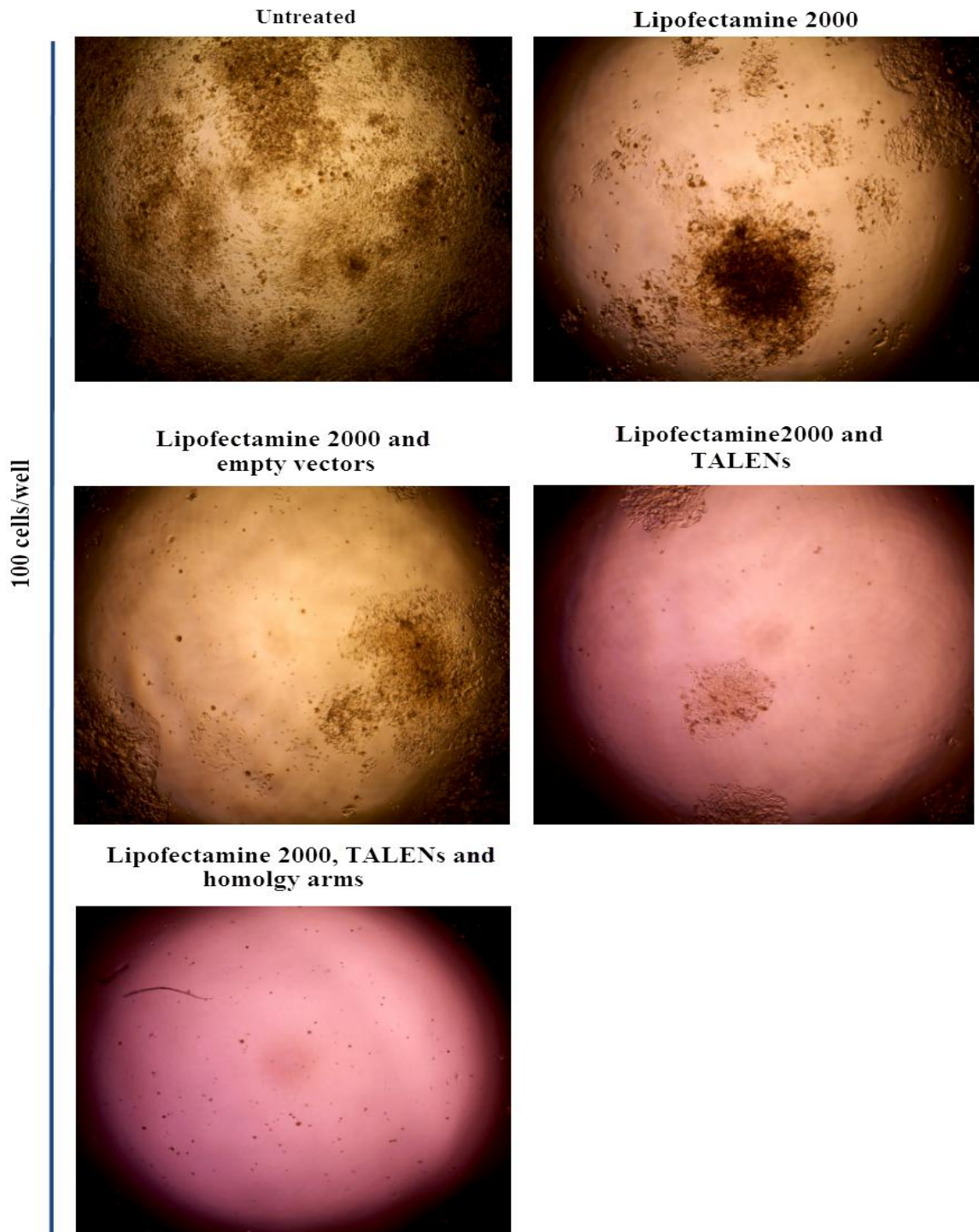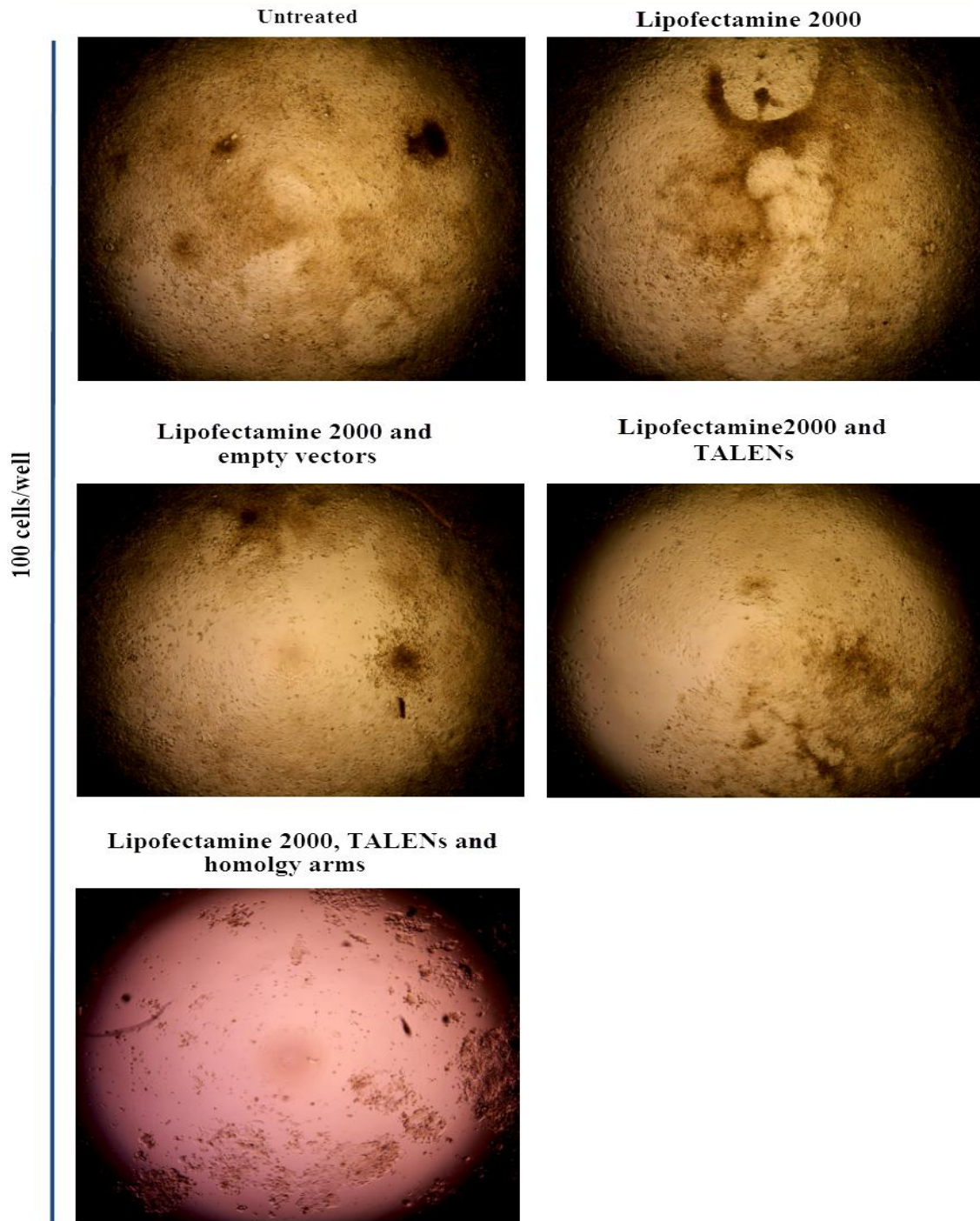
Figure 5.21 HCT116 cell line 10 days after transfection with TALENs and TALENs with homology arms with 100 cells seeded. Lipofectamine 2000, empty vectors (as a negative control) and untreated cells were used to compare the cell growth with TALENs and TALENs with homology arms. The negative controls, and cells transfected with empty vector or with TALENs showed lower growth than the untreated cells. The cells transfected with TALENs with homology arms showed much lower growth compared to the negative control or the cells transfected with TALENs or untreated (done once).

5.2.5 Quantification of the ELDA (Extreme limiting dilution analysis assay) of the HCT116 colonosphere cells using ultralow attachment plates

HCT116 cells were cultured at two dilutions – 10 and 100 cell seedings – into ultralow attachment 96 well plates. These plates enable colonies to grow as free floating spheres. The cells were transfected for the first time at the time of seeding and the second time four days after seeding. The cells were treated with Lipofectamine 2000 only (as a control for the chemical reagents) or transfected with empty vectors only (as a control for chemical reagents and vectors), with *SPO11* TALENs or with *SPO11* TALENs and homology arms. In addition, the cells were treated with transfection only (as a control for chemical reagents) and transfected with negative siRNA, siRNA-1, and siRNA-2 and siRNA-4. After 10 days, the results were based on the numbers of surviving colonies in each well, and analysed using the ELDA web-tool (http://bioinf.wehi.edu.au/software/elda/) to determine the frequencies of colonosphere forming cells.

The frequencies of colonosphere forming cells showed an approximately 8-fold decrease ($P<0.01$) in the cells transfected with *SPO11* TALENs and *SPO11* TALENs and homology arms, when compared to the cells transfected with empty vectors only (Table 5.6). No significant differences ($P> 0.01$) were found in pairwise comparisons of sphere-forming frequencies between Lipofectamine 2000 only/empty vector only transfected cells (Table 5.7). In contrast, all pairwise comparisons with the *SPO11* TALENs transfected cells *vs. SPO11* TALENs and homology arms transfected cells groups were highly significant ($p<0.01$) with Lipofectamine 2000 only, empty vector only transfected cells and untreated cells (Table 5.7).

Table 5.6. Number of wells showing colonospheres forming frequency in each treatment condition (*SPO11* TALENs and *SPO11* TALENS and homology arms), including the negative control and untreated cells (done once).

Number of cells per well	Number of wells plated	Number of wells showing colonospheres				
		Untreated cells	Cells transfected with empty vectors only	Cells treated with Lipofectamine 2000 only	Cells transfected with *SPO11* TALENs	Cells transfected with *SPO11* TALENs and homology arms
Ultralow attachment plate – HCT116 passage number P5.6						
100	6	6	6	5	1	1
10	6	6	1	0	0	0
Sphere forming frequency (95% CI)		1/1 (1/11-1/1)	1/71 (1/176-1/28)	1/31 (1/80-1/12)	1/609 (1/4301-1/87)	1/609 (1/4301-1/87)
P value *		<0.01				

* The overall test for differences in cells frequencies between any of the groups.

Table 5.7. ELDA results comparing colonosphere formation by cells transfected with *SPO11* TALENs and with *SPO11* TALENs and homology arms (done once).

Ultralow attachment plate – HCT116 passage number P5.6- *SPO11* with TALENs and *SPO11* TALENs and homology arms				
Group 1	Group 2	Chisq	DF	Pr(>Chisq)
Lipofectamine 2000 only	Cells transfected with *SPO11* TALENs	11.3	1	<0.01
Lipofectamine 2000 only	Cells transfected with *SPO11* TALENs and homology arms	11.3	1	<0.01
Lipofectamine 2000 only	Empty vectors only	1.41	1	0.235
Lipofectamine 2000 only	Untreated	10.0	1	<0.01
SPO11 TALEN transfected cells	Cells transfected with *SPO11* TALENs and homology arms	1.28e-15	1	1
SPO11 TALENs transfected cells	Empty vectors only	5.26	1	<0.01
SPO11 TALENs transfected cells	Untreated	787	1	<0.01
SPO11 TALENs and homology arms transfected cells	Empty vectors only	5.26	1	<0.01
SPO11 TALENs and homology arms transfected cells	Untreated	787	1	<0.01
Empty vectors only	Untreated	19.2	1	<0.01

The frequencies of colonosphere forming cells following transfection with negative siRNA, siRNA-1, and siRNA-2 and siRNA-4, showed an approximately 3-fold decrease (P<0.01) with SPO11 siRNA-4 compared to the negative control siRNA transfected cells (Table 5.8). In addition, no significant differences (P> 0.01) were found in pairwise comparisons of sphere-forming frequencies between untreated/ negative control siRNA transfected cells, untreated/ HiPerFect-only treated cells and HiPerFect-only treated/negative control siRNA transfected cells (Table 5.9). In addition, no significant differences (P> 0.01) were found in pairwise comparisons of sphere-forming frequencies between negative control siRNA and SPO11 siRNA-4 transfected cells (Table 5.9). In contrast, all untreated and HiPerFect-only pairwise comparisons with the SPO11 siRNA-4 transfected group were significant (Table 5.9).

Table 5.8. Number of wells showing colonospheres forming frequency in each treatment conditions (different siRNAs) including the negative controls and untreated cells (done once).

Number of cells per well	Number of wells plated	Number of wells showing colonospheres					
		Untreated cells	Negative control siRNA transfected cells	HiPerFect-only treated cells	SPO11 siRNA-1 transfected cells	SPO11 siRNA-2 transfected cells	SPO11 siRNA-4 transfected cells
Ultra low attachment plate – **HCT116 passage number P5.6**							
100	6	6	6	6	6	6	6
10	6	6	3	4	5	2	0
Sphere forming frequency (95% CI)		1/1 (1/11-1/1)	1/15 (1/43-1/5)	1/10 (1/26-1/4)	1/6 (1/15-1/3)	1/22 (1/63-1/8)	1/42 (1/103-1/17)
P value *		0.0018					

* The overall test for differences in cells frequencies between any of the groups.

Table 5.9. ELDA results comparing colonosphere formation by cells transfected with different SPO11-siRNAs (done once).

Ultra low attachment plate – HCT116 passage number P5.6- SPO11 with different siRNA				
Group 1	Group 2	Chisq	DF	Pr(>Chisq)
HiPerFect-only	Negative control siRNA	0.337	1	0.562
HiPerFect-only	SPO11 siRNA-1	0.451	1	0.502
HiPerFect-only	SPO11 siRNA-2	1.23	1	0.268
HiPerFect-only	SPO11 siRNA-4	3.92	1	0.0476
HiPerFect-only	Untreated	3.18	1	0.0748
Negative control siRNA	SPO11 siRNA-1	1.54	1	0.214
Negative control siRNA	SPO11 siRNA-2	0.275	1	0.6
Negative control siRNA	SPO11 siRNA-4	1.94	1	0.164
Negative control siRNA	Untreated	5.17	1	0.023
SPO11 siRNA-1	SPO11 siRNA-2	3.11	1	0.078
SPO11 siRNA-1	SPO11 siRNA-4	6.97	1	0.0083
SPO11 siRNA-1	Untreated	1.48	1	0.224
SPO11 siRNA-2	SPO11 siRNA-4	0.764	1	0.382
SPO11 siRNA-2	Untreated	7.48	1	0.00622
SPO11 siRNA-4	Untreated	12.6	1	0.000378

5.3 Discussion

5.3.1 SPO11 protein in normal tissues and cancer tissues/cell lines

SPO11 is a meiosis-specific protein that binds to DNA to initiate recombination by forming DNA double-strand breaks (DSBs). The *SPO11* gene (*CT35*) was identified as a CTA gene and was detected in melanoma, lung and cervical cancer (Koslowski et al., 2002). According to the literature, and until the present time, no study has been conducted on the SPO11 at the protein level in human cancer cells. Therefore, the present study focuses on the protein in normal and cancer tissues/cell lines.

SPO11 knockdown was undertaken using different siRNAs and different transfection chemicals in four different cell lines: HCT116, SW480, HepG2 and NTERA2. However, the knockdown experiments failed. The failure of the knockdown might be a result of the death of cells when *SPO11* siRNA was used, as will be discussed later (see Section 5.3.2). However, the surviving cells were used to check the protein levels after knockdown and possible these were the cells unaffected by the siRNA knockdown (i.e. the cells in which knockdown worked are lost). An analysis of the effectiveness of *SPO11* siRNA should be carried out using qRT-PCR.

In the present study, Spo11 was detected only in normal testis and widely by western blotting and immunohistochemistry in different cancer types including embryonal carcinoma, astrocytoma, cancers of the colon, lung, liver, breast, ovary and melanoma. The high levels in cancer cells could suggest that SPO11 might be essential for the growth or development of cancer cells. Taking this further, this might indicate SPO11 could be a good potential drug target.

The cell fractions (nucleus, cytoplasm) that were collected to determine the location of SPO11 confirmed that every cell line tested showed strong localisation of SPO11 in the nuclear fraction and weak localisation in the cytoplasm. The exception was the HCT116 cell line, which showed only nuclear localisation. However, SPO11 should be restricted to the nucleus because of the function of the SPO11 in meiotic recombination, but SPO11 might have other uncharacterise functions, possibly explaining the low protein levels in the cytoplasm. Previous studies have indicated that multifunctional DNA binding proteins are located in both nuclear and cytoplasmic compartments, where they serve different

functions (Wilkinson and Shyu, 2001). Therefore, the SPO11 protein could be a multifunctional protein in cancer cells.

The chromatin association assay using different salt concentrations, which showed that SPO11 was not strongly associated with the chromatin, suggests the SPO11 might load onto the DNA indirectly at a specific location with opened chromatin, perhaps in association with another chromatin binding protein (Grey et al., 2011). In meiosis chromatin is activated for SPO11 access by chromatin modifiers such as meiosis-specific histone H3K4 methyltransferase PRDM9 (Grey et al., 2011). Interestingly, the *PRDM9* gene is expressed in many of the cancer cell lines used in these analyses (Feichtinger et al., 2012a), and it could be the case that SPO11 is part of a general meiosis-like programme that becomes activated in cancer cells. Indeed, another meiotic chromosomal regulator gene has also been shown to be expressed in all cancer cell lines used here, *TEX19* (Feichtinger et al., 2012a). The exact function of *TEX19* remains unclear, but reducing TEX19 levels in cancer cells also impedes cell proliferation (McFarlane group, unpublished data). SPO11 might only have a weak direct chromatin association. Alternatively, the SPO11 that is detected as not associated with chromatin might be 'free' SPO11 which is released from a DNA association by MRN complex (Longhese et al., 2010). In addition, the 1 M salt would not remove covalently bound SPO11. The possibility of covalently bound SPO11 will be addressed in the next chapter.

The attempts at siRNA knockdown failed, and the TALEN technique results for knockout of *SPO11* levels in the cancer cell lines were equivocal. The most encouraging results were obtained when the NTERA2 cell line was transfected with TALENs and homology arms, as this line showed a reduction at the protein level in some samples for both chemical transfection and electroporation, suggesting a heterozygote might have been generated. However, full knockout was never detected in any sample. This again raises the question whether SPO11 is an essential protein in the cancer cells. One answer might be that the presence of SPO11 is essential for the cancer cell survival; i.e., cells with null SPO11 will die (See 5.3.2).

5.3.2 Is SPO11 essential in cancer cells?

When Spo11 is absent from the budding yeast, recombination is not initiated during meiosis as result of no DSBs occuring and the SC not being formed (Chua and Roeder, 1998). In mice, full knockout of *SPO11* leads to arrest of spermatocytes in the early pachytene with little or no synapsis and ultimately leads to apoptosis (Romanienko and Camerini-Otero, 2000). A recent study reported that SPO11 in the mouse testis is required for phosphorylation of HORMAD1, HORMAD2 and SMC3, which all have functions in chromosome synapsis (Fukuda et al., 2012). SMC3 also functions during mitosis and might be phosphorylated in response to DSBs, possibly initiated by SPO11 directly or due to some other SPO11-dependent function (Fukuda et al., 2012). In addition, the phosphorylation of SMC3 might be involve in pachytene checkpoint that monitors recombination and synapsis or DNA damage repair (Fukuda et al., 2012). If such a meiotic checkpoint were imposed on cancer cells, it could have an influence on cell cycle dynamics.

In the present study SPO11 was detected only in the normal testis and not in any other normal tissues by western blotting and immunohistochemistry. SPO11 is essential for multiple roles during meiotic cell division. For example, in *S. cerevisiae* Spo11 is a mediator of interhomolog associations; also, *Spo11Δ* decrease the length of the S-phase by 25% (Cha et al., 2000). In addition, Spo11 initiates a DSB via Y135 residue (Bergerat et al., 1997), but the *Spo11 Y135F* mutant does not affect S-phase but the DSB and SC were not formed (Cha et al., 2000). Given that all these roles occur during meiosis SPO11 should not normally be present in healthy somatic cells, except the testis tissues. On the other hand, SPO11 was detected in all cancer cell lines and most of the cancer tissues tested. The presence of SPO11 in all cancer cell lines and most of the cancer tissues tested open an important question whether SPO11 is essential for the cancer cells? If the SPO11 has meiotic-like functions in cancer then that might lead to mis-segregation by forming DSBs which are then repaired incorrectly leading to chromosome rearrangement which are a hallmark of tumour cells.

The differences in the survival between the cells transfected with siRNA-4, TALENs and TALENs with homology arms, comparing to the untreated and negative controls, may provide clues to other yet uncharacterized roles of SPO11, indicating that SPO11, might

be essential for cancer cell survival. The heterozygote might have the ability to survive as it retains significant levels of SPO11 (Figure 5.11). We cannot dismiss siRNA off target effects and so these observations most be validated/ extended using an additional set of *SPO11*-speicific siRNA. In addition, in the absence of homology/cassette vector the TALENs might disrupt the *SPO11* gene and reduce function. However, it might be the case that a non-specific effect of a DSB might reduce viability and extra controls should be done to address the possibility; these should include the generation of a DSB within at least one non-essential gene. In a previous study, homozygous null mutation of *SPO11* in mice can lead to arrest and spermatocyte apoptosis during the early prophase to mid-pachynema of meiosis (Smirnova et al., 2006); if the same is true in cancer cells then full knockout might lead to apoptosis.

5.4 Conclusions

SPO11 has different functions during meiosis. Thus, *SPO11* is expected to be expressed in the normal testis, where meiosis is occurring, and not in other somatic cells where meiotic cell division does not occur. In the present study, SPO11 protein was detected only in the normal testis and not in any other normal tissues by western blotting and immunohistochemistry. However, SPO11 was detected in all cancer cell lines and most of the cancer tissues tested. Knockdown of *SPO11* failed in these cell lines, which might have been due to technical failure or a lethal effect of the siRNA use. The TALEN technique was attempted as an alternative for removing SPO11 function, but appeared to be only partially successful.

Although survival of cells in two cancer cell lines (SW480 and HCT116) was reduced by treatment with SPO11 siRNA-4 and by transfection of TALENS and TALENS with homology arms. ELDA results also showed that the ability to form colonospheres was reduced using siRNA-4, TALENS and TALENS with homology arms of *SPO11* in HCT116 colonosphere colonies comparing to negative controls and untreated cells. The presence of *SPO11* during mitotic division might lead to incorrect replication or/and formation of DSBs during mitosis, which might lead to different chromosome rearrangements and ultimately to cancer, suggesting SPO11 could be an oncogenic driver. Therefore, defects in SPO11 might cause cancer cells to undergo apoptosis. The possibility of a role SPO11 during mitosis is clearly one that should be investigated

further, as it could begin to explain why SPO11 might be essential and why reduction of SPO11 levels affects the cancer cells. These results, taken together, suggest that SPO11 might be a good potential drug target.

5.5 Future Work

An essential but uncharacterised role in cancer cells is suggested for SPO11. Therefore, future studies should expand the cell growth studies in different cell lines. Covalent binding studies between SPO11 and DNA might indicate whether SPO11 forms DSB in cancer cells (see Chapter 6). Flow cytometry analysis should be undertaken to check if SPO11 has a function during the S-phase in cancer cells as it does in meiotic cell division. Mutation of Y135 should also be a focus, to establish whether SPO11 is important in initiating DSB or some other function in cancer cells. In addition, co-immunoprecipitation techniques can be used to identify potential proteins in cancer cells that could give clues to function. Additionally, using apoptotic marker such as, CASPASE3 should be used after treat the cancer cells with TALENs or siRNA against *SPO11* this will determine whether loss of *SPO11* results in apoptosis, as the case in meiotic cells. Using a *SPO11* on/off system, such as tetracycline-controlled transcriptional activation (Tet-Off system), should be constructed, then TALENs can be used to target the other *SPO11* gene copies. This technique can be used to study the function of SPO11 in the cancer cells by comparing the cells behaviours when the cells treated with tetracycline while the other cells not. Advanced approaches can then be attempted, including knockout of *SPO11* in mice to determine whether SPO11 mice have reduced cancer levels.

6 SPO11 binding to DNA

6.1 Introduction

Meiotic recombination occurs in specific loci called hotspots. A specific protein, PR domain-containing 9 (PRDM9, also known as Meisetz in mouse) interacts with hotspot locations in the genome (Paigen and Petkov, 2010). The PRDM9 has a zinc finger that makes it a master regulator of the hotspot through DNA binding at specific recombination sites (Grey et al., 2011; Parvanov et al., 2010). This binding opens the chromatin, via PRDM9 methylation of histone H3K4 residues creating a favourable chromatin configuration that allows the Spo11 to gain access to the DNA (Cole et al., 2010). Recombination is then initiated by the SPO11 protein, which creates a DNA DSB (Paigen and Petkov, 2012).

The DSB then requires repair, which is initiated by the binding of the Mre11/Rad50/Nbs1 (MRN) complex. Rad50 has a specific structure called a coiled-coil domain that ends with a zinc hook connection which allows the ATP to bind to the structure (Lee et al., 2013). ATM then phosphorylates a key protein in DSB repair (Segal-Raz et al., 2011). In addition, a recent study has suggested that ATM activated by the DSB also activates a negative feedback loop, which inhibits further DSB formation by phosphorylating SPO11 (Lange et al., 2011).

Giving that the work in the previous chapter infers a possible function for SPO11 in cancer cells, the aim of this chapter was to determine whether SPO11 is covalently bound to DNA (Hartsuiker, 2011). In addition, the effects of individual knockdown of ATM, Rad50 and PRDM9 were examined with respect to SPO11 binding to DNA.

6.2 Results

In this chapter, DNA fractions were collected from NTERA2 cells and subjected to individually after ultra-centrifugation. Fractions were taking from ultra-centrifuge tube and measured by UV 260 nm to determine the DNA containing fraction. According to the measurement of the DNA concentration, the peaks of DNA concentration were usually in fractions 3, 4 and 5 (Figure 6.1 A). These fractions were applied to a slot blot and analyses by western blotting using anti-SPO11 antibody. This resulted in the detection of SPO11 in fractions 3, 4 and 5, this indicates SPO11 binding to DNA. Free SPO11 was also detected in fractions 9 and 10 (Figure 6.1 B). The membrane then was stripped and reprobed with α-tubulin to confirm that the binding observed for SPO11 to the high DNA concentration fraction was really protein-to-DNA binding; the α-tubulin was detected only in fractions 9 and 10 (Figure 6.1 C).
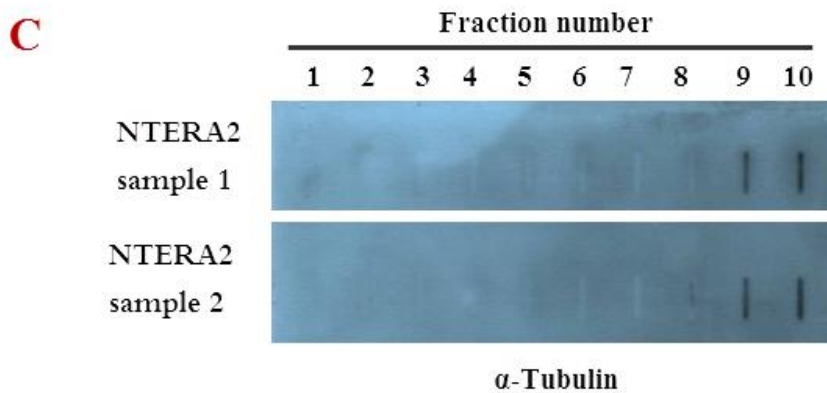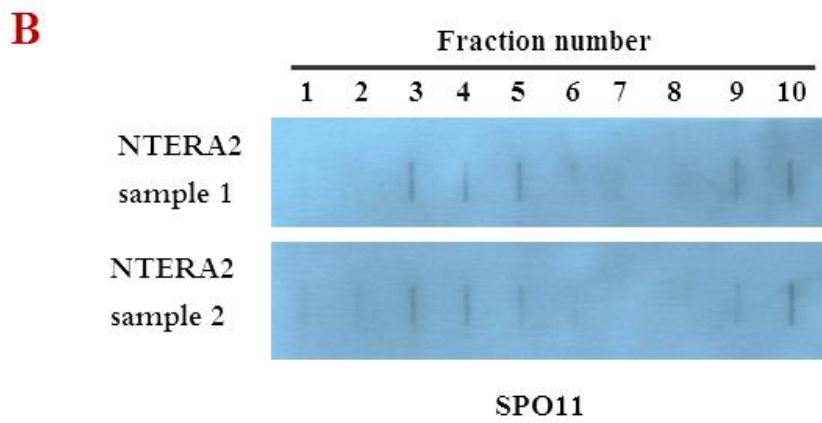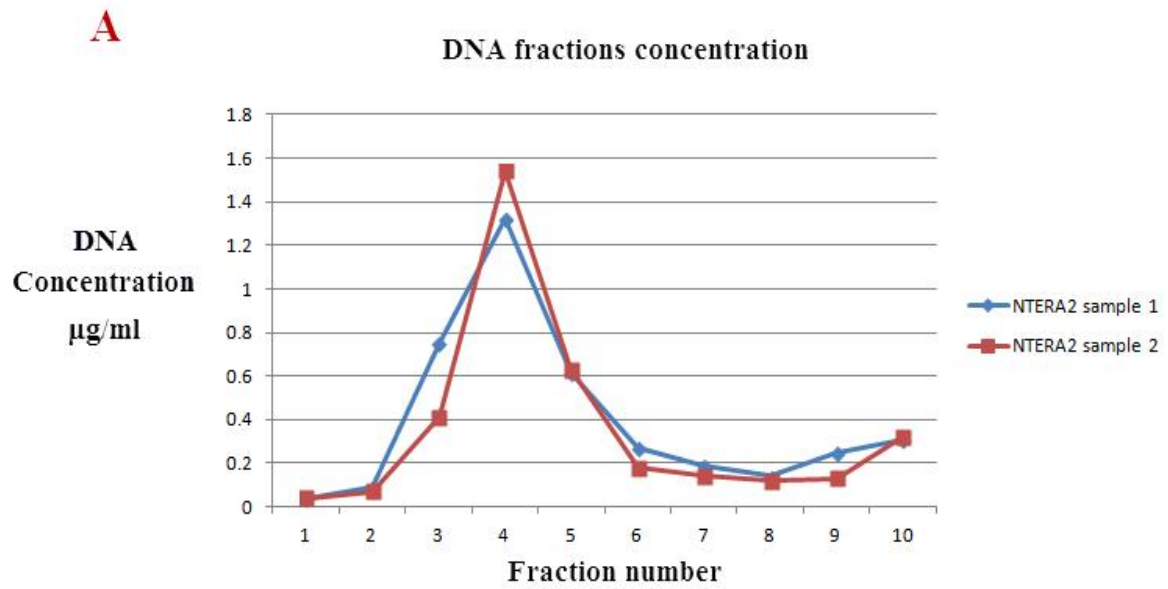
Figure 6.1. Detection of SPO11 binding to DNA. **(A)** The DNA concentration of the sample fractions shows the peak in fractions 3, 4 and 5. **(B)** SPO11 binds to DNA in fractions 3, 4 and 5 while free SPO11 was detected in fractions 9 and 10. **(C)** α-tubulin was detected in the protein fractions which are 9 and 10 (repeated twice).

In meiosis PRDM9 facilitates SPO11 DNA access. Given that PRDM9 expressed in many cancer cells, it was hypothesised that PRDM9 might be needed for the SPO11-DNA association observed here (Figure 6.2). To test this, PRDM9 was knocked-down in NTERA2 using siRNA, with clear PRDM9 knockdown observed when compared to the untreated and non-interference (negative control) samples (Figure 6.2 A). The NTERA2 cell lysates ultra-centrifuged on CsCl gradients and individual fractions were collected. These fractions were applied equally (based on the DNA concentration of the cell lysates) to the slot blot, which revealed the presence of SPO11 in the fractions 3, 4, 5 and 6 in the untreated and non-interference samples (Figure 6.2 B) as observed previously (Figure 6.1). The SPO11 binding to DNA appears to be reduced with PRDM9 knockdown when compared to the untreated and non-interference samples. However, the DNA concentration was lower than untreated and non-interference samples, which might affect the apparent level of SPO11 in the fractions (Figure 6.2 C). Thus, further analyses and quantification are required.
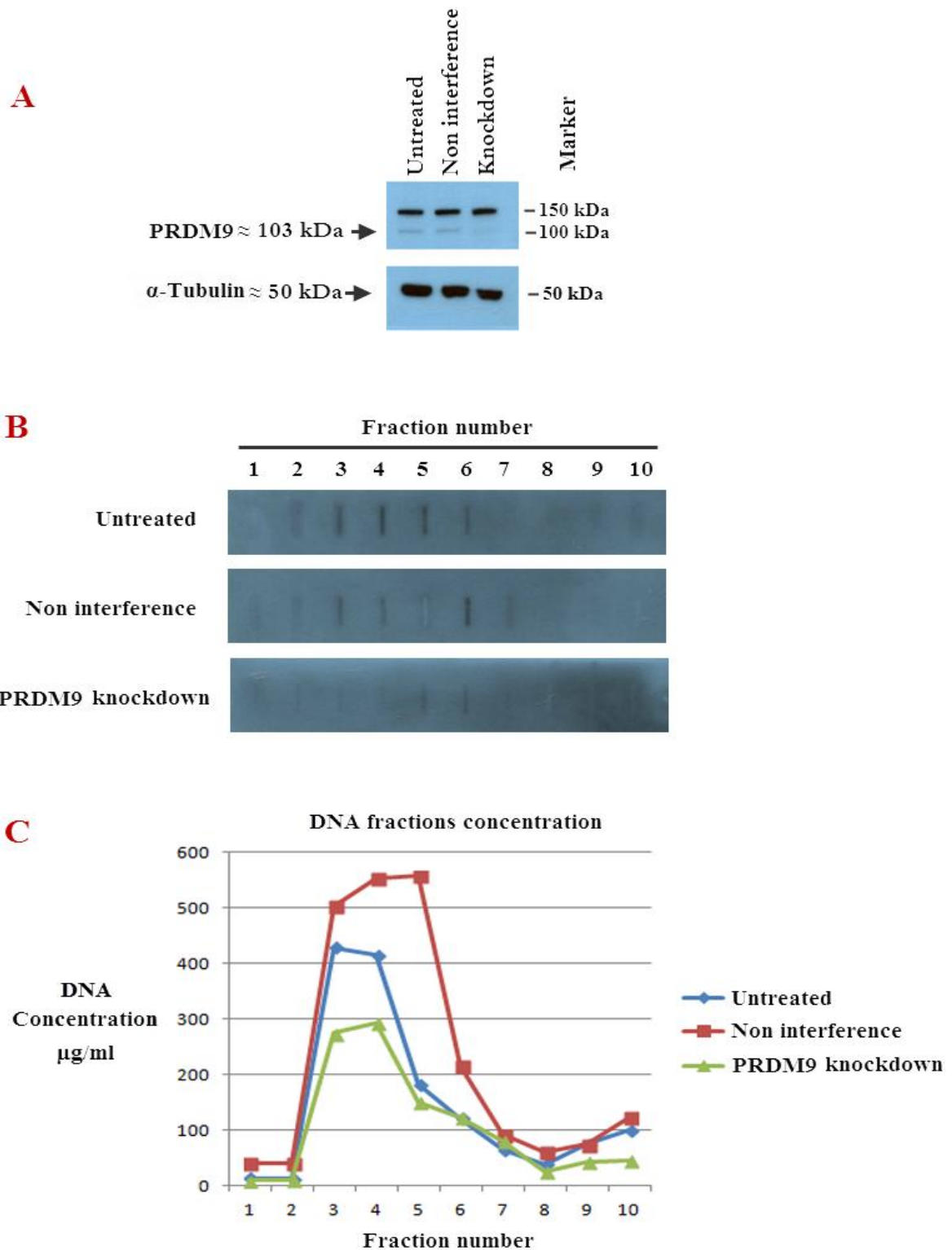
Figure 6.2. Detection of SPO11 binding to DNA following PRDM9 knockdown. (A) Western blot results show an α-tubulin band, which has similar thickness in untreated and non-interference and PRDM9 knockdown, partial PRDM9 knockdown compared to untreated and non-interference samples **(B)** SPO11 binding to the DNA occurred in fractions 3, 4, 5 and 6 in the untreated and non-interference samples; however, the SPO11 binding to DNA was reduced following PRDM9 knockdown when compared to the untreated and non-interference samples **(C)** The DNA concentration of the sample fractions shows the peak in fractions 3, 4, 5 and 6, however, the bands in fractions 9 and 10 were presented in other repeat which does not has DNA in it (repeated twice).

141

Given the importance of RAD50 in SPO11-mediated DSB end processing, and the role for ATM in regulating SPO11-mediated meiotic DSB levels, the levels of bound SPO11 were assess upon reduction of both Rad50 and ATM levels individually. The Rad50 and ATM were knocked-down in NTERA2 using siRNA. The results showed clear knockdown of both proteins when compared to the untreated and non-interference (negative control) samples (Figure 6.3 A and Figure 6.4 A). The cell lysates were ultra-centrifuged on CsCl gradients and the individual fractions were collected. These fractions were applied equally (based on the DNA concentration of the cell lysates) to the slot blot, which revealed the presence of SPO11 equally in fractions 3, 4, 5 and 6 in the untreated and non-interference samples in the Rad50 knockdown (Figure 6.3 B) and ATM knockdown (Figure 6.4 B) samples (no major difference was observed). In addition, the measurement of the DNA concentration, the peaks of DNA concentration were usually in fractions 3, 4, 5 and 6 (Figure 6.3 C and Figure 6.4 C).
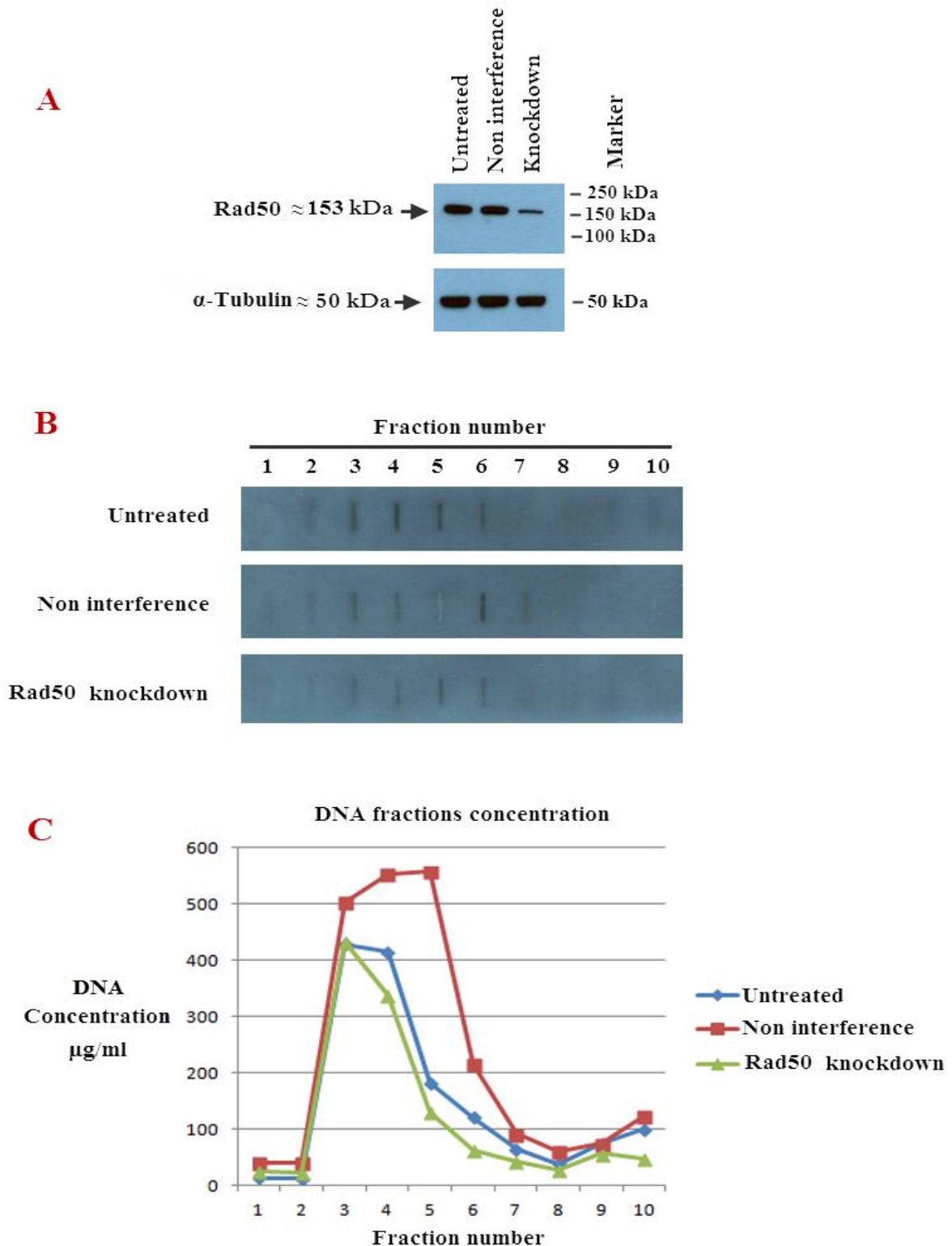
Figure 6.3. Detection of SPO11 binding to DNA following Rad50 knockdown. (A) Western blot results show an α-tubulin band, which has similar thickness in untreated and non-interference and Rad50 knockdown, partial Rad50 knockdown cell lysate fractions compared to fractions from untreated and non-interference cells. **(B)** SPO11 binding to DNA, which showed equal amounts of SPO11 in fractions 3, 4, 5 and 6 in all untreated, non-interference and Rad50 knockdown samples**(C)** The DNA concentration of the sample fractions shows the peak in fractions 3, 4, 5 and 6, however, the bands in fractions 9 and 10 were presented in other repeat which does not have DNA in it (repeated twice).

143
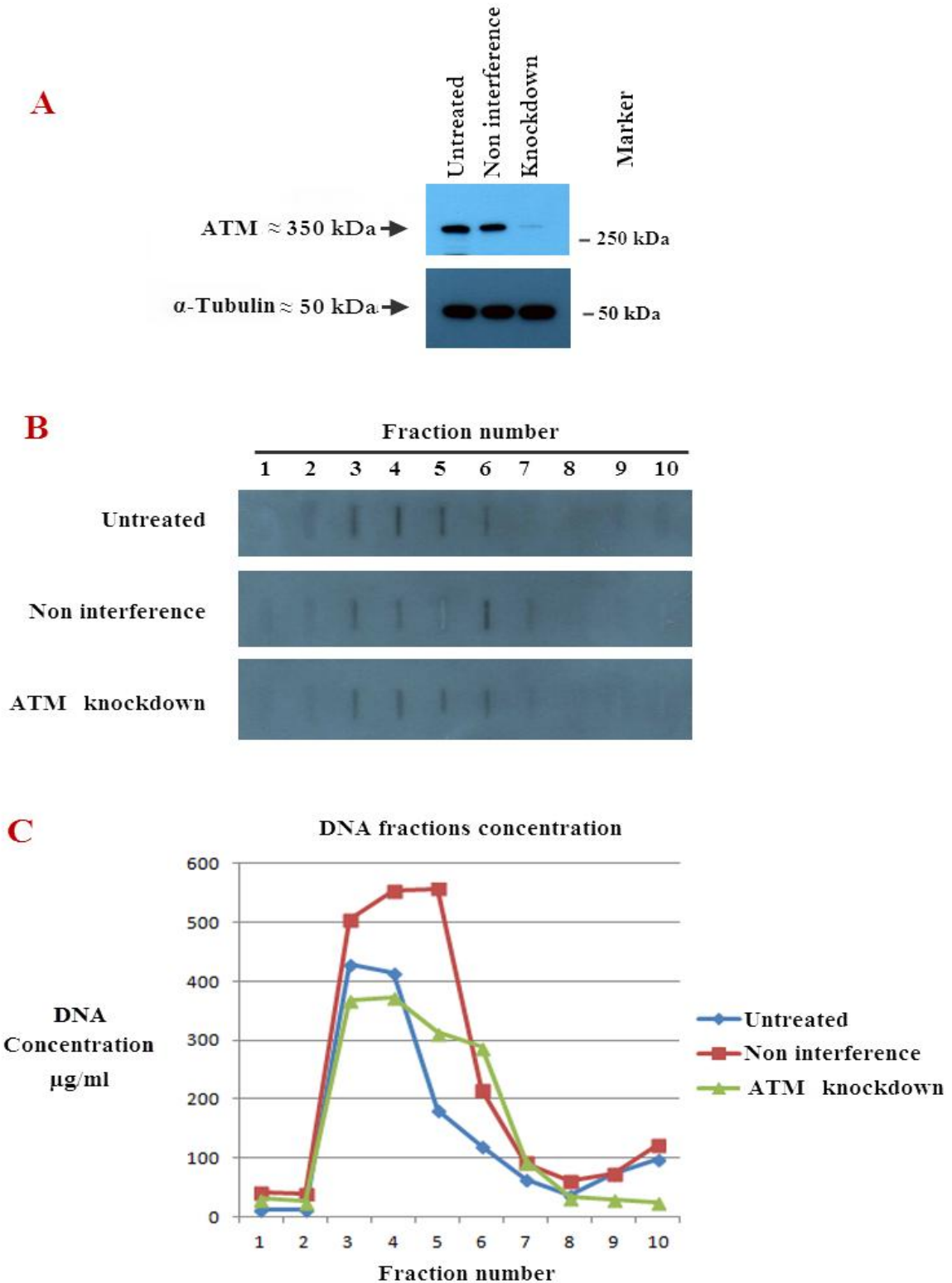
Figure 6.4. Detection of SPO11 binding to DNA following ATM knockdown. (A) Western blot results shows an α-tubulin band, which has similar thickness in untreated and non-interference and ATM knockdown, partial ATM knockdown cell lysate fractions compared to fractions from untreated and non-interference cells **(B)** SPO11 binding to DNA, which showed equal amounts of SPO11 in fractions 3, 4, 5 and 6 in all untreated, non-interference and ATM knockdown samples **(C)** The DNA concentration of the sample fractions shows the peak in fractions 3, 4, 5 and 6 however, the bands in fractions 9 and 10 were presented in other repeat which does not have DNA in it (repeated twice).

144

6.3 Discussion

As described in Chapter 5, SPO11 has been detected in different cell lines and cancer tissues. However, it has different roles during meiosis in DNA replication and DSB formation (Cha et al., 2000). Therefore, the validation of SPO11 DNA binding was very important in the present study. SPO11 was detected together with the peak of DNA in the fractionation study, as shown in the combined data obtained for the DNA concentration and the slot blot results. These findings provided good evidence that SPO11 might bind covalently to DNA, which might be linked to DSB formation in somatic cells. Therefore, the possibility that SPO11 might form DSBs during mitosis is supported by these data. SPO11 binding to DNA could therefore lead to different chromosome rearrangements and ultimately to cancer, suggesting SPO11 could be an oncogenic driver. However, this possibility does not account for why SPO11 might be required for cell proliferation (See Chapter 5).

The *PRDM9* gene is another meiosis-specific gene that performs chromatin modifications. In this case, the chromatin is opened up by PRDM9, which allows SPO11 to bind to the DNA. Therefore, knockdown of PRDM9 might be expected to lead to limited access of the SPO11 to the DNA, thereby limiting SPO11-DNA binding and ultimately limiting DSB formation. This possibility was supported in the present study by the evidence that less SPO11-DNA binding appeared to occur in the PRDM9 knockdown cells compared to the untreated and negative control cells. However, some residual SPO11-DNA binding was still evident in the PRDM9 knockdown sample, which might because of partial knockdown of PRDM9 or the possibility of other DNA hotspots that might be available for SPO11 binding.

In the present study, SPO11-DNA binding was detected at a similar level in Rad50 and ATM knockdown, untreated, and negative control cells. Both ATM and Rad50 are activated by the DSB as part of the DSB repair. Thus, the detection of SPO11-DNA binding with the Rad50 knockdown would be expected. However, in meiosis, although ATM is activated as well by the DSB, recent evidence now suggests that ATM controls a negative feedback loop which inhibits further DSBs by phosphorylation of SPO11 and ATM inactivation results in more DSBs (Lange et al., 2011). Therefore, an increased SPO11-DNA binding should occur in cancer cells if a meiotic scenario were occurring.

However, similar levels of SPO11-DNA binding were detected in the ATM knockdown compared to untreated and negative control cells. This might reflect a partial knockdown that was insufficient to prevent the SPO11 phosphorylation feedback loop. Another possibility is that the ATM does not have a negative feedback loop in cancer cells.

6.4 Conclusion

During meiosis SPO11 binds to DNA to form DSBs which initiate the recombination process. However, in the present study, SPO11 was detected in the cancer cell line DNA at a position corresponding to the peak fractions of DNA, which might indicate the SPO11 was bound to the DNA, giving rise to the possibility of the formation of DSBs in cancer cells. In addition, during meiosis, the SPO11 recognises the hotspots that are modifications in the chromatin created by PRDM9. Therefore, taking this theory to the cancer cells, knockdown of PRDM9 was shown to reduce SPO11-DNA binding. PRDM9 might open the chromatin in cancer cells to allow SPO11 to access to the DNA. If the SPO11 has meiotic-like functions in cancer then that might lead to mis-segregation by forming DSB which are then repaired incorrectly leading to multiple chromosomes rearrangement which are hallmark of most tumour cells.

7 The role of PRDM9 in cancer cells

7.1 Introduction

The PRDM9 protein in humans is a zinc finger protein and also contains a Kruppel associated box (or KRAB domain) (Oliver et al., 2009), which allows PRDM9 to recognise and bind to the C2H2 zinc finger domain (Kota and Feil, 2010). Thus, PRDM9 binds to DNA and then activates the H3K4 methyltransferase, which leads to chromatin modification (Neale, 2010). In humans and other eukaryotes, crossovers occur within hotspot regions. Sequence variation in a 13–base pair (bp) motif, 5' CCNCCNTNNCCNC 3', the target of PRDM9 among humans correlates with 40% of sperm hotspots (Myers et al., 2010). PRDM9 mediated chromatin modification activates some hotspots that allows SPO11 to recognise double stranded DNA and then to perform cleavage to initiate recombination (Figure 7.1) (Buard et al., 2009).

In addition, PRDM9 might be required for chromosomal structures such as XY body formation through searches for homologous chromosomes and synapsis (Reviewed in, Sasaki and Matsui, 2008). For instance, mice with the $Prdm9^{-/-}$ genotype show abnormality in sex-body formation in pachytene spermatocytes (Mihola et al., 2009). The Meisetz mouse (PRDM9) protein directly regulates *RIK* expression (NCBI accession NM177719), also known as *Morc2b*, which is meiosis-specific in mice (Hayashi et al., 2005) but of unknown function (Bolcun-Filas et al., 2011). However, the *RIK* gene product is a GHKL ATPase (Hayashi et al., 2005), which might be involved in the DNA-mismatch-repair machinery (Dutta and Inouye, 2000).

Mutation in PRDM9 causes human male infertility (Irie et al., 2009). In addition, mutation in *PRDM9* in one of the parents causes chromosome rearrangements. For instance, a recent study showed that mutations in *PRDM9* in one of the parents significantly increases the susceptibility to recurrent 7q11.23 microdeletions that cause Williams-Beuren syndrome (Borel et al., 2012). Another recent study reported that rare *PRDM9* alleles can cause genomic rearrangements and can also lead to aneuploidies, both of which are associated with childhood leukemogenesis (Hussin et al., 2013).

A recent study indicated that *PRDM9* was only expressed in the normal adult testis, while it was detected in different types of cancer such as embryonal carcinoma, astrocytoma, colon cancer, prostate cancer, breast cancer, melanoma and leukaemia (Feichtinger et al., 2012a). The aim of this chapter was to execute a preliminary study of PRDM9 protein in normal tissues and cancer tissues and cell lines and then to study the role of PRDM9 in cancer cells by analysing the localisation of PRDM9 (nuclear or cytoplasmic). In addition, the effects of PRDM9 knockdown on the levels of H3K4-me and the association of PRDM9 with chromatin were examined. Lastly, a potential relation between the PRDM9 and *Rik* human ortholog genes was explored.
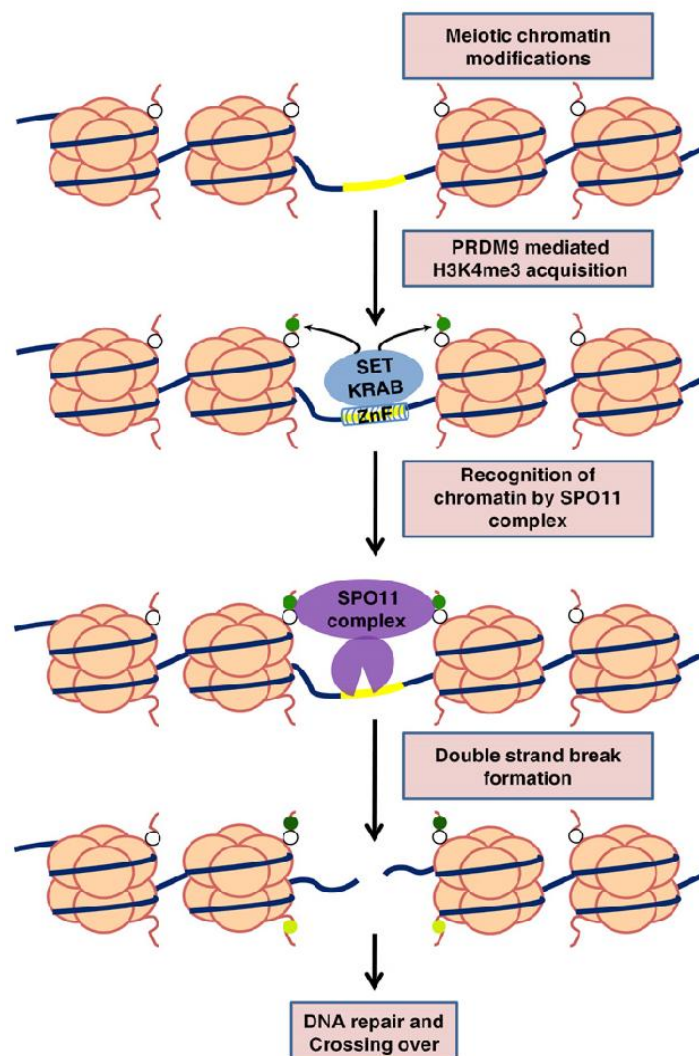

Figure 7.1. chromatin modification in meiotic recombination. In mammalian cells, PRDM9 mediates histone methyltransferase which is recruited to recombination hotspots (yellow rectangle), a process that is facilitated by specific histone modifications. PRDM9 then catalyses H3K4me3 (green circles) through its KRAB domain (blue oval). This modification allows the SPO11 to access to the DNA and create DSBs (Kota and Feil, 2010).

7.2 Results

7.2.1 Analysis of the PRDM9 protein in the normal tissues and cancer

Western blotting was carried out to test protein levels of PRDM9 in both normal tissues (14 different tissues) and cancer cell lines (17 different cell lines). The PRDM9 antibody revealed no protein in normal tissues, including the testis (Figure 7.2 A). The analysis of SPO11 in the normal testis exhibited as low levels by the western blotting which may indicate these proteins are not well represented in the this commercial supplied tissue (Figure 5.2 A). However, the PRDM9 protein was detected in embryonal carcinoma, astrocytoma, colon cancer, breast cancer, ovarian cancer and melanoma (Figure 7.2 B).

Immunohistochemistry carried out on normal and cancer tissues of the colon, ovary and liver, on normal testis tissues, and on lung cancer tissues revealed positive reactions for all three normal testis tissue samples (Table 7.1; Figure 7.3). The colon tissues were negative for both normal and cancer tissues (Table 7.1; Figure 7.4). The ovarian tissues were negative for the normal tissues and most of the cancer tissues (6/7) (Table 7.1; Figure 7.4). The liver tissues were negative for the normal tissues and one third of the cancer tissues (Table 7.1; Figure 7.5). However, the lung tissue (only cancer) was positive for most of the tissues (5/6) (Table 7.1; Figure 7.5)
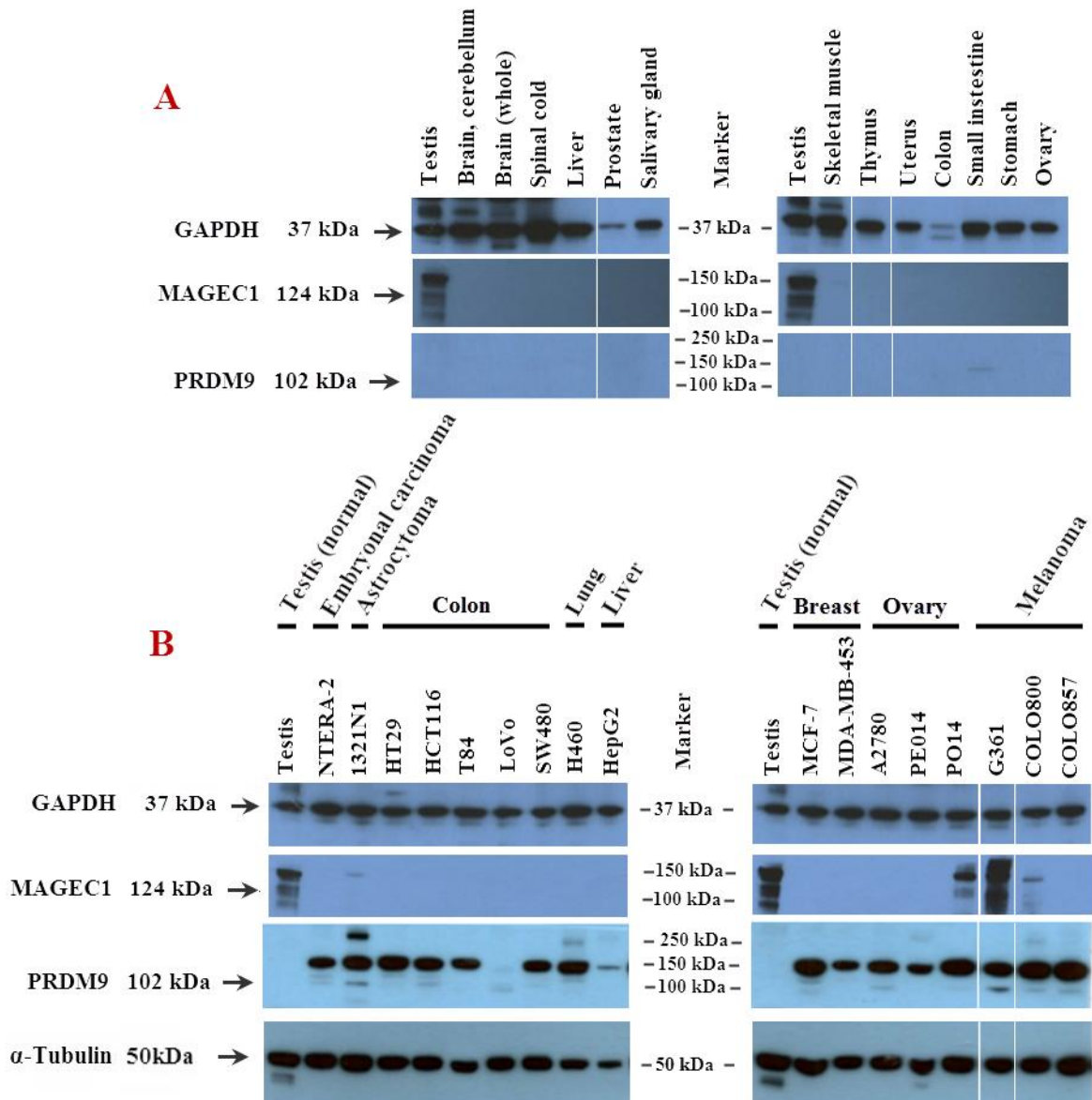
Figure 7.2. Western blot for PRDM9 in normal tissues and cancer cell line. (A) GAPDH control for the normal tissues, MAGEC1 as a CTA control. PRDM9 was not detectable in any normal tissues. (B) GAPDH and α-tubulin as controls for the cancer cell lines, MAGEC1 as a CTA control expressed in melanoma and ovarian cancer; PRDM9 was present in NTERA2, 1321N1, HCT116, LoVo, MCF-7, A2780, PO14, G361, COLO800 and COLO857 (the normal tissues repeat twice and the cancer cell lines were repeated three times).

Table 7.1. Quantification of PRDM9 IHC results in different organs tissues.

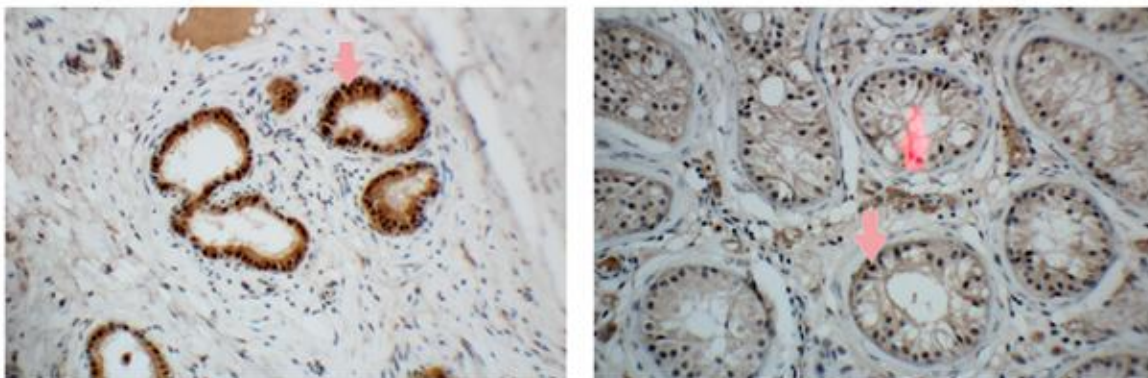| Organ	Normal tissues		Cancer tissues	
	Positive	Negative	Positive	Negative
Testis	3/3	0/3	-	-
Colon	0/8	8/8	0/8	8/8
Ovary	0/1	1/1	1/7	6/7
Liver	0/2	2/2	4/6	2/6
Lung	-	-	5/6	1/6

Normal testis tissues

Figure 7.3. PRDM9 IHC results for normal human testis tissue. Normal testis tissues were used as a positive control for CTAs. The arrows in both images show the seminiferous tubules stained brown by anti-PRDM9 antibodies, which present as positive. (These results were generated with cooperation with a pathologist consultant and were repeated several times with different samples from the same organ; see Table 7.1).

Figure 7.4. PRDM9 IHC results in the colon and ovarian normal and cancer tissues. The colon tissues shown at the top left are normal. The arrow points to the crypts in this section stained with haematoxylin, which present as negative. Moderately differentiated adenocarcinoma tissues are shown at the top right. The arrow points to the differentiated adenocarcinoma weakly stained brown by anti-PRDM9 antibody, which presents as negative. Moderately adenocarcinoma tissues are shown at the top right. The arrow points to the adenocarcinoma dose not stained by anti-PRDM9 antibody, which presents as negative (the tissues were obtained from the same patient). The normal ovarian tissues are shown at the bottom left. The arrow points to the oocyte in this section stained with haematoxylin, which presents as negative. Moderately differentiated serous cystadenocarcinoma tissues are shown at the bottom right. The arrow points to a focal positive stained brown by anti-PRDM9 antibody. (These results were generated with cooperation with a pathologist consultant and were repeated several times with different samples from the same organ; see Table 7.1).
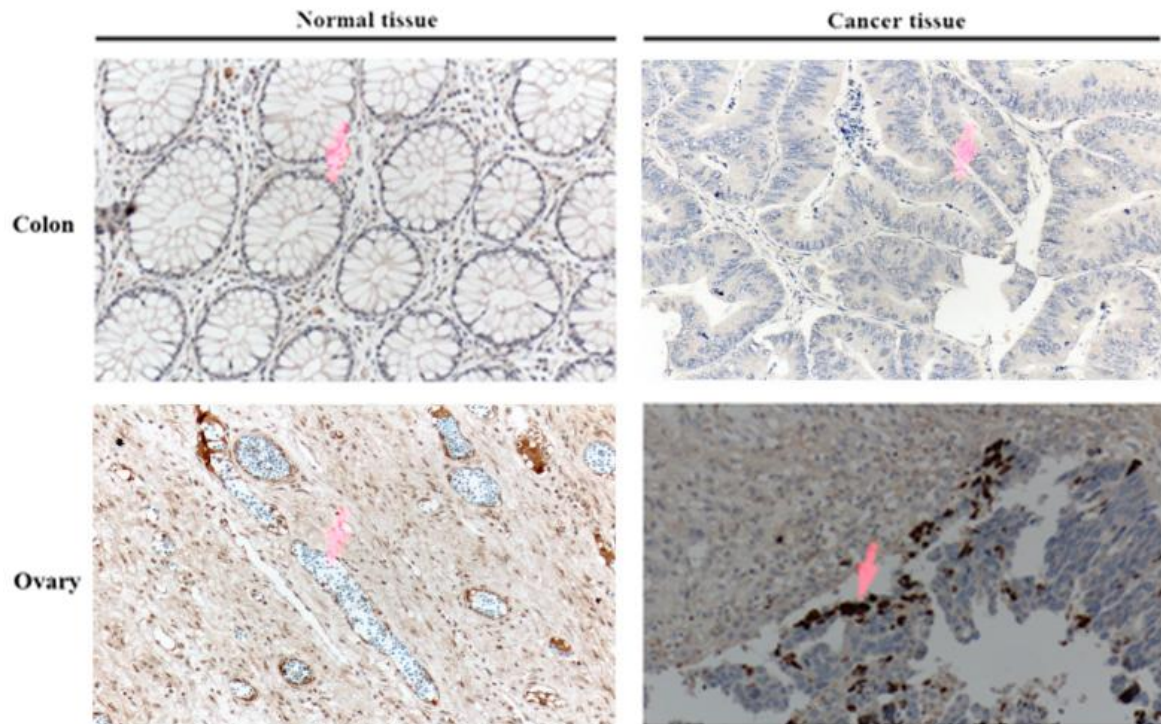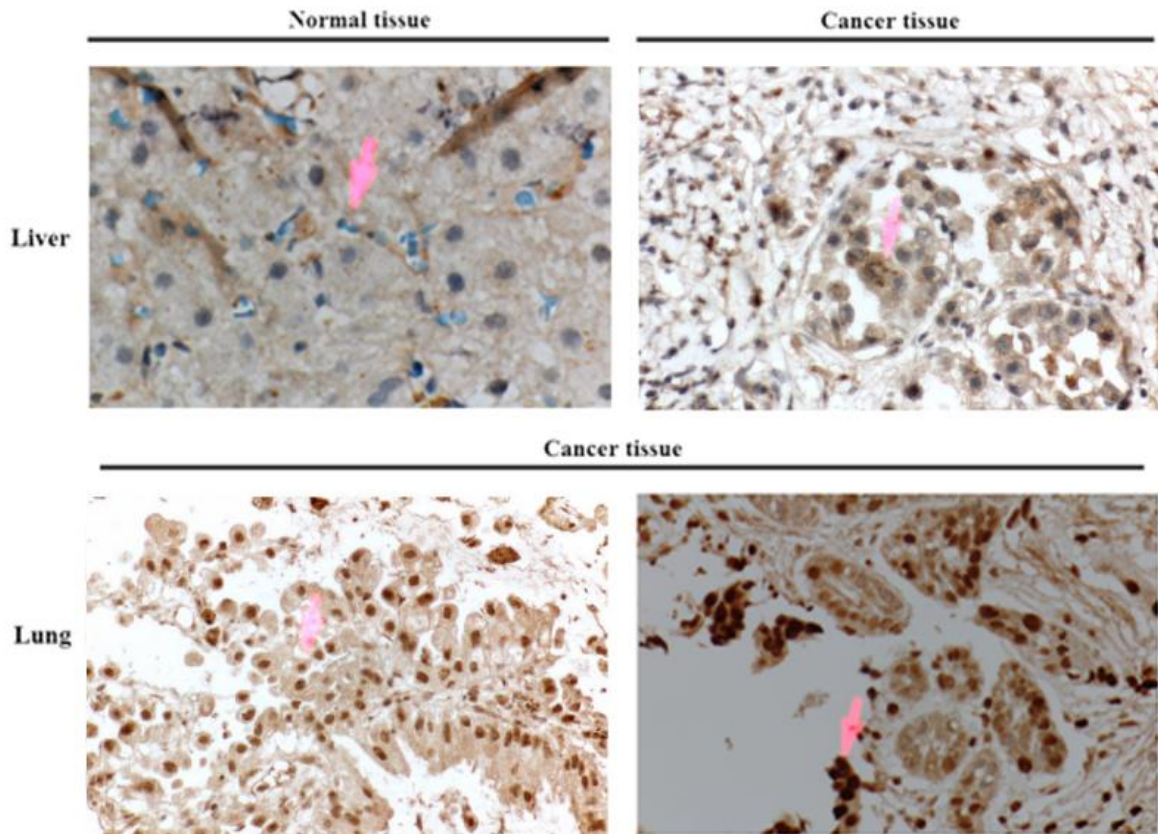
Figure 7.5. PRDM9 IHC results in the colon and ovarian normal and cancer tissues. Normal liver tissues are shown on the left. One arrow points to the cords of hepatocytes stained with haematoxylin with highly background, which presents as negative. The other arrow points to the moderately differentiated adenocarcinoma stained brown by anti-PRDM9 antibody on the right, which presents as positive. **(B)** Lung cancer tissues: the left image shows a positive reaction and the arrow points to well differentiated adenocarcinoma stained brown by anti-PRDM9 antibody. The right image shows squamous cell carcinoma, moderately differentiated and with anti-PRDM9 antibody strong positive brown staining. (These results were generated with cooperation with a pathologist consultant and were repeated several times with different samples from the same organ; see Table 7.1).

7.2.2   Cellular localisation of PRDM9 protein

The cytoplasmic and nuclear fractions were obtained separately to identify the cellular location of PRDM9 protein. In the cell lines NTERA2, 1321N1, HCT116 and A2780, the PRDM9 protein was detected in the nucleus and in the cytoplasm in NTERA2 and 1321N1. However, it was detected in both HCT116 and A2780 in the nucleus (Figure 7.6).
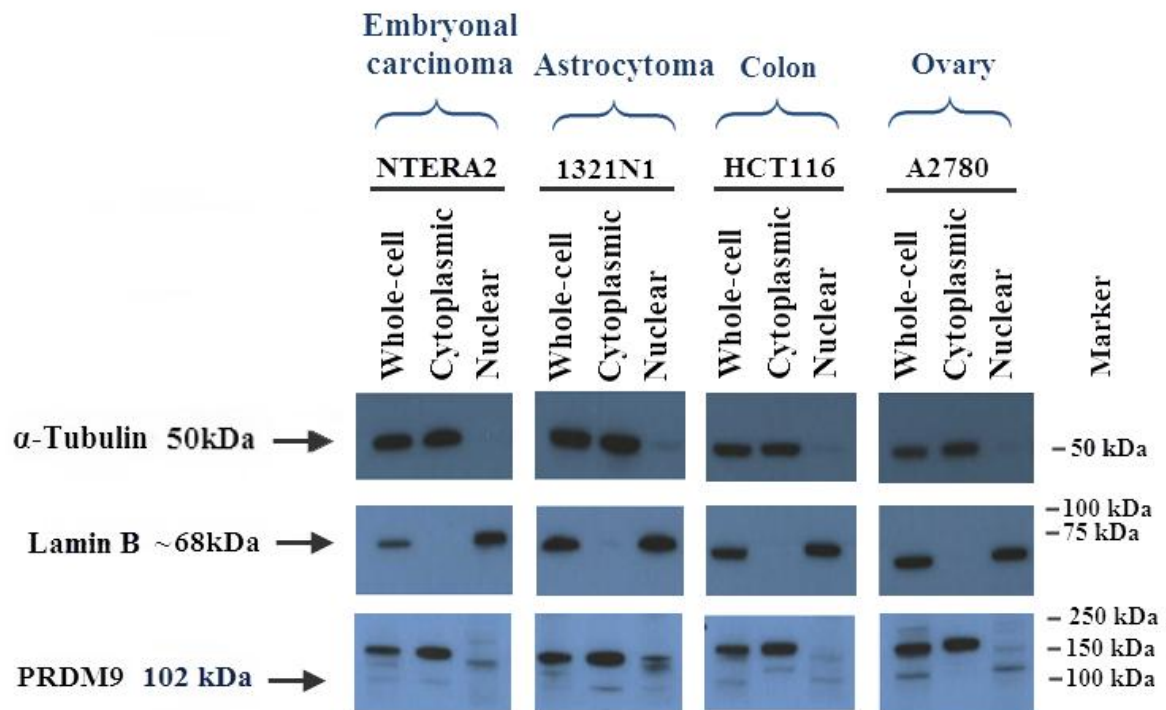

Figure 7.6. Western blot for PRDM9 in different cell line fractions. α-tubulin was used as a cytoplasmic control and lamin B was used as a nuclear control. The PRDM9 was detected in the cytoplasm with NTERA2. In the 1321N1, it was detected in the nucleus and cytoplasm. However, it was detected in both HCT116 and A2780 in the nucleus (repeated twice).

7.2.3 PRDM9 knockdown

In this study, different PRDM9 siRNAs were used to knockdown PRDM9. The PRDM9 siRNA-7 was applied to the cell lines NTERA2, 1321N1, LoVo, HCT116, G361, Colo800 and COLO857 as single or three hits. The knockdown failed with 1321N1, LoVo, Colo800 and COLO857 and it was successful with NTERA2, HCT116 and G361 (Figure 7.7). Two of the PRDM9 knockdowns, NTERA2 and G361, and two of the unsuccessful PRDM9 knockdowns, COLO800 and A2780, were then probed with antibody against H3K4 methylated to check the relationship between PRDM9 and H3K4-me in the cancer cells. The results show no mesurable change in the H3K4 trimethylation levels with or without knockdown of the PRDM9 (Figure 7.8)
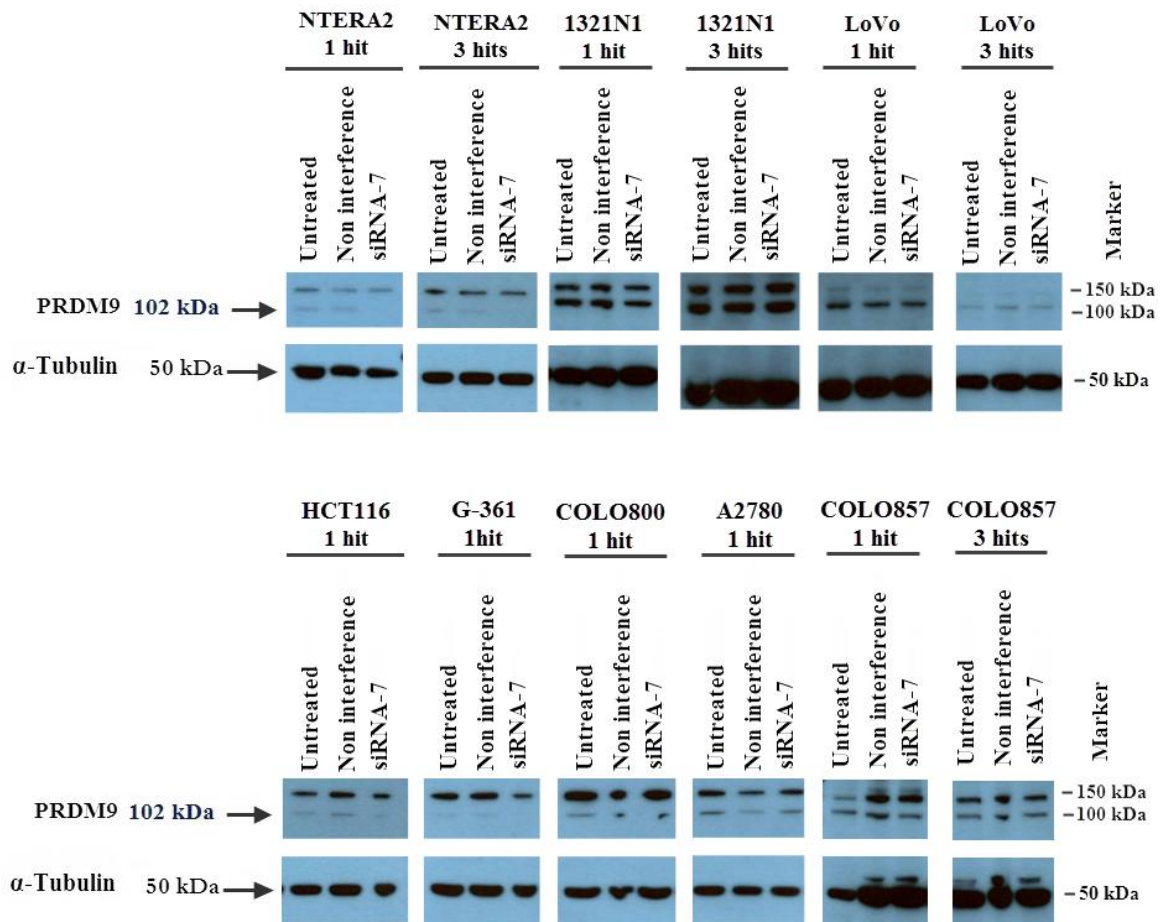
Figure 7.7. Knockdown of PRDM9 in different cell lines. The knockdown failed with 1321N1, LoVo, Colo800 and COLO857 and it was successful with NTERA2, HCT116 and G361, when compared to untreated and non-interference cells as negative controls (repeated three times).
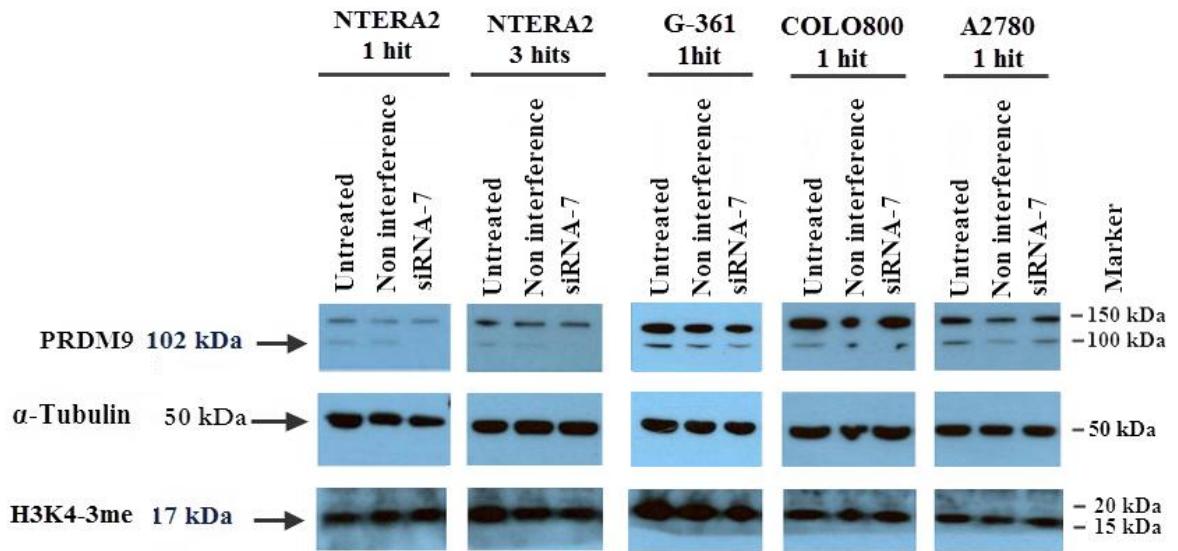
155

Figure 7.8. Validation of the relation between PRDM9 and H3K4-3me in different cell lines. Changes in H3K4-3me with or without knockdown of the PRDM9 in all cell lines (repeated twice).

7.2.4 Validation of the association between PRDM9 and chromatin

The association between the PRDM9 protein and chromatin was tested using different salt concentrations in the nuclear extraction. In addition, to determine if the association occurred before or after metaphase, the cells were treated with colcemid, which breaks the spindle accumulating cells in metaphase. Cell lines used in this experiment were two colon cancer cell lines (HCT116 and SW480), embryonal carcinoma (NTERA2) and ovarian cancer (A2780). The results revealed no evidence of a tight association between PRDM9 and chromatin in any cell lines (Figure 7.9).
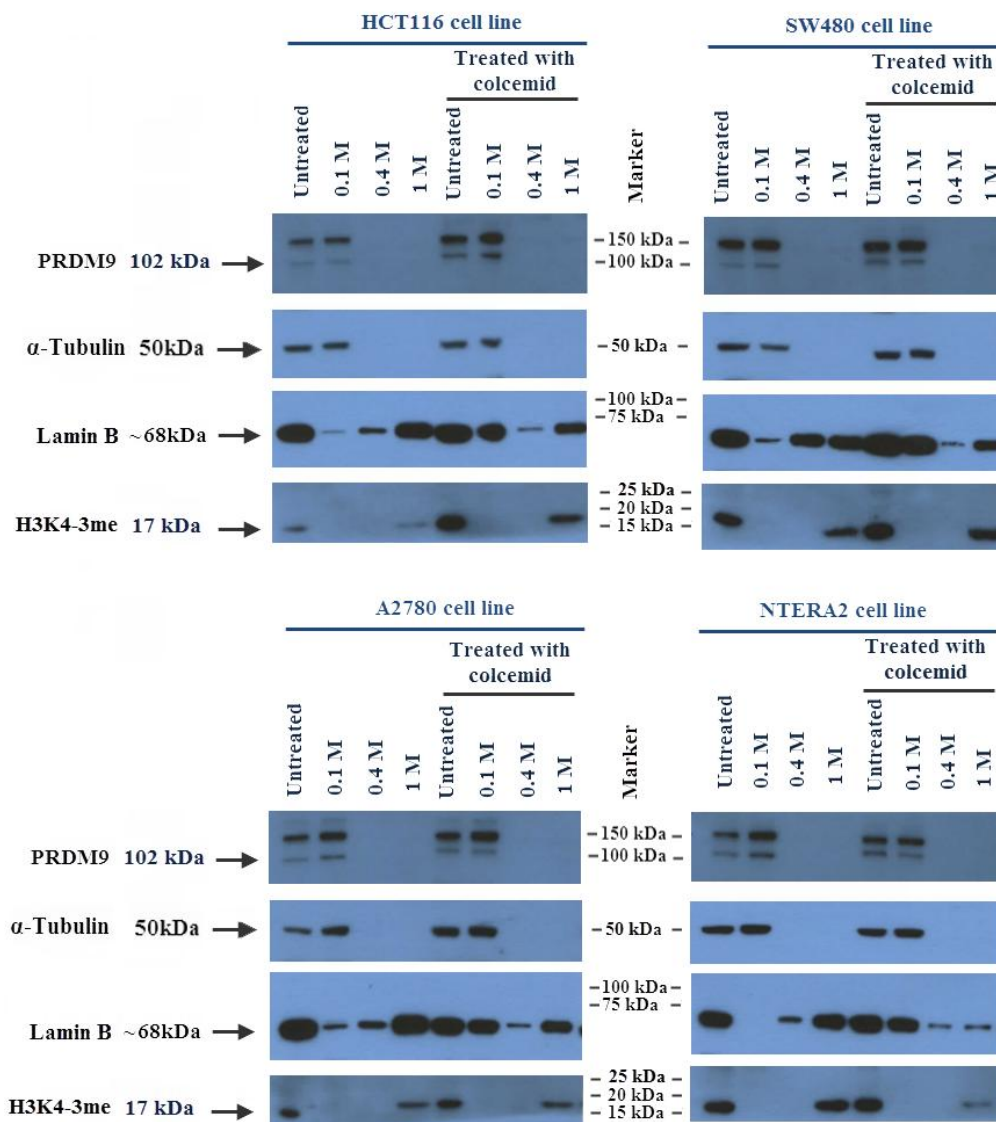

Figure 7.9. Chromatin association test for PRDM9. All cell lines used showed no association between PRDM9 and chromatin. The H3K4 line (as a control) shows high association with chromatin. (A) HCT116 cell line; (B) SW480 cell line; (C) 2780 cell line. (D) NTERA2 cell line (done once).

157

7.2.5 Relation between the *Rik* (*Morc2b*) and human ortholog genes

In the mouse, loss of the PRDM9 orthologue, Meisetz, caused altered gene expression of some meiotic genes (Hayashi et al., 2005). This indicates Meisetz (PRDM9) is not only a hotspot activator, but also a transcriptconal regulator (Hayashi et al., 2005). One of the genes under control of Meisetz was *Rik*. To explore whether PRDM9 in cancer cells is activating expression of any genes, the levels of *Rik* orthologue gene expression were measured upon expression of *PRDM9*.

The *Rik* gene orthologus were identified, which encode a MORC family proteins. Therefore, expression of all members of this gene family were validated including *MORC1*, *MORC2*, *MORC3* and *MORC4*, to determine if any were testis (meiosis) specific. Normal and cancer cell cDNA was used for RT-PCR to compare the expression of the *PRDM9* and different genes of the *MORC* family.

The expression in normal tissues showed a substantial difference, especially between *PRDM9* and *MORC2*, *MORC3* and *MORC4*. Expression of *MORC4* was observed in most tissue and expression of *MORC2* and *MORC3* was seen in all tissues, while *PRDM9* was only expressed in the normal testis (Figure 7.10). However, *MORC1* showed expression in the normal testis and spinal cord (Figure 7.10). The genes were amplified from the cancer tissues and cell lines to look for a correlation between *PRDM9* and *MORC1* expression. No matches between the *PRDM9* and *MORC1* was seen as *MORC1* was not detectable in cancer cells (Figure 7.11).
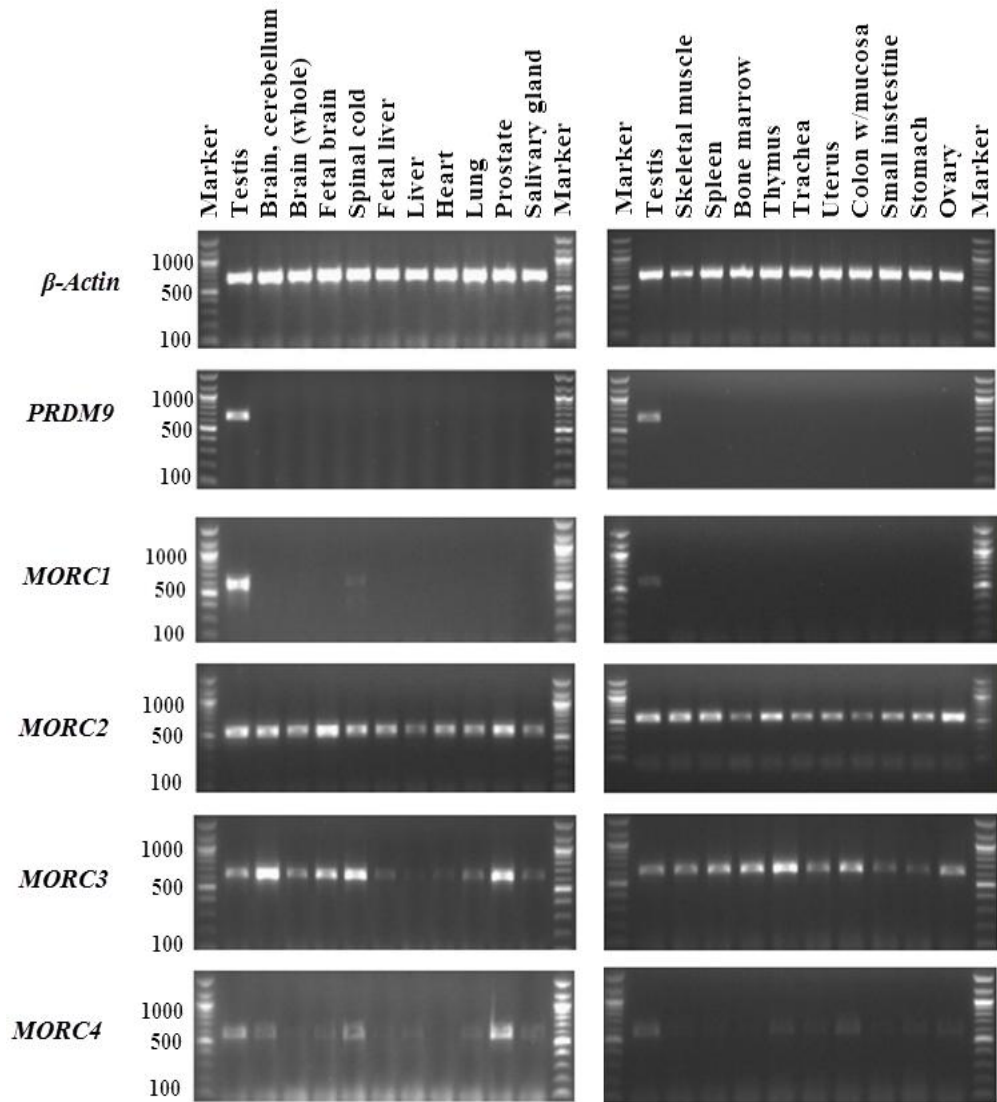
Figure 7.10. Comparing expression of *PRDM9* and *MORC* genes family in normal tissues. A negative relation is evident, especially between *PRDM9* and *MORC2*, *MORC3* and *MORC4*, whereas *MORC1* is quite similar to *PRDM9* except for the expression in the spinal cord (done once).
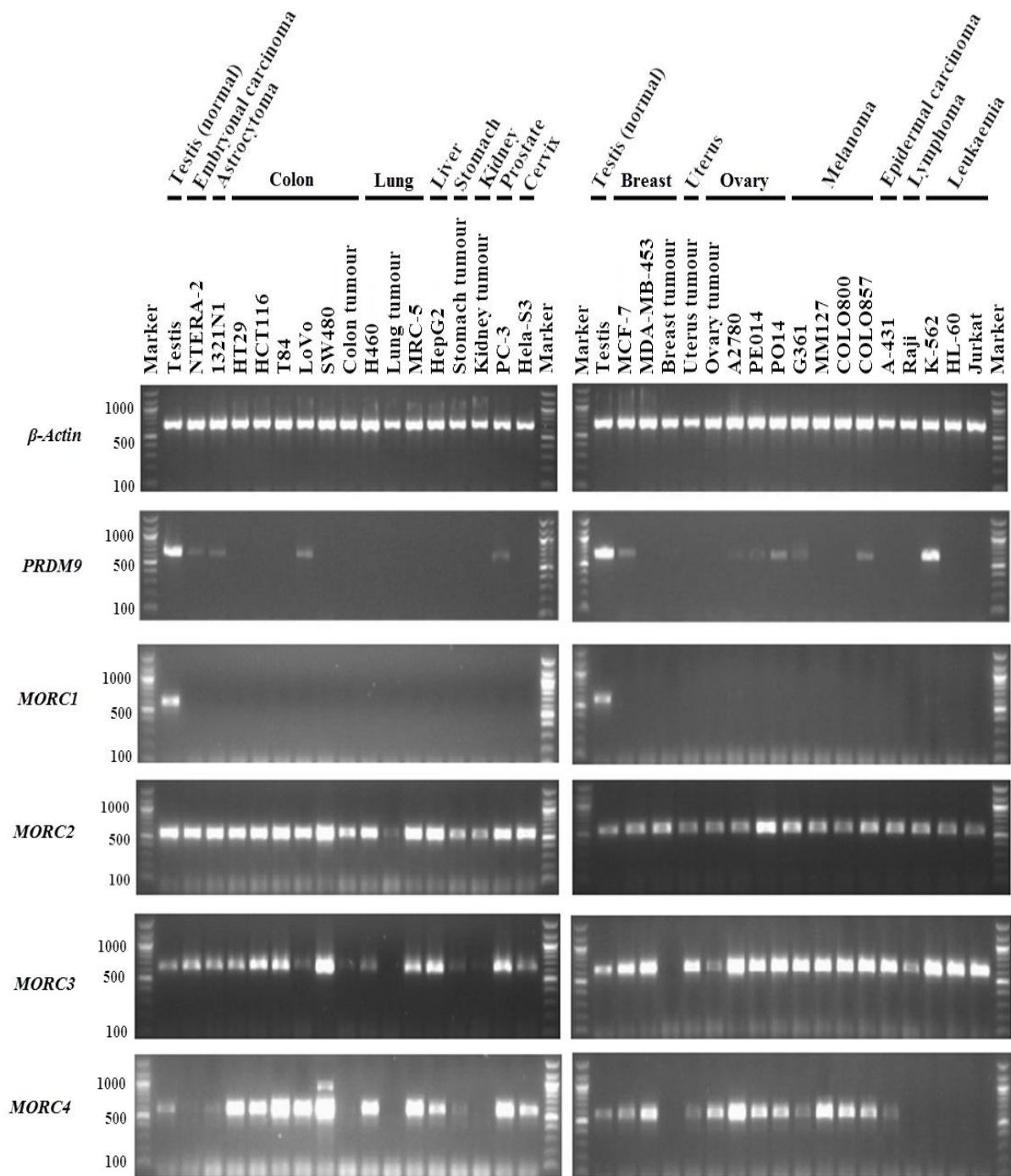
Figure 7.11. Comparison of the expression of *PRDM9* and *MORC* gene family in cancer tissues and cell lines. No expression of *MORC1* could be detected in cancer cells (done once).

7.3 Discussion

The PRDM9 protein plays important roles in mammalian meiosis (Sasaki and Matsui, 2008). However, in the present study, PRDM9 was detected in different types of cancer. Western blot results showed that PRDM9 was not detected in any normal tissues, including the testis. This failure to detect PRDM9 in the testis might indicate that the tissue samples did not include the seminiferous tubules or not enough of the tubule tissue to generate a band. However, IHC results indicated that PRDM9 was present in all three normal testis tissues but not in the other normal tissues.

In addition, PRDM9 was detected in embryonal carcinoma, astrocytoma, colon cancer, breast cancer, ovarian cancer and melanoma tissues by western blot and by IHC. In this study, one sample out of seven of the ovarian cancer, two thirds of the liver cancer and most of the lung cancer samples examined were positive for PRDM9. These findings indicate that this gene might be a good tool for early diagnosis when combined with other markers. It also might be a future cancer immunotherapy target, making PRDM9 a good protein for further study.

At this stage of this study, further experiments were carried out to address whether the function of this gene is the same in meiosis and in the cancer cells. The PRDM9 protein plays a role in recombination and formation of the sex body, which are all nuclear functions. However, although this study detected PRDM9 in the nucleus in all cancer samples used, it was also detected in both nuclear and cytoplasm which indicates that PRDM9 might have other functions in cancer cells. In addition, during meiosis, PRDM9 associates with chromatin and H3K4-3me to open up the chromatin and allow SPO11 to access and bind to the DNA, and initiate recombination. However, in the present study, no association of PRDM9 with chromatin was evident and knockdown of PRDM9 did not change the levels of the H3K4-3me.

In mice, Meisetz (PRDM9) directly regulates *Rik* expression (NCBI accession NM177719), also known as *Morc2b*, which is a meiosis-specific gene in the mouse (Hayashi et al., 2005) and serves an unknown function (Bolcun-Filas et al., 2011). The *Rik* gene might be involved in the DNA-mismatch-repair machinery (Dutta and Inouye, 2000). However, the expression of the human ortholog genes of the mouse *Rik* gene differs in

normal and cancer cells. Thus, PRDM9 might have other roles in cancer and these might differ between mice and humans.

Based on all these results together, the expression of PRDM9 in cancer cells might indicate other uncharacterised functions of PRDM9 in the cancer. Another possibility is that PRDM9 might play an important but as yet unknown role in DSB repair, perhaps by regulating other proteins involved in DSB repair (Hayashi et al., 2005). However, it might also activity in cancer cells and that the gene is simply activated due to the de-regulation of transcription in cancer cells. If this is the case, then PRDM9 might still provide a useful tool in immunotherapeutic.

7.4 Conclusion

PRDM9 is an important gene during meiosis. However, its presence in different cancer tissues and cell lines indicate that it might be a good tool for early diagnosis or/and cancer immunotherapy. However, this gene requires further investigation to address its function, if any, in cancer cells.

8 General Discussion

8.1 Screening of meiotic genes

CTA genes are normally expressed in male germ cells, and are therefore expected to be expressed in the normal adult testis but not in other healthy somatic cells. However, CTA genes are expressed in different types of cancer. The expression of CTA genes in cancer cells can potentially lead to abnormal chromosome segregation or may causes chromosome rearrangement (de Carvalho et al., 2012). CTAs can also be used as cancer biomarkers to diagnose cancers at an early stage. These antigens are also promising candidates for cancer immunotherapy and vaccination. Therefore, identifying large numbers of the CTA genes should enhance and increase therapeutic strategies.

In this study two different tools were used to identify a number of novel potential CTA genes: a manual searching of the meiotic recombination genes and the genes identified by bioinformatics tools. The genes identified using both methods were tested using RT-PCR in different normal tissues and then the good candidates were further explored in different cancer tissues and cell lines.

Surprisingly, 25 genes were expressed in different normal somatic cells and eight of these were thought to be meiotic specific genes. This might be explained in a number of ways. Firstly, these genes have specific functions during meiosis but might have other, as yet uncharacterised functions in mitotic cells. Secondly, some of the normal tissues might have undiagnosed neoplasia. For example, a previous study used a different panel of normal tissues to identify CTA genes and differences were observed in gene expression in the normal tissues from a different panel (Chen et al., 2005a). In addition, many patients may have microscopic cancers that have not progressed to reach the clinic diagnosis level and these people may die from other causes. For example, more than 38% of individuals aged 41 to 60 years who died of non-cancer related trauma had microtumours and only 0.5% were diagnosed with cancer during their lifetimes (Naumov et al., 2009). In the present study, the normal samples used might have had an underlying tumour burden. Another possibility, as seen in the fission yeast, is that specific post-transcriptional mRNA degradation may inhibit the production of meiotic proteins, such as Rec8, in mitotic cells (Harigaya et al., 2006). If this inhibition is also applicable in mammalian cells, it may explain the expression of supposedly meiosis-specific genes in somatic cells.

Six genes identified in this current study showed expression restricted to the normal testis but not in other normal or cancer tissues and cell lines. However, only 33 cancer tissues/cells were explored in the present study, which means that these genes might be expressed in other cancers not included here. For instance, a meta-analysis of microarray data carried out on these six genes through the CancerMA online tool, which is based on microarray data from 80 cancer array sets for 13 type of cancer (Feichtinger et al., 2012b), indicated a significant up-regulation of *CYLC2* and *CCDC79* in ovarian cancer; however, the RT-PCR results for both *CYLC2* and *CCDC79* in the present study did not indicate any expression in the ovarian cancer tissue or in the three different ovarian cell lines (A2780, PE014 and TO14) that were used.

Eleven genes were identified as potentially good candidates as CTA genes, as they showed expression restricted to the normal testis or normal testis and fewer than two other normal tissues, but were expressed in different type of cancers. Some of these genes were expressed abnormally in the somatic cells. One example was *NUT* which has been detected in a rare and aggressive cancer known as NUT midline carcinoma (NMC) (Stelow and French, 2009). Most patients with this cancer die within one year of developing symptoms (French, 2010). NMC occurs as result of fusions between *NUT* and *BRD4*, resulting in an oncogene which is caused by t(15;19) (q13;p13.1) (Ziai et al., 2010). The fusions between *NUT* and *BRD4* cause the NUT moiety to interact with p300 (BRD4-NUT/p300). This interaction leads to transcriptionally inactive hyperacetylated chromatin domains that inactivate *p53* expression (Reynoird et al., 2010). Therefore, knockdown of BRD4-NUT releases p300, to allow activation of *p53* expression and promotion of cell differentiation and apoptosis (Reynoird et al., 2010). There are different molecular technique to diagnose this type of cancer such as using a monoclonal antibody against NUT (Haack et al., 2009). In addition, the use of the FISH technique for both NUT and BRD4 is another useful molecular approach for detecting NMC (Hsieh et al., 2011). A previous study, found that the fusions between *NUT* and *BRD4* is associated with decreased histone acetylation and transcriptional repression (Schwartz et al., 2011). Therefore, they have successfully treated NMC patient with the FDA-approved HDAC inhibitor, vorinostat (Schwartz et al., 2011). In the present study, the *NUT* gene was expressed in colon and ovarian cancers. However, the fusions between *NUT* and *BRD4* has not tested in this study, which can be tested by FISH technique, if the fusions between *NUT* and *BRD4* detected in these two cancers then it might be useful to treat the cancer

cells by vorinostat. If the *NUT* gene not fusions with *BRD4* then the *NUT* gene function unknown, but might be still useful as target immunotherapy. The PAGE5 gene, which is a member of the CTA family, positively regulates antiapoptotic genes such as the dickkopf-1 (*DKK1*) gene, where *DKK1* expression was *p53*-independent (Nylund et al., 2012).

The *PRDM9* gene was identified in the present study as a good candidate CTA gene. Its known function is to open the chromatin and allow SPO11 to access the DNA and initiate meiotic recombination (Buard et al., 2009). *SPO11* was also identified as a CTA gene (Koslowski et al., 2002). Therefore, this study focused on these two genes (*PRDM9* and *SPO11*).

8.2   The role of SPO11 in cancer cells

The *SPO11* gene (*CT35*) was identified as a CTA gene and was detected in melanoma, lung and cervical cancer (Koslowski et al., 2002). In the present study, the SPO11 protein appeared to be detected in the normal testis tissues only, but not in other normal tissues (the antibody has not been fully validated, however it detects a band of the correct size on the western blots and only in the testis not in other normal tissues). However, it was detected in all cancer cell lines and most of the cancer tissues that were used in this study. Full knockout was not achieved, which indicates that SPO11 might be essential for cancer cell survival. Cell growth was reduced using siRNA-4, TALENs and TALENs with homology arms to *SPO11* in HCT116 and SW480 when compared to negative controls and untreated cells. In addition, the ability to form colonospheres was reduced using siRNA-4, TALENs and TALENs with homology arms for *SPO11* in HCT116 colonosphere colonies when compared to negative controls and untreated cells. Therefore, SPO11 might be essential for the cancer cells and/or it might establish the cancer by doing the same function as meiosis such as, forming DSBs which lead to chromosome rearrangement, which can cause cancer, suggesting SPO11 could be an oncogenic driver.

As shown in Chapter 6, SPO11 appears to be covalently bound to DNA indicating SPO11 binding to the DNA might occur in cancer cells. If the antibody is valid, SPO11 did bind to the DNA, which indicates that SPO11 might have a DSB forming function in cancer cells as it does in meiosis. In the case of cancer cells, this might lead to chromosome rearrangements and ultimately to cancer, so SPO11 could be oncogenic. SPO11 binding to DNA appeared to be reduced by *PRDM9* knockdown, which might indicate that PRDM9

opens the chromatin to allow the SPO11 to access and bind to the DNA in mitotic cells. However, PRDM9 might have other functions in cancer cells, as will be discussed in Section 8.3.

In meiotic cells, Rad50 and ATM are activated by DSBs, but ATM also activates a negative feedback loop that inhibits further DSB formation by phosphorylating SPO11 (Lange et al., 2011). However, knockdown of Rad50 and ATM separately did not change the level of apparent SPO11-DNA binding. The knockdown of ATM was hypothesis to have increased SPO11-DNA binding as result of inactivation of a negative feedback loop (Lange et al., 2011), but similar levels of SPO11-DNA binding were detected in the ATM knockdown when compared to untreated and negative control cells. This might reflect a partial knockdown that was insufficient to prevent the SPO11 phosphorylation feedback loop. Another possibility is that the ATM does not have a SPO11-related negative feedback loop in cancer cells.

These results indicate that SPO11 in somatic cells might have same function in common with meiotic cells. Therefore, the presence of SPO11 during mitotic division might lead to incorrect replication or/and formation of DSBs during mitosis, which might lead to different chromosome rearrangements and ultimately to cancer. In addition, the homozygous null mutation of *Spo11* in mice can lead to arrest and spermatocyte apoptosis during the early prophase to mid-pachynema meiosis (Romanienko and Camerini-Otero, 2000). If that the same function is active in the cancer cells, then SPO11 might play important roles during the DNA replication and/or forming DSBs, suggesting SPO11 could be an oncogenic driver. Therefore, cancer cells with defects in SPO11 might undergo apoptosis as results of causes a severe reduction in DNA replication or/and formation of DSBs during mitosis.

8.3   PRDM9 in cancer cells

In Chapter 6, the knockdown of PRDM9 in a cancer cell line resulted in a reduction in the apparent SPO11-DNA binding, which might indicate that PRDM9 opens the chromatin to allow SPO11 to access and bind to the DNA, which is its proposed function in meiosis. However, unlike SPO11, PRDM9 was not detected in all cell lines. Like SPO11, PRDM9 was detected in the nucleus in all samples and in the cytoplasm and nucleus in some samples. PRDM9 knockdown did not affect the global H3K4-3me levels, so evidence for a H3K4 methyl transference activity is currently missing. Whilst it can be postulated that

the function of PRDM9 in cancer cells might be the same as in meiosis, there is insufficient evidence to make any conclusions at this stage.

PRDM9 could have other roles in cancer cells, such as an as yet unknown role in DSBs repair (Hayashi et al., 2005), possibly through regulation of some other protein involved in DSBs repair (Hayashi et al., 2005). In mice, the Meisetz (PRDM9) protein directly regulates *Rik*, a meiosis-specific gene (Hayashi et al., 2005) with an unknown function (Bolcun-Filas et al., 2011), but it might be involved in the DNA-mismatch-repair machinery (Dutta and Inouye, 2000). However, the expression pattern of the human *Rik* ortholog genes differs than of *PRDM9* in normal and cancer cells; thus, *PRDM9* expression dose not correlate to the *Rik* human ortholog genes, suggesting there may not be a direct functional link.

PRDM9 is an important gene during meiosis, however, its expression in different cancer tissues and cell lines indicate that it might be a good tool for early diagnosis or/and cancer immunotherapy.

8.4   Closing remarks

This study aimed to identify novel CTA genes and found eleven of these genes. In addition, six genes were detected in the testis and not in other normal and/or cancer tissues and cell lines. Two of these six genes were up-regulated in ovarian cancers, as determined by using a microarray meta-analyses tool, which means that these two genes should be studied further in more ovarian cancer samples. These genes might show promise as biomarkers for early diagnosis of cancer and as targets for cancer immunotherapy and vaccination.

SPO11 was detected in all cell lines and most of the cancer tissues used in this study. In addition, knockdown and/or knockout of the *SPO11* gene negativly affected cancer cell growth, which might indicate that SPO11 is essential for cancer cell survival. Knockdown of PRDM9 in the cancer cell lines reduced the level of SPO11 DNA binding, which might indicate PRDM9 opens the chromatin to allow the SPO11 to access and bind to the DNA as a function in meiosis. However, PRDM9 was not detected in all cell lines, which is the case for SPO11.

Future studies should focus on protein distribution of the good candidate CTA genes identified in the present study in more normal and cancer cell types. An essential but

uncharacterised role for SPO11 in cancer cells is suggested by these findings. Therefore, future studies should expand the cell growth studies in different cell lines. Flow cytometry analysis should be undertaken to check if SPO11 has a function during the S-phase of cancer cells as it does in meiotic cell division. Mutation of Y135 should also be a focus, to establish whether SPO11 is important in initiating DSB or some other function in cancer cells.

References

Abruzzo, M. A., and Hassold, T. J. (2006). Etiology of nondisjunction in humans. Environmental and molecular *25*, 38-47.

Adair, S. J., and Hogan, K. T. (2009). Treatment of ovarian cancer cell lines with 5-aza-2′-deoxycytidine upregulates the expression of cancer-testis antigens and class I major histocompatibility complex-encoded molecules. Cancer Immunology, Immunotherapy *58*, 589-601.

Adams, J., and Cory, S. (2007). The Bcl-2 apoptotic switch in cancer development and therapy. Oncogene *26*, 1324-1337.

Adjei, A. A. (2001). Blocking oncogenic Ras signaling for cancer therapy. Journal of the National Cancer Institute *93*, 1062-1074.

Aggarwal, B. B., Shishodia, S., Sandur, S. K., Pandey, M. K., and Sethi, G. (2006). Inflammation and cancer: how hot is the link? Biochemical pharmacology *72*, 1605-1621.

Almeida, L. G., Sakabe, N. J., Silva, M. C. C., Mundstein, A. S., Cohen, T., Chen, Y.-T., Chua, R., Gurung, S., Gnjatic, S., and Jungbluth, A. A. (2009). CTdatabase: a knowledge-base of high-throughput and curated data on cancer-testis antigens. Nucleic acids research *37*, D816-D819.

Artigas, M. S., Loth, D. W., Wain, L. V., Gharib, S. A., Obeidat, M. e., Tang, W., Zhai, G., Zhao, J. H., Smith, A. V., and Huffman, J. E. (2011). Genome-wide association and large-scale follow up identifies 16 new loci influencing lung function. Nature genetics *43*, 1082–1090.

Barber, T. D., McManus, K., Yuen, K. W., Reis, M., Parmigiani, G., Shen, D., Barrett, I., Nouhi, Y., Spencer, F., and Markowitz, S. (2008). Chromatid cohesion defects may underlie chromosome instability in human colorectal cancers. Proceedings of the National Academy of Sciences *105*, 3443-3448.

Baudat, F., Buard, J., Grey, C., Fledel-Alon, A., Ober, C., Przeworski, M., Coop, G., and de Massy, B. (2010). PRDM9 is a major determinant of meiotic recombination hotspots in humans and mice. Science *327*, 836 - 840.

Behnam, B., Chahlavi, A., Pattisapu, J., and Wolfe, J. (2009). TSGA10 is Specifically Expressed in Astrocyte and Over-expressed in Brain Tumors. Avicenna Journal of Medical Biotechnology *1*, 161-166.

Bellani, M. A., Romanienko, P. J., Cairatti, D. A., and Camerini-Otero, R. D. (2005). SPO11 is required for sex-body formation, and Spo11 heterozygosity rescues the prophase arrest of Atm-/-spermatocytes. Journal of cell science *118*, 3233-3245.

Berg, I. L., Neumann, R., Lam, K.-W. G., Sarbajna, S., Odenthal-Hesse, L., May, C. A., and Jeffreys, A. J. (2010). PRDM9 variation strongly influences recombination hot-spot activity and meiotic instability in humans. Nature genetics *42*, 859-863.

Bergerat, A., de Massy, B., Gadelle, D., Varoutas, P.-C., Nicolas, A., and Forterre, P. (1997). An atypical topoisomerase II from Archaea with implications for meiotic recombination. Nature *386*, 414 - 417.

Bermudez, V. P., Farina, A., Higashi, T. L., Du, F., Tappin, I., Takahashi, T. S., and Hurwitz, J. (2012). In vitro loading of human cohesin on DNA by the human Scc2-Scc4 loader complex. Proceedings of the National Academy of Sciences *109*, 9366-9371.

Bird, A. (2007). Perceptions of epigenetics. Nature *447*, 396-398.

Bisig, C. G., Guiraldelli, M. F., Kouznetsova, A., Scherthan, H., Höög, C., Dawson, D. S., and Pezza, R. J. (2012). Synaptonemal complex components persist at centromeres and are required for homologous centromere pairing in mouse spermatocytes. PLoS Genetics *8*, e1002701.

Blanco-Rodríguez, J. (2012). Programmed phosphorylation of histone H2AX precedes a phase of DNA double-strand break-independent synapsis in mouse meiosis. Reproduction *144*, 699-712.

Blasco, M. A. (2005). Telomeres and human disease: ageing, cancer and beyond. Nature Reviews Genetics *6*, 611-622.

Boateng, K. A., Bellani, M. A., Gregoretti, I. V., Pratto, F., and Camerini-Otero, R. D. (2013). Homologous Pairing Preceding SPO11-Mediated Double-Strand Breaks in Mice. Developmental cell *24*, 196-205.

Bolcun-Filas, E., Bannister, L. A., Barash, A., Schimenti, K. J., Hartford, S. A., Eppig, J. J., Handel, M. A., Shen, L., and Schimenti, J. C. (2011). A-MYB (MYBL1) transcription factor is a master regulator of male meiosis. Development *138*, 3319-3330.

Borel, C., Cheung, F., Stewart, H., Koolen, D. A., Phillips, C., Thomas, N. S., Jacobs, P. A., Eliez, S., and Sharp, A. J. (2012). Evaluation of PRDM9 variation as a risk factor for recurrent genomic disorders and chromosomal non-disjunction. Human Genetics *131*, 1519-1524.

Brábek, J., Mierke, C. T., Rösel, D., Veselý, P., and Fabry, B. (2010). The role of the tissue microenvironment in the regulation of cancer cell motility and invasion. Cell Commun Signal *8*, 22.

Branford, W. W., Zhao, G.-Q., Valerius, M. T., Weinstein, M., Birkenmeier, E. H., Rowe, L. B., and Potter, S. S. (1997). Spxl, a novel X-linked homeobox gene expressed during spermatogenesis. Mechanisms of development *65*, 87-98.

Brar, G. A., and Amon, A. (2008). Emerging roles for centromeres in meiosis I chromosome segregation. Nature Reviews Genetics *9*, 899-910.

Buard, J., Barthès, P., Grey, C., and de Massy, B. (2009). Distinct histone modifications define initiation and repair of meiotic recombination in the mouse. The EMBO journal *28*, 2616-2624.

Buonomo, S. B., Clyne, R. K., Fuchs, J., Loidl, J., Uhlmann, F., and Nasmyth, K. (2000). Disjunction of homologous chromosomes in meiosis I depends on proteolytic cleavage of the meiotic cohesin Rec8 by separin. Cell *103*, 387-398.

Cairns, R. A., Harris, I. S., and Mak, T. W. (2011). Regulation of cancer cell metabolism. Nature Reviews Cancer *11*, 85-95.

Cammack, R., Attwood, T., Campbell, P., Parish, H., Smith, A., Vella, F., and Stirling, J. (2006). Oxford Dictionary of Biochemistry and Molecular Biology: OUP Oxford, p 479).

Carelle, N., Piotto, E., Bellanger, A., Germanaud, J., Thuillier, A., and Khayat, D. (2002). Changing patient perceptions of the side effects of cancer chemotherapy. Cancer *95*, 155-163.

Cedar, H., and Bergman, Y. (2009). Linking DNA methylation and histone modification: patterns and paradigms. Nature Reviews Genetics *10*, 295-304.

Celerin, M., Merino, S. T., Stone, J. E., Menzie, A. M., and Zolan, M. E. (2000). Multiple roles of Spo11 in meiotic chromosome behavior. The EMBO journal *19*, 2739-2750.

Cermak, T., Doyle, E. L., Christian, M., Wang, L., Zhang, Y., Schmidt, C., Baller, J. A., Somia, N. V., Bogdanove, A. J., and Voytas, D. F. (2011). Efficient design and

assembly of custom TALEN and other TAL effector-based constructs for DNA targeting. Nucleic acids research *39*, e82.

Cha, R. S., Weiner, B. M., Keeney, S., Dekker, J., and Kleckner, N. (2000). Progression of meiotic DNA replication is modulated by interchromosomal interaction proteins, negatively by Spo11p and positively by Rec8p. Genes & development *14*, 493-503.

Chen, Y.-T., Scanlan, M. J., Venditti, C. A., Chua, R., Theiler, G., Stevenson, B. J., Iseli, C., Gure, A. O., Vasicek, T., and Strausberg, R. L. (2005a). Identification of cancer/testis-antigen genes by massively parallel signature sequencing. Proceedings of the National Academy of Sciences *102*, 7940-7945.

Chen, Y.-T., Venditti, C. A., Theiler, G., Stevenson, B. J., Iseli, C., Gure, A. O., Jongeneel, C. V., Old, L. J., and Simpson, A. (2005b). Identification of CT46/HORMAD1, an immunogenic cancer/testis antigen encoding a putative meiosis-related protein. Cancer Immun *5*, 9.

Chen, Y. T., Ross, D. S., Chiu, R., Zhou, X. K., Chen, Y. Y., Lee, P., Hoda, S. A., Simpson, A. J., Old, L. J., and Caballero, O. (2011). Multiple cancer/testis antigens are preferentially expressed in hormone-receptor negative and high-grade breast cancers. PloS one *6*, e17876.

Chen, Y. T., Scanlan, M. J., Sahin, U., Türeci, Ö., Gure, A. O., Tsang, S., Williamson, B., Stockert, E., Pfreundschuh, M., and Old, L. J. (1997). A testicular antigen aberrantly expressed in human cancers detected by autologous antibody screening. Proceedings The National Academy of Sciences *94*, 1914-1918

Cheng, Y.-H., Wong, E. W., and Cheng, C. Y. (2011). Cancer/testis (CT) antigens, carcinogenesis and spermatogenesis. Spermatogenesis *1*, 209-220.

Cheung, V. G., Sherman, S. L., and Feingold, E. (2010). Genetic Control of Hotspots. Science *327*, 791 - 792.

Christian, M., Cermak, T., Doyle, E. L., Schmidt, C., Zhang, F., Hummel, A., Bogdanove, A. J., and Voytas, D. F. (2010). Targeting DNA double-strand breaks with TAL effector nucleases. Genetics *186*, 757-761.

Chua, P. R., and Roeder, G. S. (1998). Zip2, a meiosis-specific protein required for the initiation of chromosome synapsis. Cell *93*, 349-359.

Cobaleda, C., Schebesta, A., Delogu, A., and Busslinger, M. (2007). Pax5: the guardian of B cell identity and function. Nature immunology *8*, 463-470.

Cole, F., Kauppi, L., Lange, J., Roig, I., Wang, R., Keeney, S., and Jasin, M. (2012). Homeostatic control of recombination is implemented progressively in mouse meiosis. Nature Cell Biology *14*, 424-430.

Cole, F., Keeney, S., and Jasin, M. (2010). Evolutionary conservation of meiotic DSB proteins: more than just Spo11. Genes & development *24*, 1201-1207.

Costa, Y., and Cooke, H. J. (2007). Dissecting the mammalian synaptonemal complex using targeted mutations. Chromosome Research *15*, 579-589.

Costa, Y., Speed, R., Öllinger, R., Alsheimer, M., Semple, C. A., Gautier, P., Maratou, K., Novak, I., Höög, C., and Benavente, R. (2005). Two novel proteins recruited by synaptonemal complex protein 1 (SYCP1) are at the centre of meiosis. Journal of cell science *118*, 2755-2762.

Daniel, K., Lange, J., Hached, K., Fu, J., Anastassiadis, K., Roig, I., Cooke, H. J., Stewart, A. F., Wassmann, K., and Jasin, M. (2011). Meiotic homologue alignment and its quality surveillance are controlled by mouse HORMAD1. Nature cell biology *13*, 599-610.

Daum, J. R., Potapova, T. A., Sivakumar, S., Daniel, J. J., Flynn, J. N., Rankin, S., and Gorbsky, G. J. (2011). Cohesion fatigue induces chromatid separation in cells delayed at metaphase. Current Biology *21*, 1018-1024.

de Carvalho, F., Vettore, A. L., and Colleoni, G. W. B. (2012). Cancer/Testis Antigen MAGE-C1/CT7: New Target for Multiple Myeloma Therapy. Clinical and Developmental Immunology *2012*, 257695.

De Smet, C., and Loriot, A. (2010). DNA hypomethylation in cancer: Epigenetic scars of a neoplastic journey. epigenetics *5*, 206-213.

De Smet, C., Lurquin, C., Lethé, B., Martelange, V., and Boon, T. (1999). DNA methylation is the primary silencing mechanism for a set of germ line-and tumor-specific genes with a CpG-rich promoter. Molecular and cellular biology *19*, 7327-7335.

Deardorff, M. A., Bando, M., Nakato, R., Watrin, E., Itoh, T., Minamino, M., Saitoh, K., Komata, M., Katou, Y., and Clark, D. (2012). HDAC8 mutations in Cornelia de Lange syndrome affect the cohesin acetylation cycle. Nature *489*, 313-317.

Deardorff, M. A., Kaur, M., Yaeger, D., Rampuria, A., Korolev, S., Pie, J., Gil-Rodríguez, C., Arnedo, M., Loeys, B., and Kline, A. D. (2007). Mutations in cohesin complex members SMC3 and SMC1A cause a mild variant of Cornelia de Lange syndrome with predominant mental retardation. The American Journal of Human Genetics *80*, 485-494.

Dutta, R., and Inouye, M. (2000). GHKL, an emergent ATPase/kinase superfamily. Trends in biochemical sciences *25*, 24-28.

Egel, R., and Lankenau, D.-H. (2007). Recombination and meiosis: crossing-over and disjunction, (New York: Springer, pp 42-45).

Eichler, A. F., and Plotkin, S. R. (2008). Brain metastases. Current treatment options in neurology *10*, 308-314.

Espagne, E., Vasnier, C., Storlazzi, A., Kleckner, N. E., Silar, P., Zickler, D., and Malagnac, F. (2011). Sme4 coiled-coil protein mediates synaptonemal complex assembly, recombinosome relocalization, and spindle pole body morphogenesis. Proceedings of the National Academy of Sciences *108*, 10614-10619.

Farnebo, M., Bykov, V. J. N., and Wiman, K. G. (2010). The p53 tumor suppressor: a master regulator of diverse cellular processes and therapeutic target in cancer. Biochemical and biophysical research communications *396*, 85-89.

Fátima, L. M., Yamila, P. L., Fernanda, T. M., Eva, L. J., Claudio, S., and Martín, M. (2012). Tumor-specific MAGE proteins as regulators of p53 function. Cancer Letters *325*, 11-17.

Feichtinger, J., Aldeailej, I., Anderson, R., Almutairi, M., Almatrafi, A., Alsiwiehri, N., Griffiths, K., Stuart, N., Wakeman, J., and Larcombe, L. (2012a). Meta-analysis of clinical data using human meiotic genes identifies a novel cohort of highly restricted cancer-specific marker genes. Oncotarget *3*, 843–853.

Feichtinger, J., McFarlane, R. J., and Larcombe, L. D. (2012b). CancerMA: a web-based tool for automatic meta-analysis of public cancer microarray data. Database: the journal of biological databases and curation *2012*, bas055.

Feichtinger, J., McFarlane, R.J., Larcombe, L. (2013). CancerEST: a web-based tool for automatic meta-analysis of public EST data. Database, accepted pending revisions.

Fodero-Tavoletti, M. T., Hardy, M. P., Cornell, B., Katsis, F., Sadek, C. M., Mitchell, C. A., Kemp, B. E., and Tiganis, T. (2005). Protein tyrosine phosphatase hPTPN20a is targeted to sites of actin polymerization. Biochemical Journal *389*, 343.

Fraune, J., Schramm, S., Alsheimer, M., and Benavente, R. (2012). The mammalian synaptonemal complex: Protein components, assembly and role in meiotic recombination. Experimental cell research *318*, 1340-1346.

French, C., Ramirez, C., Kolmakova, J., Hickman, T., Cameron, M., Thyne, M., Kutok, J., Toretsky, J., Tadavarthy, A., and Kees, U. (2007). BRD–NUT oncoproteins: a family of closely related nuclear proteins that block epithelial differentiation and maintain the growth of carcinoma cells. Oncogene *27*, 2237-2242.

French, C. A. (2010). Demystified molecular pathology of NUT midline carcinomas. Journal of clinical pathology *63*, 492-496.

Fridkin, A., Penkner, A., Jantsch, V., and Gruenbaum, Y. (2009). SUN-domain and KASH-domain proteins during development, meiosis and disease. Cellular and molecular life sciences *66*, 1518-1533.

Fukuda, T., Pratto, F., Schimenti, J. C., Turner, J. M., Camerini-Otero, R. D., and Höög, C. (2012). Phosphorylation of chromosome core components may serve as axis marks for the status of chromosomal events during mammalian meiosis. PLoS genetics *8*, e1002485.

Gandhi, R., Gillespie, P. J., and Hirano, T. (2006). Human Wapl is a cohesin-binding protein that promotes sister-chromatid resolution in mitotic prophase. Current biology *16*, 2406-2417.

Garcia-Cruz, R., Roig, I., and Caldés, M. (2008). Maternal origin of the human aneuploidies. Are homolog synapsis and recombination to blame? Notes (learned) from the underbelly. Meiosis *5*, 128-136.

Garcia, V., Phelps, S. E., Gray, S., and Neale, M. J. (2011). Bidirectional resection of DNA double-strand breaks by Mre11 and Exo1. Nature *479*, 241-244.

Garg, M., Chaurasiya, D., Rana, R., Jagadish, N., Kanojia, D., Dudha, N., Kamran, N., Salhan, S., Bhatnagar, A., and Suri, S. (2007). Sperm-associated antigen 9, a novel cancer testis antigen, is a potential target for immunotherapy in epithelial ovarian cancer. Clinical Cancer Research *13*, 1421-1428.

Godfrey, K. M., Lillycrop, K. A., Burdge, G. C., Gluckman, P. D., and Hanson, M. A. (2007). Epigenetic mechanisms and the mismatch concept of the developmental origins of health and disease. Pediatric research *61*, 5R-10R.

Gregan, J., Polakova, S., Zhang, L., Tolić-Nørrelykke, I. M., and Cimini, D. (2011). Merotelic kinetochore attachment: causes and effects. Trends in cell biology *21*, 374-381.

Greten, T. F., and Jaffee, E. M. (1999). Cancer vaccines. Journal of Clinical Oncology *17*, 1047-1060.

Grey, C., Barthès, P., Chauveau-Le Friec, G., Langa, F., Baudat, F., and de Massy, B. (2011). Mouse PRDM9 DNA-binding specificity determines sites of histone H3 lysine 4 trimethylation for initiation of meiotic recombination. PLoS biology *9*, e1001176.

Grizzi, F., Franceschini, B., Hamrick, C., Frezza, E. E., Cobos, E., and Chiriva-Internati, M. (2007). Usefulness of cancer-testis antigens as biomarkers for the diagnosis and treatment of hepatocellular carcinoma. J Transl Med *5*.

Gure, M., Old, A., and Chen, Y. T. (2002). Cancer/testis antigens: an expanding family of targets for cancer immunotherapy. Immunological reviews *188*, 22-32.

Gutiérrez-Caballero, C., Herrán, Y., Sánchez-Martín, M., Suja, J. Á., Barbero, J. L., Llano, E., and Pendás, A. M. (2011). Identification and molecular characterization of the mammalian α-kleisin RAD21L. Cell Cycle *10*, 1477-1487.

Haack, H., Johnson, L. A., Fry, C. J., Crosby, K., Polakiewicz, R. D., Stelow, E. B., Hong, S.-M., Schwartz, B. E., Cameron, M. J., and Rubin, M. A. (2009). Diagnosis of NUT midline carcinoma using a NUT-specific monoclonal antibody. The American journal of surgical pathology *33*, 984-991.

Haering, C. H., and Nasmyth, K. (2003). Building and breaking bridges between sister chromatids. Bioessays *25*, 1178-1191.

Hamer, G., Gell, K., Kouznetsova, A., Novak, I., Benavente, R., and Hoog, C. (2006). Characterization of a novel meiosis-specific protein within the central element of the synaptonemal complex. Journal of Cell Science *119*, 4025-4032.

Hamer, G., Wang, H., Bolcun-Filas, E., Cooke, H. J., Benavente, R., and Hoog, C. (2008). Progression of meiotic recombination requires structural maturation of the central element of the synaptonemal complex. Journal of Cell Science *121*, 2445-2451.

Hanahan, D., and Weinberg, R. A. (2000). The hallmarks of cancer. cell *100*, 57-70.

Hanahan, D., and Weinberg, R. A. (2011). Hallmarks of cancer: the next generation. Cell *144*, 646-674.

Handel, M. A., and Schimenti, J. C. (2010). Genetics of mammalian meiosis: regulation, dynamics and impact on fertility. Nature Reviews Genetics *11*, 124-136.

Harigaya, Y., Tanaka, H., Yamanaka, S., Tanaka, K., Watanabe, Y., Tsutsumi, C., Chikashige, Y., Hiraoka, Y., Yamashita, A., and Yamamoto, M. (2006). Selective elimination of messenger RNA prevents an incidence of untimely meiosis. Nature *442*, 45-50.

Hartsuiker, E. (2011). Detection of Covalent DNA-Bound Spo11 and Topoisomerase Complexes. Methods in Molecular Biology *745*, 65-77.

Hauf, S., and Watanabe, Y. (2004). Kinetochore orientation in mitosis and meiosis. Cell *119*, 317-327.

Hayashi, K., Yoshida, K., and Matsui, Y. (2005). A histone H3 methyltransferase controls epigenetic events required for meiotic prophase. Nature *438*, 374-378.

Hayslip, J., and Montero, A. (2006). Tumor suppressor gene methylation in follicular lymphoma: a comprehensive review. Molecular cancer *5*, 44.

Heid, H. W., Figge, U., Winter, S., Kuhn, C., Zimbelmann, R., and Franke, W. W. (2002). Novel actin-related proteins Arp-T1 and Arp-T2 as components of the cytoskeletal calyx of the mammalian sperm head. Experimental cell research *279*, 177-187.

Hembruff, S. L., Jokar, I., Yang, L., and Cheng, N. (2010). Loss of transforming growth factor-β signaling in mammary fibroblasts enhances CCL2 secretion to promote mammary tumor progression through macrophage-dependent and-independent mechanisms. Neoplasia (New York, NY) *12*, 425–433.

Hemminger, J. A., Toland, A. E., Scharschmidt, T. J., Mayerson, J. L., Kraybill, W. G., Guttridge, D. C., and Iwenofu, O. H. (2012). The cancer-testis antigen NY-ESO-1 is highly expressed in myxoid and round cell subset of liposarcomas. Modern Pathology *26*, 282-288.

Henderson, K. A., and Keeney, S. (2004). Tying synaptonemal complex initiation to the formation and programmed repair of DNA double-strand breaks. Proceedings of the National Academy of Sciences of the United States of America *101*, 4519-4524.

Hess, H., Heid, H., Zimbelmann, R., and Franke, W. W. (1995). The protein complexity of the cytoskeleton of bovine and human sperm heads: the identification and characterization of cylicin II. Experimental cell research *218*, 174-182.

Hofmann, O., Caballero, O. L., Stevenson, B. J., Chen, Y.-T., Cohen, T., Chua, R., Maher, C. A., Panji, S., Schaefer, U., and Kruger, A. (2008). Genome-wide analysis of

cancer/testis gene expression. Proceedings of the National Academy of Sciences *105*, 20422-20427.

Hong, J. A., Kang, Y., Abdullaev, Z., Flanagan, P. T., Pack, S. D., Fischette, M. R., Adnani, M. T., Loukinov, D. I., Vatolin, S., and Risinger, J. I. (2005). Reciprocal binding of CTCF and BORIS to the NY-ESO-1 promoter coincides with derepression of this cancer-testis gene in lung cancer cells. Cancer research *65*, 7763-7774.

Hosoya, N., Okajima, M., Kinomura, A., Fujii, Y., Hiyama, T., Sun, J., Tashiro, S., and Miyagawa, K. (2011). Synaptonemal complex protein SYCP3 impairs mitotic recombination by interfering with BRCA2. EMBO reports *13*, 44-51.

Hsieh, M.-S., French, C. A., Liang, C.-W., and Hsiao, C.-H. (2011). NUT Midline Carcinoma Case Report and Review of the Literature. International Journal of Surgical Pathology *19*, 808-812.

Hu, Y., and Smyth, G. K. (2009). ELDA: extreme limiting dilution analysis for comparing depleted and enriched populations in stem cell and other assays. Journal of immunological methods *347*, 70-78.

Hunder, N. N., Wallen, H., Cao, J., Hendricks, D. W., Reilly, J. Z., Rodmyre, R., Jungbluth, A., Gnjatic, S., Thompson, J. A., and Yee, C. (2008). Treatment of metastatic melanoma with autologous CD4+ T cells against NY-ESO-1. The New England Journal of Medicine *358*, 2698-2703.

Hussin, J., Sinnett, D., Casals, F., Idaghdour, Y., Bruat, V., Saillour, V., Healy, J., Grenier, J.-C., De Malliard, T., and Busche, S. (2013). Rare allelic forms of PRDM9 associated with childhood leukemogenesis. Genome research *23*, 419-430.

Iclozan, C., and Gabrilovich, D. I. (2012). Recent Advances in Immunotherapy of Lung Cancer. Journal of Lung Cancer *11*, 1-11.

Irie, S., Tsujimura, A., Miyagawa, Y., Ueda, T., Matsuoka, Y., Matsui, Y., Okuyama, A., Nishimune, Y., and Tanaka, H. (2009). Single nucleotide polymorphisms in PRDM9 (MEISETZ) in patients with nonobstructive azoospermia. Journal of andrology *30*, 426-431.

Jiang, C.-L., Jin, S.-G., Lee, D.-H., Lan, Z.-J., Xu, X., O'Connor, T. R., Szabó, P. E., Mann, J. R., Cooney, A. J., and Pfeifer, G. P. (2002). MBD3L1 and MBD3L2, two new proteins homologous to the methyl-CpG-binding proteins MBD2 and MBD3: characterization of MBD3L1 as a testis-specific transcriptional repressor. Genomics *80*, 621-629.

Jin, J., Jin, N., Zheng, H., Ro, S., Tafolla, D., Sanders, K. M., and Yan, W. (2007). Catsper3 and Catsper4 are essential for sperm hyperactivated motility and male fertility in the mouse. Biology of reproduction *77*, 37-44.

Jones, R. G., and Thompson, C. B. (2009). Tumor suppressors and cell metabolism: a recipe for cancer growth. Genes & development *23*, 537-548.

Jukic, D. M., Rao, U., Kelly, L., Skaf, J. S., Drogowski, L. M., Kirkwood, J. M., and Panelli, M. C. (2010). Microrna profiling analysis of differences between the melanoma of young adults and older adults. J Transl Med *8*, 27.

Jungbluth, A. A., Chen, Y. T., Stockert, E., Busam, K. J., Kolb, D., Iversen, K., Coplan, K., Williamson, B., Altorki, N., and Old, L. J. (2001). Immunohistochemical analysis of NY-ESO-1 antigen expression in normal and malignant human tissues. Journal of Cancer *92*, 856-860.

Junttila, M. R., Karnezis, A. N., Garcia, D., Madriles, F., Kortlever, R. M., Rostker, F., Swigart, L. B., Pham, D. M., Seo, Y., and Evan, G. I. (2010). Selective activation of p53-mediated tumour suppression in high-grade tumours. Nature *468*, 567-571.

Kawamura, T., Suzuki, J., Wang, Y. V., Menendez, S., Morera, L. B., Raya, A., Wahl, G. M., and Belmonte, J. C. I. (2009). Linking the p53 tumour suppressor pathway to somatic cell reprogramming. Nature *460*, 1140-1144.

Keeney, S., Giroux, C. N., and Kleckner, N. (1997). Meiosis-specific DNA double-strand breaks are catalyzed by Spo11, a member of a widely conserved protein family. Cell *88*, 375-384.

Keeney, S., and Neale, M. (2006). Initiation of meiotic recombination by formation of DNA double-strand breaks: mechanism and regulation. Biochemical Society Transactions *34*, 523-525.

Kim, M. A., Lee, H. J., Yang, H. K., Bang, Y. J., and Kim, W. H. (2011a). Heterogeneous amplification of ERBB2 in primary lesions is responsible for the discordant ERBB2 status of primary and metastatic lesions in gastric carcinoma. Histopathology *59*, 822-831.

Kim, R., Kulkarni, P., and Hannenhalli, S. (2013). Derepression of Cancer/Testis Antigens in cancer is associated with distinct patterns of DNA Hypomethylation. BMC cancer *13*, 1-10.

Kim, S. H., Kim, U.-K., Lee, W.-S., Bok, J., Song, J.-W., Seong, J. K., and Choi, J. Y. (2011b). Albumin-Like Protein is the Major Protein Constituent of Luminal Fluid in the Human Endolymphatic Sac. PloS one *6*, e21656.

Kim, Y., Park, H., Park, D., Lee, Y. S., Choe, J., Hahn, J. H., Lee, H., Kim, Y. M., and Jeoung, D. (2010). Cancer/testis antigen CAGE exerts negative regulation on p53 expression through HDAC2 and confers resistance to anti-cancer drugs. Journal of Biological Chemistry *285*, 25957-25968.

Kleckner, N. (1996). Meiosis: how could it work? Proceedings of the National Academy of Sciences *93*, 8167-8174.

Kogo, H., Tsutsumi, M., Inagaki, H., Ohye, T., Kiyonari, H., and Kurahashi, H. (2012). HORMAD2 is essential for synapsis surveillance during meiotic prophase via the recruitment of ATR activity. Genes to Cells *17*, 897-912.

Kojima, K., Kuramochi-Miyagawa, S., Chuma, S., Tanaka, T., Nakatsuji, N., Kimura, T., and Nakano, T. (2009). Associations between PIWI proteins and TDRD1/MTR-1 are critical for integrated subcellular localization in murine male germ cells. Genes to Cells *14*, 1155-1165.

Koslowski, M., Türeci, Ö., Bell, C., Krause, P., Lehr, H.-A., Brunner, J., Seitz, G., Nestle, F. O., Huber, C., and Sahin, U. (2002). Multiple splice variants of lactate dehydrogenase C selectively expressed in human cancer. Cancer research *62*, 6750-6755.

Kota, S. K., and Feil, R. (2010). Epigenetic transitions in germ cell development and meiosis. Developmental cell *19*, 675-686.

Kouzarides, T. (2007). Chromatin modifications and their function. Cell *128*, 693-705.

Krishnadas, D. K., Bai, F., and Lucas, K. (2013a). Cancer testis antigen and immunotherapy. ImmunoTargets and Therapy *2*, 11-19.

Krishnadas, D. K., Shapiro, T., and Lucas, K. (2013b). Complete Remission Following Decitabine/Dendritic Cell Vaccine for Relapsed Neuroblastoma. Pediatrics *131*, e336-e341.

Lange, J., Pan, J., Cole, F., Thelen, M. P., Jasin, M., and Keeney, S. (2011). ATM controls meiotic double-strand-break formation. Nature *479*, 237-240.

Lee, J.-H., Mand, M. R., Deshpande, R. A., Kinoshita, E., Yang, S.-H., Wyman, C., and Paull, T. T. (2013). Ataxia Telangiectasia-Mutated (ATM) Kinase Activity Is

Regulated by ATP-driven Conformational Changes in the Mre11/Rad50/Nbs1 (MRN) Complex. Journal of Biological Chemistry *288*, 12840-12851.

Lee, J. H., Schütte, D., Wulf, G., Füzesi, L., Radzun, H.-J., Schweyer, S., Engel, W., and Nayernia, K. (2006). Stem-cell protein Piwil2 is widely expressed in tumors and inhibits apoptosis through activation of Stat3/Bcl-XL pathway. Human molecular genetics *15*, 201-211.

Lehtonen, H. J., Kiuru, M., Ylisaukko-oja, S. K., Salovaara, R., Herva, R., Koivisto, P. A., Vierimaa, O., Aittomäki, K., Pukkala, E., and Launonen, V. (2006). Increased risk of cancer in patients with fumarate hydratase germline mutation. Journal of medical genetics *43*, 523-526.

Lengauer, C., Kinzler, K. W., and Vogelstein, B. (1998). Genetic instabilities in human cancers. Nature *396*, 643-649.

Lesch, B. J., and Page, D. C. (2012). Genetics of germ cell development. Nature Reviews Genetics *13* 781-794.

Li, T., Huang, S., Zhao, X., Wright, D. A., Carpenter, S., Spalding, M. H., Weeks, D. P., and Yang, B. (2011). Modularly assembled designer TAL effector nucleases for targeted gene knockout and gene replacement in eukaryotes. Nucleic acids research *39*, 6315-6325.

Liu, J. G., Yuan, L., Brundell, E., Björkroth, B., Daneholt, B., and Höög, C. (1996). Localization of the N-terminus of SCP1 to the central element of the synaptonemal complex and evidence for direct interactions between the N-termini of SCP1 molecules organized head-to-head. Experimental cell research *226*, 11-19.

Liu, M., Chen, J., Hu, L., Shi, X., Zhou, Z., Hu, Z., and Sha, J. (2012). HORMAD2/CT46. 2, a novel cancer/testis gene, is ectopically expressed in lung cancer tissues. Molecular human reproduction *18*, 599-604.

Loidl, J. (2013). The Hidden Talents of SPO11. Developmental cell *24*, 123-124.

Longhese, M. P., Bonetti, D., Manfrini, N., and Clerici, M. (2010). Mechanisms and regulation of DNA end resection. The EMBO journal *29*, 2864-2874.

Loriot, A., Boon, T., and De Smet, C. (2003). Five new human cancer-germline genes identified among 12 genes expressed in spermatogonia. International Journal of Cancer *105*, 371-376.

Maeshima, K., Hihara, S., and Eltsov, M. (2010). Chromatin structure: does the 30-nm fibre exist in vivo? Current opinion in cell biology *22*, 291-297.

Mann, M. B., Hodges, C. A., Barnes, E., Vogel, H., Hassold, T. J., and Luo, G. (2005). Defective sister-chromatid cohesion, aneuploidy and cancer predisposition in a mouse model of type II Rothmund–Thomson syndrome. Human molecular genetics *14*, 813-825.

Mao-Draayer, Y., Galbraith, A. M., Pittman, D. L., Cool, M., and Malone, R. E. (1996). Analysis of meiotic recombination pathways in the yeast Saccharomyces cerevisiae. Genetics *144*, 71-86.

Marcar, L., MacLaine, N. J., Hupp, T. R., and Meek, D. W. (2010). Mage-A cancer/testis antigens inhibit p53 function by blocking its interaction with chromatin. Cancer research *70*, 10362-10370.

Mehta, G. D., Rizvi, S. M. A., and Ghosh, S. K. (2012). Cohesin: a guardian of genome integrity. Biochimica et Biophysica Acta (BBA)-Molecular Cell Research *1823*, 1324-1342.

Mellman, I., Coukos, G., and Dranoff, G. (2011). Cancer immunotherapy comes of age. Nature *480*, 480-489.

Meuwissen, R., Meerts, I., Hoovers, J., Leschot, N., and Heyting, C. (1997). Human synaptonemal complex protein 1 (SCP1): isolation and characterization of the cDNA and chromosomal localization in the gene. Genomics *39*, 377-384.

Meyerson, M., Gabriel, S., and Getz, G. (2010). Advances in understanding cancer genomes through second-generation sequencing. Nature Reviews Genetics *11*, 685-696.

Mihola, O., Trachtulec, Z., Vlcek, C., Schimenti, J. C., and Forejt, J. (2009). A mouse speciation gene encodes a meiotic histone H3 methyltransferase. Science *323*, 373 - 375.

Mirandola, L., J. Cannon, M., Cobos, E., Bernardini, G., Jenkins, M. R., Kast, W. M., and Chiriva-Internati, M. (2011). Cancer testis antigens: novel biomarkers and targetable proteins for ovarian cancer. International reviews of immunology *30*, 127-137.

Mizukami, Y., Kono, K., Daigo, Y., Takano, A., Tsunoda, T., Kawaguchi, Y., Nakamura, Y., and Fujii, H. (2008). Detection of novel cancer-testis antigen-specific T-cell responses in TIL, regional lymph nodes, and PBL in patients with esophageal squamous cell carcinoma. Cancer science *99*, 1448-1454.

Mobasheri, M. B., Jahanzad, I., Mohagheghi, M. A., Aarabi, M., Farzan, S., and Modarressi, M. H. (2007). Expression of two testis-specific genes, TSGA10 and SYCP3, in different cancers regarding to their pathological features. Cancer detection and prevention *31*, 296-302.

Mou, D. C., Cai, S. L., Peng, J. R., Wang, Y., Chen, H. S., Pang, X. W., Leng, X. S., and Chen, W. F. (2002). Evaluation of MAGE-1 and MAGE-3 as tumour-specific markers to detect blood dissemination of hepatocellular carcinoma cells. British Journal of Cancer *86*, 110-116.

Mussolino, C., and Cathomen, T. (2012). TALE nucleases: tailored genome engineering made easy. Current Opinion in Biotechnology *23*, 644-650.

Myers, S., Bowden, R., Tumian, A., Bontrop, R. E., Freeman, C., MacFie, T. S., McVean, G., and Donnelly, P. (2010). Drive against hotspot motifs in primates implicates the PRDM9 gene in meiotic recombination. Science *327*, 876-879.

Nasmyth, K. (2011). Cohesin: a catenase with separate entry and exit gates? Nature Cell Biology *13*, 1170-1177.

Natsume, A., Wakabayashi, T., Tsujimura, K., Shimato, S., Ito, M., Kuzushima, K., Kondo, Y., Sekido, Y., Kawatsura, H., and Narita, Y. (2008). The DNA demethylating agent 5-aza-2′-deoxycytidine activates NY-ESO-1 antigenicity in orthotopic human glioma. International Journal of Cancer *122*, 2542-2553.

Naumov, G. N., Folkman, J., and Straume, O. (2009). Tumor dormancy due to failure of angiogenesis: role of the microenvironment. Clinical & experimental metastasis *26*, 51-60.

Neale, M. J. (2010). PRDM9 points the zinc finger at meiotic recombination hotspots. Genome Biol *11*, 104.

Niemeyer, P., Türeci, Ö., Eberle, T., Graf, N., Pfreundschuh, M., and Sahin, U. (2003). Expression of serologically identified tumor antigens in acute leukemias. Leukemia research *27*, 655-660.

Nylund, C., Rappu, P., Pakula, E., Heino, A., Laato, L., Elo, L. L., Vihinen, P., Pyrhönen, S., Owen, G. R., and Larjava, H. (2012). Melanoma-Associated Cancer-Testis Antigen 16 (CT16) Regulates the Expression of Apoptotic and Antiapoptotic Genes and Promotes Cell Survival. Plos one *7*, e45382.

Oliver, P. L., Goodstadt, L., Bayes, J. J., Birtle, Z., Roach, K. C., Phadnis, N., Beatson, S. A., Lunter, G., Malik, H. S., and Ponting, C. P. (2009). Accelerated evolution of the Prdm9 speciation gene across diverse metazoan taxa. PLoS genetics *5*, e1000753.

Öllinger, R., Reichmann, J., and Adams, I. R. (2010). Meiosis and retrotransposon silencing during germ cell development in mice. Differentiation *79*, 147-158.

Page, J., Berríos, S., Rufas, J. S., Parra, M. T., Suja, J. Á., Heyting, C., and Fernández-Donoso, R. (2003). The pairing of X and Y chromosomes during meiotic prophase in the marsupial species Thylamys elegans is maintained by a dense plate developed from their axial elements. Journal of cell science *116*, 551-560.

Page, S. L., Khetani, R. S., Lake, C. M., Nielsen, R. J., Jeffress, J. K., Warren, W. D., Bickel, S. E., and Hawley, R. S. (2008). Corona is required for higher-order assembly of transverse filaments into full-length synaptonemal complex in Drosophila oocytes. PLoS Genetics *4*, 1-12.

Paigen, K., and Petkov, P. (2010). Mammalian recombination hot spots: properties, control and evolution. Nature Reviews Genetics *11*, 221-233.

Paigen, K., and Petkov, P. (2012). Meiotic DSBs and the control of mammalian recombination. Cell Research *22*, 1624-1626.

Pangas, S. A., Yan, W., Matzuk, M. M., and Rajkovic, A. (2004). Restricted germ cell expression of a gene encoding a novel mammalian HORMA domain-containing protein. Gene Expression Patterns *5*, 257-263.

Panizza, S., Mendoza, M. A., Berlinger, M., Huang, L., Nicolas, A., Shirahige, K., and Klein, F. (2011). Spo11-accessory proteins link double-strand break sites to the chromosome axis in early meiotic recombination. Cell *146*, 372-383.

Parvanov, E. D., Petkov, P. M., and Paigen, K. (2010). Prdm9 controls activation of mammalian recombination hotspots. Science *327*, 835-835.

Pellestor, F., Anahory, T., Lefort, G., Puechberty, J., Liehr, T., Hédon, B., and Sarda, P. (2011). Complex chromosomal rearrangements: origin and meiotic behavior. Human Reproduction Update *17*, 476-494.

Pennington, K. P., and Swisher, E. M. (2012). Hereditary ovarian cancer: beyond the usual suspects. Gynecologic oncology *124*, 347-353.

Perez, S., Papamichail, M., and Baxevanis, C. (2007). Immunotherapy for colorectal cancer. Annals of Gastroenterology *16*.

Petronczki, M., Siomos, M. F., and Nasmyth, K. (2003). Un menage a quatre: the molecular biology of chromosome segregation in meiosis. Cell *112*, 423-440.

Pezzi, N., Prieto, I., Kremer, L., Jurado, L. A. P., Valero, C., Del Mazo, J., Martinez-A, C., and Barbero, J. L. (2000). STAG3, a novel gene encoding a protein involved in meiotic chromosome pairing and location of STAG3-related genes flanking the Williams-Beuren syndrome deletion. The FASEB Journal *14*, 581-592.

Pivot-Pajot, C., Caron, C., Govin, J., Vion, A., Rousseaux, S., and Khochbin, S. (2003). Acetylation-dependent chromatin reorganization by BRDT, a testis-specific bromodomain-containing protein. Molecular and cellular biology *23*, 5354-5365.

Prieler, S., Penkner, A., Borde, V., and Klein, F. (2005). The control of Spo11's interaction with meiotic recombination hotspots. Genes & development *19*, 255-269.

Puri, P., Acker-Palmer, A., Stahler, R., Chen, Y., Kline, D., and Vijayaraghavan, S. (2011). Identification of testis 14–3-3 binding proteins by tandem affinity purification. Spermatogenesis *1*, 354-365.

Qiao, H., Chen, J. K., Reynolds, A., Höög, C., Paddy, M., and Hunter, N. (2012). Interplay between Synaptonemal Complex, Homologous Recombination, and Centromeres during Mammalian Meiosis. PLoS Genetics *8*, e1002790.

Raica, M., Cimpean, A. M., and Ribatti, D. (2009). Angiogenesis in pre-malignant conditions. European journal of cancer *45*, 1924-1934.

Revenkova, E., Eijpe, M., Heyting, C., Hodges, C. A., Hunt, P. A., Liebe, B., Scherthan, H., and Jessberger, R. (2004). Cohesin SMC1β is required for meiotic chromosome dynamics, sister chromatid cohesion and DNA recombination. Nature cell biology *6*, 555-562.

Revenkova, E., and Jessberger, R. (2006). Shaping meiotic prophase chromosomes: cohesins and synaptonemal complex proteins. Chromosoma *115*, 235-240.

Reynoird, N., Schwartz, B. E., Delvecchio, M., Sadoul, K., Meyers, D., Mukherjee, C., Caron, C., Kimura, H., Rousseaux, S., and Cole, P. A. (2010). Oncogenesis by sequestration of CBP/p300 in transcriptionally inactive hyperacetylated chromatin domains. The EMBO journal *29*, 2943-2952.

Richardson, C., Moynahan, M. E., and Jasin, M. (1998). Double-strand break repair by interchromosomal recombination: suppression of chromosomal translocations. Genes & development *12*, 3831-3842

Roman-Gomez, J., Jimenez-Velasco, A., Agirre, X., Castillejo, J. A., Navarro, G., San Jose-Eneriz, E., Garate, L., Cordeu, L., Cervantes, F., and Prosper, F. (2007). Epigenetic regulation of human cancer/testis antigen gene, HAGE, in chronic myeloid leukemia. Haematologica *92*, 153-162.

Romanienko, P. J., and Camerini-Otero, R. D. (1999). Cloning, Characterization, and Localization of Mouse and Human SPO11. Genomics *61*, 156-169.

Romanienko, P. J., and Camerini-Otero, R. D. (2000). The Mouse Spo11 Gene Is Required for Meiotic Chromosome Synapsis. Molecular cell *6*, 975-987.

Rosa, A. M., Dabas, N., Byrnes, D. M., Eller, M. S., and Grichnik, J. M. (2012). Germ Cell Proteins in Melanoma: Prognosis, Diagnosis, Treatment, and Theories on Expression. Journal of Skin Cancer *2012*, 621968.

Ross, M. T., Grafham, D. V., Coffey, A. J., Scherer, S., McLay, K., Muzny, D., Platzer, M., Howell, G. R., Burrows, C., and Bird, C. P. (2005). The DNA sequence of the human X chromosome. Nature *434*, 325-337.

Sampietro, M. L., Trompet, S., Verschuren, J. J., Talens, R. P., Deelen, J., Heijmans, B. T., de Winter, R. J., Tio, R. A., Doevendans, P. A., and Ganesh, S. K. (2011). A genome-wide association study identifies a region at chromosome 12 as a potential susceptibility locus for restenosis after percutaneous coronary intervention. Human molecular genetics *20*, 4748-4757.

Sasaki, H., and Matsui, Y. (2008). Epigenetic events in mammalian germ-cell development: reprogramming and beyond. Nature Reviews Genetics *9*, 129-140.

Scanlan, M. J., Gordon, C. M., Williamson, B., Lee, S. Y., Chen, Y. T., Stockert, E., Jungbluth, A., Ritter, G., Jäger, D., and Jäger, E. (2002). Identification of cancer/testis genes by database mining and mRNA expression analysis. International journal of cancer *98*, 485-492.

Scholey, J. M., Brust-Mascher, I., and Mogilner, A. (2003). Cell division. Nature *422*, 746-752.

Schramm, S., Fraune, J., Naumann, R., Hernandez-Hernandez, A., Höög, C., Cooke, H. J., Alsheimer, M., and Benavente, R. (2011). A novel mouse synaptonemal complex protein is essential for loading of central element proteins, recombination, and fertility. PLoS genetics *7*, e1002088.

Schultz-Thater, E., Piscuoglio, S., Iezzi, G., Le Magnen, C., Zajac, P., Carafa, V., Terracciano, L., Tornillo, L., and Spagnoli, G. C. (2011). MAGE-A10 is a nuclear

protein frequently expressed in high percentages of tumor cells in lung, skin and urothelial malignancies. International Journal of Cancer *129*, 1137-1148.

Schwartz, B. E., Hofer, M. D., Lemieux, M. E., Bauer, D. E., Cameron, M. J., West, N. H., Agoston, E. S., Reynoird, N., Khochbin, S., and Ince, T. A. (2011). Differentiation of NUT midline carcinoma by epigenomic reprogramming. Cancer research *71*, 2686-2696.

Segal-Raz, H., Mass, G., Baranes-Bachar, K., Lerenthal, Y., Wang, S.-Y., Chung, Y. M., Ziv-Lehrman, S., Ström, C. E., Helleday, T., and Hu, M. C.-T. (2011). ATM-mediated phosphorylation of polynucleotide kinase/phosphatase is required for effective DNA double-strand break repair. EMBO reports *12*, 713-719.

Serrentino, M.-E., and Borde, V. (2012). The spatial regulation of meiotic recombination hotspots: Are all DSB hotspots crossover hotspots? Experimental Cell Research *318*, 1347-1352.

Sharma, S., Kelly, T. K., and Jones, P. A. (2010). Epigenetics in cancer. Carcinogenesis *31*, 27-36.

Sharp, J. A., Plant, J. J., Ohsumi, T. K., Borowsky, M., and Blower, M. D. (2011). Functional analysis of the microtubule-interacting transcriptome. Molecular biology of the cell *22*, 4312-4323.

Siegel, R., Naishadham, D., and Jemal, A. (2012). Cancer statistics, 2012. CA: a cancer journal for clinicians *62*, 10-29.

Simpson, A. J. G., Caballero, O. L., Jungbluth, A., Chen, Y. T., and Old, L. J. (2005). Cancer/testis antigens, gametogenesis and cancer. Nature Reviews Cancer *5*, 615-625.

Slingluff, C. L., and Speiser, D. E. (2005). Progress and controversies in developing cancer vaccines. Journal of Translational Medicine *3*, 18.

Smet, C., and Loriot, A. (2013). DNA Hypomethylation and Activation of Germline-Specific Genes in Cancer. Epigenetic Alterations in Oncogenesis *754*, 149-166.

Smirnova, N. A., Romanienko, P. J., Khil, P. P., and Camerini-Otero, R. D. (2006). Gene expression profiles of Spo11−/− mouse testes with spermatocytes arrested in meiotic prophase I. Reproduction *132*, 67-77.

Stelow, E. B., and French, C. A. (2009). Carcinomas of the upper aerodigestive tract with rearrangement of the nuclear protein of the testis (NUT) gene (NUT midline carcinomas). Advances in anatomic pathology *16*, 92-96.

Suda, T., Tsunoda, T., Daigo, Y., Nakamura, Y., and Tahara, H. (2007). Identification of human leukocyte antigen-A24-restricted epitope peptides derived from gene products upregulated in lung and esophageal cancers as novel targets for immunotherapy. Cancer science *98*, 1803-1808.

Sun, H. S., Kennedy, P. J., and Nestler, E. J. (2012). Epigenetics of the Depressed Brain: Role of Histone Acetylation and Methylation. Neuropsychopharmacology *38*, 124-137.

Takahashi, K., Shichijo, S., Noguchi, M., Hirohata, M., and Itoh, K. (1995). Identification of MAGE-1 and MAGE-4 proteins in spermatogonia and primary spermatocytes of testis. Cancer research *55*, 3478-3482.

Tang, Z., Sun, Y., Harley, S. E., Zou, H., and Yu, H. (2004). Human Bub1 protects centromeric sister-chromatid cohesion through Shugoshin during mitosis. Proceedings The National Academy of Sciences *101*, 18012–18017.

Teo, M., Crotty, P., O'Sullivan, M., French, C. A., and Walshe, J. M. (2011). NUT midline carcinoma in a young woman. Journal of Clinical Oncology *29*, e336-e339.

Türeci, O., Sahin, U., Koslowski, M., Buss, B., Bell, C., Ballweber, P., Zwick, C., Eberle, T., Zuber, M., and Villena-Heinsen, C. (2002). A novel tumour associated leucine

zipper protein targeting to sites of gene transcription and splicing. Oncogene *21*, 3879-3888.

Türeci, Ö., Sahin, U., Zwick, C., Koslowski, M., Seitz, G., and Pfreundschuh, M. (1998). Identification of a meiosis-specific protein as a member of the class of cancer/testis antigens. Proceedings of the National Academy of Sciences *95*, 5211-5216.

Uhlmann, F. (2004). The mechanism of sister chromatid cohesion. Experimental cell research *296*, 80-85.

Uhlmann, F. (2011). Cohesin subunit Rad21L, the new kid on the block has new ideas. EMBO reports *12*, 183-184.

Umate, P., and Tuteja, R. (2011). Genome-wide comprehensive analysis of human helicases. Communicative & integrative biology *4*, 118-137.

Van der Bruggen, P., Traversari, C., Chomez, P., Lurquin, C., De Plaen, E., Van den Eynde, B., Knuth, A., and Boon, T. (1991). A gene encoding an antigen recognized by cytolytic T lymphocytes on a human melanoma. Science *254*, 1643-1647.

van Duin, M., Broyl, A., de Knegt, Y., Goldschmidt, H., Richardson, P. G., Hop, W. C. J., van der Holt, B., Joseph-Pietras, D., Mulligan, G., and Neuwirth, R. (2011). Cancer testis antigens in newly diagnosed and relapse multiple myeloma: prognostic markers and potential targets for immunotherapy. Haematologica *96*, 1662-1669.

van Geel, M., Dickson, M. C., Beck, A. F., Bolland, D. J., Frants, R. R., van der Maarel, S. M., de Jong, P. J., and Hewitt, J. E. (2002). Genomic analysis of human chromosome 10q and 4q telomeres suggests a common origin. Genomics *79*, 210-217.

Von Stetina, J. R., and Orr-Weaver, T. L. (2011). Developmental control of oocyte maturation and egg activation in metazoan models. Cold Spring Harbor perspectives in biology *3*, a005553.

Walczak, C. E., Cai, S., and Khodjakov, A. (2010). Mechanisms of chromosome behaviour during mitosis. Nature Reviews Molecular Cell Biology *11*, 91-102.

Wang, Q.-E., Han, C., Milum, K., and Wani, A. A. (2011). Stem cell protein Piwil2 modulates chromatin modifications upon cisplatin treatment. Mutation Research/Fundamental and Molecular Mechanisms of Mutagenesis *708*, 59-68.

Wang, S., Lee, D. P., Gong, N., Schwerbrock, N. M., Mashek, D. G., Gonzalez-Baró, M. R., Stapleton, C., Li, L. O., Lewin, T. M., and Coleman, R. A. (2007). Cloning and functional characterization of a novel mitochondrial N-ethylmaleimide-sensitive glycerol-3-phosphate acyltransferase (GPAT2). Archives of biochemistry and biophysics *465*, 347-358.

Wang, Z., Zang, C., Rosenfeld, J. A., Schones, D. E., Barski, A., Cuddapah, S., Cui, K., Roh, T. Y., Peng, W., and Zhang, M. Q. (2008). Combinatorial patterns of histone acetylations and methylations in the human genome. Nature genetics *40*, 897-903.

Weiser, T. S., Guo, Z. S., Ohnmacht, G. A., Parkhurst, M. L., Tong-On, P., Marincola, F. M., Fischette, M. R., Yu, X., Chen, G. A., and Hong, J. A. (2001). Sequential 5-Aza-2'-deoxycytidine-depsipeptide FR901228 treatment induces apoptosis preferentially in cancer cells and facilitates their recognition by cytolytic T lymphocytes specific for NY-ESO-1. Journal of Immunotherapy *24*, 151-161.

Wilkinson, M. F., and Shyu, A. B. (2001). Multifunctional regulatory proteins that control gene expression in both the nucleus and the cytoplasm. Bioessays *23*, 775-787.

Wojtasz, L., Daniel, K., Roig, I., Bolcun-Filas, E., Xu, H., Boonsanay, V., Eckmann, C. R., Cooke, H. J., Jasin, M., and Keeney, S. (2009). Mouse HORMAD1 and HORMAD2, two conserved meiotic chromosomal proteins, are depleted from

synapsed chromosome axes with the help of TRIP13 AAA-ATPase. PLoS genetics *5*, e1000702.

Yamabuki, T., Daigo, Y., Kato, T., Hayama, S., Tsunoda, T., Miyamoto, M., Ito, T., Fujita, M., Hosokawa, M., and Kondo, S. (2006). Genome-wide gene expression profile analysis of esophageal squamous cell carcinomas. International journal of oncology *28*, 1375-1384.

Yawata, T., Nakai, E., Park, K. C., Chihara, T., Kumazawa, A., Toyonaga, S., Masahira, T., Nakabayashi, H., Kaji, T., and Shimizu, K. (2010). Enhanced expression of cancer testis antigen genes in glioma stem cells. Molecular carcinogenesis *49*, 532-544.

Youds, J. L., and Boulton, S. J. (2011). The choice in meiosis–defining the factors that influence crossover or non-crossover formation. Journal of cell science *124*, 501-513.

Zakharyevich, K., Tang, S., Ma, Y., and Hunter, N. (2012). Delineation of joint molecule resolution pathways in meiosis identifies a crossover-specific resolvase. Cell *149*, 334-347.

Zhang, F., Cong, L., Lodato, S., Kosuri, S., Church, G. M., and Arlotta, P. (2011). Efficient construction of sequence-specific TAL effectors for modulating mammalian transcription. Nature biotechnology *29*, 149-153.

Zhao, L., Mou, D. C., Leng, X. S., Peng, J. R., Wang, W. X., Huang, L., Li, S., and Zhu, J. Y. (2004). Expression of cancer-testis antigens in hepatocellular carcinoma. World Journal of Gastroenterology *10*, 2034-2038.

Zhu, Z., Xu, W., Dai, J., Chen, X., Zhao, X., Fang, P., Yang, F., Tang, M., Wang, Z., and Wang, L. (2012). The alteration of protein profile induced by cigarette smoking via oxidative stress in mice epididymis. The international journal of biochemistry & cell biology *45*, 571-582.

Ziai, J., French, C. A., and Zambrano, E. (2010). NUT gene rearrangement in a poorly-differentiated carcinoma of the submandibular gland. Head and neck pathology *4*, 163-168.

Appendix

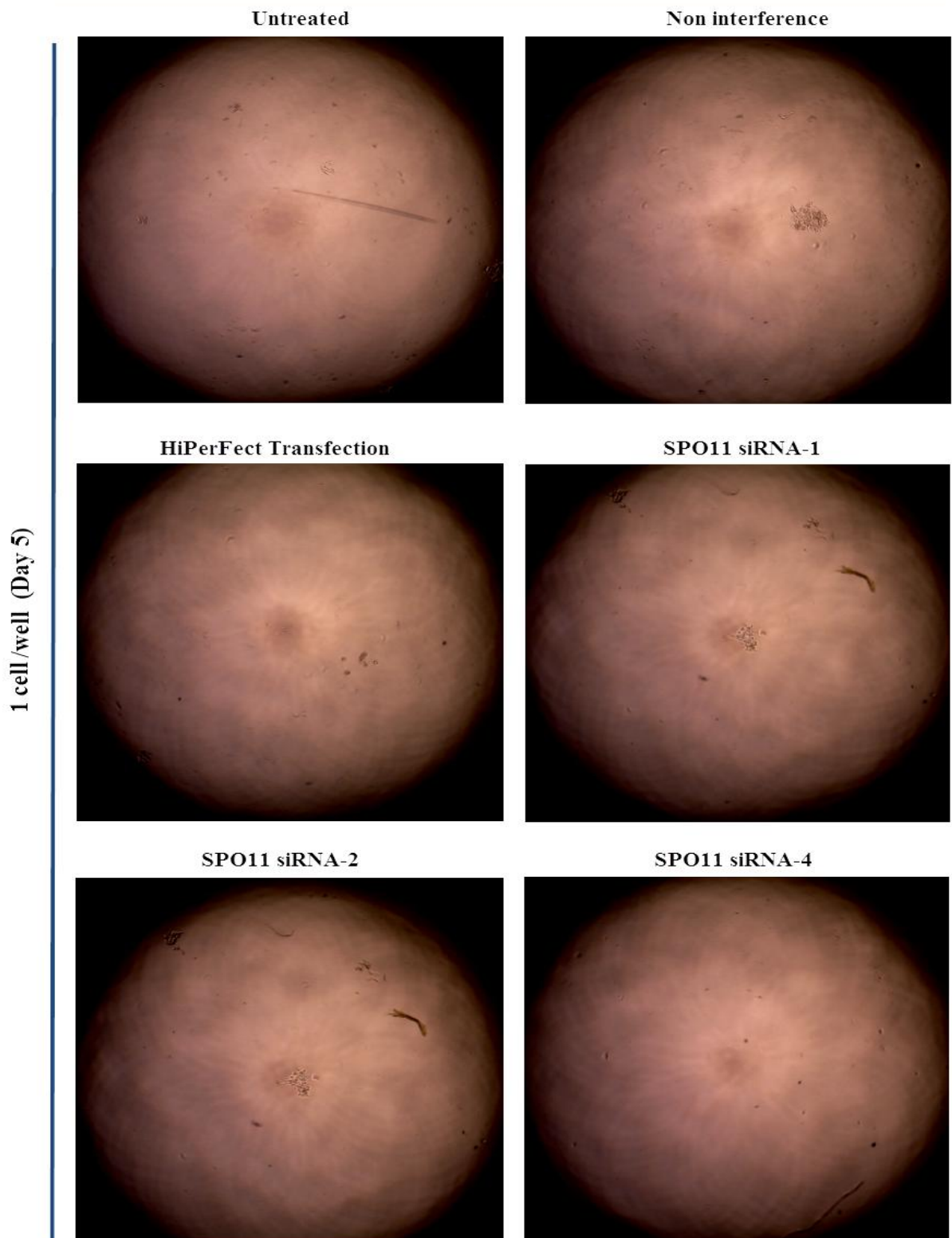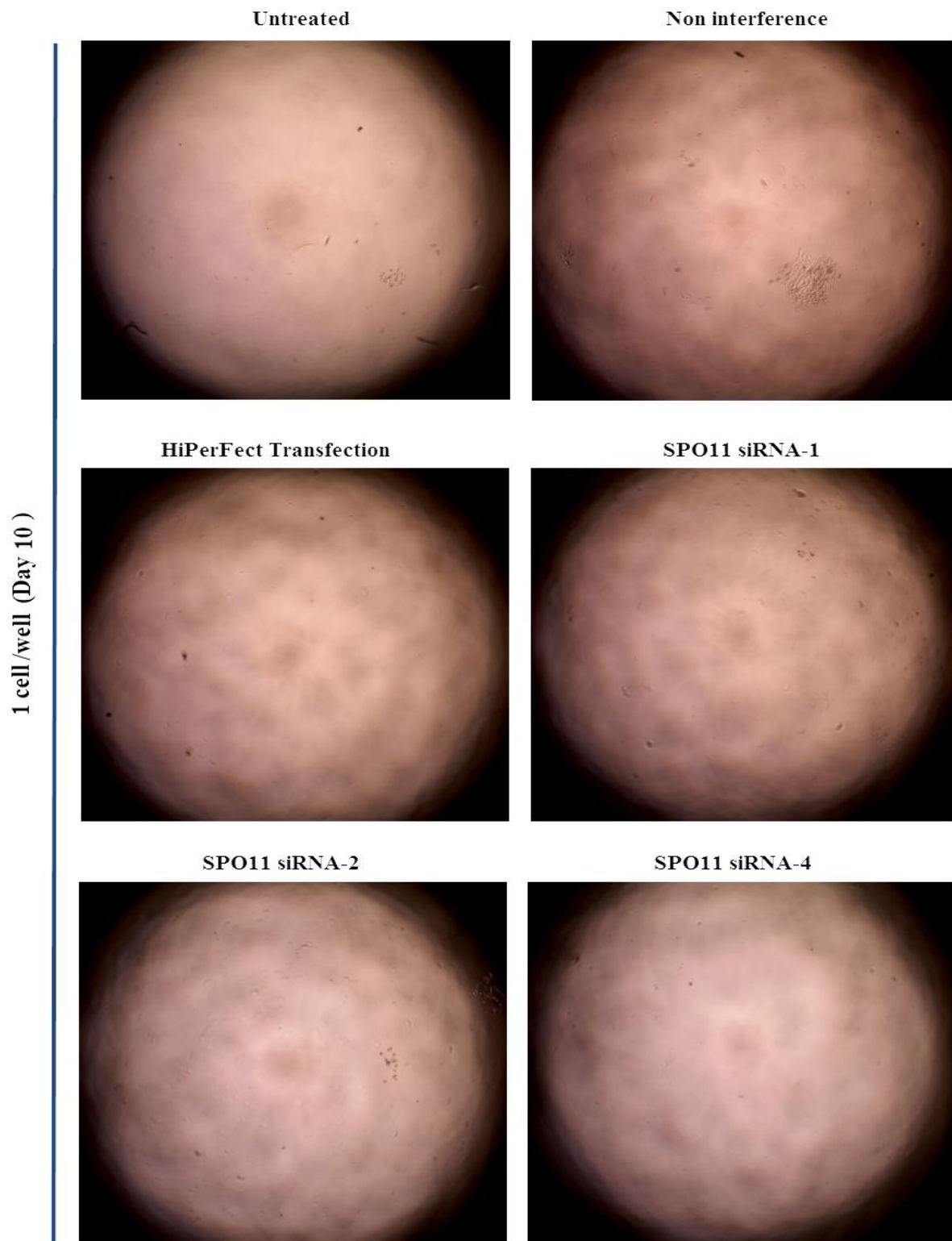## Cell growth after transfection with siRNA or TALENs
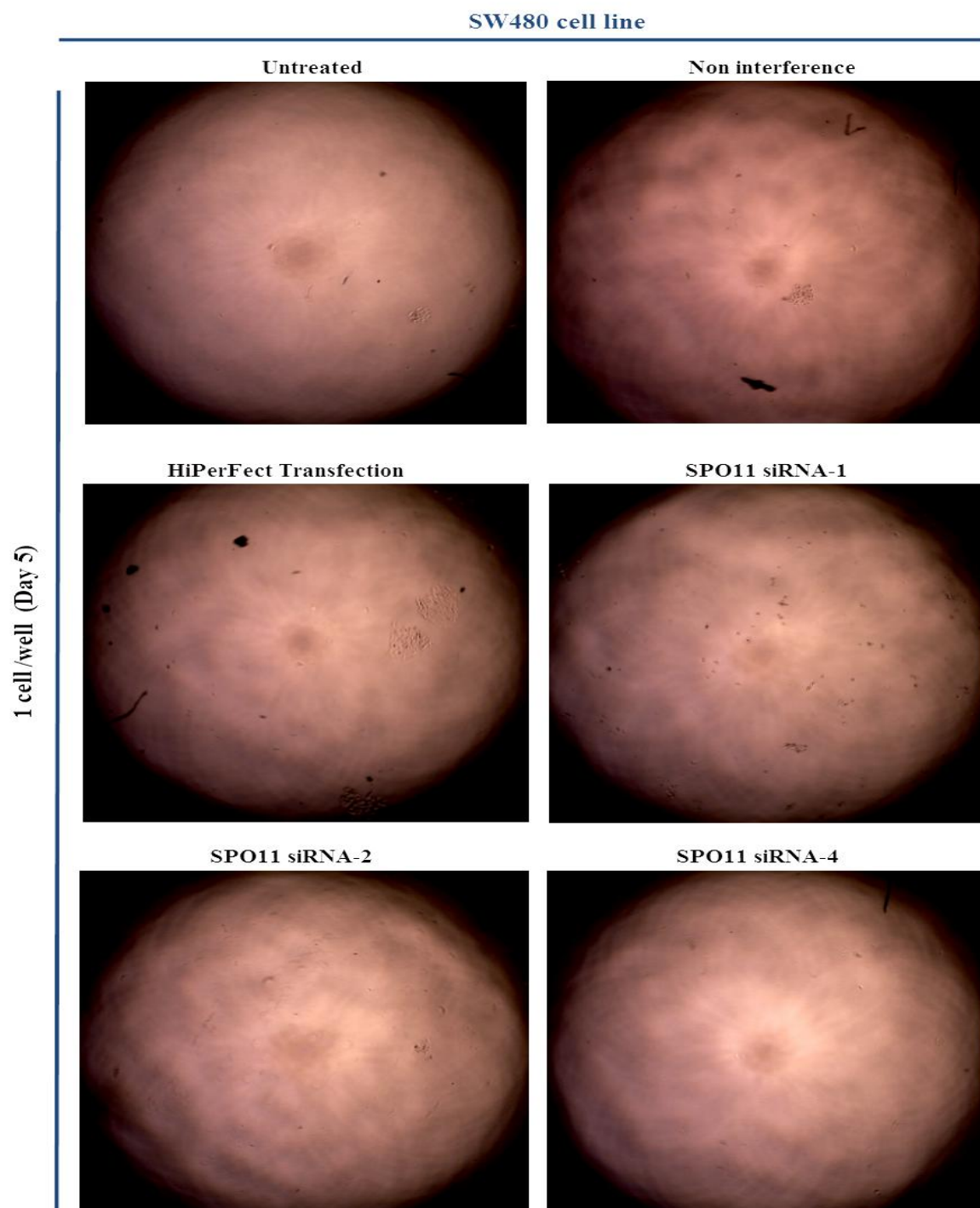
Figure A.1 SW480 cell line 5 days after treated with different siRNA with single cell seeded. Non-interference, Hirerfect transfection (as negative controls) and untreated used to compare the cells growth with different siRNA.
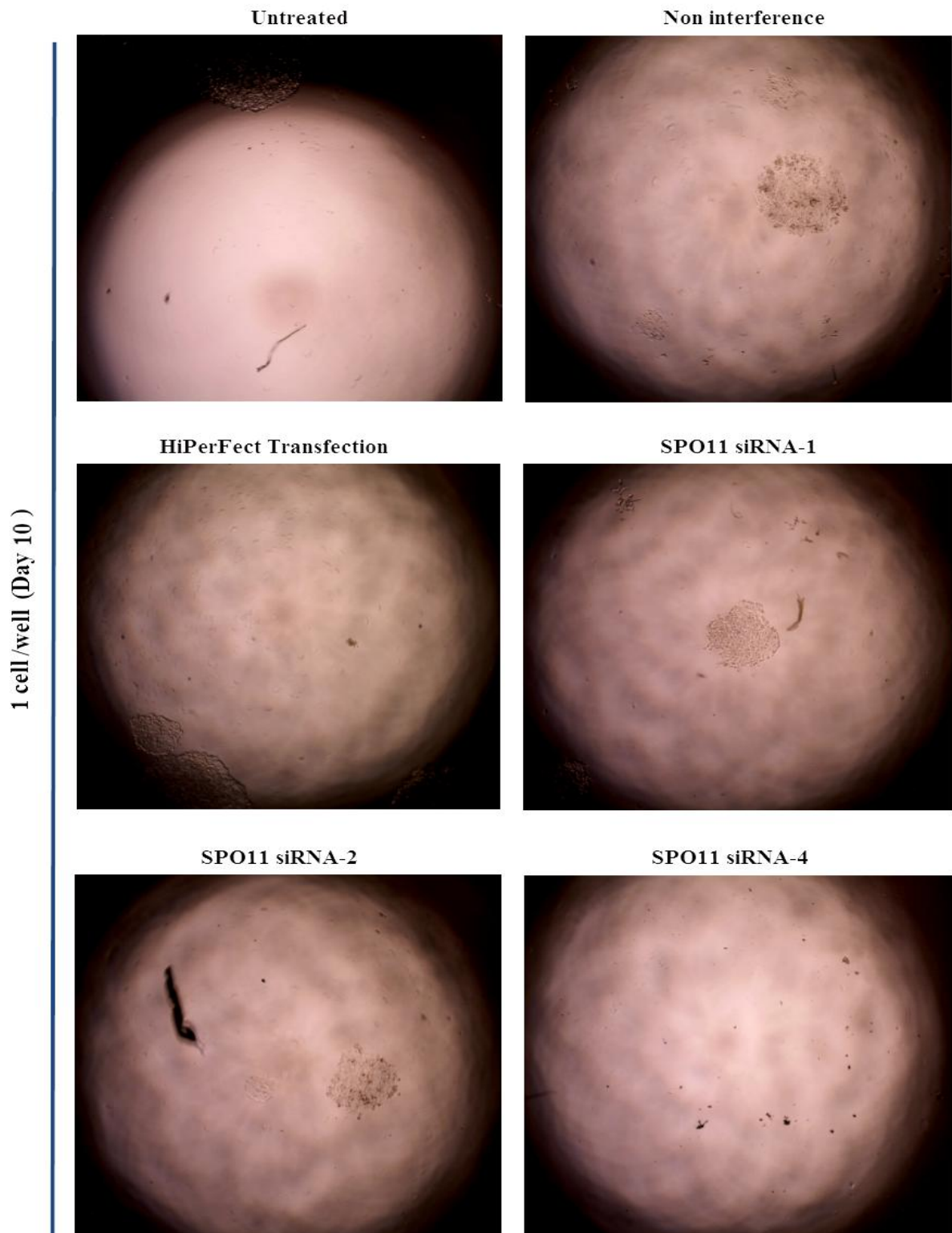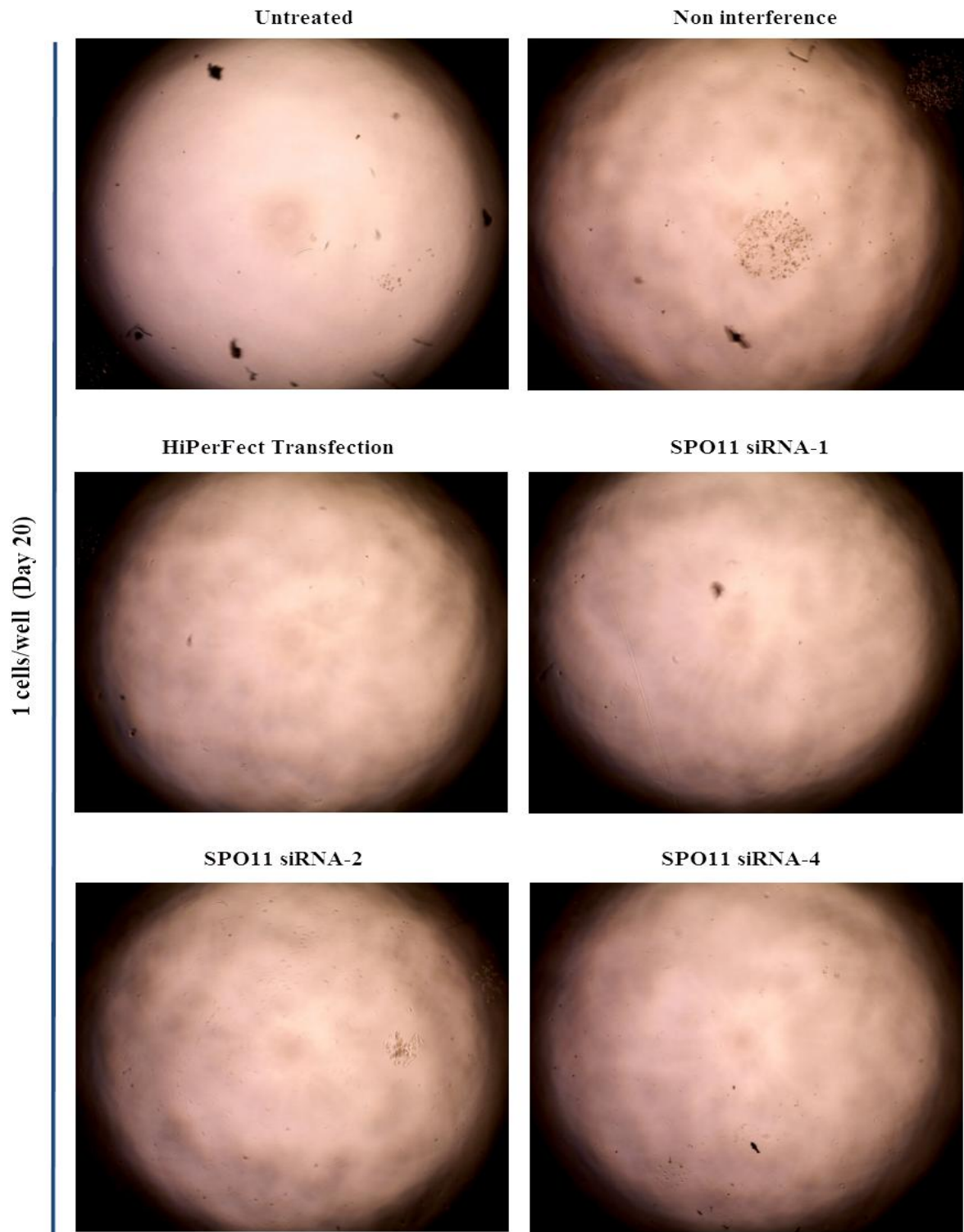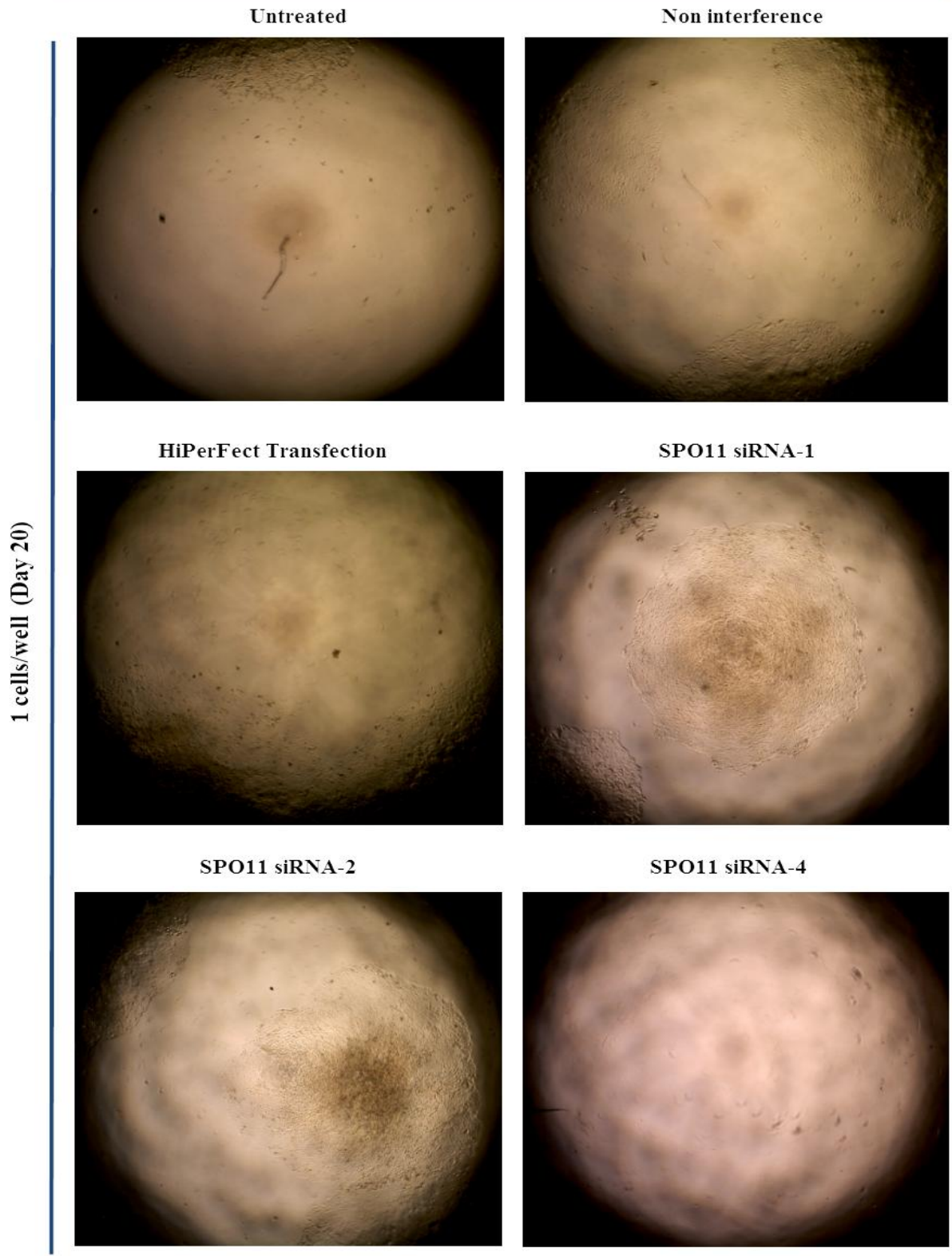
Untreated

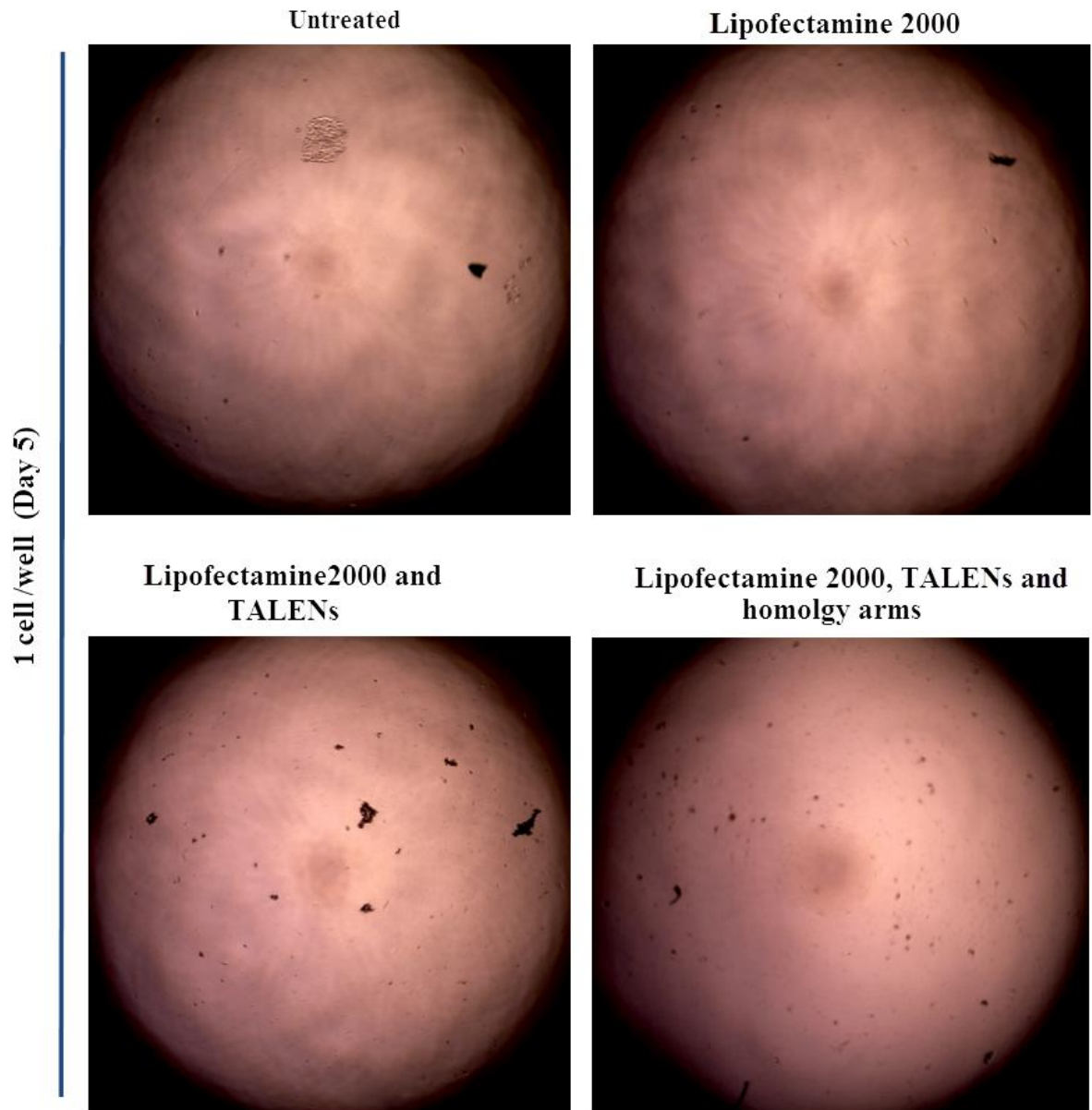Non interference

HiPerFect Transfection

SPO11 siRNA-1

SPO11 siRNA-2

SPO11 siRNA-4

1 cell/well (Day 5)

Figure A.2 HCT116 cell line 5 days after treated with different siRNA with single cell seeded. Non-interference, Hirerfect transfection (as negative controls) and untreated used to compare the cells growth with different siRNA.

1 cell /well (Day 10)

Untreated

Non interference

HiPerFect Transfection

SPO11 siRNA-1

SPO11 siRNA-2

SPO11 siRNA-4

Figure A.3 SW480 cell line 10 days after treated with different siRNA with single cell seeded. Non-interference, Hirerfect transfection (as negative controls) and untreated used to compare the cells growth with different siRNA.

Figure A.4 HCT116 cell line 10 days after treated with different siRNA with single cell seeded. Non-interference, Hirerfect transfection (as negative controls) and untreated used to compare the cells growth with different siRNA.

187

Untreated

Non interference

HiPerFect Transfection

SPO11 siRNA-1

1 cells/well (Day 20)

SPO11 siRNA-2

SPO11 siRNA-4

Figure A.5 SW480 cell line 20 days after treated with different siRNA with single cell seeded.
Non-interference, Hirerfect transfection (as negative controls) and untreated used to compare the cells growth with different siRNA.

Untreated | **Non interference**

HiPerFect Transfection | **SPO11 siRNA-1**

SPO11 siRNA-2 | **SPO11 siRNA-4**

1 cells/well (Day 20)

Figure A.6 HCT116 cell line 20 days after treated with different siRNA with single cell seeded. Non-interference, Hirerfect transfection (as negative controls) and untreated used to compare the cells growth with different siRNA.

Untreated

Lipofectamine 2000

1 cell /well (Day 5)

Lipofectamine2000 and TALENs

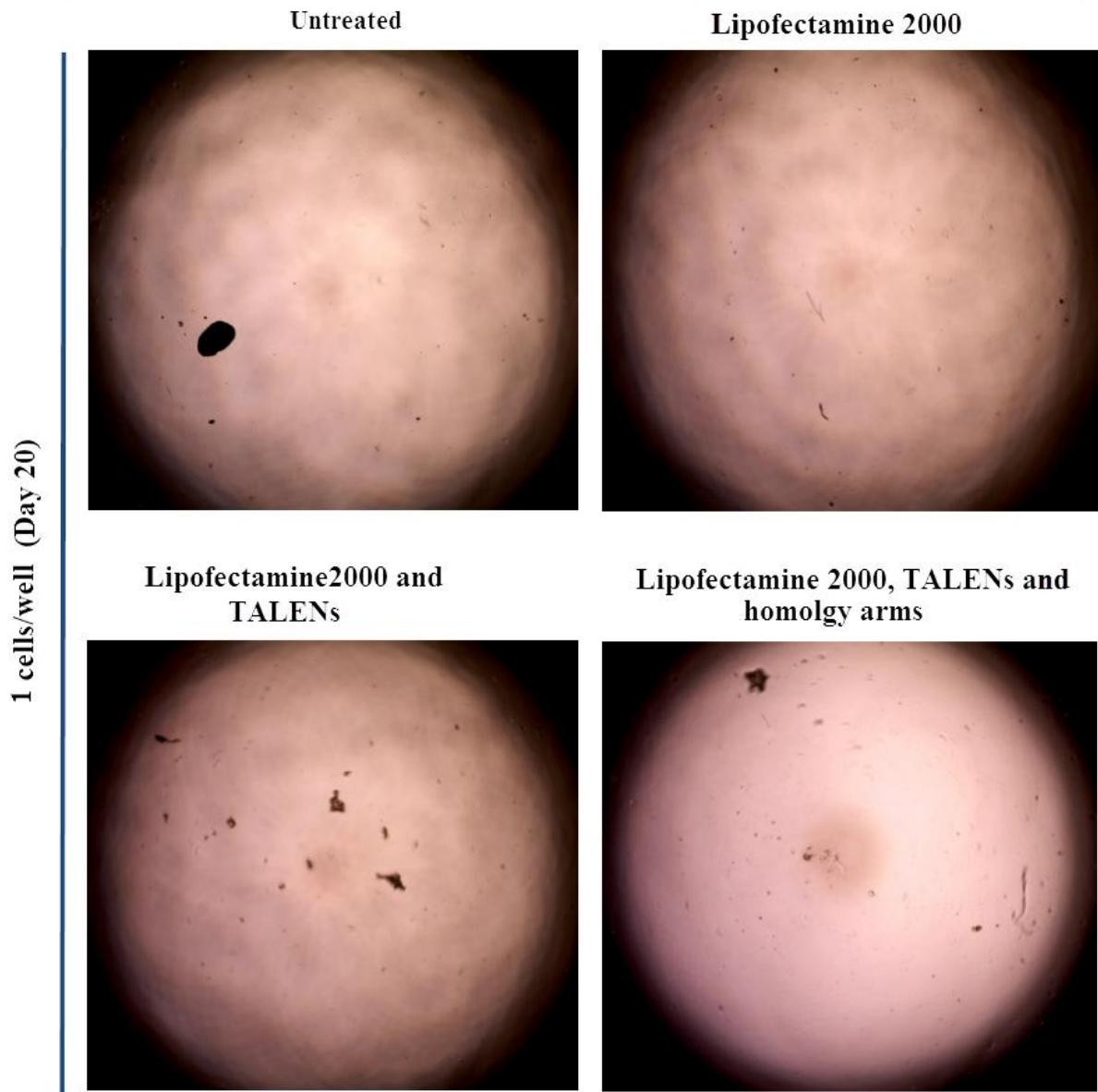**Lipofectamine 2000, TALENs and homolgy arms**

Figure A.7 SW480 cell line 5 days after treated with TALEN and TALEN with homology arms with single cell seeded. Untreated and lipofectamine 2000 (as negative control) used to compare the cells growth with TALEN and TALEN with homology arms.
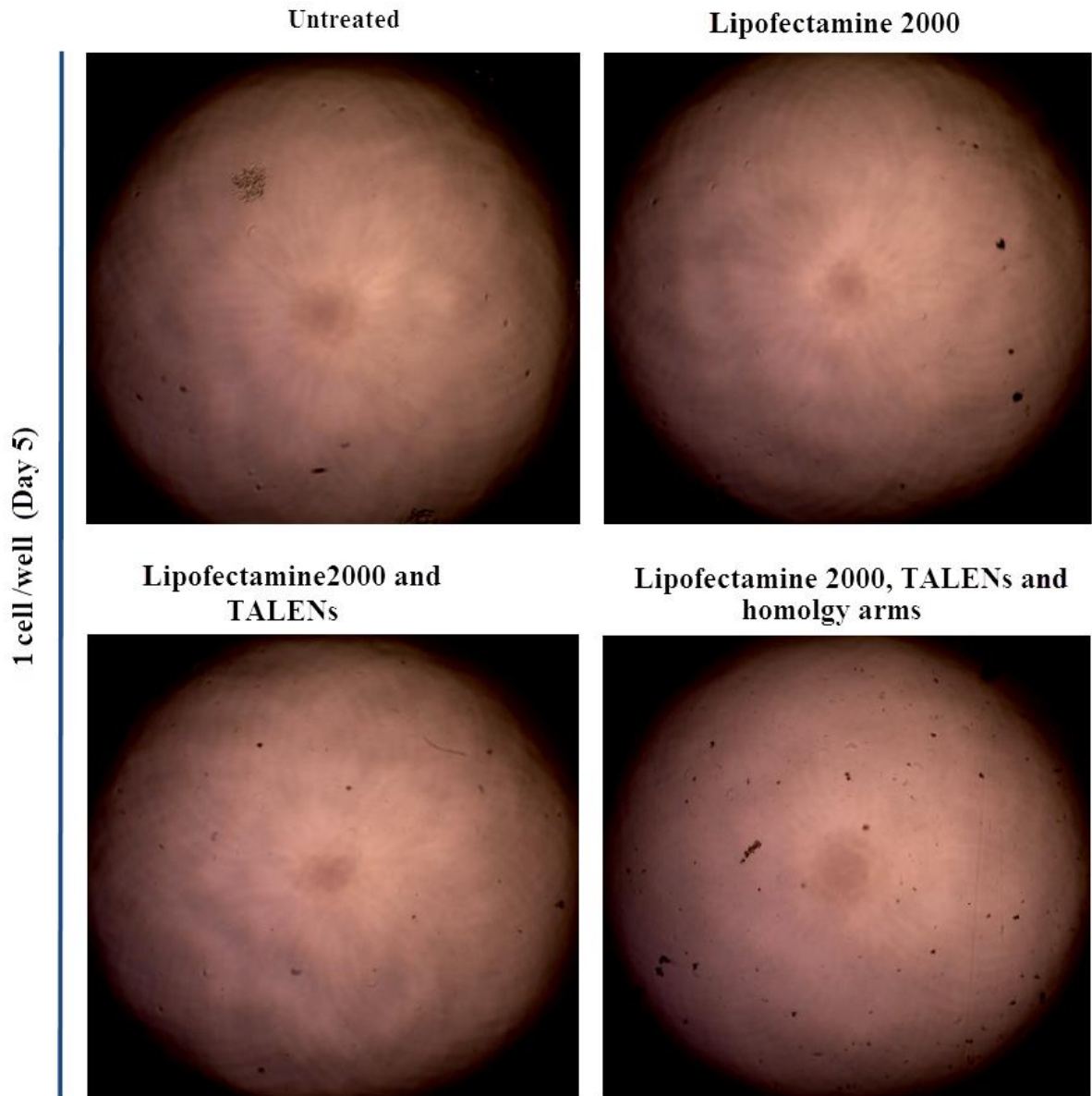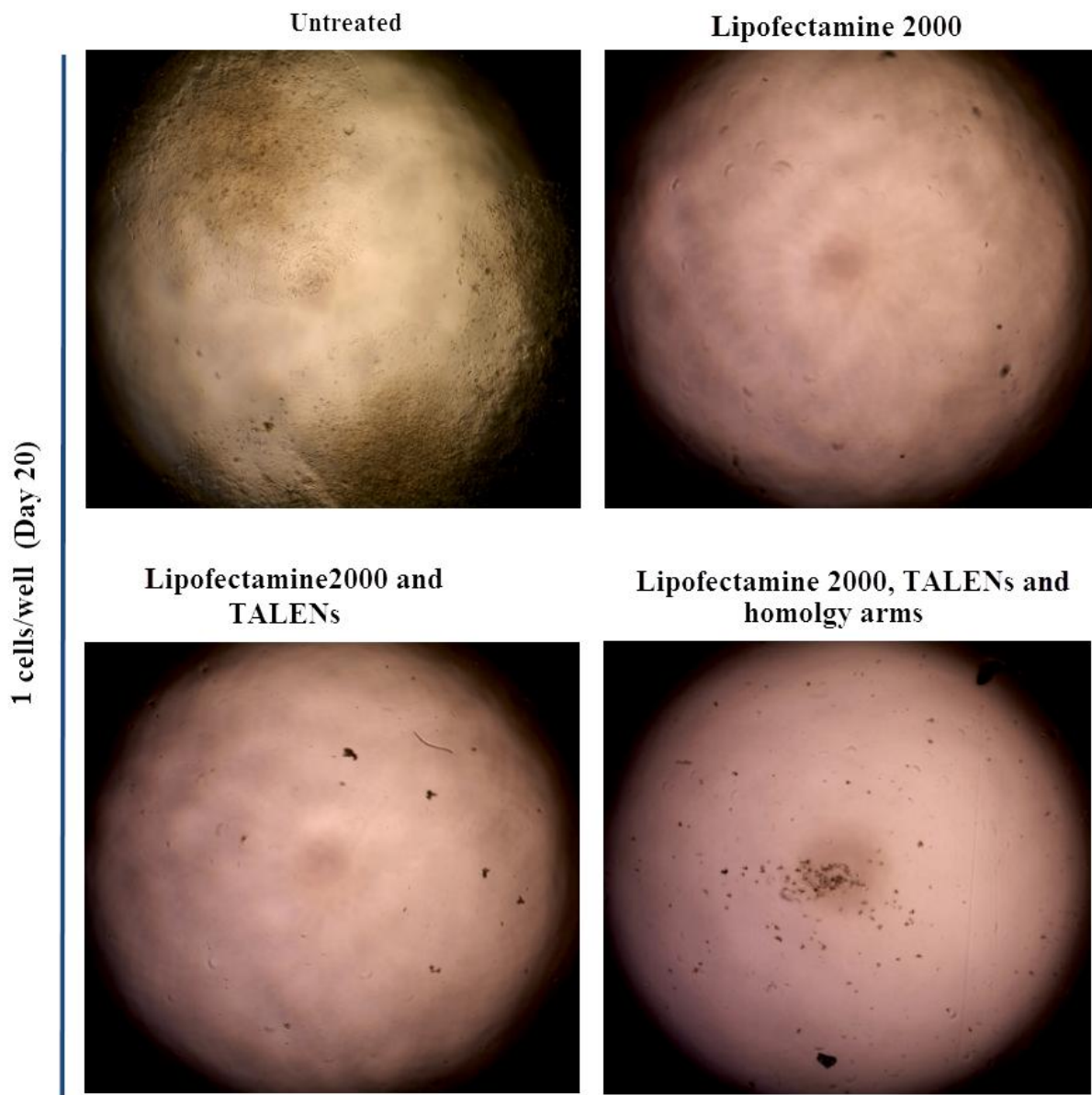
Figure A.8 HCT116 cell line 5 days after treated with TALEN and TALEN with homology arms with single cell seeded. Untreated and lipofectamine 2000 (as negative control) used to compare the cells growth with TALEN and TALEN with homology arms.
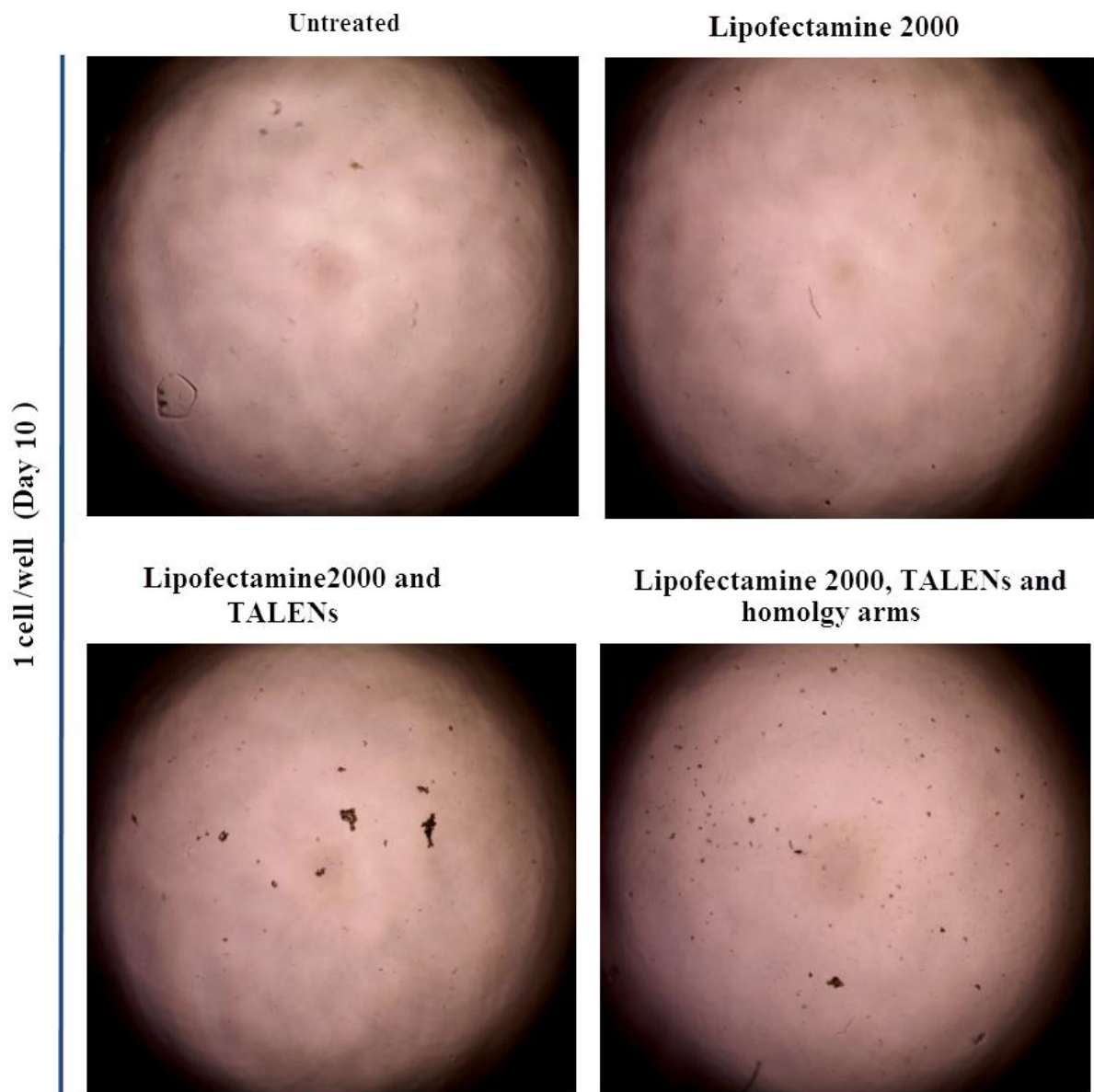
Figure A.9 SW480 cell line 10 days after treated with TALEN and TALEN with homology arms with single cell seeded. Untreated and lipofectamine 2000 (as negative control) used to compare the cells growth with TALEN and TALEN with homology arms.
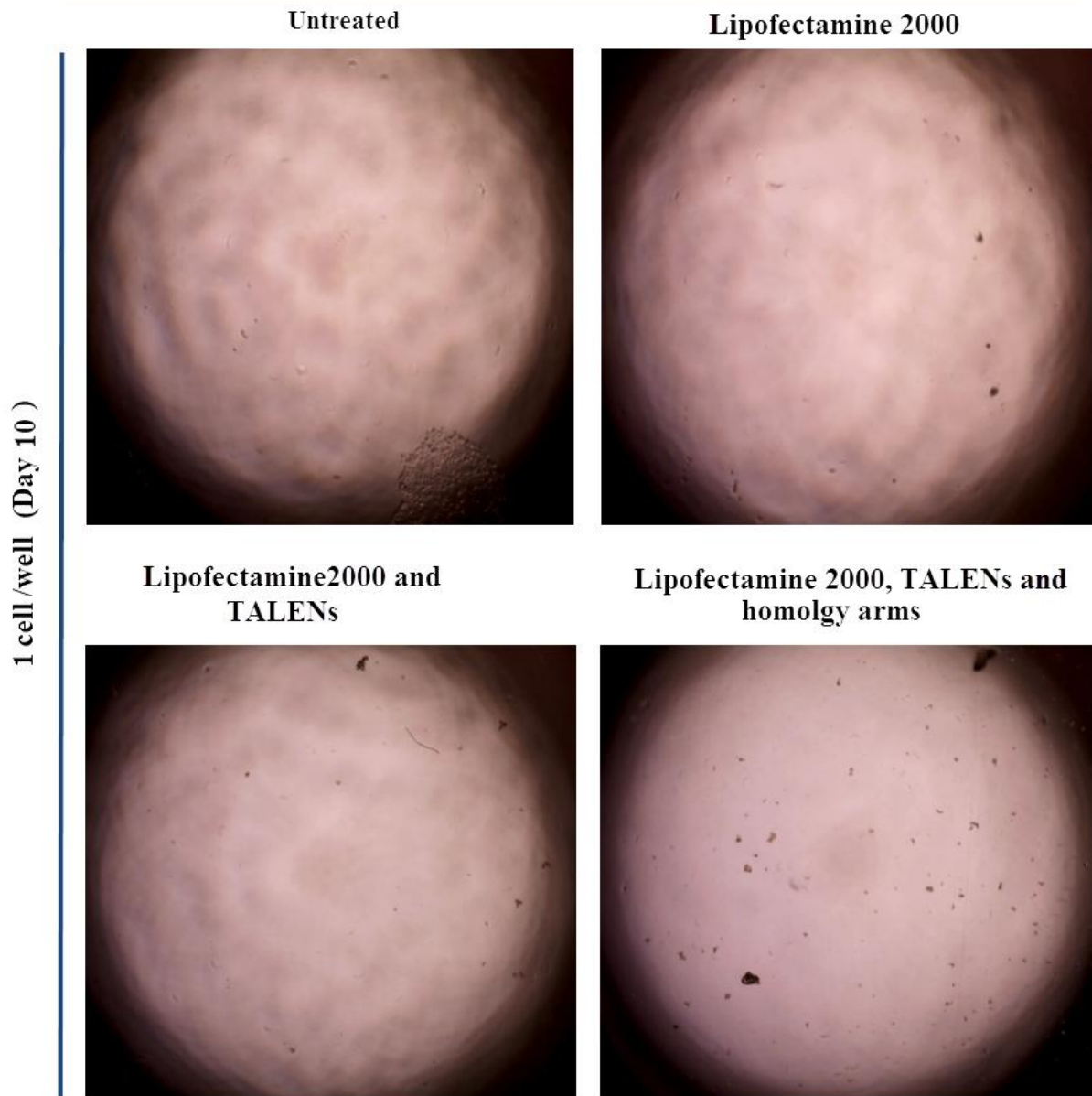
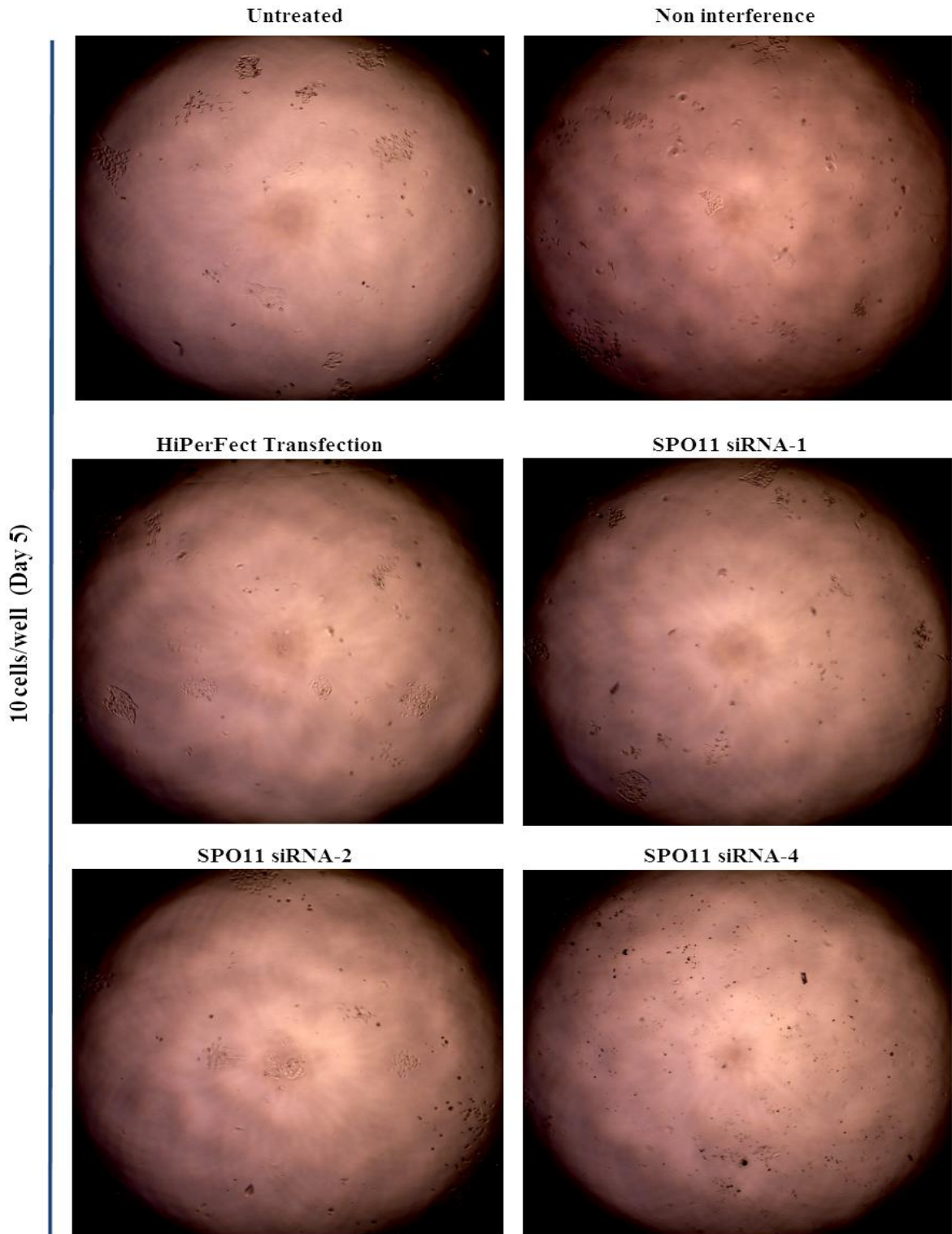**Figure A.10 HCT116 cell line 10 days after treated with TALEN and TALEN with homology arms with single cell seeded.** Untreated and lipofectamine 2000 (as negative control) used to compare the cells growth with TALEN and TALEN with homology arms.

Figure A.11 SW480 cell line 20 days after treated with TALEN and TALEN with homology arms with single cell seeded. Untreated and lipofectamine 2000 (as negative control) used to compare the cells growth with TALEN and TALEN with homology arms.

Figure A.12   HCT116 cell line 20 days after treated with TALEN and TALEN with homology arms with single cell seeded. Untreated and lipofectamine 2000 (as negative control) used to compare the cells growth with TALEN and TALEN with homology arms.

Untreated   Non interference

HiPerFect Transfection   SPO11 siRNA-1

SPO11 siRNA-2   SPO11 siRNA-4
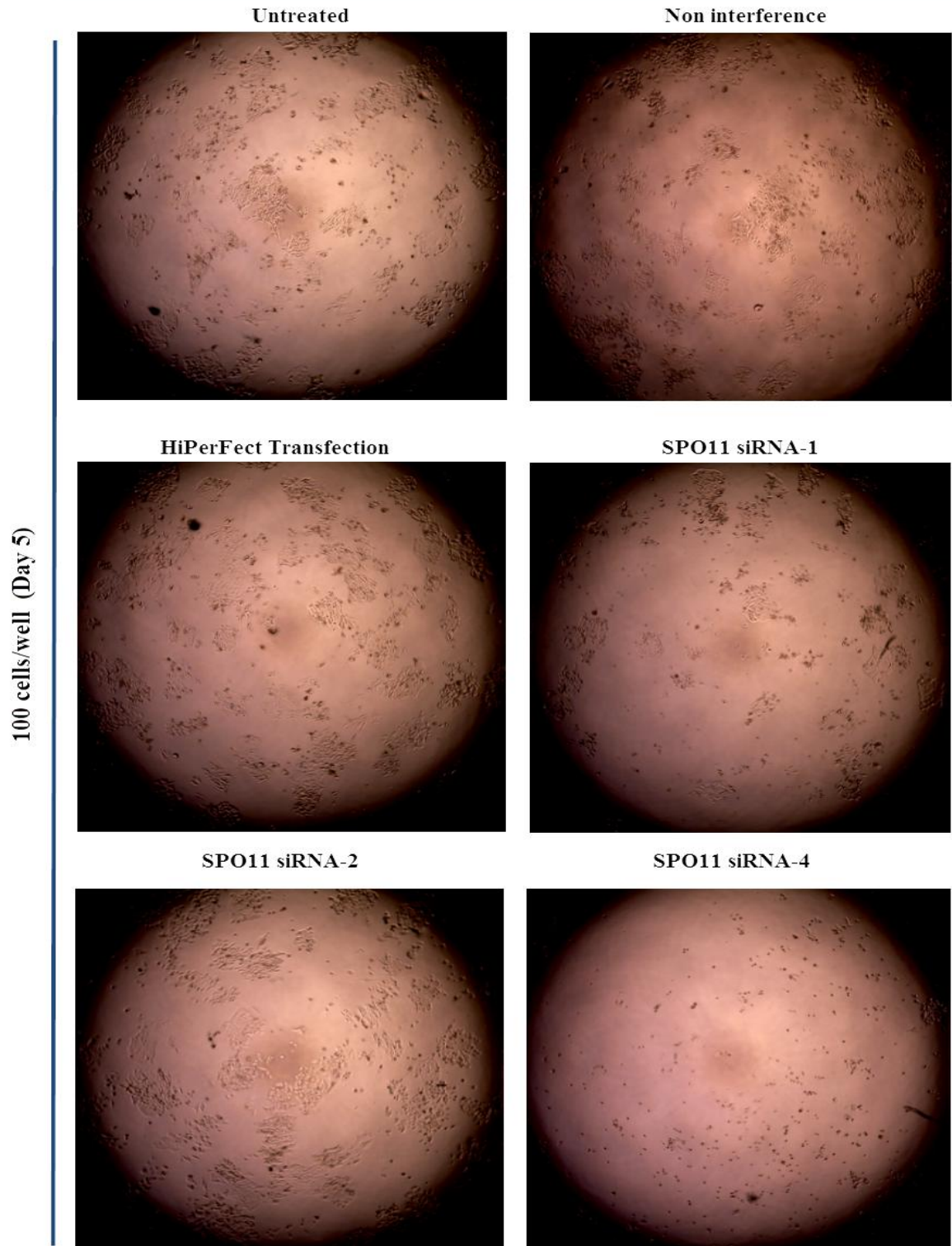
10 cells/well (Day 5)

Figure A.13 SW480 cell line 5 days after treated with different siRNA with 10 cells seeded. Non-interference, Hirerfect transfection (as negative controls) and untreated used to compare the cells growth with different siRNA. The cells treated with SPO11-siRNA4 shows clearly affected comparing to the untreated and the controls.
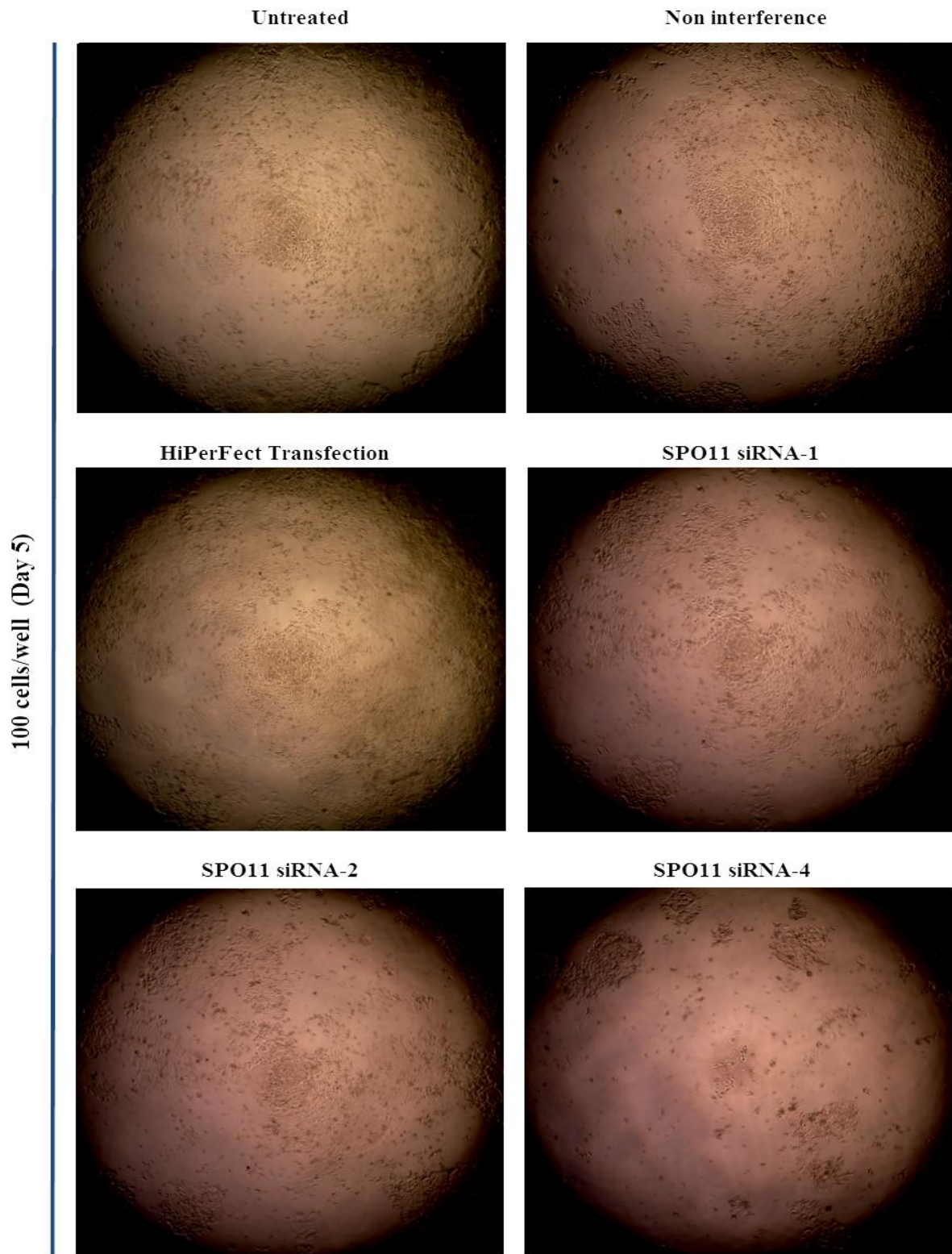
Figure A.14 HCT116 cell line 5 days after treated with different siRNA with 10 cells seeded. Non-interference, Hirerfect transfection (as negative controls) and untreated used to compare the cells growth with different siRNA. The cells treated with SPO11-siRNA4 shows clearly affected comparing to the untreated and the controls.

197

Untreated

Non interference

HiPerFect Transfection

SPO11 siRNA-1

100 cells/well (Day 5)
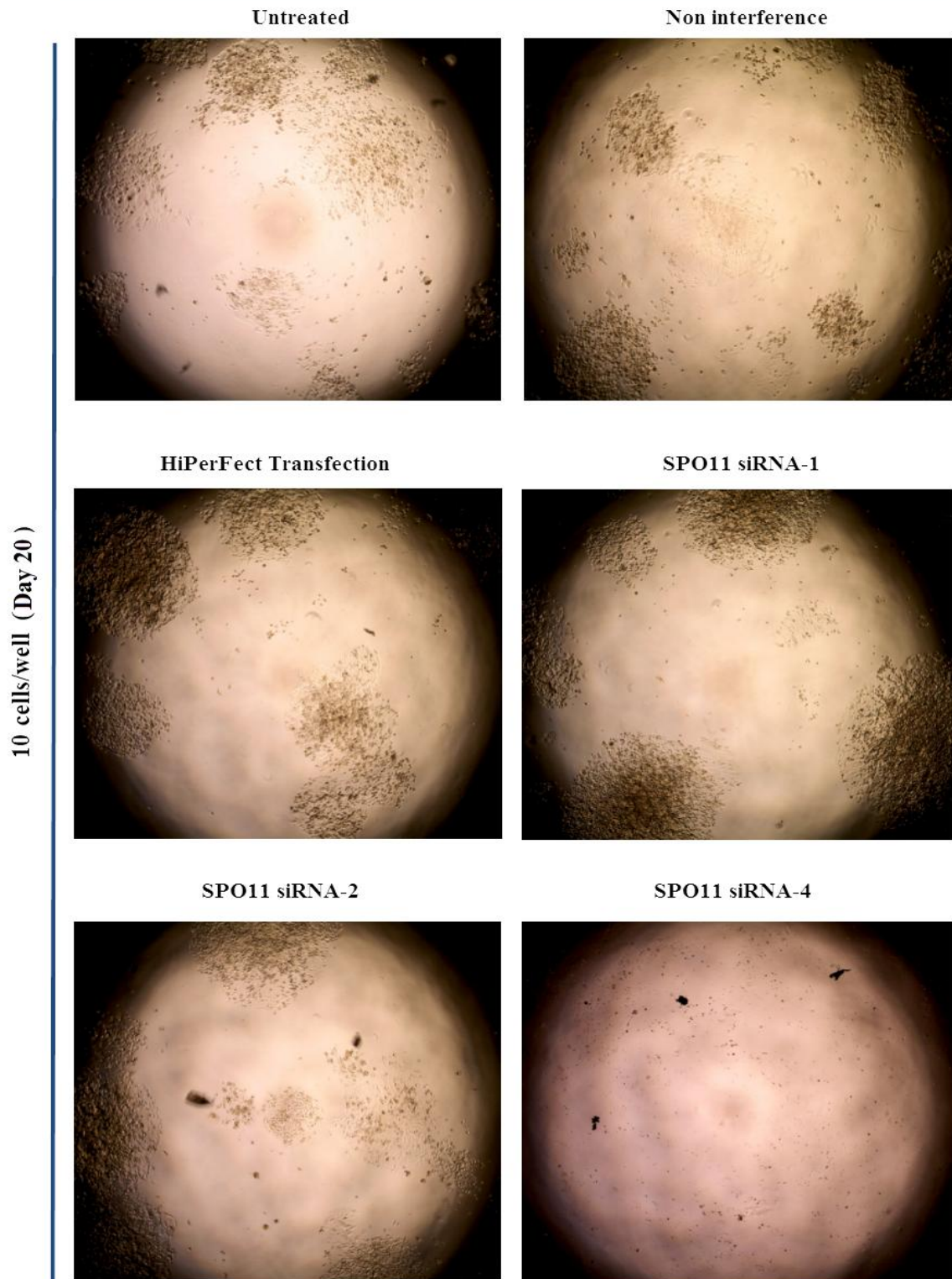
SPO11 siRNA-2

SPO11 siRNA-4

Figure A.15 SW480 cell line 5 days after treated with different siRNA with 100 cells seeded. Non-interference, Hirerfect transfection (as negative controls) and untreated used to compare the cells growth with different siRNA. The cells treated with SPO11-siRNA4 shows clearly affected comparing to the untreated and the controls.
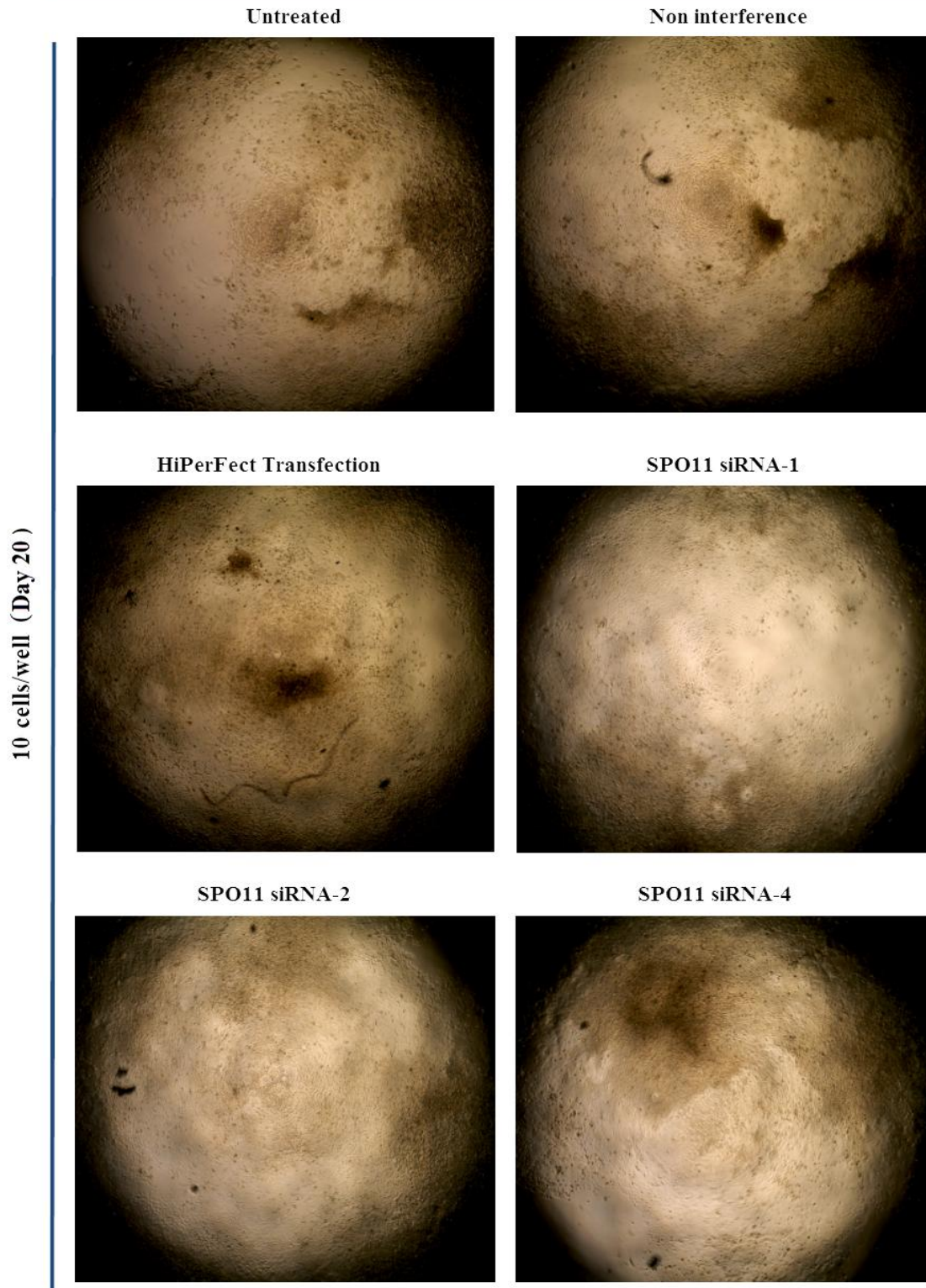
HCT116 cell line

Untreated	Non interference
HiPerFect Transfection	SPO11 siRNA-1
SPO11 siRNA-2	SPO11 siRNA-4

100 cells/well (Day 5)

Figure A.16 HCT116 cell line 5 days after treated with different siRNA with 100 cells seeded.
Non-interference, Hirerfect transfection (as negative controls) and untreated used to compare the cells growth with different siRNA. The cells treated with SPO11-siRNA4 shows clearly affected comparing to the untreated and the controls.

199

SW480 cell line

Untreated | Non interference

HiPerFect Transfection | SPO11 siRNA-1

SPO11 siRNA-2 | SPO11 siRNA-4
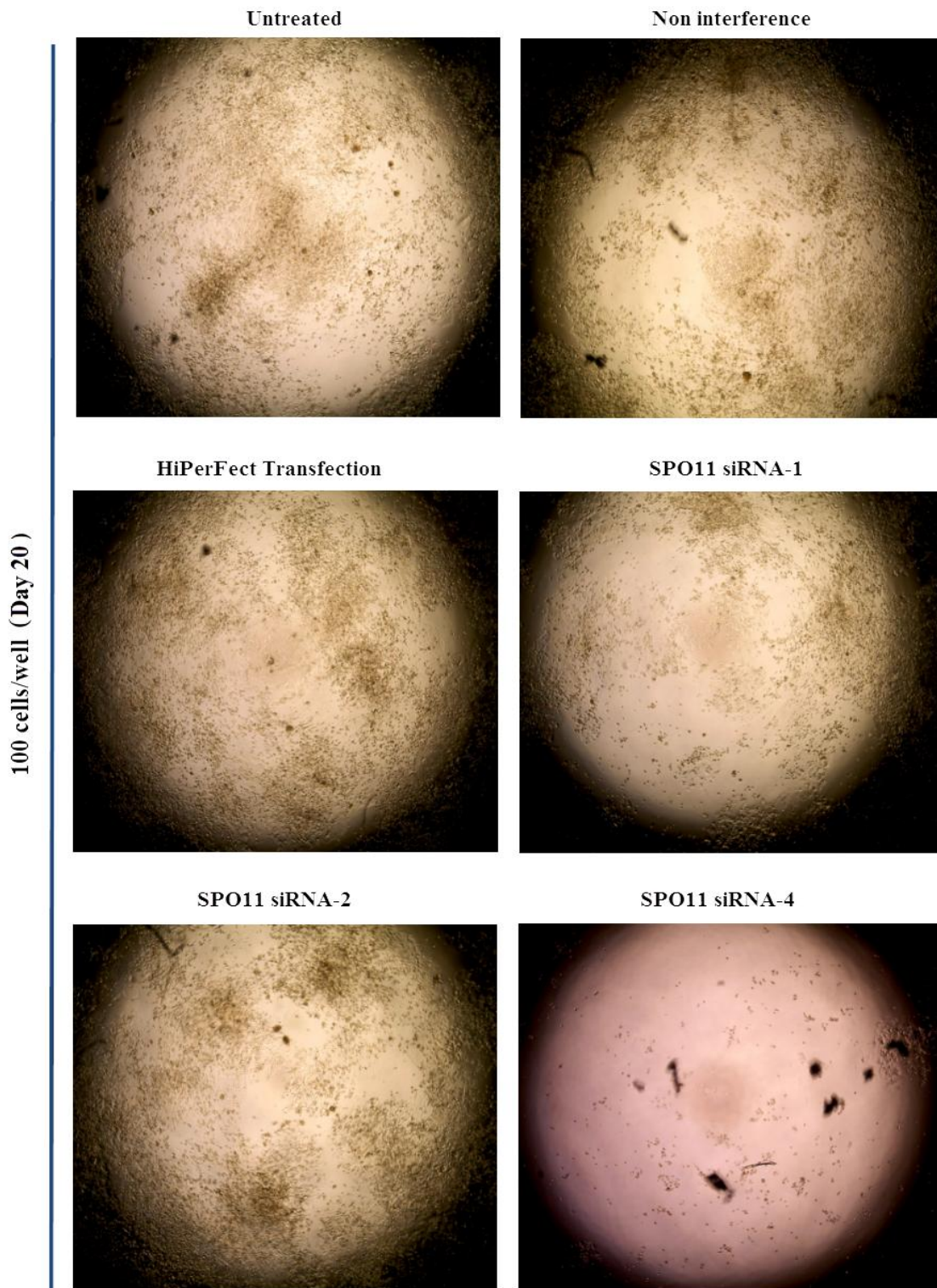
10 cells/well (Day 20)

Figure A.17 SW480 cell line 20 days after treated with different siRNA with 10 cells seeded. Non-interference, Hirerfect transfection (as negative controls) and untreated used to compare the cells growth with different siRNA. The cells treated with SPO11-siRNA4 shows clearly affected comparing to the untreated and the controls.

Figure A.18 HCT116 cell line 20 days after treated with different siRNA with 10 cells seeded. Non-interference, Hirerfect transfection (as negative controls) and untreated used to compare the cells growth with different siRNA. The cells treated with SPO11-siRNA1 and SPO11-siRNA4 shows clearly affected comparing to the untreated and the controls.

Untreated

Non interference

HiPerFect Transfection

SPO11 siRNA-1

SPO11 siRNA-2

SPO11 siRNA-4

100 cells/well (Day 20)

Figure A.19 SW480 cell line 20 days after treated with different siRNA with 100 cells seeded. Non-interference, Hirerfect transfection (as negative controls) and untreated used to compare the cells growth with different siRNA. The cells treated with SPO11-siRNA4 shows clearly affected comparing to the untreated and the controls.
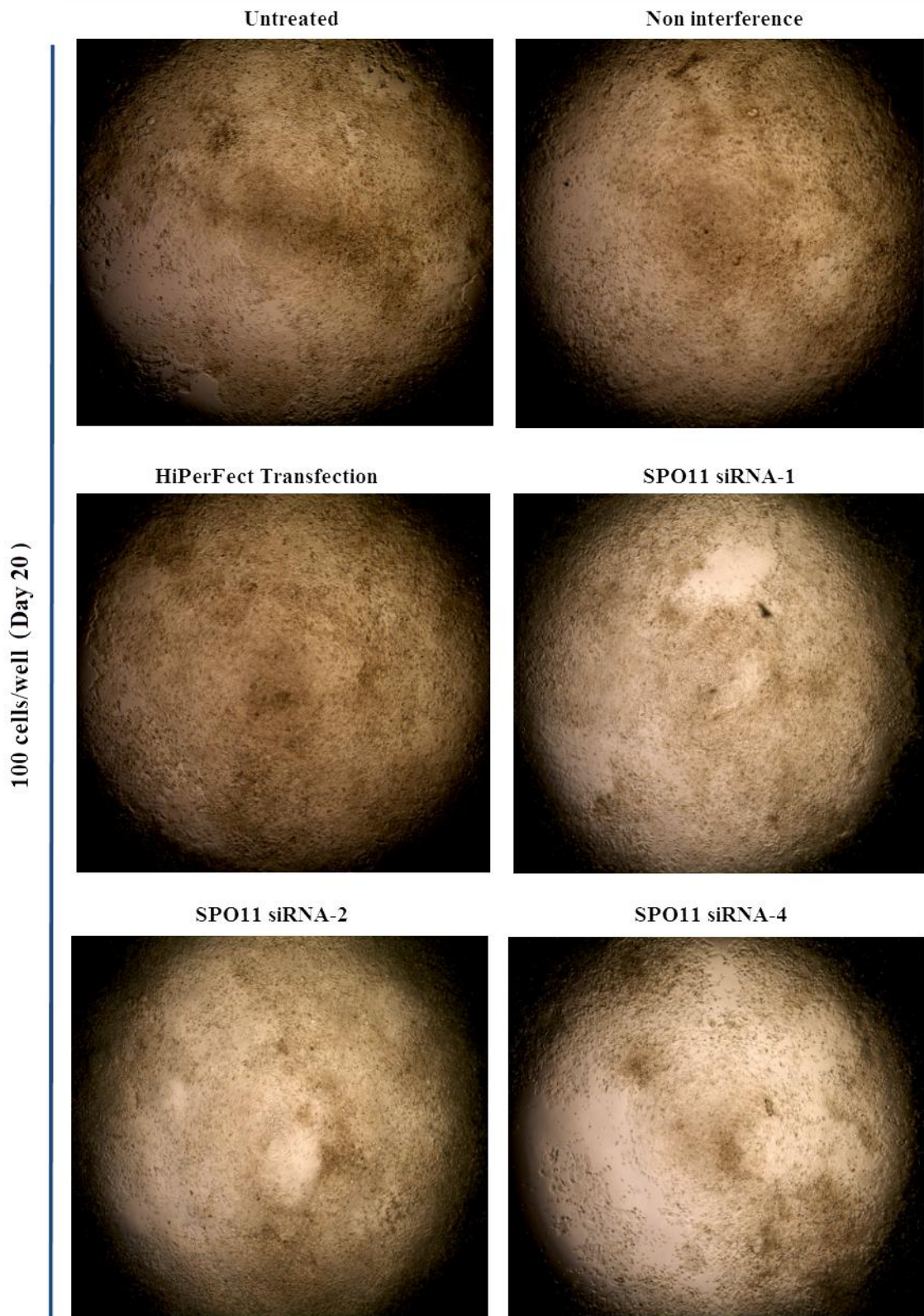
Untreated

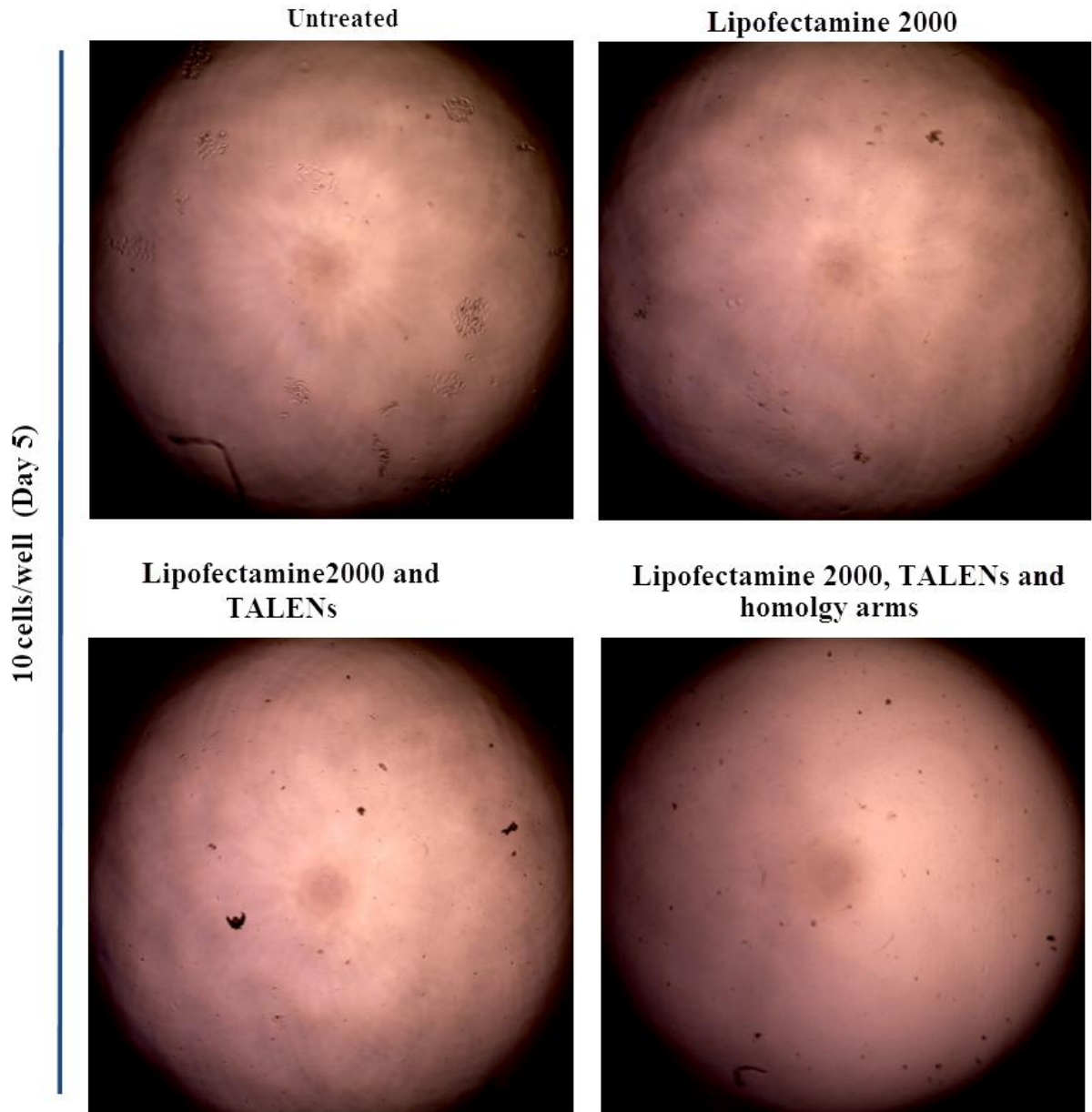Non interference

HiPerFect Transfection

SPO11 siRNA-1

SPO11 siRNA-2

SPO11 siRNA-4

100 cells/well (Day 20)

Figure A.20   HCT116 cell line 20 days after treated with different siRNA with 100 cells seeded. Non-interference, Hirerfect transfection (as negative controls) and untreated used to compare the cells growth with different siRNA. The cells treated with SPO11-siRNA4 shows clearly affected comparing to the untreated and the controls.

203

Untreated

Lipofectamine 2000

10 cells/well (Day 5)

Lipofectamine2000 and
TALENs

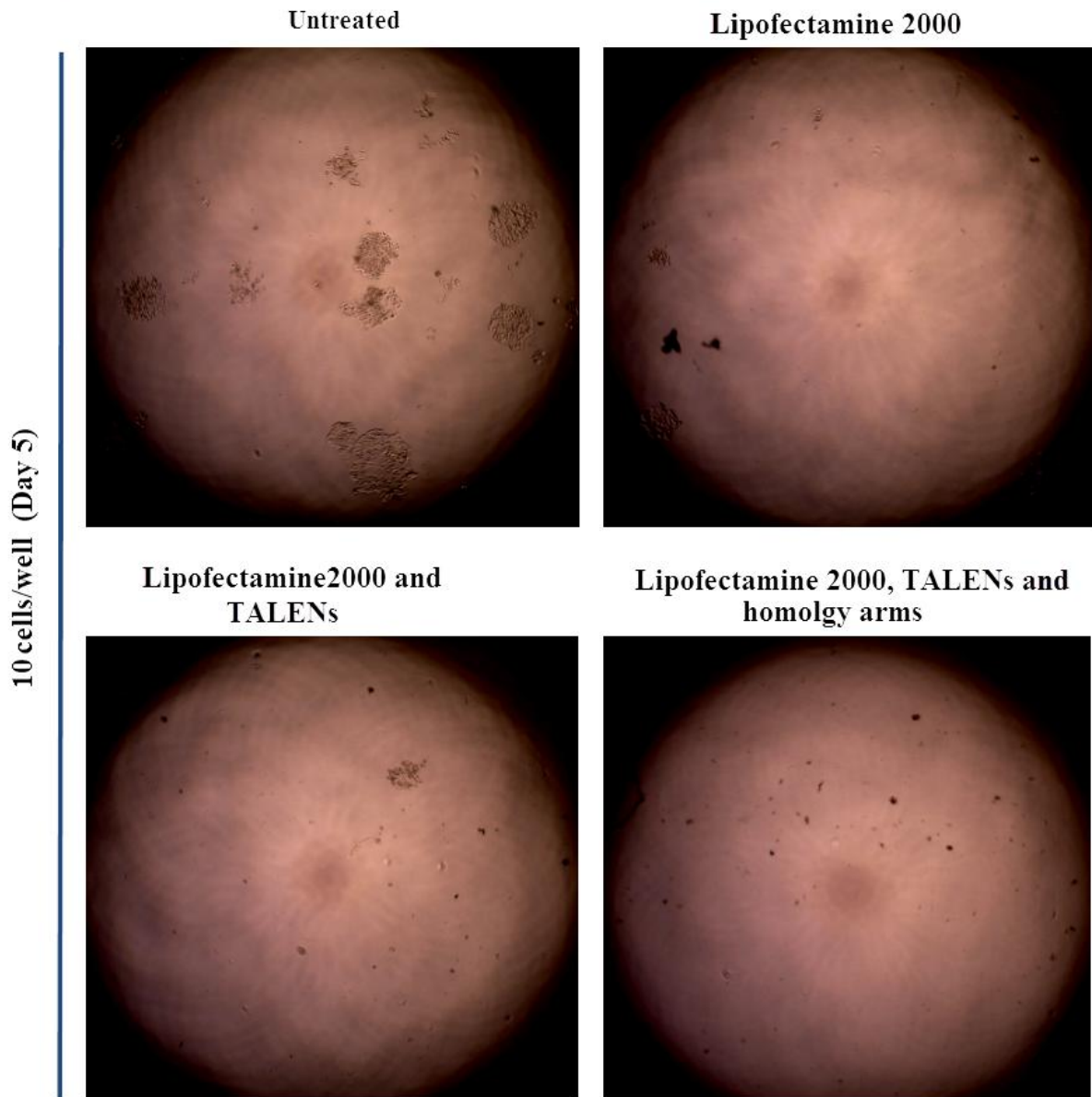Lipofectamine 2000, TALENs and
homolgy arms

Figure A.21 SW480 cell line 5 days after treated with TALEN and TALEN with homology arms with 10 cells seeded. Untreated and lipofectamine 2000 (as negative control) used to compare the cells growth with TALEN and TALEN with homology arms. The cells treated with negative control, TALENs and TALENs with homology arms were affected comparing with untreated.

Figure A.22 HCT116 cell line 5 days after treated with TALEN and TALEN with homology arms with 10 cells seeded. Untreated and lipofectamine 2000 (as negative control) used to compare the cells growth with TALEN and TALEN with homology arms. The cells treated with negative control, TALENs and TALENs with homology arms were affected comparing with untreated.
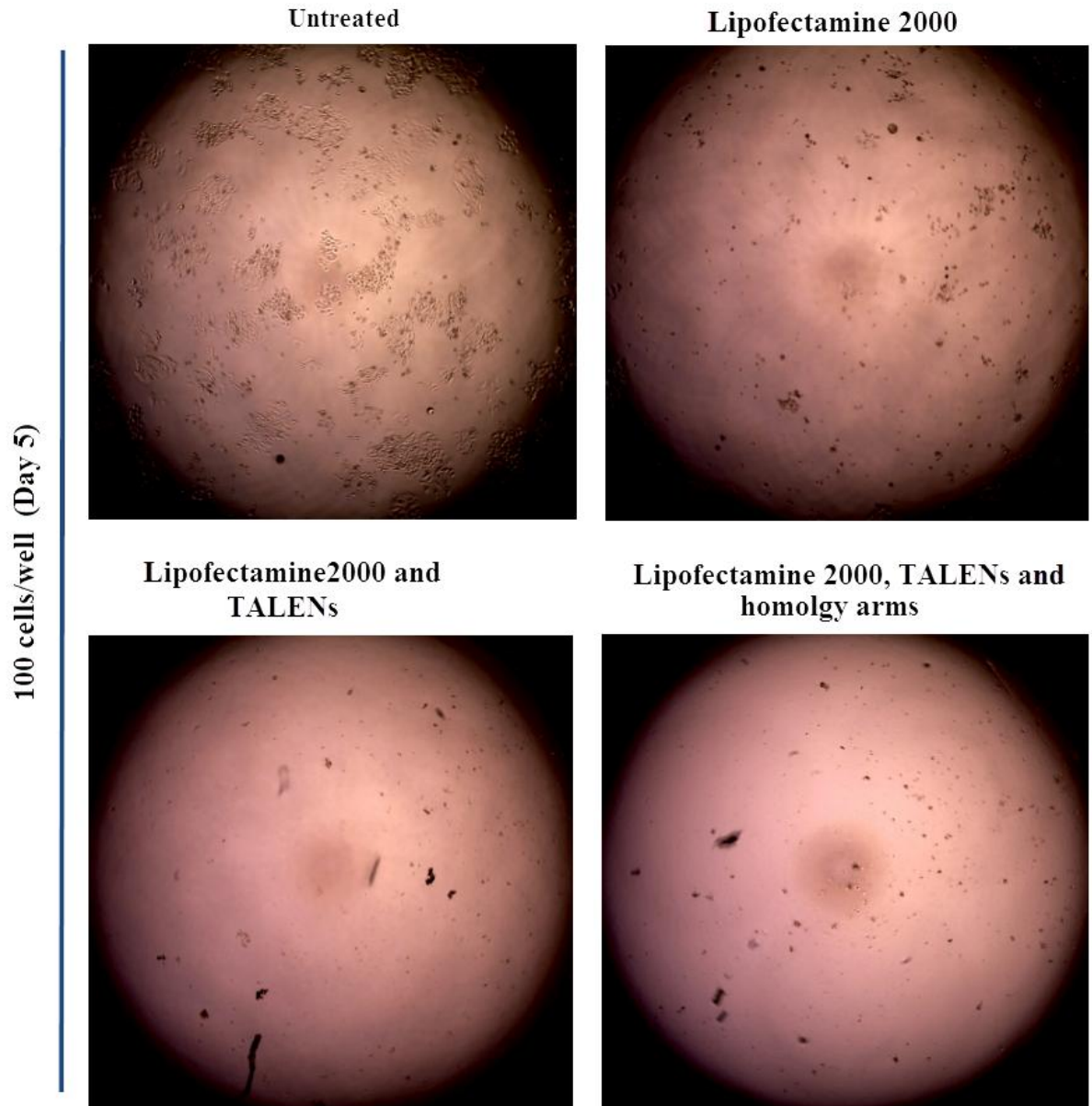
Figure A.23 SW480 cell line 5 days after treated with TALEN and TALEN with homology arms with 100 cells seeded. Untreated and lipofectamine 2000 (as negative control) used to compare the cells growth with TALEN and TALEN with homology arms. The cells treated with negative control, TALENs and TALENs with homology arms were affected comparing with untreated.
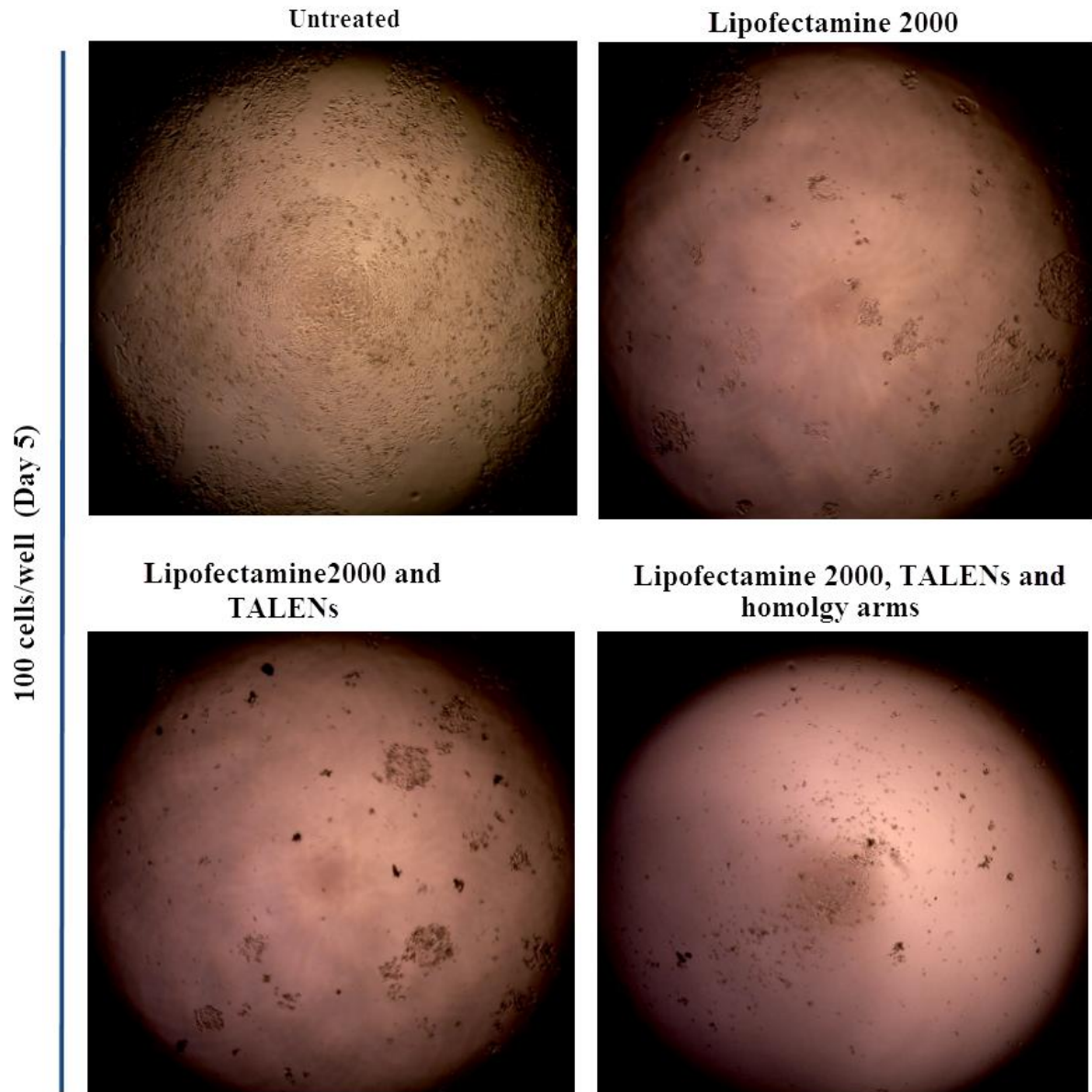
Figure A.24 HCT116 cell line 5 days after treated with TALEN and TALEN with homology arms with 100 cells seeded. Untreated and lipofectamine 2000 (as negative control) used to compare the cells growth with TALEN and TALEN with homology arms. In the cells treated with negative control and TALENs the growth were lower than untreated while no growth with the cells with TALENs with homology arms comparing to negative control, treated with TALENs and untreated.

SW480 cell line

Untreated

Lipofectamine 2000

(left margin, rotated) 10 cells/well (Day 10)

Lipofectamine2000 and TALENs

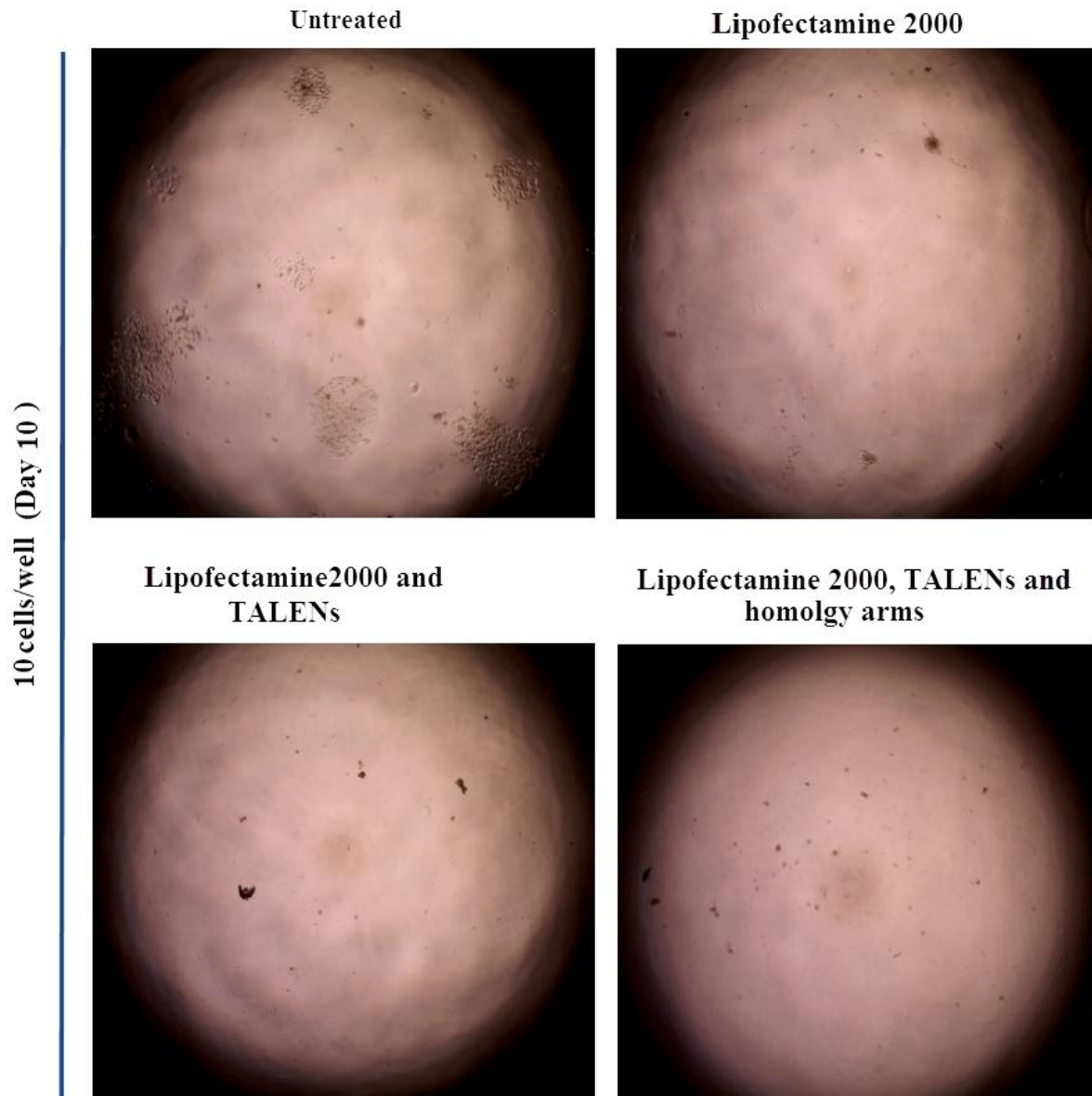**Lipofectamine 2000, TALENs and homolgy arms**

Figure A.25 SW480 cell line 10 days after treated with TALEN and TALEN with homology arms with 10 cells seeded. Untreated and lipofectamine 2000 (as negative control) used to compare the cells growth with TALEN and TALEN with homology arms. The cells treated with negative control, TALENs and TALENs with homology arms were affected comparing with untreated.
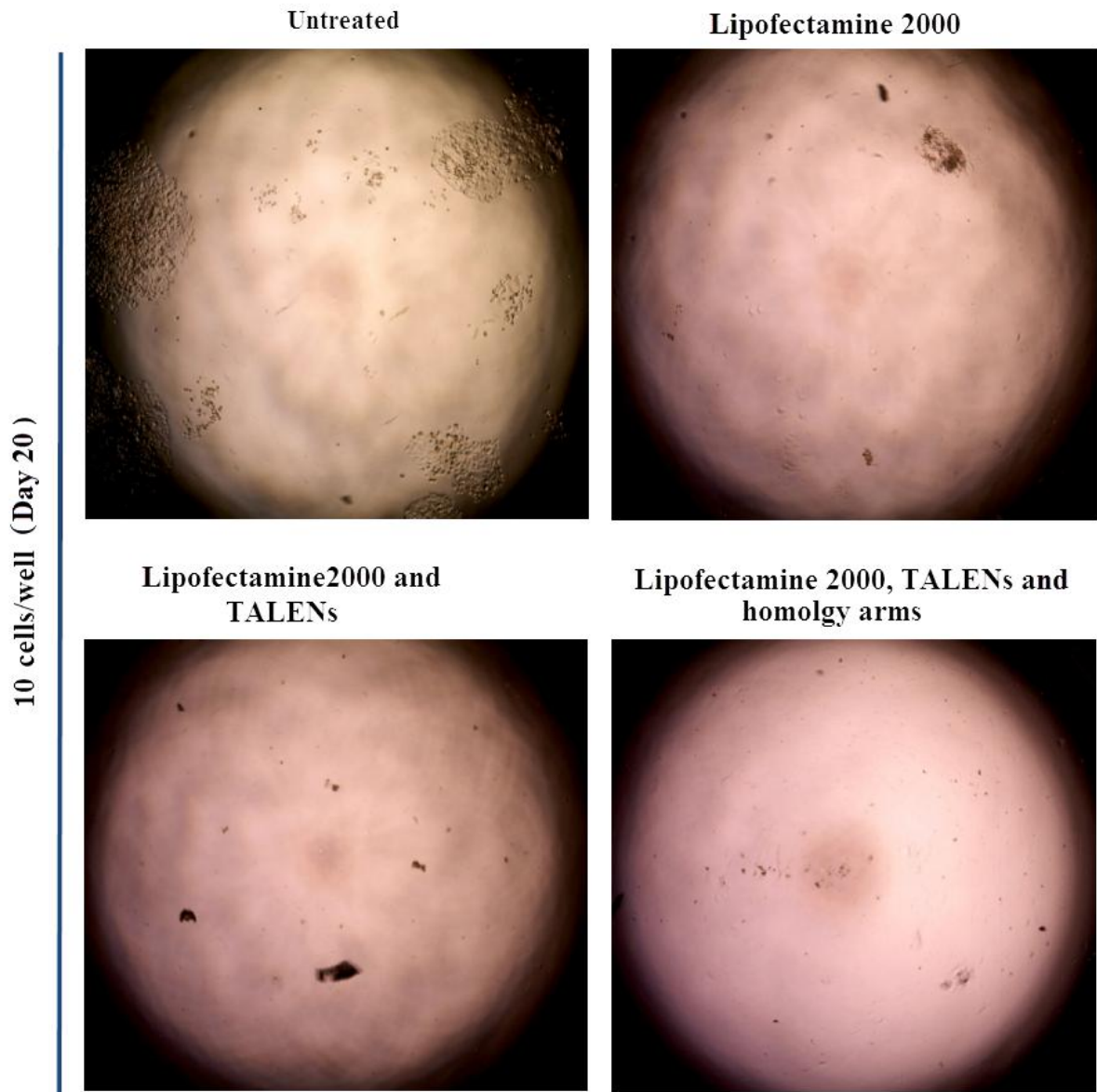
Figure A.26 SW480 cell line 20 days after treated with TALEN and TALEN with homology arms with 100 cells seeded. Untreated and lipofectamine 2000 (as negative control) used to compare the cells growth with TALEN and TALEN with homology arms. The cells treated with negative control, TALENs and TALENs with homology arms were affected comparing with untreated.

المملكة العربية السعودية

وزارة الصحة

المديرية العامة للشؤون الصحية بمنطقة الرياض

٢٧٥ / ١٠٠

وزارة الصحة
Ministry of Health

To whom it may concern :

This letter is to certify that our researcher **Mr. Ibrahim Aldeailej** will conduct his experiments on human tissues at our Central Laboratory in Riyadh for his PhD research in Bangor University. Therefore, Mr. Aldeailej will not be required for any additional permeations to use the laboratory samples which are taken based on patients approval in regard to Saudi Ministry of Health ethical standards.

However, Mr. Aldeailej will not be authorized to request additional new samples from patients for his projects.

This letter has been issued upon his request.

Medical Director & Head of Histopathology Dept.

Dr. Nayel Al-Jasser, MD

Consultant Histopathologist

Address:

King Saud Medical City
Riyadh Regional Lab. & Blood Bank
Post Box No. 59082
Riyadh, 11525
Riyadh, KSA
Email: naljasser@gmail.com

Figure A.27 Approval for used patient samples